

Development of Tyrosinase Inhibitors

Sini Radhakrishnan

This thesis is submitted in fulfilment of the requirements for the degree of
Doctor of Philosophy

Faculty of Science

School of Mathematical and Physical Sciences

University of Technology Sydney

2016

CERTIFICATE OF AUTHORSHIP/ORIGINALITY

I, Sini Radhakrishnan, certify that the work in this thesis has not been previously submitted for a degree nor has it been submitted as part of requirements for a degree.

I also certify that the thesis has been written by myself. Any assistance that I have received in my research work and the preparation of the thesis itself has been acknowledged. Furthermore, I certify that all information sources and literature used are indicated in the thesis.

Sini Radhakrishnan

ACKNOWLEDGEMENTS

This research was supported/funded by UTS International Research Scholarship (IRS) and Dr. Abdul Kalam Doctoral Scholarship. My deepest gratitude stands for the entire faculty and staff of the Faculty of Science at the University of Technology Sydney for having provided me with all the facilities and support that has led eventually to the completion of this thesis.

I take this opportunity to express my sincere gratitude and special appreciation to my Principal supervisor, Prof. Anthony Baker. His guidance and motivation has helped me throughout the tenure of my research including the drafting of this thesis. He has shown immense patience and has never deterred from sharing his knowledge and support with me. A special mention here has to be made on his efforts in improvising my skills with proof reading and scientific writing. I could not have imagined having a better advisor and mentor for my PhD study.

I would also like to thank my PhD Co-supervisor, Dr. Ronald Shimmon. I am deeply grateful to him for his guidance and advice in troubleshooting all the practical problems in the laboratory. He has been instrumental in getting me trained and competent with modern analytical techniques including NMR spectroscopy. He stands before me as an epitome of humility with brains.

I take this opportunity to express my deepest gratitude to Dr. Costa Conn, who has supervised me with a keen eye throughout my research schedule. His extensive knowledge and guidance in the field of molecular modeling has indeed been fruitful.

I am thankful to Dr. Linda Xiao and to Dr. David Bishop for their generous assistance during my research studies.

Finally, a special thanks to my mother Nirmala, and my son Vishnu, who have stood by me in my good and bad and have continuously encouraged and supported me throughout my PhD schedule. This thesis is dedicated to them.

ABSTRACT

The primary objective of this project was the drug discovery, synthesis and biological evaluation of a series of tyrosinase inhibitors. Chalcone skeleton was the chosen pharmacophore and a library of potent inhibitors of tyrosinase (polyphenol oxidase) were synthesized and their structure-activity (SAR) relationships were explored. Chalcone derivatives were synthesized by simple base catalyzed Claisen-Schmidt condensation of an aldehyde and an appropriate ketone in a polar solvent like methanol. The structures of the compounds synthesized were confirmed by ^1H NMR, ^{13}C NMR, FTIR and HRMS. Two compounds that are the reduction congeners of the pyridinyl azachalcones strongly inhibited the enzyme activity and were more potent than the positive control kojic acid. Two of the hydroxyazachalcones synthesized inhibited the diphenolase activity of tyrosinase and were identified as competitive reversible inhibitors and with their K_i values of 3.4 μM and 3.9 μM , respectively. This study showed that a more potent tyrosinase inhibitor can be obtained from methoxyazachalcones with a single step dealkylation reaction. A series of novel hydroxynaphthylchalcone compounds were synthesized and inhibited the diphenolase activity of tyrosinase in a dose dependent manner with much higher tyrosinase inhibitory activities than the positive control, kojic acid. The number and position of methoxy substituents on the aromatic rings appeared to be critical for cytotoxicity. Also placement of strongly electron-withdrawing groups such as NO_2 in ring B correlated with increase of cytotoxic activity. This study provides valuable information in utilizing methoxychalcone as a lead compound for the further design and development of potential tyrosinase inhibitors with antimelanogenic effects. Two pyridinyl methoxychalcone compounds exhibited higher tyrosinase inhibitory activities (IC_{50} values of 10.6 μM and 12.5 μM , respectively) than the control kojic acid (IC_{50} : 22.83 μM). Kinetic studies revealed them to act as competitive tyrosinase inhibitors. Both the compounds inhibited melanin production and tyrosinase activity in B16 cells. Docking results confirm that the active inhibitors strongly interact with mushroom tyrosinase residues. The current study portrays methoxychalcones with electrophilic character to be potent agents with antimelanogenic effects. A series of hydroxy substituted chalcone oxime derivatives have been synthesized and evaluated for their inhibitory activities on tyrosinase and melanogenesis in murine B16F10 melanoma cell lines. A library of 2'-acetylpyridinyl chalconeoxime compounds was also synthesized.

The study portrayed the significance of an oxime moiety on the chalcone framework that brought about better coordination with the copper metal centers at the active site of mushroom tyrosinase and also exhibited stronger hydrogen bonding interactions with the amino acid residues. From all the compounds synthesized, a novel 2'-acetylpyridinyl chalconeoxime compound exhibited the most potent tyrosinase inhibitory activity with an IC_{50} value that was found to be several times potent than the reference standard, kojic acid. The inhibition mechanism was competitive and was in complete agreement with the docking results. Furthermore, a solid-state based mechanochemical process was used to synthesize novel azachalcones and their oximes as tyrosinase inhibitors. Both the novel oxime compounds displayed competitive inhibition with their K_i values of 5.1 μ M and 2.5 μ M, respectively. This method minimizes waste disposal problems and provides a simple, efficient and benign method for the synthesis of novel tyrosinase inhibitors for use as skin whitening agents or as anti-browning food additives. The effects of novel 2,3-dihydro-1*H*-inden-1-one chalcone-like compounds for tyrosinase inhibition were studied. Hydroxy substituted 1-indanone chalcone-like compounds were found to be significantly more potent than kojic acid.

Assays were performed with L-DOPA as the substrate, using kojic acid, a well-known strong tyrosinase inhibitor as the positive control. The kinetic parameters and inhibition mechanisms of active tyrosinase inhibitors were illustrated with the help of Lineweaver-Burk plots and Dixon plots. Furthermore, the experimental results were integrated with simulation studies using Accelrys Discovery Studio 4.5 suite. Few of the active tyrosinase inhibitors were further evaluated for the *in vitro* cytotoxic activity on B16 F10 melanoma cell lines. The results suggested substituted chalcone derivatives to serve as an interesting candidate for the treatment of tyrosinase related disorders and as the lead compounds for the development of new and potent tyrosinase inhibitors.

TABLE OF CONTENTS

Certificate of Authorship/ Originality	ii
Acknowledgements	iii
Abstract	iv
List of papers published	xiii
List of Tables.....	xiv
List of Figures	xv
List of Abbreviations.....	xviii
CHAPTER 1: Introduction.....	1
1.1. Melanin & melanogenesis.....	2
1.1.1.Physiological roles of melanin	5
1.2. Mushroom tyrosinase	6
1.2.1. Biochemical characteristics of tyrosinase	7
1.2.2. Domain structure	8
1.2.3. Reaction mechanism of tyrosinase	9
1.2.4. Tyrosinase substrates	13
1.3. Potential uses of tyrosinase inhibitors.....	15
1.4. Mechanisms of tyrosinase inhibition	18
1.5. Rational drug design of tyrosinase inhibitors.....	18
1.6. Classification of known tyrosinase inhibitors	19
1.6.1. Simple monocyclic inhibitors	19
1.6.2. Polyphenols	22
1.6.3. Stilbenes	25
1.6.4. Phenolic compounds as tyrosinase inhibitors	27
1.6.5. Coumarins as tyrosinase inhibitors	28

1.6.6. Benzaldehyde and benzoate derivatives as tyrosinase inhibitors.....	29
1.6.7. Other inhibitors	30
1.6.8. Chalcones as tyrosinase inhibitors	33
1.7. References	37
CHAPTER 2: Hydroxyazachalcones	64
2.1. Introduction	65
2.2. Experimental	65
2.2.1. Method for synthesis of compound 5b.....	65
2.3. Results and Discussion.....	67
2.3.1. Chemistry	67
2.3.2. Enzyme kinetics	70
2.3.3. In silico docking studies.....	76
2.4. Conclusion	78
2.5. References	80
CHAPTER 3: Hydroxynaphthylchalcones	84
3.1. Introduction	85
3.2. Experimental	85
3.2.1. Method for synthesis of compound 10b.....	86
3.3. Results and Discussion.....	90
3.3.1. Chemistry	90
3.3.2. Kinetics	922
3.3.3. Docking studies	96
3.4. Conclusion	99
3.5. References	100
CHAPTER 4: Allyl alcohols of Azachalcones	1033
4.1. Introduction	104
4.2. Experimental	1044

4.2.1. Method for synthesis of compound 11b.....	1055
4.3. Results and Discussion.....	106
4.3.1. Synthesis	1066
4.3.2. Chemistry	11010
4.3.3. Kinetics	1122
4.3.4. Docking results	1144
4.4. Conclusion	121
4.5. References	12222
CHAPTER 5: Methoxychalcone compounds	1233
5.1. Introduction	1244
5.2. Experimental	1255
5.2.1. Method for synthesis of compound 3c.....	1255
5.3. Results and Discussion.....	13131
5.3.1. Chemistry & inhibition kinetics	131
5.3.2. Effect on melanogenesis	1344
5.3.3. Docking studies	137
5.4. Conclusion	1399
5.5. References	14040
CHAPTER 6: Chalconeoximes (Phenyl & naphthyl derivatives)	1455
6.1. Introduction	1466
6.2. Experimental	1466
6.2.1. Method for the synthesis of compound 17b.....	1477
6.2.2. Spectral data	1488
6.3. Results and Discussion.....	15151
6.3.1. Chemistry & inhibition kinetics	15151
6.3.2. Docking studies	1555
6.3.3. Effect on melanogenesis	1599

6.4. Conclusion	16161
6.5. References	16262
CHAPTER 7: Solid state synthesis of Chalconeoximes	1644
7.1. Introduction	1655
7.2. Experimental	1666
7.2.1. Method for synthesis of 23b	167
7.2.2. Spectral data	168
7.3. Results and Discussion	172
7.3.1. Effect of compounds on tyrosinase activity: inhibition kinetics	17272
7.3.2. Inhibition mechanism of the selected compounds on mushroom tyrosinase	1733
7.3.3. Lineweaver–Burk analysis of tyrosinase inhibition by compounds 22b and 23b...	1755
7.3.4. Docking studies	1788
7.4. Conclusion	18080
7.5. References	18181
CHAPTER 8: Aminochalcones	1855
8.1. Introduction	1866
8.2. Experimental	1866
8.2.1. Method for the synthesis of compound 30b	1877
8.2.2. Spectral data	1888
8.3. Results and Discussion	19393
8.3.1. Chemistry	19393
8.3.2. Kinetics	1944
8.3.3. Docking studies	1988
8.3.4. Effect on melanogenesis	201
8.4. Conclusion	204
8.5. References	204

CHAPTER 9: 2,3-Dihydro-1H-inden-1-one (1-indanone) Chalcone-like derivatives	206
9.1. Introduction	2077
9.2. Experimental	2077
9.2.1. Method for the synthesis of compound 41b	2077
9.2.2. Spectral data	2087
9.3. Results and Discussion	2118
9.3.1. Chemistry and inhibition kinetics	211
9.3.2. In silico docking studies	2177
9.4. Conclusion	22020
9.5. References	220
CHAPTER 10: Chalconeoximes (2'-acetylpyridinyl derivatives)	223
10.1. Introduction	22424
10.2. Experimental	22424
10.2.1. Method for synthesis of compound 46b	22525
10.2.2. Spectral data	22626
10.3. Results and Discussion	2299
10.3.1. Chemistry	22929
10.3.2. Inhibition mechanism of the selected compounds on mushroom tyrosinase	23232
10.3.3. Lineweaver–Burk analysis by inhibitor compounds 46b and 48b	23333
10.3.4. Docking studies	2355
10.4. Conclusion	2388
10.5. References	23939
CHAPTER 11: Conclusion	24141
11.1. Future prospects	2533
CHAPTER 12: General Experimental	255
12.1. Chemical reagents and instruments	256
12.2. General method for the synthesis of chalcone derivatives	256

12.3. Method for the synthesis of hydroxy derivatives of methoxychalcones.....	256
12.4. Method for the synthesis of allyl alcohols of chalcone compounds.....	257
12.5. General method for the synthesis of hydroxy chalcone oxime compounds....	257
12.6. General method for the synthesis of amino chalcones.....	257
12.7. Method for the synthesis of chalcone compounds by solid state synthesis....	258
12.8. Method for the synthesis of chalcone oximes by solid state synthesis.....	258
12.9. Tyrosinase inhibition assay.....	258
12.10. Determination of the inhibition type of respective active compounds on mushroom tyrosinase.....	259
12.11. <i>In silico</i> docking between tyrosinase and target compounds.....	259
12.12. <i>In vitro</i> cytotoxicity studies.....	260
12.12.1. Cell culture.....	260
12.12.2. Cell viability.....	260
12.12.3. Assay of murine tyrosinase activity.....	260
12.12.4. Determination of melanogenesis in B16 cells.....	261
12.13. References.....	261
CHAPTER 13: Appendix.....	263
13.1. Kinetics of mushroom tyrosinase.....	264
13.2. Enzyme inhibitors.....	266
13.2.1. Reversible enzyme inhibition.....	267
13.2.2. Competitive inhibition.....	267
13.2.3. Non-competitive inhibition.....	268
13.2.4. Mixed type inhibition	268
13.2.5. Uncompetitive inhibition.....	270
13.2.6. Irreversible inhibitors.....	271
13.2.7. Suicide inhibition.....	271
13.3. Docking and ligand-receptor interactions.....	273
13.3.1. Target Characterization.....	276
13.3.2. Hot spot identification.....	276

13.3.3. Current challenges or limitations facing molecular docking.....	277
13.4. Receptor-Ligand Interactions.....	278
13.5. Applications of Docking.....	279
13.6. References.....	279

LIST OF PAPERS PUBLISHED

1. Radhakrishnan, SK, Shimmon, R, Conn, C, Baker, AT 2015, 'Azachalcones: A novel class of polyphenol oxidase inhibitors', *Bioorganic and Medicinal Chemistry Letters*, Vol 25, pp. 1753-1756.
2. Radhakrishnan, SK, Shimmon, R, Conn, C, Baker, AT 2015, 'Development of hydroxylated naphthylchalcones as polyphenol oxidase inhibitors: Synthesis, biochemistry and molecular docking studies', *Bioorganic Chemistry*, Vol 63, pp. 116–122.
3. Radhakrishnan, SK, Shimmon, R, Conn, C, Baker, AT 2015, 'Integrated kinetic studies and computational analysis on naphthyl chalcones as mushroom tyrosinase inhibitors', *Bioorganic and Medicinal Chemistry Letters*, Vol 25, pp. 4085–4091.
4. Radhakrishnan, SK, Shimmon, R, Conn, C, Baker, AT 2015, 'Evaluation of novel chalcone oximes as inhibitors of tyrosinase and melanin formation in B16 cells', *Archiv der Pharmazie*, Vol 348, pp. 1–10.
5. Radhakrishnan, SK, Shimmon, R, Conn, C, Baker, AT 2015, 'Inhibitory kinetics of novel 2, 3-dihydro-1H-inden-1-one chalcone like-derivatives on mushroom tyrosinase', *Bioorganic and Medicinal Chemistry Letters*, Vol 25, pp. 5495–5499.
6. Radhakrishnan, SK, Shimmon, R, Conn, C, Baker, AT 2015, 'Design, synthesis and biological evaluation of hydroxy substituted amino chalcone compounds for antityrosinase activity in B16 cells', *Bioorganic Chemistry*, Vol 62, pp. 117-123.
7. Radhakrishnan, SK, Shimmon, R, Conn, C, Baker, AT 2016, 'Inhibitory kinetics of azachalcones and their oximes on mushroom tyrosinase: a facile green synthesis', *Chemistry and Biodiversity*, Vol 13, pp. 531–538.

LIST OF TABLES

Table 1 Properties of various tyrosinases.....	8
Table 2 Inhibition Effects and docking results of hydroxy azachalcones.....	722
Table 3. Effect on mushroom tyrosinase activity and kinetic analysis of compounds .	733
Table 4 Inhibition and docking results of hydroxynaphthylchalcones	91
Table 5 Effect on mushroom polyphenol oxidase activity and kinetic analysis of compounds.	966
Table 6 Docking results and tyrosinase inhibition effects of allyl alcohols	11111
Table 7 Effect on mushroom polyphenol oxidase activity and kinetic analysis of compounds	11212
Table 8 Docking results, tyrosinase inhibition and cytotoxic effects of methoxychalcones	13232
Table 9 Inhibitory effects of kojic acid, 17b and 19b on mushroom tyrosinase.....	15353
Table 10 Kinetic analysis of compounds 17b and 19b.	15353
Table 11 Inhibition effects and docking results of phenyl & naphthyl chalconeoximes	1566
Table 12 Inhibition effects and docking results of chalconeoximes.....	17474
Table 13 Effect on mushroom tyrosinase activity and kinetic analysis	1788
Table 14 Docking results and tyrosinase inhibition effects of amino chalcones	19595
Table 15 Inhibitory effects of kojic acid, 29b and 30b on mushroom tyrosinase.....	1966
Table 16 Substitution Pattern and Inhibition Effects of 1-indanonechalcones	21212
Table 17 Effect on tyrosinase activity and kinetic analysis of compounds	21616
Table 18 Docking results of active indanone chalcone-like compounds.....	2177
Table 19 Inhibition effects and docking results of acetylpyridinylchalconeoximes.	23030
Table 20 Inhibitory effects of kojic acid, 46b and 48b on mushroom tyrosinase.	23232
Table 21 Inhibition effects and docking results of chalcone derivatives on mushroom tyrosinase	24444

LIST OF FIGURES

Figure 1 Biosynthetic pathway of melanin	3
Figure 2 Reaction pathway involving tyrosinase	7
Figure 3 Geometry of the active site of tyrosinase with tropolone in sticks.....	9
Figure 4 The three states of the active site of tyrosinase.	13
Figure 5 Active site of mushroom tyrosinase	19
Figure 6 Monocyclic tyrosinase inhibitors.....	22
Figure 7 Polyphenols as tyrosinase inhibitors.....	23
Figure 8 Stilbenes as tyrosinase inhibitors.....	27
Figure 9 Phenolic compounds as tyrosinase inhibitors	28
Figure 10 Miscellaneous tyrosinase inhibitors.....	32
Figure 11 Structures of chalcone, garcinol and curcumin.....	33
Figure 12 Chalcones as tyrosinase inhibitors.....	35
Figure 13 The inhibitory mechanism of compounds 5b and 2b	744
Figure 14 Lineweaver Burk plot for inhibition of compounds 5b and 2b.	755
Figure 15 Dixon plot for the inhibitory effect of compounds 5b and 2b.	766
Figure 16 Docking and 2D results of compounds 1b–5b.....	80
Figure 17 Inhibition effects of compounds 10b and 7b.	922
Figure 18 The inhibitory mechanism of compounds 10b and 7b.....	933
Figure 19 Lineweaver Burk plot for inhibition of compounds 10b and 7b.	944
Figure 20 Dixon plot for the inhibitory effect of compounds 10b and 7b	955
Figure 21 Docking and 2D results of compounds 10b, 7b	988
Figure 22 Lineweaver-Burk plots for inhibition of active compounds 11b and 13b..	1133
Figure 23 Dixon plot for the inhibitory effect of compounds 11b and 13b.	1144
Figure 24 Docking and 2D results of compounds 11b –16b	1199
Figure 25 Lineweaver Burk plot for inhibition of compounds 3c and 1c.....	13333
Figure 26 Effect of compounds 3c and 1c on B16 cell viability.....	1355
Figure 27 Inhibitory effect of compounds 3c and 1c after treatment with 100 nM α -MSH	1366
Figure 28 Inhibitory effect of compounds 3c and 1c on B16 cells tyrosinase.....	1377
Figure 29 Docking and 2D results of compounds 3c and 1c	1399
Figure 30 Inhibitory effects of chalcone oximes on mushroom tyrosinase activity.	15252

Figure 31 Lineweaver Burk plot for inhibition of compounds 17b and 19b.	15454
Figure 32 Dixon plot for the inhibitory effect of compounds 17b and 19b	155
Figure 33 Docking and 2D results of compounds 17b and 19b	1588
Figure 34 Effect of compounds 17b and 19b on cell viability.....	1599
Figure 35 Inhibitory effect of compounds 17b and 19b in B16 cells.....	16060
Figure 36 Inhibitory effect of compounds 17b and 19b on B16 cells tyrosinase.	16161
Figure 37 Principles of green chemistry	1666
Figure 38 The inhibitory mechanism of compounds 22b and 23b.....	1755
Figure 39 Lineweaver-Burk plots for inhibition of compounds 22b and 23b.	1766
Figure 40 Dixon plot for the inhibitory effect of compounds 22b and 23b.	1777
Figure 41 Docking and 2D results of compounds 22b and 23bet.	18080
Figure 42 Lineweaver Burk plot for inhibition of compounds 29b and 30b.	1977
Figure 43 Dixon plot for the inhibitory effect of compounds 30b and 29b.	1988
Figure 44 Docking and 2D results of compounds 29b and 30b	201
Figure 45 Effect of compounds 29b and 30b on cell viability.....	202
Figure 46 Inhibitory effect of 29b and 30b after treatment with 100 nM α -MSH	203
Figure 47 Inhibitory effect of compounds 29b and 30b on B16 cells of tyrosinase.	203
Figure 48 Inhibition effects of compounds 41b and 42b.	21313
Figure 49 Inhibitory mechanism of compounds 41b and 42b.....	21414
Figure 50 Lineweaver Burk plot for inhibition of compounds 41b and 42b.	21515
Figure 51 Dixon plot for the inhibitory effect of compounds 41b and 42b.	21616
Figure 52 Docking and 2D results of compounds 41b and 42b.....	2199
Figure 53 The inhibitory mechanism of compounds 46b and 48b.....	23333
Figure 54 Lineweaver Burk plot for inhibition of compounds 46b and 48b.	23434
Figure 55 Dixon plot for the inhibitory effect of compounds 46b and 48b.	23535
Figure 56 Docking and 2D results of compounds 46b and 48b.....	23838
Figure 58 Tyrosinase assay	26566
Figure 59 Lineweaver –Burk plot.	26667
Figure 60 A simplified model of competitive inhibition	26768
Figure 61 Kinetics of competitive inhibition	2688
Figure 62. A simplified model of noncompetitive inhibition	2699
Figure 63 Kinetics of noncompetitive inhibition	2699
Figure 64 Kinetics of mixed inhibition	27070

Figure 65 Kinetics of uncompetitive inhibition	27070
Figure 66 Molecule docked to a protein	27373

LIST OF ABBREVIATIONS

DHI	5, 6-dihydroxyindole
DMSO	Dimethyl sulfoxide
DHICA	5, 6-dihydroxyindole-2-carboxylic acid
UV	Ultraviolet
DOPA	3, 4-dihydroxyphenylalanine
TOPA	2, 4, 5-trihydroxyphenylalanine
DHICA	5, 6-dihydroxyindole-2-carboxylic acid
TRP-1	tyrosinase related protein-1
PPO	polyphenol oxidase
HC	hemocyanins
GHB	glutaminyl-4-hydroxybenzene
NMR	Nuclear magnetic resonance
HRMS	High resolution mass spectroscopy
FTIR	Fourier transform infra-red
PDB	Protein data bank
SAR	Structure activity relationship
RT	Room temperature
TLC	Thin layer chromatography
SE	Standard error
Mp	Melting point
DNA	Deoxyribonucleic acid
ROS	Reactive oxygen species
MeOH	Methanol
MTT	3-(4, 5-dimethylthiazol-2-yl) 2, 5-diphenyltetrazolium bromide

CHAPTER 1

INTRODUCTION

1.1. Melanin & melanogenesis

Melanin (Greek: melas, "black, dark") is a broad term used to describe a group of natural pigments found in most organisms. They are predominantly indolic polymer pigments present in surface structures of most vertebrates (Riley 1997). The name is derived from Greek "melanos", meaning dark colored and it was first used by the Swedish chemist Berzelius.

Human skin colour originates from melanins present in the epidermis; the outermost layer of skin, where the pigment producing cells or melanocytes are located. (Spritz & Hearing 1994; Lozumi *et al* 1993). Melanocytes are also located in hair follicles, eyes and even in the brain. Found within melanocytes, are special organelles called melanosomes, from the Golgi apparatus (Raposo & Marks 2007). Melanosomes are highly mobile within the cell, and their actions are controlled by hormonal signals. They are tracked by microtubules and motor proteins which transfer them to the periphery of the cells (Wu *et al* 2002). This tracking mechanism of melanosomes helps the insoluble melanins to be transferred to other cells such as keratinocytes or brain cells, from melanocytes. In mammals, melanin granules are distributed to hair and epidermis by a process known as cytotrine transfer, in which portions of melanocyte cytoplasm are endocytosed by epithelial cells (Wolff, Jimbow & Fitzpatrick 1974). As stated earlier, melanins are one of the most widely distributed pigments and are found in bacteria, fungi, plants and animals. The family of melanin includes eumelanins, and pheomelanins. The latter are sulphur containing melanins that on degradation by hydroiodic acid, give rise to about 20% of aminohydroxyphenylalanine (Ito & Fujita 1985). Eumelanin is a black/brown colored chromophore which is a cross-linked polymer molecule of the monomer 5,6-dihydroxyindole (DHI) and 5, 6-dihydroxyindole-2-carboxylic acid (DHICA). Pheomelanin is a monomer derived from dopaquinone following nucleophilic addition of glutathione or cysteine. It consists of a benzothiazine monomer, a lightly colored pigment (Costin & Hearing 2007). Even though all the functions of melanins in humans have yet to be identified, several biological functions of melanins have been reported previously. These include its role as a redox buffer (free radical scavenger), as a cation binding material, and as a radiation sink (providing protection from UV radiation) (Riley 2003). The latter function occurs via the transformation of light energy into heat through an internal conversion process, keeping the generation of free radicals at a minimum (Lin & Fisher 2007; Park *et al* 2009). The

amount of melanins produced varies in different ethnic groups and determines their skin color. The characteristic skin patterns of zebra, giraffes and piebald animals in general are due to this uneven distribution of melanocytes (Frenk 1995).

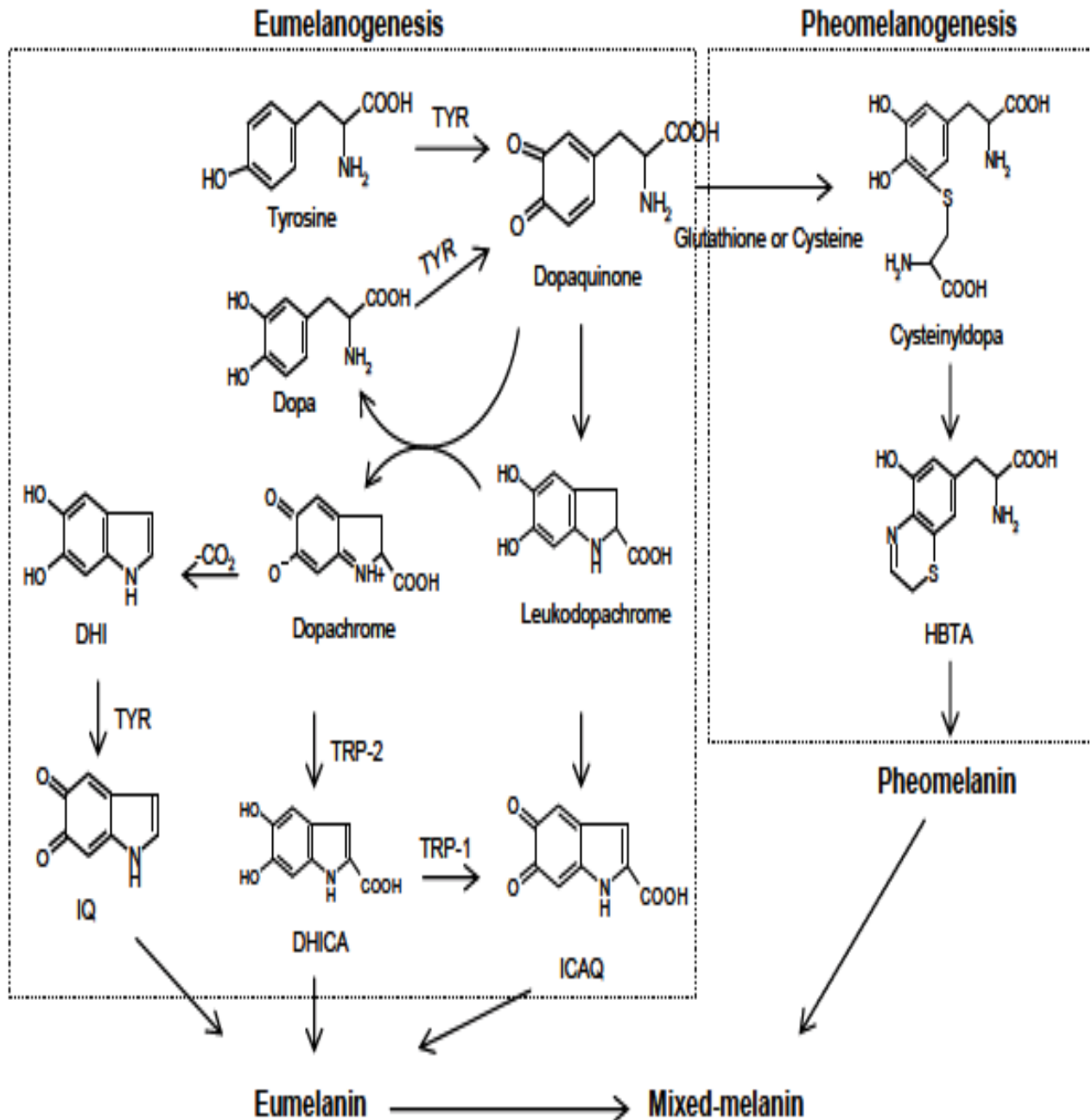


Figure 1 Biosynthetic pathway of melanin

(Reproduced from Lima *et al* 2013)

The biosynthetic pathway for melanin formation (**Figure 1**) in various life forms, firstly elucidated by Raper and Mason and recently been modified by Cooksey and Schallreuter (Raper 1928; Mason 1948; Cooksey *et al* 1997; Schallreuter *et al* 2008).

Melanin biogenesis in animals occurs by an oxidation process starting with the amino acid L-tyrosine. The pathway of eumelanogenesis may be divided into two phases referred to as proximal and distal. The proximal phase consists of the enzymatic oxidation of tyrosine or L-DOPA to its corresponding *o*-dopaquinone (Alam *et al* 2011; Kobayashi *et al* 1995). This first step is the rate-limiting step. It is the only step controlled by an enzyme. The remainder of the reaction sequence proceeds spontaneously at a physiological pH value and not under enzymatic control (Halaban *et al* 2002). There are two other enzymes involved in the formation of eumelanin: tyrosinase related protein-1 (TRP-1: DHICA oxidase), and tyrosinase-related protein-2 (TRP-2) (Korner & Pawelek 1982; Kameyama *et al* 1993). Given this, the remainder of the reaction sequence may also be rate-limited as they are under enzymatic control.

This nascent *o*-dopaquinone can undergo two different types of reactions. Firstly, the amino group of the *o*-dopaquinone side chain undergoes intra-molecular 1,4-addition to the quinone double bond, leading to cyclization into leukodopachrome. This intermediate is involved in redox cycling where upon it is quickly oxidized into dopachrome by another *o*-dopaquinone molecule, which is in turn reduced back to L-DOPA (Brun & Rosset 1974; Pawelek 1991; Aroca *et al* 1990). DOPA is also the substrate of tyrosinase and oxidized to dopaquinone again by the enzyme.

The second reaction occurs with cyclizable and noncyclizable quinones and consists of a water addition to the benzene ring which leads to the formation of 3-hydroxylated phenol 2,4,5-trihydroxyphenylalanine (TOPA) that is chemically oxidized to para-topaquinone by another ortho-dopaquinone (Garcia-Carmona *et al* 1982). Para-topaquinone is converted through a series of slow reactions to dopachrome which is the final product of the proximal phase. The distal phase is represented by the chemical and enzymatic reactions which occur after dopachrome formation and lead to the synthesis of eumelanins (Pawelek 1991; Aroca *et al* 1990). This phase starts with the slow chemical decarboxylation of dopachrome to 5,6-dihydroxyindole (DHI) and its subsequent oxidation to indole-5,6-quinone. As an alternative to this pathway in the distal phase, dopachrome may be enzymatically transformed into 5,6-dihydroxyindole-2-carboxylic acid (DHICA) by dopachrome tautomerase. 5,6-dihydroxyindole-2-carboxylic acid is further oxidized by a redox reaction with *o*-dopaquinone to form indole-5,6-quinone carboxylic acid, which can exist in three tautomeric forms, including the quinone-imine and the corresponding highly reactive quinone-methide (Lambert *et*

al 1989; Sugumaran & Semensi 1991). The physical and spectral properties of 5,6-dihydroxyindole and 5,6-dihydroxyindole-2-carboxylic acid derived melanins differ in each other; the former are black and flocculent, while the latter are yellowish-brown and finely dispersed.

During pheomelanogenesis, the thiol group of sulfhydryl compounds such as glutathione and cysteine nucleophilically attacks ortho-dopaquinone formed from tyrosinase producing cysteinyl-dopa or glutathionyl-dopa. This thiol group can attack different ring positions, although the 5-position is the favored position. Subsequent cyclization and polymerization of cysteinyl-dopa or glutathionyl-dopa in an uncharacterized series of reactions result in the production of pheomelanins (Sugumaran & Semensi 1991; Hearing & King 1993). The interaction between the eumelanin and pheomelanin compounds gives rise to a heterogeneous pool of mixed-type melanins. In addition to eumelanin and pheomelanin, other “melanins” formed from other phenolic monomers different from tyrosine are named allomelanins (Te-Sheng Chang 2009; Prota 1992). The main difference resides in the fact that allomelanins do not contain dopaquinone derived motifs as the main monomers in their structure and, on the contrary, are based on other quinoid building blocks.

1.1.1. Physiological roles of melanin

Fruits, fungi, vegetables: Here, melanins are responsible for the browning of damaged tissue when exposed to air and the browning occurring during post-harvest storage (Francisco *et al* 1997). In agriculture, this poses a significant problem with huge economic impact, making the identification of compounds that inhibit melanin formation extremely important. In other plants, (raisins, tea and cocoa), the tyrosinase activity is needed for the production of distinct organoleptic properties. In fungi, the role of melanin is correlated with the differentiation of reproductive organs and spore formation, virulence of pathogenic fungi, and tissue protection after injury. The role of browning in fruits and vegetables may serve a defensive role, although the exact reasons remain unclear at present (Gadd 1980; Bell & Wheeler 1986; Zimmerman *et al* 1995).

Invertebrates: Apart from providing pigmentation, melanin is also involved in three physiologically important processes. These are: (1) defense reactions involving the immune system, (2) wound healing and (3) cuticular hardening (sclerotization). Insects and other arthropods use melanin production as a defense mechanism to encapsulate

foreign organisms (Sugumaran 1998; Gillespie, Kanost & Trenczek 1997; Nappi & Sugumaran 1993; Söderhäll, Aspán & Duvic 1990; Sugumaran & Kanost 1993; Sugumaran 1996; Ashida & Brey 1995). Furthermore, deposition of melanin at a wound site prevents the loss of blood, while the cytotoxic melanogenic quinonoid precursors may kill invading microorganisms at the wound site (Nappi & Sugumaran 1993; Sugumaran 1996). Finally, melanogenesis closely resembles the sclerotinogenic pathway. Sclerotization reactions employ catecholamines that are similar to melanogenic precursors, using a similar set of enzymes. During sclerotization, N-catecholamines are converted to quinones. These and other reactive metabolites are involved in cross-linking structural proteins, resulting in the formation of the hard cuticle. Arrest or even delay of this process has devastating consequences on insects which has led to the proposed use of tyrosinase inhibitors as insecticides (Sugumaran 1991).

Mammals: As stated earlier, in mammals, melanin is produced in specialized pigment-producing cells known as melanocytes, which originate in the neural crest during embryogenesis and are spatially distributed throughout the organism during development. This distribution is under strict genetic control and leads to interesting skin patterns, such as in zebras and leopards. In mammals, melanin pigments play several diverse and important roles, including thermoregulation, camouflage and sexual attraction (Tadokoro *et al* 2003).

Although melanin has a photoprotective function in human skin, the accumulation of an abnormal amount of melanin in different specific parts of the skin resulting in more pigmented patches can become an esthetic problem in humans (Ando *et al* 2007; Priestly 1993). Hyper-pigmentary disorders such as actinic and senile lentigines, melasma and post-inflammatory hyperpigmentation are major cosmetic problems and sufferers often pursue medical advice. These conditions affect the populations with darker skin complexion, particularly Hispanics and Asians with greater severity and frequency (Stratigos & Katsambas 2004).

1.2. Mushroom tyrosinase

The use of mushrooms with therapeutic properties is growing day by day due to the range of side effects caused by conventional medicines. Amongst naturally occurring alternatives to conventional medicine, mushrooms have been recognized as potent

candidates, as demonstrated in clinical studies, with the added advantage that because they are readily obtained in relatively large quantities and are inexpensive. Mushroom tyrosinase is popular among researchers as it is commercially available and inexpensive and also there are simple tools available to investigate features of this enzyme. Among mushrooms *Agaricus bisporus* is the most commonly consumed species worldwide, and it is also a good representative of its family; this is the reason, most research work is carried out on this particular species. Moreover, all of the tyrosinases obtained from various species of mushroom have similar properties, so the studies reported here are related to *A. bisporus*.

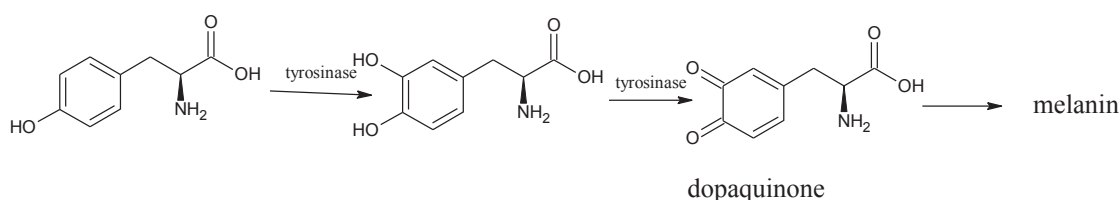


Figure 2 Reaction pathway involving tyrosinase

1.2.1. Biochemical characteristics of tyrosinase

In higher plants and fungi, tyrosinases exist in immature, mature latent and active isoforms (Sánchez-Ferrer, Villalba & García-Carmona 1989; Sánchez-Ferrer, Bru & García-Carmona 1990). The best-characterized tyrosinases are derived from *Streptomyces glaucescens*, the fungi *Neurospora crassa* and *Agaricus bisporus*. The enzyme extracted from the champignon mushroom *A. bisporus* is highly homologous with the mammalian ones, and this renders it well suited as a model for studies on melanogenesis (Khan 2007). In fact, almost all studies on tyrosinase inhibition conducted so far have used mushroom tyrosinase because the enzyme is commercially available. However, the application of mushroom tyrosinase inhibitors for human use has some limitations for human use because of key differences between the fungal and human tyrosinase. Mushroom tyrosinase is a cytosolic enzyme while the human tyrosinase is membrane bound (Nishioka 1978). Mushroom tyrosinase is a tetramer while the human form is a monomer that is highly glycosylated during

its complex maturation process. Many of these tyrosinases have been sequenced (**Table 1**), including ones from *N. crassa* and humans (Lerch 1982; Kwon *et al* 1987; Kupper *et al* 1989).

Table 1 Classification and properties of various tyrosinases

(Solomon *et al* 1996)

Source	Number of subunits	Molecular weight of subunit (kDa)
<i>Streptomyces glaucescens</i> (Eubacteria)	1	30.9
<i>Neurospora crassa</i> (Fungi)	1	46
<i>Agaricus bisporus</i> (Fungi)	2	13.4 43
<i>Beta vulgaris</i> (Plant)	1	40
Human melanocyte (Animal)	1	66.7

1.2.2. Domain structure

Tyrosinase from *A. bisporus* was reported to be a heterotetramer comprising two heavy (H) and light (L) chains with a molecular mass of 120 kDa (Strothkemp, Jolley & Mason 1976).

The enzyme tyrosinase has three domains, of which the central domain contains two Cu binding sites, called CuA and CuB. Six conserved histidine residues bind this pair of copper ions in the active site of the enzyme tyrosinase, both Cu atoms also interact with both molecular oxygen (**Figure 3**) and its phenolic substrate (Jackman, Hajnal & Lerch 1991). The binuclear copper-binding site is located at the bottom of a spacious cavity in the surface of the H subunit. The cavity is readily accessible from the solvent, and is not occluded by the L subunit or by loops of side chains of the H subunit (Robb & Gutteridge 1981; Wichers, Gerritsen & Chapelon 1996). Tyrosinase inhibitors such as tropolone binds in this cavity without the need for conformational changes of the protein. Tropolone interacts through van der Waals forces with the side chains of

Val283 and the copper ligand His263. In addition, there is edge-to-face aromatic interaction with Phe264. The space of the active site cavity is so large that it even accommodates phenolic steroids as substrate like 17 β -estradiol (Ismaya *et al* 2011).

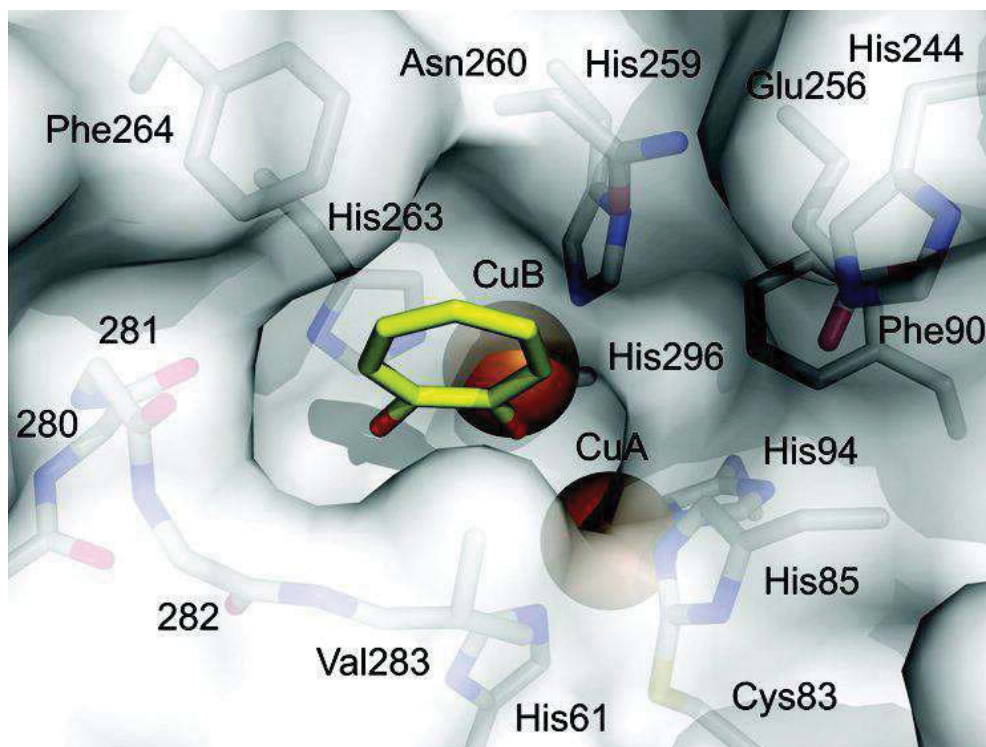


(Figure taken from Ismaya *et al* 2011).

Figure 3 Geometry of the active site of tyrosinase with tropolone in sticks

1.2.3. Reaction mechanism of tyrosinase

Copper is involved in many biological processes such as antioxidant defenses, pigmentation, mitochondrial respiration, neurotransmitter synthesis, connective tissue formation, peptide amidation, and iron metabolism (Camakarisa, Voskoboinika & Mercer 1999). The toxicity of Cu is partially associated with its potential to bind and activate dioxygen (O_2), leading to generation of reactive oxygen species (Stohs & Bogchi 1995). The versatility and reactivity of copper is largely owing to its flexibility in ligand binding via oxidation states +1 and +2 (Da Silva & Williams 2001). This property enables copper to play a key role in the active site of enzymes such as tyrosinase, hemocyanin, cytochrome c oxidase and laccase. The di-copper centre of tyrosinases resembles that of hemocyanins (HC) (Della Longa *et al* 1996; Sa'nchez-Ferrer *et al* 1995). Tyrosinase is a Type 3 copper protein. Type 3 copper proteins

possess two copper atoms located adjacent to each other, with both copper atoms being tetrahedral, and are coordinated to histidine residues. Type 2 copper proteins contain one copper atom that possess distorted tetragonal coordination. Type 1 copper proteins also have a single copper, that possesses distorted tetrahedral coordination. Tyrosinase, like all Type 3 copper proteins is composed of two Cu(II) ions bridged by O₂, when in its oxy form, thus the two Cu(II) ions are electronically coupled through the oxygen. The reactivity of copper is mainly because of its flexibility in binding with ligands and by the ease with which it passes through its two oxidation states, Cu(I) and Cu(II) (Cooksey *et al* 1998; Galindo *et al* 1983).

Removal of only one of the copper- binding histidine residues results in loss of the copper ions, thereby abolishing dioxygen binding and enzyme activity (Huber & Lerch 1988; Tsai & Lee 1998). The location of cysteine also plays an important role in the formation of disulfide linkages, which stabilize protein structure (Jackman, Hajnal & Lerch, 1991). In addition to this in *A. bisporus* tyrosinase, Cys83 forms a thioether bond with His85, locking the orientation of this histidine (Ismaya *et al* 2011). The number of cysteine residues varies with species; human and mouse tyrosinases have 17 cysteine residues and plants have 11, whereas the C-terminal domain contains 1 cysteine residue. Interestingly, *N. crassa*, *A. bisporus* and prokaryotic tyrosinases contain 0 or 1 cysteine in the mature protein. In the mushroom tyrosinase sequence, only two cysteine residues are found in the C-terminal domain (van Gelder, Flurkey & Wichers 1997). The enzyme extracted from the champignon mushroom *A. bisporus* is highly homologous with the mammalian ones, and this renders it well suited as a model for studies on melanogenesis. In fact, almost all studies on tyrosinase inhibition conducted so far have used mushroom tyrosinase because the enzyme is commercially available. The human tyrosinase gene family has three members: tyrosinase (TYR), tyrosinase related protein 1 (TRP1), and tyrosinase related protein 2 (DCT, TRP2). • They bind different divalent metal cations and have different catalytic properties. They act in a complex. DCT1 (trp2) binds zinc, tyrosinase binds copper, and it is unclear which cation is bound by TRP1. • Trp1 and tyrosinase share 40% AA identity. DCT and TYR share 32% identity; both were identified because they are recognized by tyrosinase antibodies.

In the formation of melanin pigments, three types of tyrosinase (oxy-, met-, and deoxytyrosinase, **Figure 4**) with different binuclear copper structures of the active site are involved. The oxygenated form (oxytyrosinase, E_{oxy}) consists of two tetragonal

copper(II) atoms, each coordinated by two strong equatorial and one weaker axial NHis ligands. In the oxy form, molecular oxygen binds in the form of peroxide in a $\mu\text{-}\eta^2\text{:}\eta^2$ side-on bridging ($\text{Cu(II)-O}_2^{2-}\text{-Cu(II)}$) mode, which destabilizes the O-O bond and activates it. Mettyrosinase (E_{met}), similar to the oxy form, contains two tetragonal copper(II) ions coupled through an endogenous bridge, although hydroxide exogenous ligands other than peroxide are bound to the copper site. Deoxytyrosinase (E_{deoxy}) contains two copper(I) ions with a co-ordination arrangement similar to that of the met form, but without the hydroxide bridge. The resting form of tyrosinase, i.e., the enzyme as obtained after purification, is found to be a mixture of 85% met and 15% oxy forms (Himmelwright, Eickman & Solomon 1979; Solomon 1981). The oxy form can catalyze both monophenolase and oxidase reactions, whereas the met form lacks monooxygenase activity (Solomon, Sundaram & Machonkin 1996).

In the monophenolase cycle, the monophenol can react only with the oxy form and undergoes oxidation to the *o*-quinone, resulting in a deoxy tyrosinase ready for further dioxygen binding. Oxytyrosinase is, then, regenerated after the binding of molecular oxygen to deoxytyrosinase. If only an *o*-diphenol is present as the substrate (the diphenolase cycle), both the oxy and met forms react with the *o*-diphenol, oxidizing it to the *o*-quinone. During this oxidation the *o*-diphenol binds to the oxy form yielding both the *o*-quinone and the met form of the enzyme.

The regeneration of oxy-tyrosinase through the reaction with oxygen results in a characteristic lag time that exists until a sufficient amount of diphenol, needed to reduce the met form to the deoxy form is produced by the small amount of the oxy form generally present in the resting enzyme preparations (Sa'nchez-Ferrer *et al* 1995; Lerch 1981; Wilcox *et al* 1985).

The length of the lag time depends on several factors: the enzyme source; the concentration of monophenol; the enzyme concentration and finally, the presence of catalytic amounts of *o*-diphenol or transition metal ions, which completely abolish the lag period (Burton 1994; Sanjust *et al* 2003). Met-tyrosinase, the resting form of tyrosinase, contains two tetragonal Cu(II) ions antiferromagnetically coupled through an endogenous bridge, although hydroxide exogenous ligands other than peroxide are bound to the copper site. The antiferromagnetic coupling between the Cu(II) ions of mettyrosinase triggers the lack of an electron paramagnetic resonance (EPR) signal, which requires a super exchange pathway associated with a bridging ligand (Ros,

Rodríguez-López & García-Cánovas 1993; Fenoll *et al* 2001). This species can be converted by addition of peroxide to oxytyrosinase, which in turn decays back to mettyrosinase when the peroxide is lost.

In addition to this monooxygenase (cresolase) activity (phenols to *o*-quinones), tyrosinase can also oxidize catechols to orthoquinones. This latter oxidase activity (catecholase activity) is accompanied by irreversible enzyme inactivation (**suicide inactivation**). This inactivation occurs when the catechol substrate is oxidized leading to the reduction of Cu(II) and elimination of Cu(0) from the enzyme. This inactivation is linearly correlated with the loss of 50% of the copper atoms from the active site.

It is proposed that this loss of copper may be the result of oxidative modification of histidine residues that coordinate the copper atoms at the enzyme active site. This mechanism postulates that *oxy*-tyrosinase sometimes binds catechol substrates in the oxygenase mode, i.e. as if they were phenols. This processing of catechols as phenols in the oxygenase cycle accounts for the observed suicide-inactivation mechanism (Land, Ramsden & Riley 2007; Land *et al* 2008; Ramsden, Stratford & Riley 2009). However, a slightly different mechanism has also been proposed.

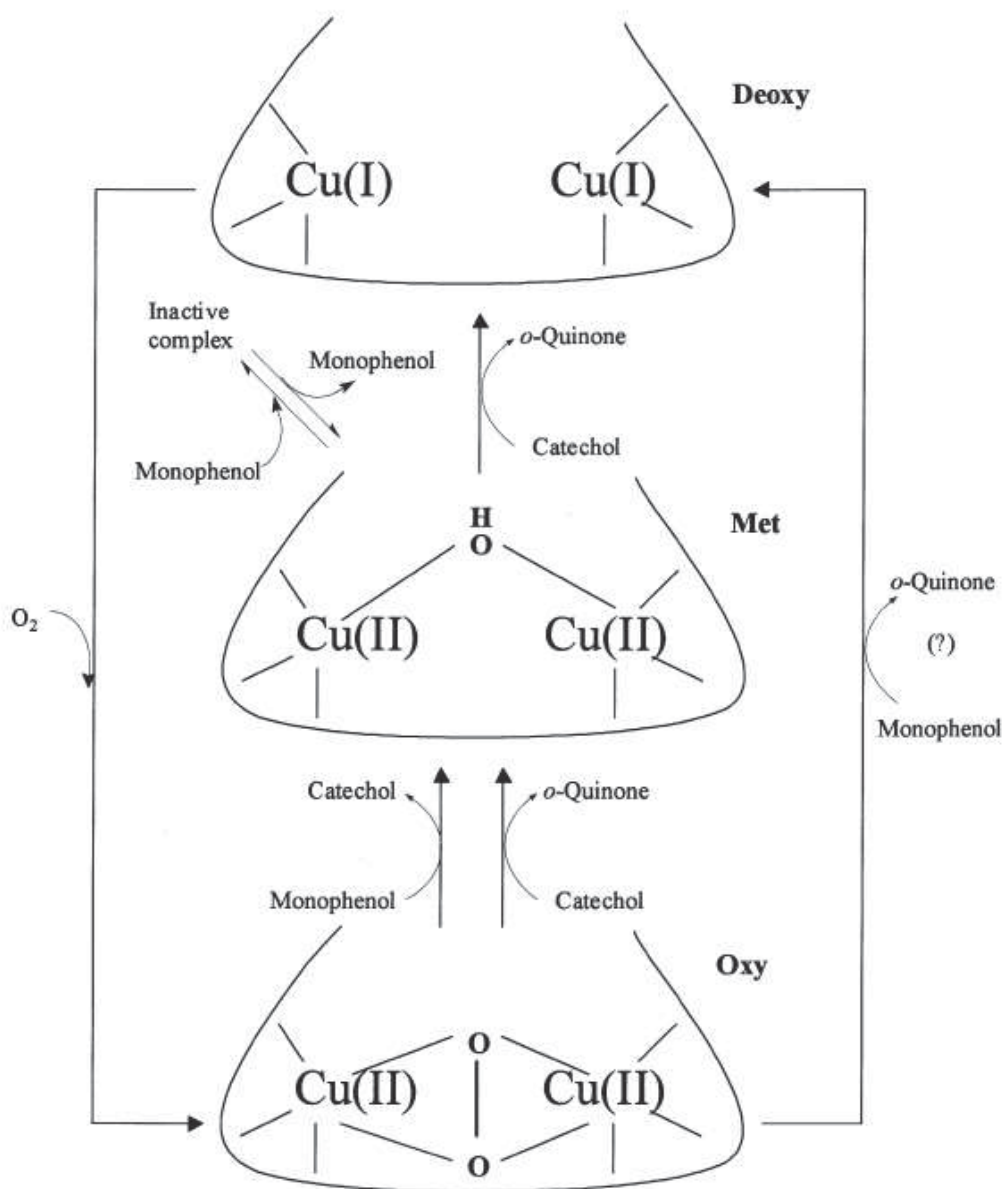


Figure 4 The three states of the active site of tyrosinase

(Reproduced from Rescigno *et al* 2002)

1.2.4. Tyrosinase substrates

As with many enzymes, tyrosinase's name is derived from its substrate, tyrosine. The principal endogenous substrates of mushroom tyrosinase are L-tyrosine, *p*-aminophenol, and its condensation product with glutamate-glutaminy-4-hydroxybenzene (GHB), all three being derived from the shikimate pathway (Stüssi & Rast 1981). Labeling studies demonstrated that the oxygen incorporated into the phenolic substrate derives from molecular O₂. The two electrons required to reduce the second oxygen atom to H₂O

were supplied by the substrate (Mason, Fowlks & Peterson 1955). Both types of tyrosinase activities (monophenolase and diphenolase) appear to have broad substrate specificities, however for chiral substrates the enzyme displays higher affinity for the L-isomers of the substrates than for the corresponding D-isomers. Tyrosinase substrates can be divided into three groups, depending upon the nature of the quinonoid intermediate:

- (i) *o*-quinone products contain a sidechain capable of intramolecular 1,4-addition to the quinone double bond.
- (ii) *o*-quinone products do not contain a sidechain and are uncyclizable but can undergo addition of water to the quinone double bond (Dawson & Tarpley 1951).
- (iii) *o*-quinone products are highly stable through the reaction and do not undergo nucleophilic attack (Ros-Martinez *et al* 1993).

Mono, di and trihydroxyphenols are tyrosinase substrates, however tyrosinase has greater affinity for dihydroxyphenols. Also, among the monohydroxyphenols (*p*-cresol and tyrosine), dihydroxyphenols (catechol, L-DOPA, D-DOPA, catechin and chlorogenic acid) and trihydroxyphenols (pyrogallol), catechol showed maximum activity, indicating that the enzyme is most active with catechol as a substrate (Zhang *et al* 1999). In principle, any simple monophenol and the corresponding catechol could behave as a PPO substrate, taking into due account that catechols are quinonised much faster than monophenols. As a general rule, bulky and/or crowded substituents too close to the phenolic hydroxyl prevent or at least render more difficult any enzyme/substrate interaction (Espin *et al* 1998).

Apart from this remarkable limitation, among homologous mono- and di-phenol series, a clear correlation between the electron-donating power of substituents and ease of enzymic action can be seen, and therefore phenols (and of course catechols), substituted with electron-withdrawing functional groups such as $-\text{NO}_2$, $-\text{COOH}$, $-\text{CHO}$ etc. tend to behave as competitive inhibitors rather than substrates for tyrosinase (Prota 1992). This is a convincing indication of an electrophilic character for the oxygenation mechanism of monophenols. Hydroquinone has been described as a tyrosinase inhibitor, but was shown later to act both as a substrate and an inhibitor (Prota 1992). In contrast to these observations, an increasing oxidation rate for catechols, with increasing electron-

withdrawing power of substituents in the para position, has been reported for some plant tyrosinases (Mayer & Harel 1979).

1.3. Potential uses of tyrosinase inhibitors

Treatment of hyperpigmentation disorders

As stated in Section 1.1, pigmentation in mammals results from the synthesis and distribution of melanin in the skin and hair bulbs. Melanins also play a crucial role in the absorption of free radicals generated within the cytoplasm and in shielding the host from various types of ionizing radiations, including UV light. Cumulative exposure to UV light can result in an increased risk of skin cancer and skin damage (e.g., premature aging and wrinkles), albinism and leukoderma. The main physiological stimulus of melanogenesis is solar UV radiation, which acts either directly or indirectly on melanocytes or indirectly inducing the release of keratinocyte-derived factors such as α -melanocyte stimulating hormone (α -MSH) ((Fistarol and Itin 2013; Chang 2009). Alterations in tyrosinase dysfunction can culminate in serious maladies including café au lait macules, ephelides (freckles), solar lentigo (age spots), and melasma (Spritz & Hearing 1994; Fu *et al* 2005; Maeda & Fukuda 1991; Mcevely, Iyengar & Otwell 1992). Melanin biosynthesis can be inhibited by avoiding UV exposure, the inhibition of tyrosinase, the inhibition of melanocyte metabolism and proliferation, or the removal of melanin with corneal ablation (Nerya *et al* 2003). Whitening agents reduce hyperpigmentation such as darkened age spots, whereas pigmenting agents are designed to increase pigmentation for increased sun protection. Standard topical treatments for hyperpigmentation disorders such as melasma and post-inflammatory hyperpigmentation include bleaching with hydroquinones, anti-inflammatory therapy using retinoids and use of tyrosinase inhibitors. The development and screening of potent inhibitors of tyrosinase is therefore of particular interest in both the health and cosmetic industries.

As the major rate limiting step in melanin biosynthesis are the reactions catalyzed by tyrosinase, inhibitors should be clinically useful for the treatment of some dermatological disorders and also important in cosmetics as whitening agents.

Anti-browning agents in fruits and vegetables

Tyrosinase is responsible for undesired enzymatic browning of fruits and vegetables that take place during senescence or damage in post-harvest handling, making tyrosinase inhibitors potentially useful in the food industry. Browning can be both enzymatic and non-enzymatic in origin. The enzymatic browning of plant-derived foods and beverages takes place in the presence of oxygen when tyrosinase and its substrates are released from damaged cells after brushing, peeling or crushing (Zheng *et al* 2008). Browning after harvest is a common phenomenon in crops such as apples, pears, potatoes and mushrooms which decreases the commercial value of the products. Quinones formed by the diphenolase activity of tyrosinase are strong electrophiles and can polymerize to form high molecular weight compounds that undergo nucleophilic attack by amino acids, proteins, polyphenols, or water to form Michael type addition products that enhance the production of the brown colour.

Non-enzymatic browning is an outcome of caramelization (pyrolysis of sugar) and the Maillard reaction and does not involve tyrosinase (McWeeny, Knowles & Hearne 1974). The conventional processes used to eliminate browning includes autoclaving and blanching, whereby the food products are immersed in a liquid at 80-90 C for 10-12 min or passed through a forced steam flow. However, these methods are subjective to crucial weight and nutritional losses (Carpenter 1981; Mauron 1990; Konanayakam & Sastry 1988). One of the other proposed alternative is the use of microwave energy but this is restricted due to the generation of temperature gradient that leads to uneven distribution of enzyme inactivation (Decareau 1985). Anti-browning food additives include sulfiting agents and formulations of ascorbic acid and citric acid. Sulfiting agents have been re-evaluated by the US Food and Drug Administration due to health concerns whereas ascorbic acid suffers from the drawback of being quickly consumed in the process of reducing quinones formed by tyrosinase (Son, Moon & Lee 2000; Seo, Sharma & Sharma 2003; Soliva-Fortuny & Martin-Belloso 2003). Recently, 4-hexyl resorcinol has been found to be quite effective for browning control in fresh and dried fruit slices (McEvily, Iyengar & Otwell 1991). Despite reports of a large number of tyrosinase inhibitors, only a few are used today because of their limitations with regard to cytotoxicity, selectivity, and stability (Loizzo *et al* 2007).

Other applications

It has been reported that neuronal melanin and neuronal tyrosinase in the *substantia nigra* in mice and human brains may play significant roles in dopamine neurotoxicity and neurodegeneration related to Parkinson's disease (Xu *et al* 1997). Excess dopamine is oxidized by tyrosinase to produce dopamine quinones, inducing neural damage and cell death, and in turn causing Parkinson's and other neurodegenerative diseases.

Tyrosinase inhibitors have been used as herbicides to control weeds. Tyrosinase also plays an important role in the developmental and defensive functions of insects (Ashida & Brey 1995). In insects, tyrosinase is uniquely associated with three different physiologically important biochemical processes, including sclerotization of the insect cuticle, defensive encapsulation and melanization of foreign organisms, and wound healing (Pawelek & Korner 1982; Mayer 1987; Whitaker 1995; Friedman 1996; Barrett 1984; Sugumaran 1988). The development of tyrosinase inhibitors has thus become an active alternative approach in controlling insect pests.

Studies on tyrosinase inhibitors have gained immense significance mainly due to its wide range of applications in cosmetics as a depigmentation agent and in agriculture for controlling the quality and economics of fruits and vegetables. Inhibition of the enzyme tyrosinase has been a major goal for researchers, and has resulted in several inhibitors that are currently used as cosmetic additives and medicinal products for the treatment of hyperpigmentation. Although hydroquinone has been the mainstay treatment for hyperpigmentation, its clinical potential has been complicated by a number of adverse reactions including contact dermatitis, irritation, transient erythema, burning, prickling sensation, leukoderma, chestnut spots on the nails, hypochromia and ochronosis (Ennes, Paschoalick & Alchorne 2000; Engasser 1984; Fisher 1983; Romaguera & Grimalt 1985; Curto *et al* 1999). Moreover, hydroquinone is potentially mutagenic to mammalian cells. Hydroquinone and its derivative arbutin are both catabolized to quinonoid metabolites potentially possessing bone marrow toxicity (Zhou *et al* 2009). Another alternative, kojic acid is currently applied as a cosmetic skin whitener and food additive to prevent enzymatic browning (Kahn 1995). However, its use in cosmetics has been limited, because of its instability during storage. In addition, kojic acid has been shown to promote thyroid and liver carcinogenicity in rodent models, leading to its ban in Switzerland (Fujimoto *et al* 1999). On these grounds, further investigation of potential polyphenol oxidase inhibitors could be applied during food processing, to

melanin hyperpigmentation treatment, and in cosmetics for skin whitening and depigmentation.

1.4. Mechanisms of tyrosinase inhibition

It has been proved that presently known inhibitors possess different mechanisms for expressing their tyrosinase inhibitory activity. Some of these mechanisms are:

- a) Reducing agents causing chemical reduction of dopaquinone such as ascorbic acid, which is used as a melanogenesis inhibitor because of its capacity to reduce back *o*-dopaquinone to DOPA, thus preventing dopachrome and melanin formations.
- b) *o*-dopaquinone scavenger such as most thiols are well-known melanogenesis inhibitors, reacting with dopaquinone and preventing the formation of melanins. The melanogenetic process is therefore slowed until all the scavenger is consumed, and then it goes at its original rate.
- c) Alternative enzyme substrates such as some phenolic compounds, whose quinoid reaction products absorb in a spectral range different from that of melanins. When these phenolics show a good affinity for the enzyme, dopachrome formation is prevented. These compounds can be mistakenly classified as inhibitors of tyrosinase.
- d) Nonspecific enzyme inactivators such as acids or bases, which nonspecifically denature the enzyme, thus inhibiting its activity.
- e) Specific tyrosinase inactivators such as mechanism-based inhibitors or suicide substrates. These inhibitors can act as tyrosinase substrates and form covalent bond with the enzyme, thus irreversibly inactivating the enzyme.
- f) Specific tyrosinase inhibitors which bind reversibly to tyrosinase and reduce its catalytic capacity.

Working on the latter 2 types of inhibitors, researchers so far have been able to design and discover a huge library of small molecule bioactive ligands as tyrosinase inhibitors (Sheng Chang 2009).

1.5. Rational drug design of tyrosinase inhibitors

In an effort to discover small molecule drug candidates with attractive activities, the pharmaceutical industry has predominantly sought compounds that modulate target proteins through noncovalent interactions. Therefore, high throughput screening

strategies and screening collections have been tailored to identify leads that display good binding profile (Michele 2009). With the advent of structural genomics projects, the structures of many proteins are now available, sometimes well before their activities are known. Even more structures are now available through comparative modeling of close homologues (Pieper *et al* 2006; Specker *et al* 2005; Schapira, Abagyan & Totrov 2003; Rao & Olson 1999; Jorgensen 2004; Li *et al* 2004; Schnecke & Kuhn 2000; Fernandes, Kairys & Gilson 2004). For these proteins, it is a pleasant conceit to imagine that one might predict activities on the basis of structure. One way to exploit protein structures in searching for active compounds is the use of molecular docking (**Figure 5**). Docking techniques are useful since they allow a better understanding of the molecular events that occur at the binding interface of ligand-protein interaction site (See appendix).

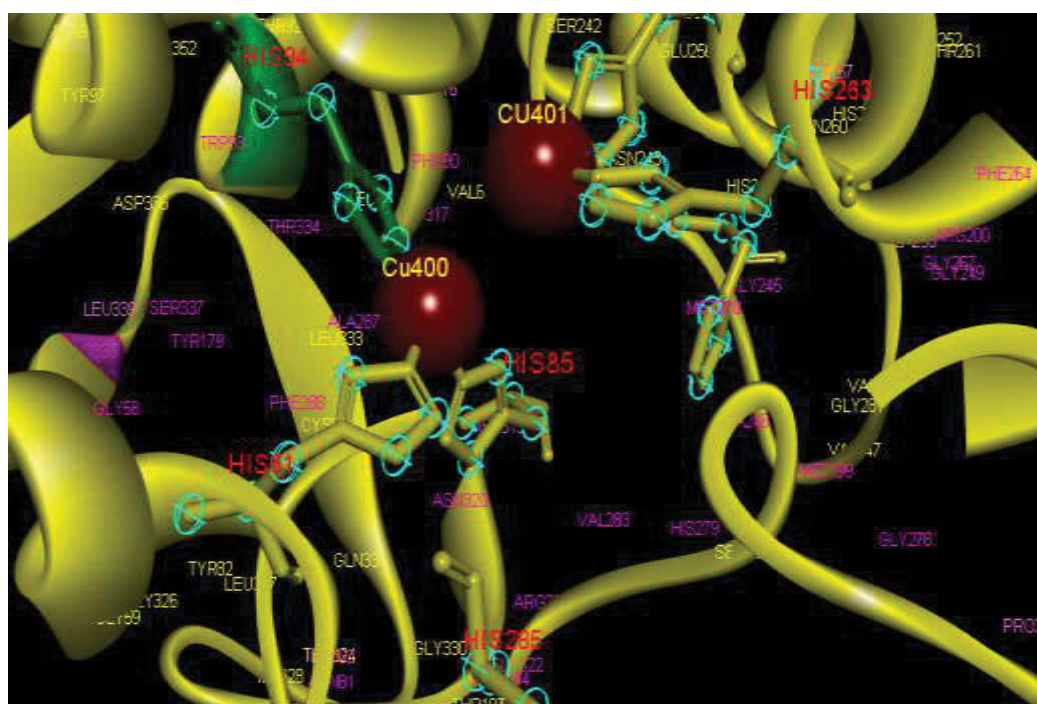


Figure 5 Active site of mushroom tyrosinase

1.6. Classification of known tyrosinase inhibitors

1.6.1. Simple monocyclic inhibitors

The monocyclic inhibitors shown in **Figure 6** have a structural similarity to endogenous phenolic substrates, and all display slow binding competitive inhibition kinetics. Kojic

acid, the most intensively studied inhibitor of tyrosinase, is a fungal metabolite produced by many species of *Aspergillus* and *Penicillium*, and is currently used as a cosmetic skin-whitening agent and as a food additive for preventing enzymatic browning (Chen, Wei & Marshall 1991). Kojic acid shows a competitive inhibitory effect on the monophenolase activity and a mixed inhibitory effect on the diphenolase activity of mushroom tyrosinase. The ability of kojic acid to chelate copper at the active site of the enzyme has been postulated to explain the observed competitive inhibitory effect. In addition, kojic acid is reported to be a slow-binding inhibitor of the diphenolase activity of tyrosinase (Cabanes, Chazarra & García-Carmona 1994). Kojic acid along with hydroquinone is used in a gel formulation to treat melasma, a patchy discoloration that appears in the face of mostly pregnant woman taking hormone replacement therapy or using contraceptive patches (Chen *et al* 1991; Robb 1984). However, its use in cosmetics has been limited, because of its instability during storage. In addition, kojic acid has been shown to promote thyroid and liver carcinogenicity in rodent models, leading to its ban in Switzerland (Fujimoto *et al* 1999). Kojic acid, along with tropolone and arbutin are often used as the positive control in tyrosinase inhibitor research for comparing the inhibitory strength of the newly synthesized inhibitors (Briganti 2003; Chang 2009; Khan 2007; Parvez 2007). It has been proposed that kojic acid inhibits the activity of tyrosinase by forming a chelate with the copper ion in the tyrosinase through the 5-hydroxyl and/or 4-carbonyl groups. A series of kojic acid derivatives have been synthesized to try and improve the properties by modification of the C-7 hydroxyl group forming an ester, hydroxyphenyl ether, glycoside and amide derivatives by numerous researchers (Kobayashi *et al* 1995; Kadokawa *et al.* 2003; Nishimura *et al* 1994; Kobayashi *et al* 1996). Kojic acid thioether derivatives containing lipophilic alkyl chains (pentyl, hexyl, and cyclohexyl) showed potent inhibitory activity. However, sulfoxides and sulfones exhibited decreased activity (Rho *et al* 2010). A potential issue that may hinder the commercialization of kojic acid is that it causes allergies and has been shown to cause hepatic tumors in heterozygous mice deficient in p53 (Nakagawa & Kawai, 1995; Takizawa *et al* 2003).

Other slow-binding inhibitors of tyrosinase are the very potent inhibitor tropolone and the substrate analog, L-mimosine (Cabanes *et al* 1987). Tropolone (2-hydroxy-2,4,6-cycloheptatriene) is one of the most potent tyrosinase inhibitors (Espín & Wichers 1999). It is structurally analogous to *o*-diphenolic substrates of tyrosinase, as well as an

effective copper chelator, however it does not act as an irreversible inhibitor as do *o*-catechols. Tropolone displayed slow-binding inhibition on tyrosinase but could only bind the oxy form (Kahn & Andrawis 1985; Sculley, Morrison & Cleland 1996). Historically, hydroquinone has been widely used as a skin bleaching cream despite its potential hepatotoxicity and skin irritant properties. In Australia and some other Countries, its use is controlled due to these concerns. It does not bleach skin in the sense that it does destroy melanin, rather it inhibits pigmentation in newly-formed skin cells. To speed up its effects, it is often combined with α -hydroxy acids, which act as exfoliants, removing pigmented cells from the surface of the skin, thus enhancing skin penetration. Although hydroquinone has been the mainstay treatment for hyperpigmentation, its clinical potential has been complicated by a number of adverse reactions including contact dermatitis, irritation, transient erythema, burning, prickling sensation, leukoderma, chestnut spots on the nails, hypochromia and ochronosis (Ennes, Paschoalick & Alchorne 2000; Engasser 1984; Fisher 1983; Romaguera & Grimalt 1985; Curto *et al* 1999). Moreover, hydroquinone is potentially mutagenic to mammalian cells. Hydroquinone and its derivative arbutin are both catabolized to quinonoid metabolites with the potential for bone marrow toxicity (Zhou *et al* 2009). Deoxyarbutin has been identified as an excellent tyrosinase inhibitor which is attributed to its chemical structure. Deoxysugars display a significant increase in both skin penetration ability and binding affinity for tyrosinase. Moreover, deoxyarbutin completely lacks skin irritation and its skin lightening effect is reversible, suggesting the absence of permanent destruction of melanocytes (Boissy, Visscher & Delong 2005).

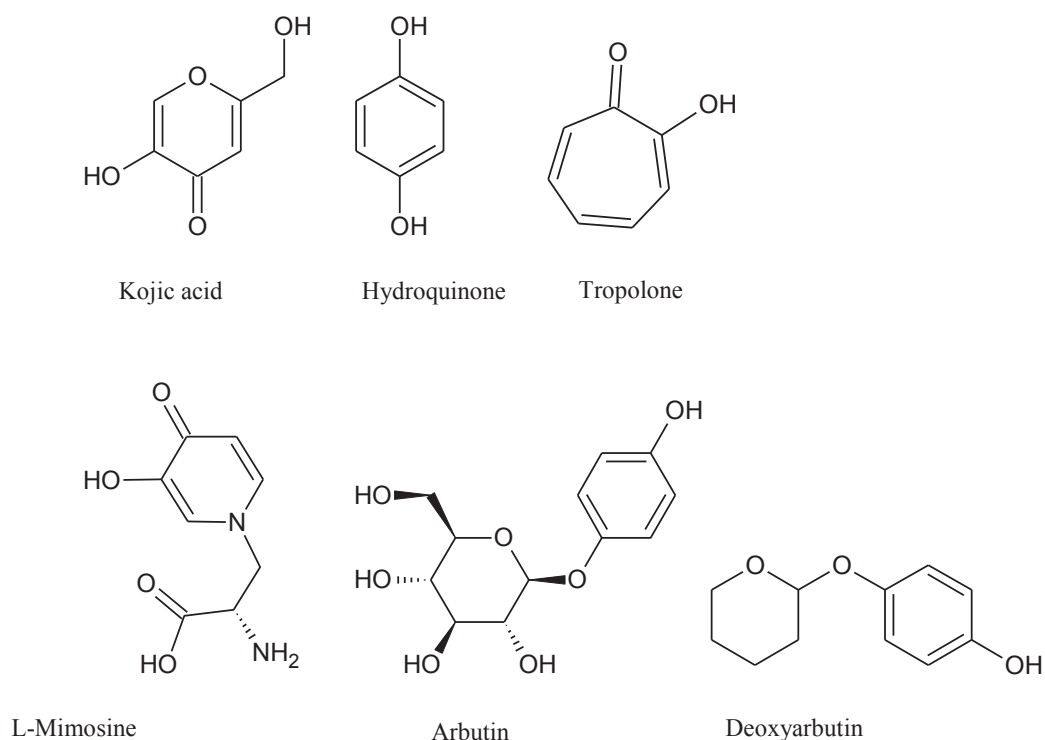


Figure 6 Monocyclic tyrosinase inhibitors

1.6.2. Polyphenols

Plant polyphenols are useful secondary metabolites with abundant biological activities in our system. Flavonoids (**Figure 7**) are among the most numerous and most studied polyphenols. Flavonoids are a group of naturally occurring antioxidants, and are proposed to act as metal chelators of the copper at the tyrosinase active site forming the copper-flavonoid complexes (van Acker *et al* 1996; Jacob, Hagai & Soliman 2011). Some flavonoids, such as kaempferol, quercetin and morin, show the inhibitory activity of tyrosinase, while others, e.g. catechin and rhamnetin, act as cofactors or substrates of tyrosinase (No *et al* 1999; Gómez-Cordovés *et al* 2001; Kermasha, Bao & Bisakowski 2001). At a concentration of 50 $\mu\text{g mL}^{-1}$, it was reported that quercetin had the best inhibitory effect with a decreased activity of 68%; meanwhile the flavonoids, myricetin and myricetin 3-*O*-rhamnoside displayed a decrease of only 21% (Matsuda *et al* 1995). In addition, the flavonol glycosides of quercetin or kaempferol were found to be less active than their corresponding aglycones (Nugroho *et al* 2009).

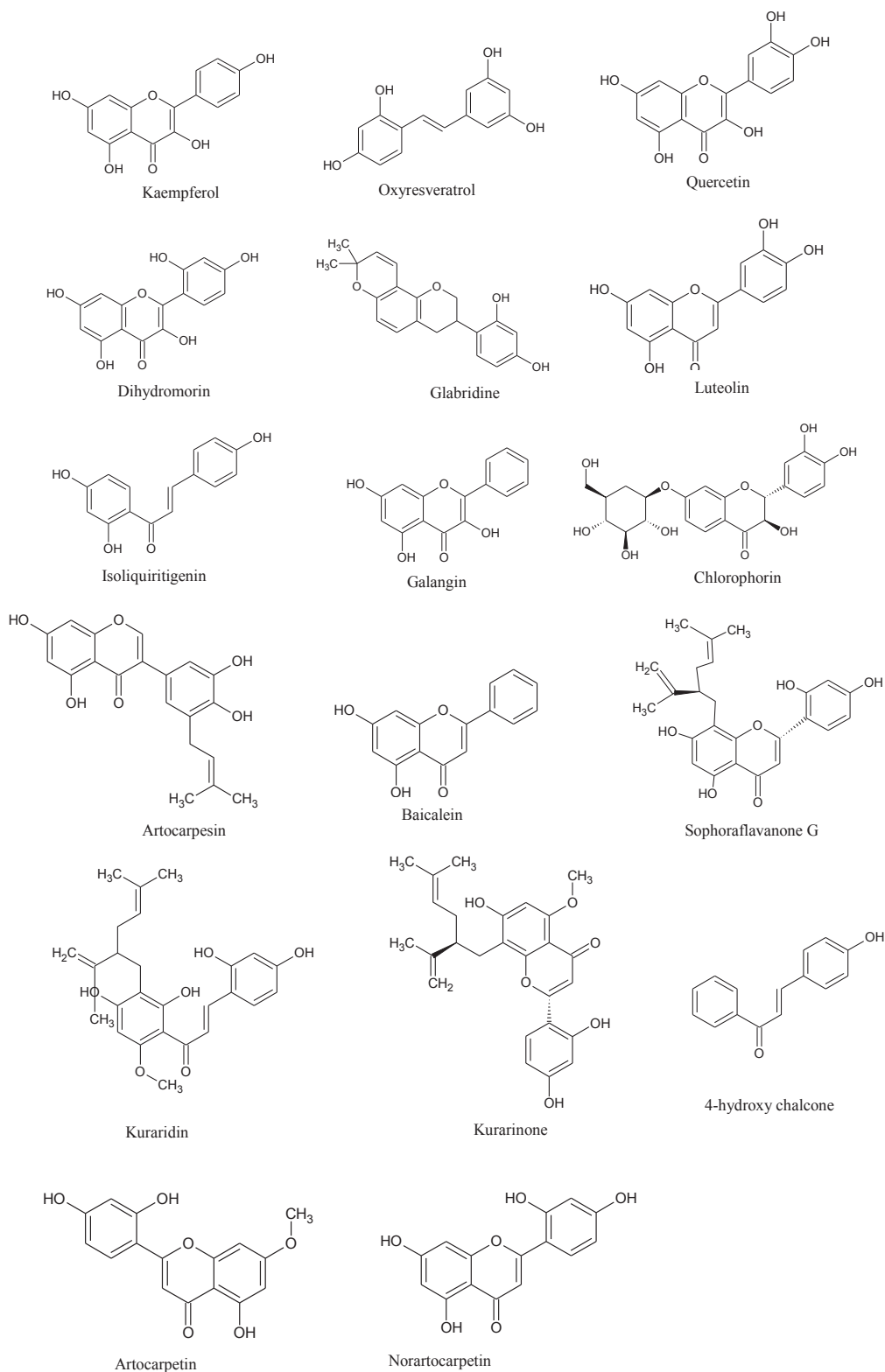


Figure 7 Polyphenols as tyrosinase inhibitors

Recently, 6-hydroxykaempferol was synthesized and confirmed to possess two times more activity than kaempferol (Gao *et al* 2007). The most active flavonol, quercetin, showed only 20% of the inhibitory activity compared to kojic acid with regard to the diphenolase activity on mushroom tyrosinase. It has been proposed that all flavanoids inhibit the enzyme due to their ability to chelate copper in the active site (Kubo & Kinst-Hori 1999; Kubo *et al* 2000). However, complexation with copper is only possible if the 3-hydroxy group is not functionalized. This work further elucidated that the 3-hydroxy group is not an essential requirement for inhibition as other types of flavonoids such as luteolin 4'-O-glucoside and luteolin 7-O-glucoside, lacking this 3-hydroxy group, still showed inhibitory activity (Kubo, Yokokawa & Kinst-Hori 1995). Some flavonols possessing a 3-hydroxy-4-keto moiety, analogous to that present in tropolone, such as kaempferol and quercetin, competitively inhibit tyrosinase, probably due to their ability to chelate the copper in the active site, leading to irreversible inactivation of tyrosinase (Kubo *et al* 1994). Another flavanol, taxifolin (5,7,3',4'-tetrahydroxyflavanol, isolated from the sprout of *Polygonum hydropiper*, showed equal inhibitory activity of kojic acid toward monophenolase activity of mushroom tyrosinase (Miyazawa & Tamura 2007).

Flavonoids containing a carbonyl group in the 4-position have been reported to possess potent tyrosinase inhibitory activity (Badria & El-Gayyar 2001). This may be explained in terms of the similarity between the dihydroxyphenyl group in L-DOPA and the keto group in flavonoids. Flavonoids containing a 4-carbonyl group also show potent tyrosinase inhibitory activity. Licorice root extracts containing glabridin, glabrene and isoliquiritigenin showed dose dependent high inhibitory activity. Glabridin is a very potent inhibitor due to presence of isoflavan moiety (Nerya *et al* 2003). Kinetics studies showed that glabridin and glabrene inhibited the tyrosinase displaying non-competitive and uncompetitive inhibition, respectively.

Another important inhibitor is gallic acid, which occurs as multiple esters with D-glucose, and their esters are widely used as additives in food industries. Gallic acid and other gallates have been shown to inhibit the oxidation of L-DOPA by tyrosinase, however, gallic acid itself acts as a substrate (Kim and Uyama 2005).

Azelaic acid (1,7-heptanedicarboxylic acid), a natural occurring, straight-chain, saturated dicarboxylic acid was found to inhibit the formation of melanin through

lipoperoxidation in melanocyte cells. However, a major side effect of azelaic acid, also a weak competitive tyrosinase inhibitor, was its melanocytotoxicity.

The flavonoids, isoartocarpesin, dihydromorin, chlorophorin, artocarpesin and artocarbene isolated from *Artocarpus incisus* (Moraceae) extract displayed tyrosinase inhibitory activity with comparative strength to that of kojic acid. These extracts suppressed pigment biosynthesis of both cultured B16-F10 melanoma cells with no sign of cytotoxicity or skin irritation on brown guinea pig backs (Shimizu *et al* 1998). Extracts from *Sophora flavescens* afforded three prenylated flavonoids, sophoraflavanone G, kuraridin and kurarinone which inhibited tyrosinase activities more than kojic acid with their IC₅₀ values of 6.6 μ M, 0.6 μ M, and 6.2 μ M, respectively (Kim *et al* 2003).

Isoflavenes, glabrene and isoliquiritigenin (2',4',4'-trihydroxychalcone) isolated from licorice roots effectively inhibited both mono- and di-phenolase tyrosinase activity (Vaya, Belinky & Aviram 1997). Transdihydromorin, oxyresveratrol and steppogenin, isolated from the twigs of *Cudrania tricuspidata* showcased IC₅₀ values of 21.54 μ M, 2.85 μ M and 2.52 μ M, respectively. Structure–activity relationship (SAR) suggested that the hydroxyl group substitutions at 2 and 4 positions of aromatic ring from phenolic compounds might play a vital role in inhibiting tyrosinase activity (Zheng *et al* 2013). A novel biflavonoid, 2,3-dihydro-4',4'-di-*O*-methyl- amentoflavone, isolated from *Podocarpus macrophyllus* var. *macrophyllus* showed a potent antityrosinase effect with an IC₅₀ value of 0.098 μ M in human epidermal melanocytes (Cheng *et al* 2007).

1.6.3. Stilbenes

Stilbenes consists of an ethene double bond substituted with a phenyl ring on both carbon atoms of the double bond (**Figure 8**). So far, only one dioxygenated stilbene, *i.e.*, pinosylvin has been studied for its tyrosinase inhibitory potential (Shimizu, Kondo & Sakai 2000). Amongst trioxxygenated stilbenes, resveratrol (3,5,4'-Trihydroxy-*trans*-stilbene) possesses free phenolic groups at positions 4', 3 and 5. It has shown stronger L-DOPA oxidase inhibitory activity than kojic acid. Dihydroresveratrol was shown to be less active than the parent compound (Ohguchi *et al* 2003).

Oxyresveratrol (2,4,3',5'-tetrahydroxy- *trans*-stilbene) was found to act as a non-competitive inhibitor of both the monophenolase and the diphenolase activity of mushroom tyrosinase. Notably, it contains resorcinol moieties in both A and B rings.

Amongst the tetra-oxygenated stilbenes, oxyresveratrol (2, 4, 3', 5'-Tetrahydroxy-*trans*-stilbene) with an IC₅₀ value of 1.5 µM displayed a nine-fold stronger inhibitory effect on mushroom tyrosinase than resveratrol (IC₅₀: 14.4 µM), due to the additional hydroxy group at position 2 of resveratrol (Likhitwitayawuid, Sritularak & De-Eknamkul 2000; Likhitwitayawuid, Sritularak & De-Eknamkul 2002). Oxyresveratrol has been suggested to be a promising anti-browning agent for food products (Li *et al* 2007). It also had the ability to suppress dermal melanogenesis in animals (Tengamnuay, Pengrungruangwong & Likhitwitayawuid 2003). Other hydroxy stilbene derivatives, chloroporphin ((4-geranyl-3,5,2',4'-tetrahydroxy-*trans*-stilbene) and gnetol (2,6,3',5'-tetrahydroxy-*trans*-stilbene) are also diphenolase inhibitors of mushroom tyrosinase. Gnetol, a naturally occurring compound isolated from the roots of *Gnetum gnemon*, exhibited 30-fold more diphenolase inhibitory activity for murine tyrosinase than that shown by kojic acid (Ohguchi *et al* 2003).

Recently, hydroxy-2-phenylnaphthalenes, which are isosteric with resveratrol and oxyresveratrol respectively, were synthesized and found to be potent tyrosinase inhibitors (Song *et al* 2007). A naphthalene analogue of resveratrol, 5-HNB [5-(6-hydroxy-2-naphthyl)-1,2,3-benzenetriol] inhibits mushroom tyrosinase in a noncompetitive manner, suggesting that it is an allosteric inhibitor, binding to tyrosinase somewhere other than the active site (Ha *et al* 2007). Recently, piceatannol (3,4,3',5'-Tetrahydroxy-*trans*stilbene), isolated from grapes and red wine, has been found to exhibit 32.7 times stronger inhibition of monophenolase activity than kojic acid towards mushroom tyrosinase (Yokozawa & Kim 2007). The inhibitory mechanism of piceatannol which contains *o*-3',4'-dihydroxy groups may be exerted by both direct tyrosinase inhibition or by quinone product scavenging, and is not the same with that of oxyresveratrol. In contrast to dihydroresveratrol, reduction of the stilbene double bond of piceatannol leads to increased diphenolase inhibition. This was attributed to the increased flexibility proposed to enhance the interactions of the resorcinol ring with the active site of the enzyme. It has been found that the phenolic hydroxy groups and *trans*-olefin structure of the parent stilbene skeleton contribute to the inhibitory potency of hydroxystilbene for tyrosinase inhibitory activity (Ohguchi *et al* 2003).

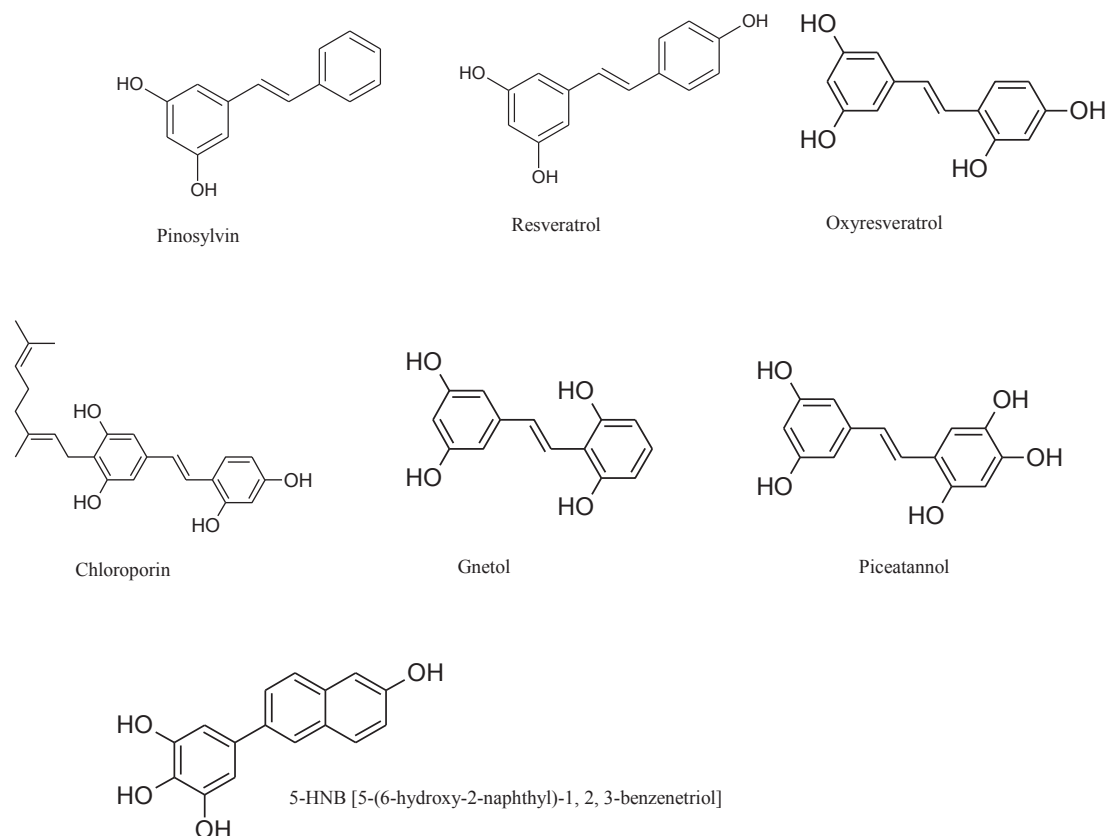


Figure 8 Stilbenes as tyrosinase inhibitors

1.6.4. Phenolic compounds as tyrosinase inhibitors

Phenolic compounds (**Figure 9**) like anacardic acids, 2-methylcardols, and cardols were isolated from various parts of cashew (*Anacardium occidentale*, Anacardiaceae) fruit, which have been found to exhibit tyrosinase inhibitory activities (Kubo, Kinst-Hori & Yokokawa 1994). Arbutin was isolated from the fresh fruit of California buckeye, *Aesculus californica* (Spach) Nutt. Hippocastanaceae and has been widely used as a whitening agent in cosmetic ingredients (Maeda & Fukuda 1996). Arbutin has been reported to show a dose-dependent competitive inhibition of the oxidation of L-dopa catalyzed by mushroom tyrosinase with an IC_{50} of 10 μ M (Funayama *et al* 1995). It was also shown to have differences in the inhibitory effects between the mushroom and human tyrosinase, specifically the inhibition of mushroom tyrosinase was half as the inhibition on the human tyrosinase. Another compound, 4,4'-dihydroxybiphenyl exhibited strong tyrosinase inhibitory activity with an IC_{50} of 1.91 μ M (Kim & Uyama 2005).

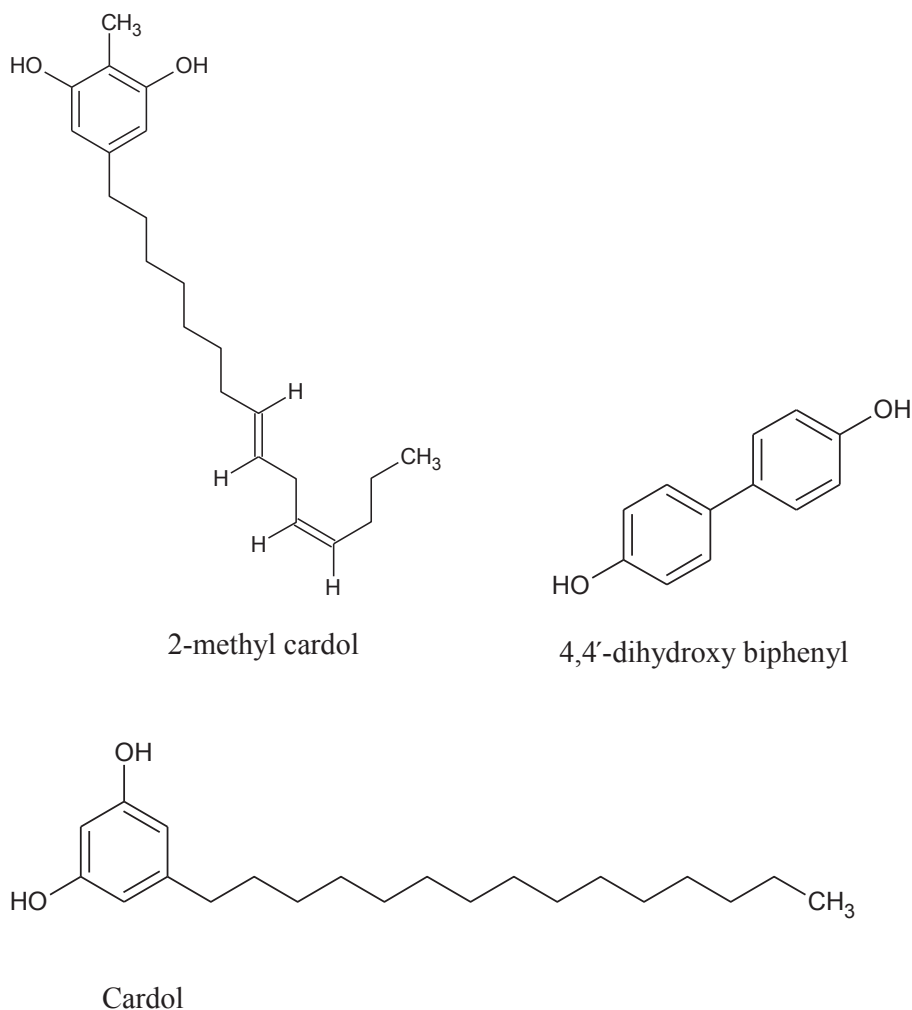


Figure 9 Phenolic compounds as tyrosinase inhibitors

1.6.5. Coumarins as tyrosinase inhibitors

Coumarins are lactones of phenylpropanoid acid with an *H*-benzopyranone nucleus. Among the coumarin-type tyrosinase inhibitors, aloesin is a natural hydroxy coumarin glucoside isolated from *Aloe vera*. Aloesin (**Figure 10**) showed significant inhibition against murine tyrosinase and has been recently used in topically applied cosmetics due to its natural source and multifunctional activity in skin care (Jones *et al* 2002; Choi *et al* 2002). A coumarin analog, esculetin, isolated from the seeds of *Euphorbia lathyris* showed one-quarter of the antityrosinase activity of kojic acid (Masamoto *et al* 2003). However, the compound was seen to be a substrate for mushroom tyrosinase (Sollai *et al* 2008).

Another coumarin analog, 9-hydroxy-4-methoxypsoralen was isolated from *Angelica dahurica* and exhibited six times more tyrosinase inhibitory activity than that of kojic

acid (Piao *et al* 2004). Recently, a new coumarin derivative, 8'-epi-cleomiscosin A was isolated from the aerial parts of *Rhododendron collettianum* and showed 12.8-fold diphenolase inhibitory activity of kojic acid toward mushroom tyrosinase (Ahmad *et al* 2004).

1.6.6. Benzaldehyde and benzoate derivatives as tyrosinase inhibitors

A large number of aldehydes and other derivatives were also isolated and characterized as tyrosinase inhibitors such as *trans*-cinnamaldehyde (Lee *et al* 2000), (2E)-alkenals, 2-hydroxy-4-methoxybenzaldehyde (Kubo &Kinst-Hori 1999), anisaldehyde, cuminaldehyde and cumic acid (Kubo &Kinst-Hori 1988), 3,4-dihydroxycinnamic acid, anisic acid, p-coumaric acid, hydroxycinnamoyl derivatives and 4-hydroxy-3-methoxycinnamic acid (Lee 2002). As the aldehyde group is known to react with biologically important nucleophilic groups such as sulfhydryl, amino and hydroxy groups, it has been proposed that its inhibitory effect is due to the formation of a Schiff base with the primary amino group of the enzyme.

It is interesting to note that the Schiff base hypothesis has been contradicted by the recent finding that these 4-substituted benzaldehyde derivatives behave as competitive inhibitors of L-DOPA oxidation (Jimenez *et al* 2001). In the case of benzoic acid derivatives, the mechanism of inhibition may involve the formation of a copper–carboxylic acid complex at the binuclear copper site of the enzyme (Conrad *et al* 1994); further substitution of a phenolic group at the para position increased the extent of inhibition (Wilcox *et al* 1985).

Hydroxy- and methoxysubstituted benzaldehyde thiosemicarbazones, HBT and MBT (**Figure 10**) have been synthesized and shown to inhibit B16 mouse melanoma mushroom tyrosinase and free-cell tyrosinase (Chen *et al* 2012). HBT and MBT reduced monophenolase activity (IC_{50} : 0.76 and 7.0 μ M, respectively) and both compounds also inhibited diphenolase activity dose dependently (IC_{50} : 3.80 μ M and 2.62 μ M, respectively). Their inhibitory mechanisms were shown to be both reversible and mixed-type inhibitors. A modified Curtius rearrangement and diazotization followed by a coupling reaction with various phenolic compounds was applied to form

azo-resveratrol. Azo-resveratrol and azooxyresveratrol analogs were shown to inhibit tyrosinase at 50 μM demonstrating 56.25% and 72.75% inhibition, respectively. In a further study, azo-resveratrol presented an IC_{50} value of 36.28 μM , thus it was less potent than resveratrol which has an IC_{50} of 26.63 μM (Song *et al* 2012).

1.6.7. Other inhibitors

Captopril, a known copper chelator, and angiotensin converting enzyme inhibitor (**Figure 10**), used to treat hypertension, shows irreversible non-competitive inhibition of the monophenolase activity of mushroom tyrosinase while exhibiting irreversible competitive inhibition for the diphenolase activity of tyrosinase (Espin & Wichers 2001; Schweikardt *et al* 2007). Recently, *p*-hydroxybenzyl alcohol was shown to irreversibly inhibit mushroom tyrosinase (Liu *et al* 2007). The suppression of melanin synthesis by the compound was attributed to its behavior in directly inhibiting cellular tyrosinase activity without effecting the expression level of tyrosinase mRNA. Methimazole (1-methyl-2-mercaptoimidazole) also displays mixed inhibition against both the mono and diphenolase activities of mushroom tyrosinase. Methimazole is believed to inhibit tyrosinase in two ways: first by conjugation with the *o*-quinone tyrosinase metabolite of L-DOPA and second, by chelation with copper at the active site of the enzyme (Andrawis and Kahn 1986). Cetylpyridinium chloride can bind to the tyrosinase molecule and induce enzyme conformational changes, which leads to a slow irreversible inactivation of the enzyme (Chen, Huang & Kubo 2003).

Competitive tyrosinase inhibition was observed in a biphenyl analog of a natural product fortuneanoside E (Bao *et al* 2010). Extraction of the methanolic phase of *Dictyophora indusiata* yielded 5-(hydroxymethyl)-2-furfural, that demonstrated inhibition in a dose-dependent manner of the oxidation of L-dopa in mushroom tyrosinase assay, and the value of ID_{50} was measured as 0.98 μM (Sharma *et al* 2004). Phenylthiourea (PTU) is a well-known inhibitor of diphenolase activity of type-3 copper proteins. The sulfur atom of the compound is believed to bind to both copper ions in the active site of the enzyme and to thus block enzyme activity (Gerdemann, Eicken & Krebs 2002). When the amino group and the sulfur moieties of *N*-phenylthiourea are replaced by *N*-hydroxylamine and oxygen, respectively, the resulting compound exhibits six times more activity than that of the parent compound (Criton & Le Mellay-Hamon 2008).

N-Substituted-*N*-nitrosohydroxylamines inhibited mushroom tyrosinase, supposedly by interacting with the copper ions at the active site of the enzyme (Shiino, Watanabe & Umezawa 2001). As removal of nitroso or hydroxyl moiety completely diminished the inhibitory activity, both functional groups were suggested to be essential for chelating activity. Among other derivatives, the authors found that *N*-hydroxybenzyl-*N*-nitrosohydroxylamines showed the best inhibitory activity, which is comparable to that of kojic acid (Shiino, Watanabe & Umezawa 2003). *N*-Substituted-*N*-nitrosohydroxylamines inhibited mushroom tyrosinase in a pH-dependent manner due to the non-ionized, electrically neutral form of the compounds (Shiino, Watanabe & Umezawa 2008).

Recently, an anthraquinone, physcion (1, 8-dihydroxy-2-methoxy-3-methylantraquinone), was found to show similar tyrosinase inhibitory activity with that of kojic acid (Leu *et al* 2008). Interestingly, another anthraquinone, 1, 5- dihydroxy-7-methoxy-3-methylantraquinone, with hydroxyl and methoxyl groups at different positions compared with those of physcion exhibited a 72-fold increase on antityrosinase activity (Devkota *et al* 2007). (+)-Lyoniresinol, a lignin from the roots of *Vitex negundo* (**Figure 10**) was found to be 5.2-fold more active than that of kojic acid (Azhar-Ul-Haq Malik *et al* 2006). The phloroglucinol, dieckol, isolated from a marine brown alga, *Ecklonia stolonifera*, displayed three times more inhibitory activity than that of kojic acid.

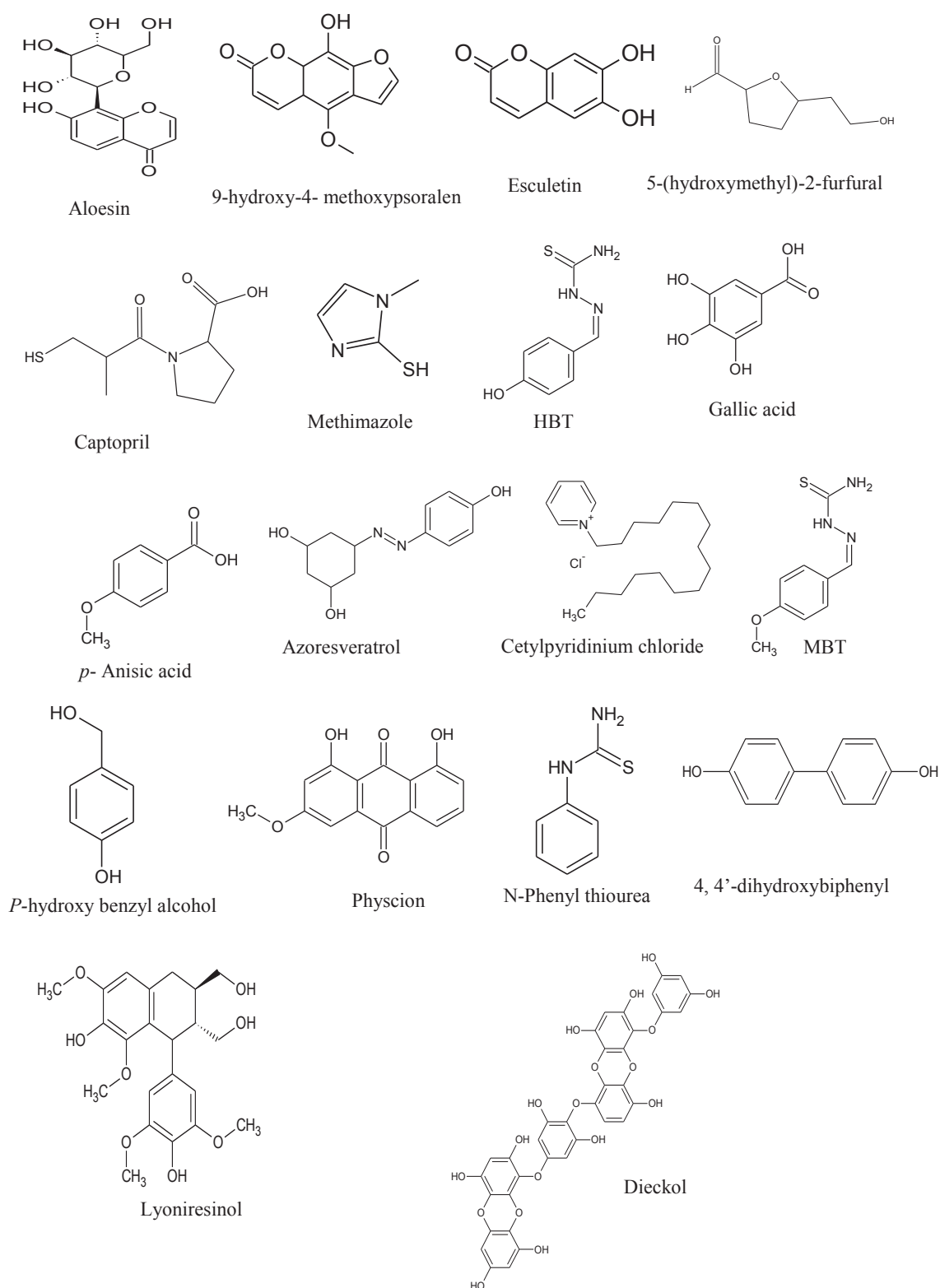


Figure 10 Miscellaneous tyrosinase inhibitors

1.6.8. Chalcones as tyrosinase inhibitors

Chalcones (1,3-diaryl-2-propen-1-ones) are flavonoids containing two aromatic rings in *trans* configuration, separated by three carbons α , β - unsaturated carbonyl group. The presence of a conjugated double bond in chalcones and a completely delocalized π electron system reduces their redox potentials and makes them prone to electron transfer reactions. The free radical scavenging potential of chalcones itself is attributed to the presence of the enone functionality (Mukherjee *et al* 2001). Their occurrence in nature, their simple structure and their diversity has led to interest in these molecules for their therapeutic potential. The compounds can be broadly classified based on substitution pattern of the parent chalcone as: hydroxylated chalcones, methoxylated chalcones, aminochalcones, N-containing chalcones (i.e. azachalcones) etc. (Boumendjel, Ronot & Boutonnat 2009).

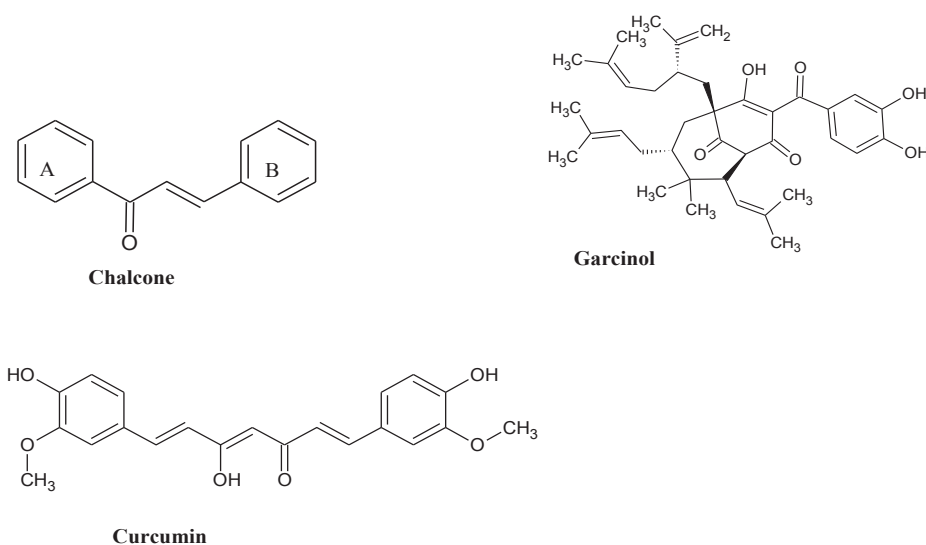


Figure 11 Structures of chalcone, garcinol and curcumin

Chalcones are readily synthesized by the base catalyzed Claisen-Schmidt condensation of an aldehyde and an appropriate ketone in a polar solvent such as methanol. The method is versatile and convenient, though yields can be variable.

One of the most important factors determining tyrosinase inhibition efficiency is the number and position of hydroxyl groups on the aromatic rings (Khatib *et al* 2005). This can be attributed to the fact that phenolic hydroxyl groups can act both as hydrogen-bond donors and acceptors in biological systems. Electron donating groups (*e.g.* -OMe,

-OH) on the π -system activate the aromatic ring by increasing the electron density on the ring through a resonance donating effect. Hydroxyl groups in compounds can also oxygen bound between the two copper atoms of tyrosinase and can also be directly involved by transferring protons during catalysis, which can result in inactivation of tyrosinase (Muñoz-Muñoz *et al* 2008).

Chalcones are abundant in plants and are precursors in the biosynthesis of flavonoids and isoflavonoids (**Figure 11**). The most common chalcone derivatives found in foods, such as citrus fruit and apples, are phloretin and 2',4,4',6'-tetrahydroxychalcone. Chalcones possessing a resorcinol ring and a catechol moiety on the other have high tyrosinase inhibition. For example, butein with a catechol subunit on ring A and resorcinol on ring B displays good monophenolase activity, but weaker diphenolase activity. Three chalcones derivatives, including licuraside, isoliquiritin, and licochalcone A have been isolated from the roots of the *Glycyrrhiza* species and shown to competitively inhibit the monophenolase activity of mushroom tyrosinase (**Figure 12**). Licochalcone A has been shown to be 5.4-fold more active than kojic acid (Fu *et al* 2005). Another prenylated chalcone, kuraridin, was isolated from the plant *Sophora flavescens* and identified as a potent tyrosinase inhibitor, with 34 times the activity of kojic acid against the monophenolase activity of mushroom tyrosinase (Kim *et al* 2003). Interestingly, its hydroxylated analog, kuraridinol, was found to be 18.4-fold more active compared to kojic acid (Hyun *et al* 2008).

Recently, 2,4,2',4'-tetrahydroxy-3-(3-methyl-2-butenyl)-chalcone (TMBC), which was isolated from the stems of *Morus nigra*, was shown to be 26-fold more potent than kojic acid in diphenolase inhibitory activity of mushroom tyrosinase. The kinetic study showed that the compound is competitive to the L-DOPA binding site of the enzyme with a K_i value of 1 to 1.5 μ M. Moreover, the melanin content of melanoma cells was reduced by TMBC (Zhang *et al* 2009).

Studies had shown the 4-hydroxyl group in the B ring of the chalcone skeleton to be a major factor affecting monophenolase inhibitory potency, because it results in a molecular skeleton closely similar to that of L-tyrosine (Nerya *et al* 2004). In addition, 2,4,2',4'-tetrahydroxychalcone was reported to possess more potent monophenolase inhibitory activity compared to both 3,4,2',4'-tetrahydroxychalcone and 2,4,3',4'-

tetrahydroxychalcone (Khatib *et al* 2005). It was concluded that 4-resorcinol moiety in the chalcone skeleton played a key role in exhibiting inhibitory potency. It was interesting to note that previously identified potent tyrosinase inhibitors with a flavone, flavanone, or flavonol skeleton such as artocarpetin, norartocarpetin, and streppogenin all contain a 4-resorcinol as the B ring. Thus, the 4-resorcinol moiety played an important role in the inhibition of tyrosinase activity not only in chalcones but also in other flavonoid structures.

Hydroxychalcones such as isoliquiritigenin, butein and 4-hydroxychalcone decreased tyrosinase activity and reduced the lag period of enzyme monophenolase function. However, 4'-hydroxychalcone showed no inhibitory properties. Butein exhibits competitive inhibition while isoliquiritigenin and 4-hydroxychalcone exhibit semi-competitive inhibition (Nerya *et al* 2004).

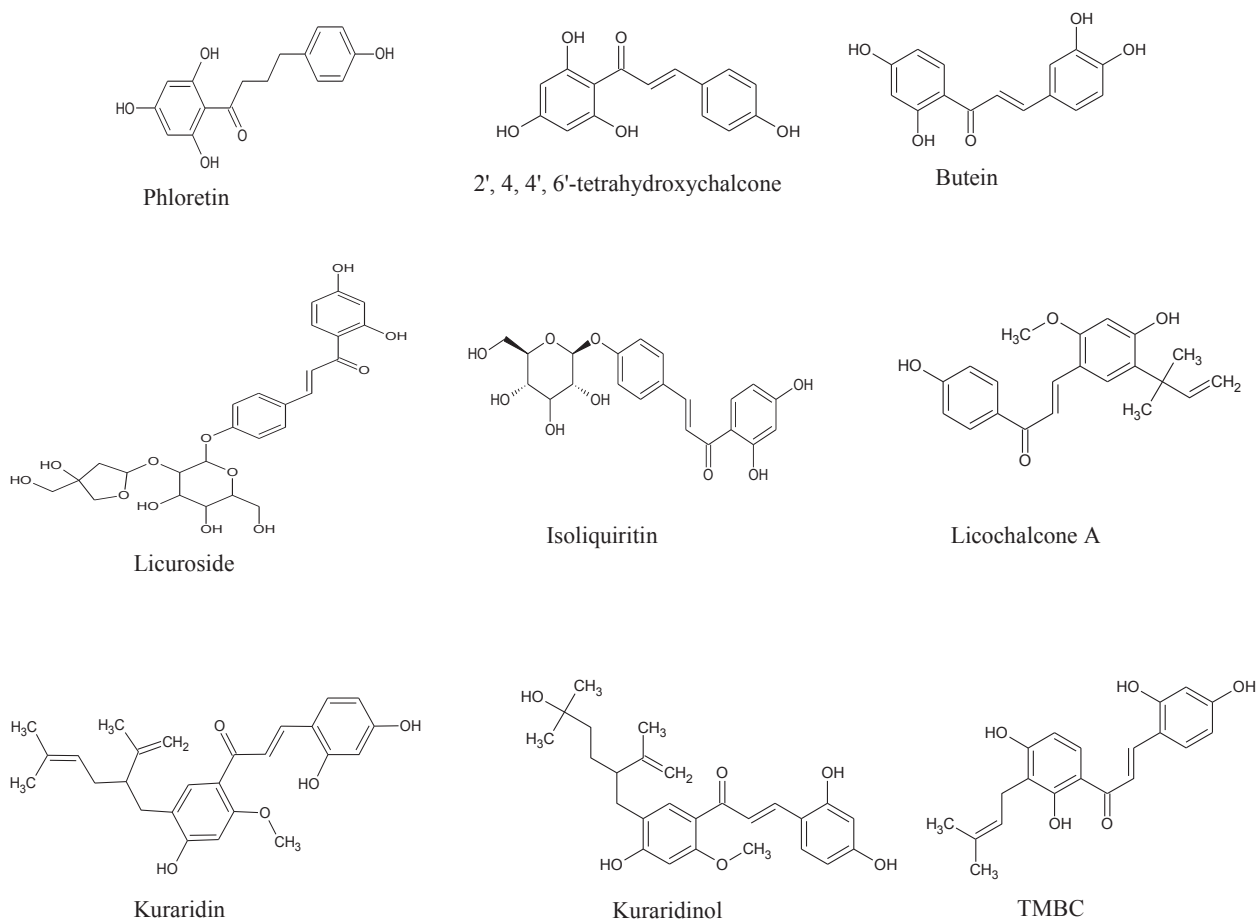


Figure 12 Chalcones as tyrosinase inhibitors

Chapters **2&3** discussed the design, synthesis and kinetics of hydroxy substituted azachalcone compounds as tyrosinase inhibitors. This implicated the significance of phenolic hydroxyl groups that acted both as hydrogen-bond donors and acceptors. *In silico* studies further showed the hydroxyl group of the ligand to block the tyrosinase activity by binding with the copper atoms in the active site of the enzyme. SAR studies identified hydroxyl as the functional group indispensable for tyrosinase inhibitory activity. Another structural advantage was attributed to the naphthyl ring that could exert a nucleophilic action on the dihydroxy phenyl ring.

Chapter **4** attempted the design and synthesis of a whole new class of allyl alcohol derivatives of azachalcones by employing a facile method of Luche reduction. This was found to lessen the steric hindrance by providing increased flexibility. Eliminating the carbonyl group progressively increased tyrosinase inhibitory activity thereby demonstrating the negative effect of carbonyl group in the chalcone skeleton.

Although few methoxychalcone derivatives were reported before, not much research was done to explore their anti-melanogenesis effects. Chapter **5** investigated the effect of methoxyazachalcones and methoxynaphthylchalcones on melanin formation in murine B16F10 melanoma cell lines. The number and position of methoxy substituents on the aromatic rings appeared to be critical for cytotoxicity. Also placement of strongly electron-withdrawing groups such as NO₂ in ring B correlated with increase of cytotoxic activity. This study provided valuable information in utilizing methoxychalcone as a lead compound for the further design and development of potential tyrosinase inhibitors with antimelanogenic effects.

Chapters **6 & 10** focused on the significance of an oxime moiety on the chalcone framework that brought about better coordination with the copper metal centers at the active site of mushroom tyrosinase and also exhibited stronger hydrogen bonding interactions with the amino acid residues. From all the compounds synthesized, a novel 2'-acetylpyridinyl chalconeoxime compound exhibited the most potent tyrosinase inhibitory activity with an IC₅₀ value that was found to be several times potent than the reference standard, kojic acid. The inhibition mechanism was competitive and was in complete agreement with the docking results.

Chapter **7** discussed an interesting feature of the facile synthesis of chalconeoximes by a solid-state solvent free method, thus generating an environmentally benign protocol.

Chapter 8 attempted the design and synthesis of aminochalcones and their structure-activity relationships. Cell based experiments on aminochalcone compounds showed very effective inhibitions of both melanin production and tyrosinase activity, suggesting amino chalcones to be a promising candidate for use as depigmentation agents in the field of cosmetics or as anti-browning food additives in the field of agriculture.

Chapter 9 attempted to explore the effects of novel 2,3-dihydro-1*H*-inden-1-one chalcone-like compounds for tyrosinase inhibition. Hydroxy substituted 1-indanone chalcone-like compounds were found to be significantly more potent than kojic acid.

1.7. References

Ahmad, VU, Ullah, F, Hussain, J, Farooq, U, Zubair, M, Khan, MT, Choudhary, MI 2004, 'Tyrosinase inhibitors from *Rhododendron collettianum* and their structure-activity relationship (SAR) studies', *Chemical and Pharmaceutical Bulletin*, Vol 52, pp. 1458–1461.

Ahmad, A, Wang, Z, Ali, R, Maitah, MY, Kong, D, Banerjee, S, Padhye, S, Sarkar, FH 2010, 'Apoptosis-inducing effect of garcinol is mediated by NF-kappaB signaling in breast cancer cells', *Journal of Cellular Biochemistry*, Vol 109, pp. 1134–1141.

Alam, N, Yoon, KN, Lee, JS, Lee, MW, Lee, TS 2011, 'Pleurotus nebrodensis ameliorates, atherogenic lipid and histological function in hypercholesteremic rats', *International Journal of Pharmacology*, Vol7, pp. 455–462.

Ando, H, Kondoh, H, Ichihashi, M, Hearing, VJ 2007, 'Approaches to identify inhibitors of melanin biosynthesis via the quality control of tyrosinase', *Journal of Investigative Dermatology*, Vol 127, pp. 751–61.

Andrawis, A, Kahn, V 1996, 'Effect of methimazole on the activity of mushroom tyrosinase', *Biochemical Journal*, Vol 235, pp. 91–96.

Aroca, P Garica-Borron, JC, Solano, F, Lozano, JA 1990, 'Regulation of mammalian melanogenesis I: partial purification and characterization of a dopachrome converting factor: dopachrome tautomerase', *Biochemistry and Biophysics Acta*, Vol 1035, pp. 266–275.

Ashida, M, Brey, P 1995, 'Role of integument in insect defense: prophenoloxidase cascade in the cuticular matrix', *Proceedings of the National Academy of Sciences USA*, Vol 92, pp. 10698–10702.

Awasthi, SK, Mishra, N, Kumar, B, Sharma, M, Bhattacharya, A, Mishra, LC, Bhasin, VK 2009, 'Potent antimalarial activity of newly synthesized substituted chalcone analogs in vitro', *Medicinal Chemistry Research*, Vol 18, pp. 407–420.

Azhar-Ul-Haq Malik, A, Khan, MT, Anwar-Ul-Haq Khan, SB, Ahmad, A, Choudhary, MI 2006, 'Tyrosinase inhibitory lignans from the methanol extract of the roots of *Vitex negundo* Linn and their structure-activity relationship', *Phytomedicine*, Vol 13, pp. 255–260.

Badria, F, El-Gayyar, M 2001, 'A new type of tyrosinase inhibitors from natural products as potential treatments for hyperpigmentation', *Bollettino Chimico Farmaceutico*, Vol 140, pp. 267–271.

Bao, K, Dai, Y, Zhu, BZ, Tu, FJ, Zhang, GW, Yao, SX 2010, 'Design and synthesis of biphenyl derivatives as mushroom tyrosinase inhibitors', *Bioorganic and Medicinal Chemistry*, Vol 18, pp. 6708–6714.

Barrett, FM 1984, 'Wound-healing phenoloxidase in larval cuticle of *Calpododes ethulius* (Lepidoptera: Hesperidae)', *Canadian Journal of Zoology*, Vol 62, pp. 834–838.

Bell, AA, Wheeler, MH 1986, 'Biosynthesis and functions of fungal melanins', *Annual Review of Phytopathology*, Vol 24, pp. 411–451.

Boissy, RE, Visscher, M, Delong, MA 2005, 'Deoxy arbutin: a novel reversible tyrosinase inhibitor with effective in vivo skin lightening potency', *Experimental Dermatology*, Vol 8, pp. 601–608.

Boumendjel, A, Ronot, X, Boutonnat, J 2009, 'Chalcone derivatives acting as cell cycle blockers: potential anti-cancer drugs?', *Current Drug Targets*, Vol 10, pp. 363–371.

Briganti, S, Camera, E, Picardo, M 2003, 'Chemical and instrumental approaches to treat hyperpigmentation', *Pigment Cell Research*, Vol 16, pp. 101–110.

Brun, A, Rosset, R 1974, 'Étude électrochimique de l'oxydation de la dihydroxy-3, 4 phénylalanine (Dopa): Mécanisme d'oxydation des catéchols en milieu acide', *Journal of Electroanalytical Chemistry and Interfacial Electrochemistry*, Vol 10, pp. 287–300.

Burton, SG 1994, 'Biocatalysis with polyphenol oxidase: a review', *Catalysis Today*, Vol 22, pp. 459–487.

Cabanes, J, García-Cánovas, F, Tudela, J, Lozano, JA, García-Carmona, F 1987, 'L-mimosine a slow-binding inhibitor of mushroom tyrosinase', *Phytochemistry*, Vol 26, pp. 917–919.

Cabanes, J, Chazarra, S, García-Carmona, F 1994, 'Kojic acid, a cosmetic skin whitening agent, is a slow-binding inhibitor of catecholase activity of tyrosinase', *Journal of Pharmacy and Pharmacology*, Vol 46, pp. 982–985.

Camakarisa, J, Voskoboinika, I, Mercer, JF 1999, 'Molecular mechanisms of copper homeostasis', *Biochemical and Biophysical Research Communications*, Vol 261, pp. 225–232.

Carpenter, KJ 1981, 'Individual amino acid levels and bioavailability. In: Protein Quality in Humans: Assessment and In Vitro Estimation', Bodwell CE, Adkins JS. and Hopkins DT. (eds), AVI, Westport, CT, pp. 239–160.

Chang, TS 2007, 'Two potent suicide substrates of mushroom tyrosinase', *Journal of Agricultural and Food Chemistry*, Vol 55, pp. 2010–2015.

Chang, TS 2009, 'An updated review of tyrosinase inhibitors', *International Journal of Molecular Sciences*, Vol 10, pp. 2440–2475.

Chen, JS, Wei, C, Marshall, MR 1991, 'Inhibition mechanism of kojic acid on polyphenol oxidase', *Journal of Agricultural and Food Chemistry*, Vol 39, pp. 1897–1901.

Chen, JS, Wei, CI, Rolle, RS, Otwell, WS, Balaban, MO, Marshall, MR 1991, 'Inhibitory effect of kojic acid on some plant and crustacean polyphenol oxidases', *Journal of Agricultural and Food Chemistry*, Vol 39, pp. 1396–1401.

Chen, QX, Huang, H, Kubo, I 2003, 'Inactivation kinetics of mushroom tyrosinase by cetylpyridinium chloride', *Journal of Protein Chemistry*, Vol 22, pp. 481–487.

Chen, LH, Hu, YH, Song, W, Song, KK, Liu, X, Jia, YL, Zhuang, JX, Chen, QX 2012, 'Synthesis and antityrosinase mechanism of benzaldehyde thiosemicarbazones: Novel tyrosinase inhibitors', *Journal of Agricultural and Food chemistry*, Vol 60, pp. 1542–1547.

Cheng, KT, Hsu, FL, Chen, SH, Hsieh, PK, Huang, HS, Lee, CK, Lee, MH 2007, 'New constituent from *Podocarpus macrophyllus* var. *macrophyllus* shows anti-tyrosinase effect and regulates tyrosinase-related proteins and mRNA in human epidermal melanocytes', *Chemical and Pharmaceutical Bulletin*, Vol 55, pp. 757–761.

Choi, S, Lee, SK, Kim, JE, Chung, MH, Park, YI 2002, 'Aloesin inhibits hyperpigmentation induced by UV radiation', *Clinical and Experimental Dermatology*, Vol 27, pp. 513–515.

Conrad, JS, Dawson, SR, Hubbard, ER, Meyers, TE, Strothkamp, KG 1994, 'Inhibitor binding to the binuclear active site of tyrosinase: Temperature, pH, and solvent deuterium isotope effects', *Biochemistry*, Vol 33, pp. 5739–5744.

Cooksey, CJ, Garratt, PJ, Land, EJ, Pavel, S, Ramsden, CA, Riley, PA, Smit, NPM 1997, 'Evidence of the indirect formation of the catecholic intermediate substrate responsible for the auto activation kinetics of tyrosinase', *The Journal of Biological Chemistry*, Vol 272, pp. 26226–26235.

Cooksey, CJ, Garratt, PJ, Land, EJ, Ramsden, CA, Riley, PA 1998, 'Tyrosinase kinetics: failure of the auto-activation mechanism of monohydric phenol oxidation by rapid formation of a quinomethane intermediate', *Biochemical Journal*, Vol 333, pp. 685–691.

Costin, GE, Hearing, VJ 2007, 'Human skin pigmentation: melanocytes modulate skin color in response to stress', *The FASEB Journal*, Vol 21, pp. 976–994.

Criton, M, Le Mellay-Hamon, V 2008, 'Analogues of *N*-hydroxy-*N'*-phenylthiourea and *N*-hydroxy-*N'*-phenyl urea as inhibitors of tyrosinase and melanin formation', *Bioorganic and Medicinal Chemistry Letters*, Vol 18, pp. 3607–3610.

Curto, EV, Kwong, C, Hermersdorfer, H, Glatt, H, Santis, C, Virador, V, Hearing, VJ, Dooley, TP 1999, 'Inhibitors of mammalian melanocyte tyrosinase; in vitro comparisons of alkyl esters of gentisic acid with other putative inhibitors', *Biochemical Pharmacology*, Vol 57, pp. 663–672.

Da Silva, JJRF, Williams, RJP 2001, 'Copper: extracytoplasmic oxidases and matrix formation. In: The Biological Chemistry of the Elements', *The Inorganic Chemistry of Life*, 2nd Ed.; Oxford University Press: New York, Chapter 15, pp. 418435.

Dawson, CR, Tarpley, WB 1951, 'The copper oxidases', In: *The Enzymes*, Sumner JB, Myrback K (eds). Academic Press: New York, pp. 454–459.

Decareau, RV 1985, 'Microwaves in the Food Processing Industry', Academic Press, London.

Della Longa, S, Ascone, I, Bianconi, A, Bonfigli, A, Congiu Castellano, A, Zarivi, O, Miranda, M 1996, 'The Dinuclear Copper Site Structure of *Agaricus bisporus* Tyrosinase in Solution Probed by X-ray Absorption Spectroscopy', *The Journal of Biological Chemistry*, Vol 271, pp. 21025–21030.

Devkota, KP, Khan, MT, Ranjit, R, Lannang, AM, Samreen Choudhary, MI 2007, 'Tyrosinase inhibitory and antileishmanial constituents from the rhizomes of *Paris polyphylla*', *Natural Product Research*, Vol 21, pp. 321–327.

Ennes, SBP, Paschoalick, R, Alchorne, MMDA 2000, 'A double-blind comparative, placebo-controlled study of the efficacy and tolerability of 4% hydroquinone as a depigmenting agent in melasma', *Journal of Dermatological Treatment*, Vol 11, pp. 173–179.

Engasser, PG 1984, 'Ochronosis caused by bleaching creams', *Journal of the American Academy of Dermatology*, Vol 10, pp. 1072–1073.

Espín, JC, García-Ruiz, PA, Tudela, J, García-Cánovas, F 1998, 'Study of stereo specificity in mushroom tyrosinase', *Biochemical Journal*, Vol 331, pp. 547–551.

Espín, JC, Wichers, HJ 1999, 'Slow-binding inhibition of mushroom (*Agaricus bisporus*) tyrosinase isoforms by tropolone', *Journal of Agricultural and Food Chemistry*, Vol 47, pp. 2638–2644.

Espin, JC, Wichers, HJ 2001, 'Effect of captopril on mushroom tyrosinase activity *in Vitro*', *Biochimica et Biophysica Acta*, Vol 1554, pp. 289–300.

Fenoll, LG, Rodríguez-López, JN, García-Sevilla, F, García-Ruiz, PA, Varón, R, García-Cánovas, F, Tudela, J 2001, 'Analysis and interpretation of the action mechanism of mushroom tyrosinase on monophenols and diphenols generating highly unstable *o*-quinones', *Biochimica et Biophysica Acta*, Vol 1548, pp. 1–22.

Fernandes, MX, Kairys, V, Gilson, MK 2004, 'Comparing ligand interactions with multiple receptors via serial docking', *Journal of Chemical Information and Computer Sciences*, Vol 44, pp. 1961–1970.

Fisher, AA 1983, 'Current contact news. Hydroquinone uses and abnormal reactions, Current contact news', *Cutis*, Vol 31, pp. 240–244, 250.

Fistarol, SK, Itin, PH 2013, 'Disorders of pigmentation', *Journal der Deutschen Dermatologischen Gesellschaft*, Vol 8, pp. 187–201.

Francisco, A Toma's-Barbera'n, AF, Mari'a, I, Gil, IM, Castan~ er, M, Arte's, F, Saltveit, EM 1997, 'Effect of Selected Browning Inhibitors on Phenolic Metabolism in Stem Tissue of Harvested Lettuce', *Journal of Agricultural and Food Chemistry*, Vol 45, pp. 583–589.

Frenk, E, 1995, 'Treatment of melasma with depigmenting agents. In: Melasma: New Approaches to Treatment', Martin Dunitz, London, pp. 9–15.

Friedman, M 1996, 'Food browning and its prevention: an overview', *Journal of Agricultural and Food Chemistry*, Vol 44, pp. 631–653.

Fu, B, Li, H, Wang, X, Lee, FS, Cui, S 2005, 'Isolation and identification of flavonoids in licorice and a study of their inhibitory effects on tyrosinase', *Journal of Agricultural and Food Chemistry*, Vol 53, pp. 7408–7414.

Fujimoto, N, Onodera, H, Mitsumori, K, Tamura, T, Maruyama, S, Ito, A 1999, 'Changes in thyroid function during development of thyroid hyperplasia induced by kojic acid in F344 rats', *Carcinogenesis*, Vol 20, pp. 1567–1571.

Funayama, M, Arakawa, H, Yamamoto, R, Nishino, T, Shin, T, Murao, S 1995, 'Effects of alpha- and beta-arbutin on activity of tyrosinases from mushroom and mouse melanoma', *Bioscience, Biotechnology Biochemistry*, Vol 59, pp. 143–144.

Gadd, GW 1980, 'Melanin production and differentiation in batch cultures of the polymorphic fungus', *FEMS Microbiology Letters*, Vol 9, pp. 237–240.

Galindo, JD, Pedren˜ o, E, Garcı'a-Carmona, F, Garcı'a-Ca'novas, F, Solano, F, Lozano, JA 1983, 'Steady-state study of the mechanism of dopa-oxidase activity of tyrosinase', *International Journal of Biochemistry*, Vol 15, pp. 1455–1461.

Gao, H, Nishida, J, Saito, S, Kawabata, J 2007, 'Inhibitory effects of 5, 6, 7-trihydroxyflavones on tyrosinase', *Molecules*, Vol 12, pp. 86–97.

Garcia-Carmona, F, Garcia-Canovas, F, Iborra, JL, Lozano, JA 1982, 'Kinetic study of the pathway of melanisation between L-dopa and dopachrome', *Biochimica et Biophysica Acta*, Vol 717, pp. 124–131.

Garcıa-Molina, F, Mu˜ noz, JL, Var˜ on, R, Rodrıguez-L˜ opez, JN, Garcıa-C˜ anovas, F, Tudela, J 2007, 'A review on spectrophotometric methods for measuring the monophenolase and diphenolase activities of tyrosinase', *Journal of Agricultural and Food Chemistry*, Vol 55, pp. 9739–49.

Gerdemann, C, Eicken, C, Krebs, B 2002, 'The crystal structure of catechol oxidase: new insight into the function of type-3 copper proteins', *Accounts of Chemical Research*, Vol 35, pp. 183–191.

Gillespie, JP, Kanost, MR, Trenczek, T 1997, 'Biochemical mediators of insect immunity', *Annual Review of Entomology*, Vol 42, pp. 611–643.

Go, ML, Wu, X, Liu, XL 2005, 'Chalcones: an update on cytotoxic and chemoprotective properties', *Current Medicinal Chemistry*, Vol 12, pp. 481–99.

Go, ML, Wu, X, Liu, XL 2005, 'Chalcones: an update on cytotoxic and chemoprotective properties', *Current Medicinal Chemistry*, Vol 12, pp. 481–499.

Gómez-Cordovés, C, Bartolomé, B, Vieira, W, Virador, VM 2001, 'Effects of wine phenolics and surghum tannins on tyrosinase activity and growth of melanoma cells', *Journal of Agricultural and Food Chemistry*, Vol 49, pp. 1620–1624.

Ha, YM, Chung, SW, Song, S, Lee, H, Suh, H, Chung, HY 2007, '4-(6- Hydroxy-2-naphthyl)-1, 3-benzendiol: A potent, new tyrosinase inhibitor', *Biological and Pharmaceutical Bulletin*, Vol 30, pp. 1711–1715.

Halaban, R Patton, RS, Cheng, E, Svedine, S, Trombetta, ES, Wahl, ML, Ariyan, S, Hebert, DN, 2002, 'Abnormal acidification of melanoma cells induces tyrosinase retention in the early secretory pathway', *The Journal of Biological. Chemistry*, Vol 277, pp.14821–14828.

Hearing, VJ, King, RA 1993, 'Determinants of skin colour: melanocytes and melanization', In: Levine N, ed. *Pigmentation and pigmentary Abnormalities*. CRC, New York, NY, pp, 3–32.

Himmelwright, RS, Eickman, NC, Solomon, EI 1979, 'Reactions and interconversion of met and dimer hemocyanin', *Biochemical and Biophysical Research Communications*, Vol 86, pp. 628–634.

Huber, M, Lerch, K 1988, 'Identification of two histidines as copper ligands in *Streptomyces glaucescens* tyrosinase', *Biochemistry*, Vol 27, pp. 5610–5615.

Hyun, SK, Lee, WH, Jeong, da, M, Kim, Y, Choi, JS 2008, 'Inhibitory effect of kurarinol, kuraridinol, and trifolirhizin from *Sophora flavescens* on tyrosinase and melanin synthesis', *Biological and Pharmaceutical Bulletin*, Vol 31, pp. 154–158.

Ismaya, WT, Rozeboom, HJ, Weijn, A, Mes, JJ, Fusetti, F, Wichers, HJ, Dijkstra, BW 2011, 'Crystal structure of *Agaricus bisporus* mushroom tyrosinase: identity of the tetramer subunits and interaction with tropolone', *Biochemistry*, Vol 50, pp. 5477–5486.

Ito, S, Fujita, K 1985, 'Microanalysis of eumelanin and phaeomelanin in hair and melanomas by chemical degradation and liquid chromatography', *Analytical Biochemistry*, Vol 144, pp. 527–536.

Jackman, MP, Hajnal, A, Lerch, K 1991, 'Albino mutants of *Streptomyces glaucescens* tyrosinase', *Biochemical Journal*, Vol 274, pp. 707–713.

Jacob, V, Hagai, T, Soliman, K 2011, 'Structure-activity relationships of flavonoids', *Current Organic Chemistry*, Vol 15, pp. 2641–2657.

Jiménez, M, Chazarra, S, Escribano, J, Cabanes, J, García-Carmona, F 2001, 'Competitive inhibition of mushroom tyrosinase by 4-substituted benzaldehydes', *Journal of Agricultural and Food Chemistry*, Vol 49, pp. 4060–4063.

Jones, K, Hughes, J, Hong, M, Jia, Q, Orndorff, S 2002, 'Modulation of melanogenesis by aloesin: a competitive inhibitor of tyrosinase', *Pigment Cell Research*, Vol 15, pp.335–340.

Jorgensen, WL 2004, 'The many roles of computation in drug discovery', *Science*, Vol 303, pp. 1813–1818.

Kahn, V, Andrawis, A 1985, 'Inhibition of mushroom tyrosinase by tropolone', *Phytochemistry*, Vol 24, 905–908.

Kameyama, K, Takemura T, Hamada, Y, Sakai, C, Kondoh, S, Nishiyama, S, Urabe, K, Hearing, VJJ 1993, 'Pigment production in murine melanoma cells is regulated by tyrosinase, tyrosinase-related protein 1 (TRP1), DOPAchrome tautomerase (TRP2), and a melanogenic inhibitor', *Journal of Investigative Dermatology*, Vol 100, pp. 126–131.

Kadokawa, J, Nishikura, T, Muraoka, R, Tagaya, H, Fukuoka, N 2003, 'Synthesis of Kojic Acid Derivatives Containing Phenolic Hydroxy Groups', *Synthetic Communications*, Vol 33, pp. 1081–1086.

Kahn V. 1995, 'Effect of kojic acid on the oxidation of DL- DOPA, Norepinephrine, and Dopamine by mushroom tyrosinase', *Pigment Cell Research*, Vol 8, 234–240.

Kermasha, S, Bao, H, Bisakowski, B 2001, 'Biocatalysis of tyrosinase using catechin as substrate in selected organic solvent media', *Journal of Molecular Catalysis B: Enzymatic*, Vol 11, pp. 929–938.

Khan, MTH 2007, 'Heterocyclic Compounds against the Enzyme Tyrosinase Essential for Melanin Production: Biochemical Features of Inhibition', *Heterocyclic Chemistry*, Vol 9, 119–138.

Khatib, S, Nerya, O, Musa, R, Shmuel, M, Tamir, S, Vaya, J 2005, 'Chalcones as potent tyrosinase inhibitors: the importance of a 2, 4-substituted resorcinol moiety', *Bioorganic and Medicinal Chemistry*, Vol 13, pp. 433–441.

Kim, SJ, Son, KH, Chang, HW, Kang, SS, Kim, HP 2003, 'Tyrosinase inhibitory prenylated flavonoids from *Sophora flavescens*', *Biological and Pharmaceutical Bulletin*, Vol 26, pp. 1348–1350.

Kim, YJ, Uyama, H 2005, 'Tyrosinase inhibitors from natural and synthetic sources: structure, inhibition mechanism and perspective for the future', *Cellular and Molecular Life Sciences*, Vol 62, pp. 1707–1723.

Kobayashi, Y, Kayahara, H, Tadasa, K, Nakamura, T, Tanaka, H 1995, 'Synthesis of Amino Acid Derivatives of Kojic Acid and Their Tyrosinase Inhibitory Activity', *Bioscience, Biotechnology and Biochemistry*, Vol 59, pp. 1745–1746.

Kobayashi, Y, Kayahara, H, Tadasa, K, Nakamura, T, Tanaka, H 1996, 'Synthesis of N-kojic-amino acid and N-kojic-amino acid-kojiolate and their tyrosinase inhibitory activity', *Bioorganic and Medicinal Chemistry Letters*, Vol 6, pp. 1303–1308.

Konanayakam, M, Sastry, SK 1988, 'Kinetics of shrinkage of mushrooms during blanching', *Journal of the Science of Food and Agriculture*, Vol 53, pp. 1406–1411.

Korner, AM, Pawelek J 1982, 'Mammalian tyrosinase catalyzes three reactions in the biosynthesis of melanin', *Science*, Vol 217, pp. 1163–1165.

Kubo, I, Kinst-Hori, I, Yokokawa, Y 1994, 'Tyrosinase inhibitors from *Anacardium occidentale* fruits', *Journal of Natural Products*, Vol 57, pp. 545–551.

Kubo, I, Kinst-Hori, I, Ishiguro, K, Chaudhuri, SK, Sanchez, Y, Oruga, T 1994, 'Tyrosinase inhibitory flavonoids from *Heterotheca inuloides* and their structural functions', *Bioorganic and Medicinal Chemistry Letters*, Vol 4, pp. 1443–1446.

Kubo, I, Yokokawa, Y, Kinst-Hori, I 1995, 'Tyrosinase inhibitors from bolivian medicinal plants', *Journal of Natural Products*, Vol 58, pp. 739–743.

Kubo, I, Kinst-Hori, I 1988, 'Tyrosinase inhibitors from cumin', *Journal of Agricultural and Food Chemistry*, Vol 46, 5338–5341.

Kubo, I, Kinst-Hori, I 1998, 'Tyrosinase inhibitors from anise oil', *Journal of Agricultural and Food Chemistry*, Vol 46, pp. 1268–1271.

Kubo, I, Kinst-Hori, I 1999, 'Tyrosinase inhibitory activity of the olive oil flavour compounds', *Journal of Agricultural and Food Chemistry*, Vol 47, pp. 4574–4578.

Kubo, I, Kinst-Hori, I 1999, '2-Hydroxy-4-methoxy benzaldehyde: a potent tyrosinase inhibitor from African medicinal plants', *Planta Medica*, Vol 65, pp. 19–22.

Kubo, I, Kinst-Hori, I 1999, 'Flavonols from saffron flower: tyrosinase inhibitory activity and inhibition mechanism', *Journal of Agricultural and Food Chemistry*, Vol 47, pp. 4121–4125.

Kubo, I, Kinst-Hori, I, Chaudhuri, SK, Kubo, Y, Sánchez, Y, Ogura, T 2000, 'Flavonols from *Heterotheca inuloides*: tyrosinase inhibitory activity and structural criteria', *Bioorganic and Medicinal Chemistry*, Vol 8, pp. 1749–1755.

Kupper, U, Niedermann, DM, Travaglini, G, Lerch, K 1989, 'Isolation and characterization of the tyrosinase gene from *Neurospora crassa*', *The Journal of Biological Chemistry*, Vol 264, pp. 17250–17258.

Kwon, BS, Haq, AK, Pomerantz, SH, Halaban, R 1987, 'Isolation and sequence of a cDNA clone for human tyrosinase that maps at the mouse c-albino locus', *Proceedings of the National Academy of Science. USA*, Vol 84, pp. 7473–7477.

Lambert, C, Chacon, JN, Chedekel, MR, Land, EJ, Riley, PA, Thompson, A, Truscott, TG 1989, 'A pulse radiolysis investigation of the oxidation of indolic melanin precursors: evidence for indolequinones and subsequent intermediates', *Biochimica et Biophysica Acta*, Vol 993, pp. 12–20.

Land, EJ, Ramsden, CA, Riley, PA 2007, 'The mechanism of suicide-inactivation of tyrosinase: a substrate structure investigation', *The Tohoku Journal of Experimental Medicine*, Vol 212, pp. 341–348.

Land, EJ, Ramsden, CA, Riley, PA, Stratford, MRL 2008, 'Evidence consistent with the requirement of cresolase activity for suicide inactivation of tyrosinase', *The Tohoku Journal of Experimental Medicine*, Vol 216, pp. 231–238.

Lee, HS 2002, 'Tyrosinase inhibitors of *Pulsatilla cernua* root-derived materials', *Journal of Agricultural and Food Chemistry*, Vol 50, pp. 1400–1403.

Lee, SE, Kim, MK, Lee, SG, Ahn, YJ, Lee, HS 2000, 'Inhibitory effects of *Cinnamomum cassia* bark-derived materials on mushroom tyrosinase', *Food Science and Biotechnology*, Vol 9, pp. 330–333.

Lerch, K 1981, 'In: Metal Ions in Biological Systems' Sigel H. (ed.), Marcel Dekker, New York, pp.143–186.

Lerch, K 1982, 'Primary structure of tyrosinase from *Neurospora crassa*. II. Complete amino acid sequence and chemical structure of a tripeptide containing an unusual thioether', *The Journal of Biological Chemistry*, Vol 257, pp. 6414–6419.

Lerner, AB, Thomas, B, Fitzpatrick, T, Calkins, E, Summerson, WH 1950, 'Mammalian tyrosinase: The relationship of copper to enzymatic activity', *The Journal of Biological Chemistry*, Vol 187, pp.793–802.

Leu, YL, Hwang, TL, Hu, JW, Fang, JY 2008, 'Anthraquinones from *Polygonum cuspidatum* as tyrosinase inhibitors for dermal use', *Phytotherapy Research*, Vol 22, pp. 552–556.

Li, C, Xu, L, Wolan, DW, Wilson, IA, Olson, AJ 2004, 'Virtual screening of human 5-aminoimidazole-4-carboxamide ribonucleotide transformylase against the NCI diversity set by use of AutoDock to identify novel nonfolate inhibitors', *Journal of Medicinal Chemistry*, Vol 47, pp. 6681–6690.

Li, H, Cheng, WC, Cho, CH, He, Z, Wang, M 2007, 'Oxyresveratrol as an anti-browning agent for cloudy apple juices and fresh cut apples', *Journal of Agricultural and Food Chemistry*, Vol 55, pp. 2604–2610.

Likhitwitayawuid, K, Sritularak, B, De-Eknamkul, W 2000, 'Tyrosinase inhibitors from *Artocarpus gomezianus*', *Planta Medica*, Vol 66, pp. 275–277.

Likhitwitayawuid, K, Sritularak, B, De-Eknamkul, W 2002, 'Tyrosinase inhibitors from plants', In Proceedings of the Tenth Special CU-af Seminar, Chulalongkorn University, Bangkok, Thailand, 31 May 2002.

Lim, SS, Kim, HS, Lee, DU 2007, 'In vitro antimalarial activity of flavonoids and chalcones', *Bulletin of the Korean Chemical Society*, Vol 28, pp. 2495–2497.

Lima, LL, Lima, RM, da Silva, AF, do Carmo, AMR, da Silva, AD, Raposo, NRB 2013, 'Azastilbene analogs as tyrosinase inhibitors: New molecules with depigmenting potential', *The Scientific World Journal*, Vol 2013, pp. 1–7.

Lin, JY, Fisher, DE 2007, 'Melanocyte biology and skin pigmentation', *Nature*, Vol 445, pp. 843–50.

Liu, SH, Pan, IH, Chu, IM 2007, 'Inhibitory effect of *p*-hydroxybenzyl alcohol on tyrosinase activity and melanogenesis', *Biological and Pharmaceutical Bulletin*, Vol 30, pp. 1135–1139.

Loizzo, MR, Tundis, R, Menichini, F, Saab, MA, Rtatti, GA, Menichini, F 2007, 'Cytotoxic activity of essential oils from labiatae and lauraceae families against *in vitro* human tumor models', *Anticancer Research*, Vol 27, pp. 3293–300.

Iozumi, K, Hoganson, GE, Pennella, R, Everett, MA, Fuller, BB 1993, 'Role of tyrosinase as the determinant of pigmentation in cultured human melanocytes', *Journal of Investigative Dermatology*, Vol 100, pp. 806–811.

Maeda, K, Fukuda, M 1996, 'Arbutin: Mechanism of its depigmenting action in human melanocyte culture', *Journal of Pharmacology and Experimental Therapeutics*, Vol 276, pp. 765–769.

Masamoto, Y, Ando, H, Murata, Y, Shimoishi, Y, Tada, M, Takahata, K 2003, 'Mushroom tyrosinase inhibitory activity of esculetin isolated from seeds of *Euphorbia lathyris* L.', *Bioscience Biotechnology Biochemistry*, Vol 67, pp. 631–634.

Mason, HS 1948, 'The chemistry of melanin. III. Mechanism of the oxidation of trihydroxyphenylalanine by tyrosinase', *The Journal of Biological Chemistry*, Vol 172, pp. 83–99.

Mason, HS, Fowlks, WL, Peterson, E 1955, 'Oxygen transfer and electron transport by the phenolase complex', *Journal of the American Chemical Society*, Vol 77, pp. 2914–2915.

Matsuda, H, Higashino, M, Chen, W, Tosa, H, Iinuma, M, Kubo, M 1995, 'Studies of cuticle drugs from natural sources. III. Inhibitory effect of *Myrica rubra* on melanin biosynthesis', *Biological and Pharmaceutical Bulletin*, Vol 18, pp. 1148–1150.

Mayer, AM, Harel, E 1979, 'Polyphenol oxidases in plants', *Phytochemistry*, Vol 18, pp. 193–215.

Mayer, AM 1987, 'Polyphenol oxidases in plants: recent progress', *Photochemistry*, Vol 26, pp. 11–20.

Mauron, J 1990, 'Influence of processing on nutritional quality', *Journal of Nutritional Science and Vitaminology*, Vol 111, pp. 383–387.

McEvily, AJ, Iyengar, R, Otwell, WS 1991, 'Sulfite alternative prevents shrimp melanosis', *Food Technology*, Vol 45, pp. 80–86.

Mcevily, JA, Iyengar, R, Otwell, QS 1992, 'Inhibition of enzymatic browning in foods and beverages', *Critical Reviews in Food Science and Nutrition*, Vol 32, pp. 253–273.

McWeeny, DJ, Knowles, ME, Hearne, JF 1974, 'The chemistry of non-enzymic browning in foods and its control by sulphites', *Journal of the Science of Food and Agriculture*, Vol 25, pp. 735–746.

Michele, H 2009, 'Potashman and Mark E. Duggan, Covalent Modifiers: An Orthogonal Approach to Drug Design', *Journal of medicinal chemistry*, Vol, 52, pp. 1231–1246.

Miyazawa, M, Tamura, N 2007, 'Inhibitory compound of tyrosinase activity from the sprout of *Polygonum hydropiper* L. (Benitade)', *Biological and Pharmaceutical Bulletin*, Vol 30, pp. 595–597.

Mukherjee, VK, Prasad, AK, Raj, AG, Brakhe, ME, Olsen, CE, Jain, SC, Parmer, VP 2001, 'Synthetic and biological activity evaluation studies on novel 1, 3-diarylpropenones', *Bioorganic and Medicinal Chemistry* Vol 9, pp. 337–345.

Muñoz-Muñoz, JL, Garcia-Molina, F, Garcia-Ruiz, PA, Molina-Alarcon, M, Tudela, J, Garcia-Canovas, F, Rodriguez-Lopez, JN 2008, 'Phenolic substrates and suicide inactivation of tyrosinase: kinetics and mechanism', *Biochemical Journal*, Vol 416, pp. 431–440.

Nakagawa, M, Kawai, K 1995, 'Contact allergy to kojic acid in skin care products', *Contact Dermatitis*, Vol 32, pp. 9–13.

Nappi, AJ, Sugumaran, M 1993, 'Some biochemical aspects of eumelanin formation in insect immunity', In: Pathak JPN. *Insect Immunity*. New Delhi: Oxford & IBH Publishing Co, pp. 131–148.

Nerya, O, Vaya, J, Musa, R, Izrael, S, Ben-Arie, R, Tamir, S 2003, 'Glabrene and isoliquiritigenin as tyrosinase inhibitors from licorice roots', *Journal of Agricultural and Food Chemistry*, Vol 51, pp. 1201–1207.

Nerya, O, Musa, R, Khatib, S, Tamir, S, Vaya, J 2004, 'Chalcones as potent tyrosinase inhibitors: the effect of hydroxyl positions and numbers', *Phytochemistry*, Vol 65, pp. 1389–1395.

Nishimura, T, Kometani, T, Takii, H, Tanaka, H, Okada, S 1994, 'Acceptor specificity in the glucosylation reaction of *Bacillus subtilis* X-23 α -amylase towards various phenolic compounds and the structure of kojic acid glucoside', *Journal of Fermentation and Bioengineering*, Vol 78, pp. 37–41.

Nishioka, K 1978, 'Particulate tyrosinase of human malignant melanoma. Solubilization, purification following trypsin treatment and characterization', *European Journal of Biochemistry*, Vol 85, pp. 137–146.

No, JK, Soung, DY, Kim, YJ, Shim, KH, Jun, YS, Rhee, SH, Yokozawa, T, Chung, HY 1999, 'Inhibition of tyrosinase by green tea components', *Life Sciences*, Vol 65, pp. 241–246.

Nowakowska, Z 2007, 'A review of anti-infective and anti-inflammatory chalcones', *European Journal of Medicinal Chemistry*, Vol 42, pp. 125–137.

Nugroho, A, Choi, JK, Park, JH, Lee, KT, Cha, BC, Park, HJ 2009, 'Two new flavonol glycosides from *Lamium amplexicaule* L. and their *in vitro* free radical scavenging and tyrosinase inhibitory activities', *Planta Medica*, Vol 75, pp. 364–366.

Ohguchi, K, Tanaka, T, Ito, T, Iinuma, M, Matsumoto, K, Akao, Y, Nozawa, Y 2003, 'Inhibitory effects of resveratrol derivatives from Dipterocarpaceae plants on tyrosinase activity', *Bioscience Biotechnology Biochemistry*, Vol 67, pp. 1587–1589.

Ohguchi, K, Tanaka, T, Iliya, I, Ito, T, Iinuma, M, Matsumoto, K, Akao, Y, Nozawa, Y 2003, 'Gnetol as a potent tyrosinase inhibitor from genus *Gnetum*', *Bioscience Biotechnology Biochemistry*, Vol 67, pp. 663–665.

Ohguchi, K, Tanaka, T, Kido, T, Baba, K, Iinuma, M, Matsumoto, K, Akao, Y, Nozawa, Y 2003, 'Effects of hydroxystilbene derivatives on tyrosinase activity', *Biochemical and Biophysical Research Communications*, Vol 307, pp. 861–863.

Park, HY, Kosmadaki, M, Yaar, M, Gilchrest, BA 2009, 'Cellular mechanisms regulating human melanogenesis', *Cellular and Molecular Life Sciences*, Vol 66, pp. 1493–1506.

Parrish, FW, Wiley, BJ, Simmons, EG, Long, Jr, L 1966, 'Production of aflatoxins and kojic acid by species of *Aspergillus* and *Penicillium*', *Applied Microbiology*, Vol 14, pp. 136–139.

Parvez, S, Kang, M, Chung, HS, Bae, H 2007, 'Naturally occurring tyrosinase inhibitors: mechanism and applications in skin health, cosmetics and agriculture industries', *Phytotherapy Research*, Vol 21, pp. 805–816.

Pawelek, JM 1991, 'After dopachrome?', *Pigment Cell Research*, Vol 4, pp. 53–62.

Pawelek, JM, Korner, AM 1982, 'The biosynthesis of mammalian melanin', *AMSCA*, Vol 70, pp. 136–145.

Piao, XL, Baek, SH, Park, MK, Park, JH 2004, 'Tyrosinase-inhibitory furanocoumarin from *Angelica dahurica*', *Biological and Pharmaceutical Bulletin*, Vol 27, pp. 1144–1146.

Pieper, U, Eswar, N, Davis, FP, Braberg, H, Madhusudhan, MS, Rossi, A, Marti-Renom, M, Karchin, R, Webb, BM, Eramian, D, Shen, MY, Kelly, L, Melo, F, Sali, A 2006, 'MODBASE: a database of annotated comparative protein structure models and associated resources', *Nucleic Acids Research*, Vol 34, pp. 291–295.

Priestly, GC 1993, 'Molecular Aspects of Dermatology', John Wiley, Chichester, pp. 226.

Prota, G 1992, 'Melanins and Melanogenesis', Academic Press, New York, pp. 1–290.

Ramsden, CA, Stratford, MRL, Riley, PA 2009, 'The influence of catechol structure on the suicide inactivation of tyrosinase', *Organic and Biomolecular Chemistry*, Vol 7, pp. 3388–3390.

Rao, MS, Olson, AJ 1999, 'Modelling of Factor Xa-inhibitor complexes: a computational flexible docking approach', *Proteins*, Vol 34, pp. 173–183.

Raper, HS 1928, 'The anaerobic oxidases', *Physiological Reviews*, Vol 8, pp. 245–282.

Raposo, G, Marks, SM 2007, 'Melanosomes—dark organelles enlighten endosomal membrane transport', *Nature Reviews Molecular Cell Biology*, Vol 8, pp. 786–797.

Rescigno, A, Sollai, F, Pisu, B, Rinaldi, A, Sanjust, E 2002, 'Tyrosinase inhibition: General and applied aspects', *Journal of Enzyme Inhibition and Medicinal Chemistry*, Vol 17, pp. 207–218.

Rho, HS, Ahn, SM, Yoo, DS, Kim, MK, Cho, DH, Cho, JY 2010, 'Kojyl thioether derivatives having both tyrosinase inhibitory and anti-inflammatory properties', *Bioorganic and Medicinal Chemistry Letters*, Vol 20, pp. 6569–6571.

Riley, PA 1997, 'Melanin', *International Journal of Biochemistry and Cell Biology*, Vol 29, pp.1235–1239.

Riley, PA 2003, 'Melanogenesis and melanoma', *Pigment Cell Research*, Vol 16, pp. 548–552.

Robb, DA, Gutteridge, S 1981, 'Polypeptide composition of two fungal tyrosinases', *Phytochemistry*, Vol 20, pp. 1481–1485.

Robb, DA 1984, 'In: Copper Proteins and Copper Enzymes', Lontie R. (ed.), CRC Press, Boca Raton, FL, Vol 2, pp. 207.

Romaguera, C, Grimalt, F 1985, 'Leukoderma from hydroquinone', *Contact Dermatitis* Vol 12, pp. 183.

Ros, JR, Rodríguez-López, JN, García-Cánovas, F 1993, 'Effect of ferrous ions on the monophenolase activity of tyrosinase', *Biochimica et Biophysica Acta*, Vol 1163, pp. 303–308.

Ros-Martinez, JR, Rodríguez-López, JN, Castellanos, RV, García-Cánovas, F 1993, 'Discrimination between two kinetic mechanisms for the monophenolase activity of tyrosinase', *Biochemical Journal*, Vol 294, pp. 621–623.

Sánchez-Ferrer, Á, Villalba, J, García-Carmona, F 1989, 'Triton X-114 as a tool for purifying spinach polyphenol oxidase', *Phytochemistry*, Vol 28, pp. 1321–1325.

Sánchez-Ferrer, Á, Bru, R, García-Carmona, F 1990, 'Partial purification of a thylakoid-bound enzyme using temperature-induced phase partitioning', *Analytical Biochemistry*, Vol 184, pp. 279–282.

Sánchez-Ferrer, A, Rodríguez-López, JN, García-Cánovas, F, García-Carmona, F 1995, 'Tyrosinase: a comprehensive review of its mechanism', *Biochimica et Biophysica Acta*, Vol 1247, pp. 1–11.

Sanjust, E, Cecchini, G, Sollai, F, Curreli, N, Rescigno, A 2003, '3-Hydroxykynurenine as a substrate/activator for mushroom tyrosinase', *Archives of Biochemistry and Biophysics*, Vol 412, pp. 272–278.

Schallreuter, KU, Kothari, S, Chavan, B, Spencer, JD, 2008, 'Regulation of melanogenesis-controversies and new concepts', *Experimental Dermatology*, Vol 17, pp. 395–404.

Schapira, M, Abagyan, R, Totrov, M 2003, 'Nuclear hormone receptor targeted virtual screening', *Journal of Medicinal Chemistry*, Vol 46, pp. 3045–3059.

Schnecke, V, Kuhn, LA 2000, 'Virtual screening with solvation and ligand-induced complementarity', *Perspectives in Drug Discovery and Design*, Vol 20, pp. 171–190.

Schweikardt, T, Olivares, C, Solano, F, Jaenicke, E, García-Borrón, JC, Decker, H 2007, 'A three-dimensional model of mammalian tyrosinase active site accounting for loss of function mutations', *Pigment Cell Research*, Vol 20, pp. 394–401.

Sculley, MJ, Morrison, JF, Cleland, WW 1996, 'Slow binding inhibition: the general case', *Biochimica et Biophysica Acta*, Vol 1298, pp. 78–86.

Seo, S, Sharma, VK, Sharma, N 2003, 'Mushroom Tyrosinase: Recent Prospects', *Journal of Agricultural and Food Chemistry*, Vol 51, pp. 2837–2853.

Sharma, VK, Choi, J, Sharma, N, Choi, M, Seo, SY 2004, 'In vitro antityrosinase activity of 5-(hydroxymethyl)-2-furfural isolated from *Dictyophora indusiata*', *Phytotherapy Research*, Vol 18, pp. 841–844.

Sheng Chang, T 2009, 'An updated review of tyrosinase inhibitors', *International Journal of Molecular Sciences*, Vol 10, pp. 2440–2475.

Shiino, M, Watanabe, Y, Umezawa, K 2001, 'Synthesis of *N*-substituted *N*-nitrosohydroxylamines as inhibitors of mushroom tyrosinase', *Bioorganic and Medicinal Chemistry*, Vol 9, pp. 1233–1240.

Shiino, M, Watanabe, Y, Umezawa, K 2003, 'Synthesis of tyrosinase inhibitory activity of novel *N*-hydroxybenzyl-*N*-nitrosohydroxylamines', *Bioorganic Chemistry*, Vol 31, pp. 129–135.

Shiino, M, Watanabe, Y 2008, 'Umezawa, K. pH-dependent inhibition of mushroom tyrosinase by *N*-substituted *N*-nitrosohydroxylamines', *Journal of Enzyme Inhibition and Medicinal Chemistry*, Vol 23, pp. 16–20.

Shimizu, K, Kondo, R, Sakai, K, Lee, SH, Sato, H 1998, 'The inhibitory components from *Artocarpus incisus* on melanin biosynthesis', *Planta Medica*, Vol 64, pp. 408–412.

Shimizu, K, Kondo, R, Sakai, K 2000, 'Inhibition of tyrosinase by flavonoids, stilbenes and related 4-substituted resorcinols: Structure–activity investigations', *Planta Medica*, Vol 66, pp. 11–15.

Silverman, RB 1995, 'Mechanism-based enzyme inactivators', *Methods in Enzymology*, Vol 249, pp. 240–283.

Söderhäll, K, Aspán, A, Duvic, B 1990, 'The proPO-system and associated proteins; role in cellular communication in arthropods', *Research in Immunology*, Vol 141, pp. 896–907.

Soliva-Fortuny, RC, Martin-Belloso, O 2003, 'New advances in extending the shelf-life of fresh-cut fruits: A review', *Trends in Food Science and Technology*, Vol 14, pp. 341–353.

Sollai, F, Zucca, P, Sanjust, E, Steri, D, Resciqno, A 2008, 'Umbelliferone and esculetin: inhibitors or substrates for polyphenol oxidases?', *Biological and Pharmaceutical Bulletin*, Vol 31, pp. 2187–2193.

Solomon, EI 1981, 'In: Copper Proteins, Vol. III, Spiro T. G. (ed.), Wiley-Interscience, New York, pp. 41–108.

Solomon, EI, Sundaram, UM, Machonkin, TE 1996, 'Multicopper oxidases and Oxygenases', *Chemical Reviews*, Vol 96, pp. 2563–2606.

Son, SM, Moon, KD, Lee, CY 2000, 'Rhubarb juice as a natural antibrowning agent', *Journal of Food Science*, Vol 65, pp. 1288–1289.

Song, S, Lee, H, Jin, Y, Ha, YM, Bae, S, Chung, HY, Suh, H 2007, 'Syntheses of hydroxy substituted 2-phenyl-naphthalenes as inhibitors of tyrosinase', *Bioorganic and Medicinal Chemistry Letters*, Vol 17, pp. 461–464.

Song, YM, Mi, HY, Kim, JA, Moon, HR 2012, 'Synthesis of novel azo-resveratrol and their derivatives as potent tyrosinase inhibitors', *Bioorganic and Medicinal Chemistry Letters*, Vol 22, pp.7451–7455.

Specker, E, Bottcher, J, Heine, A, Sottriffer, CA, Lilie, H, Schoop, A, Muller, G, Griebenow, N, Klebe, G 2005, 'Hydroxyethylene sulfones as a new scaffold to address aspartic proteases: design, synthesis, and structural characterization', *Journal of Medicinal Chemistry*, Vol 48, pp. 6607–6619.

Spritz, RA, Hearing, VJ 1994, 'Genetic disorders of pigmentation', *Advanced Human Genetics*, Vol 22, pp. 1–45.

Strothkemp, KG, Jolley, RL, Mason, HS 1976, 'Quaternary structure of mushroom tyrosinase', *Biochemical and Biophysical Research Communications*, Vol 70, pp. 519–524.

Stüssi, H, Rast, DM 1981, 'The biosynthesis and possible function of γ -glutaminy-4-hydroxybenzene in *Agaricus bisporus*', *Phytochemistry*, Vol 20, pp. 2347–2352.

Stratigos, AJ, Katsambas, AD 2004, 'Optimal management of recalcitrant disorders of hyperpigmentation in dark-skinned patients', *American Journal of Clinical Dermatology* Vol 5, pp. 161–168.

Sugumaran M 1988, 'Molecular mechanism for cuticular sclerotization', *Advances in insect physiology*, Vol 21, pp. 179–231.

Sugumaran, M 1991, 'Molecular mechanisms of mammalian melanogenesis: comparison with insect cuticular sclerotization (mini review)', *FEBS Letters*, Vol 293, pp.:4–10.

Sugumaran, M, Semensi, V 1991, 'Quinone methide as a new intermediate in eumelanin biosynthesis', *The Journal of Biological Chemistry*, Vol 266, pp. 6073–6078.

Sugumaran, M, Kanost, M 1993, 'Regulation of insect hemolymph phenol-oxidases', In: Beckage NE, Thompson SN, Frederick B. A, 'Parasites and Pathogens', Vol. I. Parasites. San Diego: Academic Press; pp. 317–342.

Sugumaran, M 1996, 'Role of insect cuticle in immunity', In: SoÈ derhaÈ ll K, Iwanaga S. Vastha, G, 'New Directions in Invertebrate Immunology', Fair Haven, N. J: SOS Publications, pp. 355–374.

Sugumaran, M 1998, 'Unified mechanism for sclerotization of insect cuticle', *Advances in Insect Physiology*, Vol 27, pp. 229–334.

Tadokoro, T, Kobayashi, N, Zmudzka, BZ, Ito, S, Wakamatsu, K, Yamaguchi, Y, Korossy, KS, Miller, SA, Beer, JZ, Hearing, VJ 2003, 'UV-induced DNA damage and melanin content in human skin differing in racial/ethnic origin', *FASEB Journal*, Vol 17, pp. 1177–1179.

Takizawa, T, Mitsumori, K, Tamura, T, Nasu, M, Ueda, M, Imai, T, Hirose, M 2003 'Hepatocellular tumor induction in heterozygous p53-deficient CBA mice by a 26-week dietary administration of kojic acid', *Toxicological Sciences*, Vol 73, pp. 287–293.

Te-Sheng Chang 2009, 'An Updated Review of Tyrosinase Inhibitors', *International Journal of Molecular Sciences*, Vol 10, pp. 2440–2475.

Tengamnuay, P, Pengrungruangwong, K, Likhitwitayawuid, K 2003, 'A potent tyrosinase inhibitor from *Artocarpus lakoocha* heartwood extract', In Proceedings of the IFSCC Conference, Seoul, Korea, 22–24 September 2003, pp. 201–212.

- Tsai, TY, Lee, YH 1998, 'Roles of copper ligands in the activation and secretion of *Streptomyces tyrosinase*', *The Journal of Biological Chemistry*, Vol 273, pp. 19243–19250.
- van Acker, SA, van den Berg, DJ, Tromp, MN, Griffioen, DH, van Bennekom, WP, van der Vijgh, WJ, Bast, A 1996, 'Structural aspects of antioxidant activity of flavonoids', *Free Radical Biology and Medicine*, Vol 20, pp. 331–342.
- van Gelder, CWG, Flurkey, WH, Wichers, HJ 1997, 'Sequence and structural features of plant and fungal tyrosinases', *Phytochemistry*, Vol 45, pp. 1309–1323.
- Vaya, J, Belinky, PA, Aviram, M 1997, 'Antioxidant constituents from licorice roots: Isolation, structure elucidation and antioxidative capacity toward LDL oxidation', *Free Radical Biology and Medicine*, Vol 23, pp. 302–313.
- Whitaker, JR 1995, Polyphenol oxidase. In Wong DWS. (ed), 'Food Enzymes, Structure and Mechanism', Chapman & Hall, New York, pp. 271–307.
- Wichers, HJ, Gerritsen, YAM, Chapelon, CGJ 1996, 'Tyrosinase isoforms from the fruiting bodies of *Agaricus bisporus*', *Phytochemistry*, Vol 43, pp. 333–337.
- Wilcox, DE, Porras, AG, Hwang, YT, Lerch, K, Winkler, ME, Solomon, EI 1985, 'Substrate analogue binding to the coupled binuclear copper active site in tyrosinase', *Journal of the American Chemical Society*, Vol 107, pp. 4015–4027.
- Wolff, K, Jimbow, K, Fitzpatrick, TB 1974, 'Experimental pigment donation in vivo', *Journal of Ultrastructure Research*, Vol 47, pp. 400–419.
- Wu, XS, Rao, K, Zhang, H, Wang, F, Sellers, JR, Matesic, LE, Copeland, NG, Jenkins, NA, Hammer, JA 2002, 'Identification of an organelle receptor for myosin-Va', *Nature Cell Biology*, Vol 4, pp. 271–278.

Xu, Y, Stokes, AH, Freeman, WM, Kumer, SC, Vogt, BA, Vrana, KE 1997, 'Tyrosinase mRNA is expressed in human substantia nigra', *Molecular Brain Research*, Vol 45, pp. 159–162.

Yamamura, T, Onishi, J, Nishiyama, T 2002, 'Antimelanogenic activity of hydrocoumarins in cultured normal human melanocytes by stimulating intracellular glutathione synthesis', *Archives of Dermatological Research*, Vol 294, pp. 349–354.

Yokozawa, T, Kim, YJ 2007, 'Piceatannol inhibits melanogenesis by its antioxidative actions', *Biological and Pharmaceutical Bulletin*, Vol 30, pp. 2007–2011.

Zhang, X, Hu, X, Hou, A, Wang, H 2009, 'Inhibitory effect of 2, 4, 2', 4'-tetrahydroxy-3-(3-methyl-2-butenyl)-chalcone on tyrosinase activity and melanin biosynthesis', *Biological and Pharmaceutical Bulletin*, Vol 32, pp. 86–90.

Zhang, X, van Leeuwen, J, Wichers, HJ, Flurkey, WH 1999, 'Characterization of tyrosinase from the cap flesh of *Portabella* mushrooms', *Journal of Agricultural and Food Chemistry*, Vol 47, pp. 374–378.

Zheng, ZP, Cheng, KW, To, JT, Li, H, Wang, M 2008, 'Isolation of tyrosinase inhibitors from *Artocarpus heterophyllus* and use of its extract as antibrowning agent', *Molecular Nutrition and Food Research*, Vol 52, pp. 1530–1538.

Zheng, ZP, Tan, HY, Chen, J, Wang, M 2013, 'Characterization of tyrosinase inhibitors in the twigs of *Cudrania tricuspidata* and their structure-activity relationship study', *Fitoterapia*, Vol 84, pp. 242–247.

Zhou, H, Kepa, JK, Siegel, D, Miura, S, Hiraki, Y, Ross, D 2009, 'Benzene Metabolite Hydroquinone Up-Regulates Chondromodulin-I and Inhibits Tube Formation in Human Bone Marrow Endothelial Cells', *Molecular Pharmacology*, Vol 76, pp. 579–587.

Zimmerman, WC, Blanchette, RA, Burnes, TA, Farrel, RL 1995, 'Melanin and perithecial development in *Ophiostoma piliferum*', *Mycology*, Vol 87, pp. 857–863.

CHAPTER 2

HYDROXYAZACHALCONES

2.1. Introduction

Azachalcones and their derivatives have been reported to have a wide variety of biological activities such as antibacterial, tuberculostatic, and anti-inflammatory potential (Nowakowska, Wyrzykiewicz & Kedzia 2001; Nowakowska, Wyrzykiewicz & Kedzia 2002; Yaylı *et al* 2007; Yaylı *et al* 2006). These activities are largely attributed to the unsaturated ketone moiety (Rao, Fang & Tzeng 2009). The hypothesis of the present study is that the presence of the 2'-hydroxyl group attached to ring A of the azachalcone has major importance. This is primarily because previous studies have recognized an apparently potent inhibitory effect of compounds with hydroxyl groups on tyrosinase (Kanade *et al* 2007; Kim *et al* 2006; Shiino, Watanabe & Umezawa 2001; Shiino, Watanabe & Umezawa 2003; Yamazaki *et al* 2009; Yan *et al* 2009). Phenolic hydroxyl groups can act both as hydrogen-bond donors and acceptors. The hydroxyl groups in compounds carry out the nucleophilic attack on the coppers of tyrosinase active site and are directly involved in transferring protons during catalysis, which resulted in inactivation of tyrosinase (Muñoz-Muñoz *et al* 2008; Gao *et al* 2007). Therefore, a series of azachalcones (**Scheme 1**) and their derivatives have been synthesized and investigated for their inhibitory effects on tyrosinase activity. It is hypothesized that the hydroxyl group of the ligand may block the tyrosinase activity by binding to the copper atoms in the active site of the enzyme based on the fact that previous findings have shown the role of hydroxyl groups in tyrosinase inhibition (Gao *et al* 2007; Kanade *et al* 2007).

2.2. Experimental

The parent azachalcones are synthesized by the base catalyzed Claisen-Schmidt condensation of 2'-acetylpyridine with an appropriate aldehyde in a polar solvent like methanol (See **12.2**). Dealkylation of the methoxy azachalcones in the presence of boron tribromide resulted in their corresponding hydroxy compounds (**Scheme 1**).

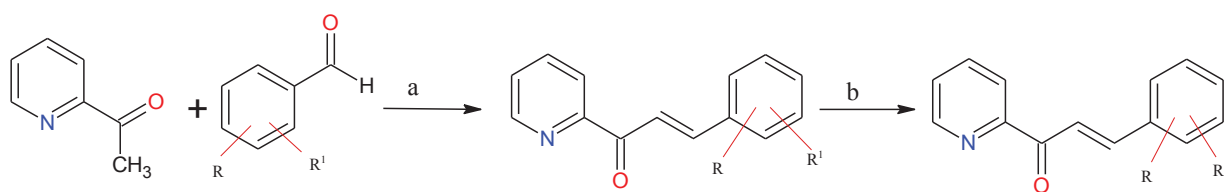
2.2.1. Method for synthesis of compound **5b**

To a stirred solution of 2'-acetylpyridine (1mM, 1.21 mL) and 3,5-dimethoxybenzaldehyde (1mM, 166mg) in 25 mL methanol, are added pulverized NaOH (2mM) and the mixture was stirred at room temperature for 24–36 h. The reaction is monitored by TLC using *n*-hexane: ethyl acetate (7:3) as mobile phase. The

reaction mixture is cooled to 0°C (ice-water bath) and acidified with HCl (10 % v/v aqueous solution) to afford total precipitation of the compound. A yellowish orange precipitate is formed, which is filtered and washed with 10% aqueous HCl solution. The product obtained is recrystallized with ethylacetate to give the pure chalcone product **5a**. A solution of BBr₃ (5.0mL) is added to a cooled solution of the chalcone compound **5a** (1 mM, 269 mg) in CH₂Cl₂ under argon. The cooling bath is removed and the dark solution is warmed to RT and stirred for 1-5hrs. The dark solution is then poured into ice water and filtered. The aqueous layer is extracted twice with chloroform. The organic extract is washed with water followed by brine and dried over anhydrous sodium sulfate. This is then rotary evaporated to give the respective hydroxy derivative **5b**.

Assays are performed with L-DOPA as the substrate, using kojic acid, a well-known strong tyrosinase inhibitor as the positive control (See **12.9**). Further investigations are carried on the kinetic parameters and inhibition mechanisms of active tyrosinase inhibitor compounds (See **12.10**). In addition, the IC₅₀, that is, the concentration of compound that causes 50% inhibition for kojic acid and the active inhibitors is determined. Dose-dependent inhibition experiments are performed in triplicate to determine the IC₅₀ of test compounds.

The hypothesis is further confirmed by conducting docking simulations between the ligands and tyrosinase (See **12.11**) using Discovery Studio 4.5. From the docking results, possible hydrogen-bonding and non-bonding interactions with the amino acid residues are studied. For the control simulation, the docking simulation of kojic acid, a well-known tyrosinase inhibitor, with tyrosinase is performed.



1a: R = 2-OMe; R¹ = 5-OMe

2a: R = 2-OMe; R¹ = 4-OMe

3a: R = 2-OMe; R¹ = 4-NO₂

4a: R = 3- NO₂; R¹ = 4- OMe

5a: R = 3-OMe; R¹ = 5-OMe

1b: R = 2-OH; R¹ = 5-OH

2b: R = 2-OH; R¹ = 4-OH

3b: R = 2-OH; R¹ = 4-NO₂

4b: R = 3- NO₂; R¹ = 4- OH

5b: R = 3-OH; R¹ = 5-OH

Scheme 1. (General method for synthesis of hydroxy azachalcones **1b-5b**). Reagents and conditions: (i) MeOH, NaOH, 0°C, 24hrs; (ii) BBr₃, CH₂Cl₂

2.3. Results and Discussion

2.3.1. Chemistry

The structures of the compounds synthesized are confirmed by ¹H NMR, ¹³C NMR, FTIR and HRMS. The most noticeable feature of the structural characterization of compounds synthesized is the assignment of the proton resonances of their α , β -unsaturated moiety, which is confirmed from the values of the vicinal coupling constants. The signals for aromatic hydrogens are seen between 6.40 and 8.40 ppm. The coupling constants for vinylic protons appear between 10.5–13.5 Hz which confirms their *trans* conformations.

Spectral data for parent azachalcone compounds (**1a-5a**)

(1a). (2*E*)-3-(2, 5-dimethoxyphenyl)-1-(pyridin-2-yl)prop-2-en-1-one. Yield: 87%; M.p: 110–112°C). ¹H NMR (CDCl₃ δ 8.36 (1H, dd, J = 9.0 Hz, H-3), 8.02 (1H, dd, J = 8.8, 9.2 Hz, H-6), 7.89 (1H, d, J = 10.5 Hz, H $_{\alpha}$), 7.82 (1H, dd, J = 9.5, 9.7 Hz, H-5) 7.65 (1H, dd, J = 10.5, 10.7 Hz, H-4'), 7.49 (1H, dd, J = 8.8, 10.2 Hz, H-4), 6.95 (1H, d, J = 12.5 Hz, H $_{\beta}$), 6.42 (s, 1H, H-6'), 6.47 (1H, dd, J = 8.3, 8.7 Hz, H-3'), 3.87 (s, 3H, Me), 3.80 (s, 3H, Me); ¹³C NMR (125MHz, DMSO-d₆) δ 205.1 (C=O), 150.8 (C1), 145.9 (C3), 137.2 (C4), 135.2 (C5), 120.9 (C6), 109.2 (C5'), 125.4 (vinylic), 140.6 (vinylic), 165.8 (C4'), 160.1 (C6'), 109.1 (C3'), 129.1 (C2'), 120.5 (C1'), 59.1 (CH₃), 55.5 (CH₃); IR (KBr) ν (cm⁻¹): 3389, 3045, 2942, 2855, 1865, 1694, 1642, 1550, 1450, 1224, 1024, 722; MS (ESI): 269.2([M + H])⁺.

(2a). (2*E*)-3-(2, 4-dimethoxyphenyl)-1-(pyridin-2-yl)prop-2-en-1-one. Yield: 85%; M.p: 122–124°C). ¹H NMR (CDCl₃ δ 8.56 (1H, dd, J = 9.5 Hz, H-3), 8.03 (1H, d, J = 9.0 Hz, H-6), 7.97 (1H, d, J = 11.0 Hz, H $_{\alpha}$), 7.84 (1H, t, J = 9.0 Hz, H-5), 7.70 (1H, d, J = 10.5 Hz, H-5'), 7.47 (1H, dd, J = 10.0 Hz, H-4), 6.97 (1H, d, J = 11.5 Hz, H $_{\beta}$), 6.47 (1H, d, J = 8.5 Hz, H-6'), 6.40 (s, 1H, H-3'), 3.89 (s, 3H, Me), 3.82 (s, 3H, Me); ¹³C NMR (125MHz, DMSO-d₆) δ 200.2 (C=O), 152.2 (C1), 147.5 (C3), 136.4 (C4), 136.7 (C5), 121.9 (C6), 109.2 (C5'), 124.9 (vinylic), 142.5 (vinylic), 165.8 (C4'), 160.1 (C6'), 109.1 (C3'), 129.1 (C2'), 120.5 (C1'), 55.1 (CH₃); IR (KBr) ν (cm⁻¹):); 3375, 3055,

2924, 2865, 1871, 1695, 1659, 1568, 1465, 1255, 1186, 1020, 742; MS (ESI): 269.2([M + H])⁺.

(3a). (2*E*)-3-(2-methoxy-4-nitrophenyl)-1-(pyridin-2-yl)prop-2-en-1-one. Yield: 78%; M.p: 127-129°C). ¹H NMR (CDCl₃ δ 8.15 (s, 1H), 7.94 (1H, m, H-6', *J* = 8.5 Hz), 7.79 (1H, d, H-5', *J* = 10.5 Hz), 8.34 (1H, dd, *J* = 9.0 Hz, H-3), 8.09 (1H, dd, *J* = 9.3, 9.6 Hz, H-6), 7.87 (1H, t, *J* = 8.0 Hz, H-5), 7.99 (1H, d, *J* = 10.0 Hz, H_α), 7.52 (1H, dd, *J* = 8.8, 9.0 Hz, H-4), 6.95 (1H, d, *J* = 10.5 Hz, H_β), 3.80 (s, 3H, Me); ¹³C NMR(125 MHz, DMSO-d₆) δ 199.2 (C=O), 150.6 (C1), 145.7 (C3), 140.2 (C4), 142.2 (C5), 120.8 (C6), 137.2 (C1'), 116.2 (C2'), 112.2 (C3'), 138.2 (C4'), 125.3 (C5'), 118.2 (C6'), 130.2 (vinylic), 144.5 (vinylic); IR (KBr) ν (cm⁻¹); 3375, 2965, 2928, 2860, 1700, 1565, 1352, 1250, 1209, 1124, 872, 715; HRMS *m/z*: 285.0869 ([M + H])⁺; Calcd: 285.0875.

(4a). (2*E*)-3-(4-methoxy-3-nitrophenyl)-1-(pyridin-2-yl)prop-2-en-1-one. Yield: 72%; M.p: 119–121°C). ¹H NMR(CDCl₃ δ 8.18 (s, 1H), 7.89 (1H, m, H-6', *J* = 8.5 Hz), 7.80 (1H, dd, H-5', *J* = 9.5 Hz), 8.39 (1H, dd, *J* = 9.8, 10.0 Hz, H-3), 8.07 (1H, dd, *J* = 8.6, 9.0 Hz, H-6), 7.85 (1H, t, *J* = 8.0 Hz, H-5), 7.94 (1H, d, *J* = 9.5 Hz, H_α), 7.53 (1H, dd, *J* = 9.0 Hz, H-4), 6.95 (1H, d, *J* = 10.0 Hz, H_β), 3.84 (s, 3H, Me); ¹³C NMR(125 MHz, DMSO-d₆) δ 200.2 (C=O), 151.4 (C1), 146.2 (C3), 140.7 (C4), 142.4 (C5), 122.4 (C6), 137.2 (C1'), 116.2 (C2'), 142.2 (C3'), 118.2 (C4'), 126.7 (C5'), 120.2 (C6'), 132.2 (vinylic), 145.2 (vinylic); IR (KBr) ν (cm⁻¹); 3450, 2950, 2924, 2854, 1690, 1535, 1295, 1224, 1122, 877, 722; HRMS *m/z*: 285.0871 ([M + H])⁺; Calcd: 285.0875.

(5a). (2*E*)-3-(3, 5-dimethoxyphenyl)-1-(pyridin-2-yl)prop-2-en-1-one. Yield: 84%; M.p: 128–130°C). ¹H NMR (CDCl₃ δ 8.38 (1H, dd, *J* = 9.8, 10.0 Hz, H-3), 8.02 (1H, dd, *J* = 8.6, 9.0 Hz, H-6), 7.89 (1H, t, *J* = 8.0 Hz, H-5), 7.97 (1H, d, *J* = 10.5 Hz, H_α), 7.07 (s, 2H, H-2' & H-6'), 7.47 (1H, dd, *J* = 8.6, 9.0 Hz, H-4), 6.94 (1H, d, *J* = 11.0 Hz, H_β), 6.47 (1H, dd, *J* = 8.5 Hz, H-3'), 3.84 (s, 6H, Me); ¹³C NMR (125MHz, DMSO-d₆) δ 199.2 (C=O), 152.3 (C1), 144.7 (C3), 139.2 (C4), 140.2 (C5), 122.8 (C6), 124.1 (vinylic), 144.5 (vinylic), 160.1 (C3' & C5'), 108.1 (C4'), 138.5 (C1'), 107.6 (C2' & C6'), 56.1(CH₃); IR (KBr) ν (cm⁻¹); 3420, 3047, 2954, 2874, 1874, 1700, 1654, 1524, 1435, 1250, 1172, 1052, 975, 722; MS (ESI); 269.2([M + H])⁺.

Spectral data for hydroxy azachalcone compounds (**1b-5b**)

(1b). (2*E*)-3-(2, 5-dihydroxyphenyl)-1-(pyridin-2-yl)prop-2-en-1-one. Yield: 62%; M.p: 140–142°C). ¹H NMR (CDCl₃ δ 10.55 (s, OH), 8.25 (1H, dd, *J* = 9.5 Hz, H-3), 8.07

(1H, dd, $J = 9.0$ Hz, H-6), 7.92 (1H, d, $J = 11.0$ Hz, H_a), 7.80 (1H, dd, $J = 7.3, 7.5$ Hz, H-5), 7.50 (1H, dd, $J = 9.5$ Hz, H-4), 6.94 (1H, d, $J = 11.5$, H_β), 7.04 (1H, s, H-6'), 7.12 (1H, t, $J = 10.5$ Hz, H-4'), 6.97 (dd, 1H, $J = 7.4, 8.0$ Hz, H-3'), 5.70 (s, OH); ¹³C NMR (125 MHz, DMSO-d₆) δ 208.1 (C=O), 150.2 (C1), 144.6 (C3), 134.8 (C4), 133.7 (C5), 122.1 (C6), 128.4 (vinyl), 144.2 (vinyl), 120.4 (C1'), 155.6 (C2'), 119.2 (C3'), 125.7 (C4'), 150.2 (C5'), 118.2 (C6'); IR (KBr) ν (cm⁻¹): 3289, 3035, 2962, 2855, 2755, 1765, 1694, 1660, 1560, 1430, 1214, 924, 722; HRMS m/z : 242.0811 ([M + H])⁺; Calcd: 242.0817.

(2b). (2*E*)-3-(2, 4-dihydroxyphenyl)-1-(pyridin-2-yl)prop-2-en-1-one. Yield: 65%; M.p: 152–154°C). ¹H NMR (CDCl₃ δ 10.57 (s, OH), 9.54 (1H, s, OH), 8.19 (1H, dd, $J = 7.5$ Hz, H-3), 8.05 (1H, dd, $J = 9.0$ Hz, H-6), 7.90 (1H, d, $J = 10.5$ Hz, H_a), 7.85 (1H, dd, $J = 8.2, 8.5$ Hz, H-5), 7.69 (1H, d, $J = 10.0$ Hz, H-5'), 7.54 (1H, dd, $J = 8.4, 9.0$ Hz, H-4), 6.90 (1H, d, $J = 11.0$ Hz, H_β), 6.47 (1H, d, $J = 8.5$ Hz, H-6'), 6.39 (1H, s, H-3'); ¹³C NMR (125 MHz, DMSO-d₆) δ 196.2 (C=O), 152.2 (C1), 145.2 (C3), 135.2 (C4), 132.3 (C5), 122.0 (C6), 125.5 (vinyl), 149.2 (vinyl), 119.7 (C1'), 166.4 (C2'), 120.3 (C3'), 170.2 (C4'), 108.5 (C5'), 128.2 (C6'); IR (KBr) ν (cm⁻¹): 3145, 3029, 2655, 2685, 1720, 1654, 1608, 1515, 1427, 1335, 1235, 1065, 925; HRMS m/z : 242.0820 ([M + H])⁺; Calcd: 242.0817.

(3b). (2*E*)-3-(2-hydroxy-4-nitrophenyl)-1-(pyridin-2-yl)prop-2-en-1-one. Yield: 47%; M.p: 138–140°C). ¹H NMR (CDCl₃ δ 10.57 (s, OH), 8.24 (s, 1H), 7.92 (1H, d, $J = 12.0$ Hz, H_β), 7.81 (1H, m, $J = 9.6, 10.0$ Hz, H-6'), 7.82 (1H, d, $J = 11.5$ Hz, H_a), 7.72 (1H, d, $J = 8.5$ Hz, H-5'), 8.10 (1H, dd, $J = 7.6, 8.0$ Hz, H-3), 8.09 (1H, dd, $J = 8.2, 9.0$ Hz, H-6), 7.87 (1H, dd, $J = 7.5, 8.0$ Hz, H-5), 7.52 (1H, dd, $J = 7.3, 10.0$ Hz, H-4); ¹³C NMR (125 MHz, DMSO-d₆) δ 194.7 (C=O), 130.4 (C1'), 167.2 (C2'), 114.7 (C3'), 139.2 (C4'), 124.2 (C5'), 120.2 (C6'), 140.2 (vinyl), 139.7 (vinyl), 154.4 (C1), 147.1 (C3), 133.2 (C4), 130.3 (C5), 124.2 (C6); IR (KBr) ν (cm⁻¹): 3152, 3129, 2645, 2350, 1745, 1648, 1525, 1435, 1325, 1234, 1128, 965, 672; HRMS m/z : 242.0824 ([M + H])⁺; Calcd: 242.0817.

(4b). (2*E*)-3-(4-hydroxy-3-nitrophenyl)-1-(pyridin-2-yl)prop-2-en-1-one. Yield: 52%; Mp: 137–139°C. ¹H NMR (500 MHz, CDCl₃): δ 10.52 (s, OH), 8.09 (s, 1H), 7.84 (1H, d, $J = 12.5$ Hz, H_β), 7.65 (1H, d, $J = 9.0$ Hz, H-5'), 7.58 (1H, d, $J = 7.0$ Hz, H-6'), 7.79 (1H, d, $J = 12.0$ Hz, H_a), 8.15 (1H, dd, $J = 9.2, 10.0$ Hz, H-3), 8.12 (1H, dd, $J = 9.0, 9.5$ Hz, H-6), 7.86 (1H, d, $J = 7.5$ Hz, H-5), 7.59 (1H, dd, $J = 10.2, 11.0$ Hz, H-4); ¹³C NMR

(125 MHz, DMSO- d_6) δ 198.6 (C=O), 124.7 (C1'), 122.1 (C2'), 137.7 (C3'), 160.4 (C4'), 116.1 (C5'), 112.9 (C6'), 129.4 (vinylic), 149.5 (vinylic), 157.2 (C1), 149.9 (C3), 134.6 (C4), 129.6 (C5), 125.8 (C6); IR (KBr) ν (cm^{-1}): 3147, 3125, 2638, 2325, 1742, 1635, 1522, 1340, 1244, 1135, 962, 662; HRMS m/z : 242.0820 ($[\text{M} + \text{H}]^+$); Calcd: 242.0817.

(5b). (2*E*)-3-(3, 5-dihydroxyphenyl)-1-(pyridin-2-yl)prop-2-en-1-one. Yield: 57%; M.p: 127–129°C). ^1H NMR (500 MHz, CDCl_3): δ 10.49 (s, OH), 7.87 (1H, d, J = 12.5 Hz, H_α), 7.27 (2H, s, H-2' & H-6'), 6.95 (1H, d, J = 13.0 Hz, H_β), 6.77 (1H, s, H-4'), 8.20 (1H, dd, J = 9.0, 9.5 Hz, H-3), 8.07 (1H, dd, J = 9.0 Hz, H-6), 7.84 (1H, dd, J = 8.2, 8.5 Hz, H-5), 7.62 (1H, dd, J = 9.5, 10.0 Hz, H-4), 5.97 (s, OH); ^{13}C NMR (125 MHz, DMSO- d_6) δ 200.6 (C=O), 145.2 (vinylic), 137.2 (vinylic), 139.4 (C1'), 110.1 (C2' & C6'), 158.3 (C3' & C5'), 109.7 (C4'), 159.2 (C1), 150.2 (C3), 135.7 (C4), 130.2 (C5), 127.4 (C6); IR (KBr) ν (cm^{-1}): 3152, 3137, 2639, 2319, 1755, 1624, 1520, 1329, 1225, 935, 662; HRMS m/z : 242.0823 ($[\text{M} + \text{H}]^+$); Calcd: 242.0817.

2.3.2. Enzyme kinetics

In the present study, tyrosinase extracted from the edible mushroom *Agaricus bisporus* is used due to its easy availability and high homology with the mammalian enzyme that renders it well suited as a model for studies on melanogenesis (Song *et al* 2005). All the hydroxy azachalcone compounds (**1b–5b**) display better tyrosinase inhibitions in comparison with the reference standard, kojic acid (**Table 2**). In particular, compounds **5b** (2*E*)-3-(3, 5-dihydroxyphenyl)-1-(pyridin-2-yl) prop-2-en-1-one and **2b** (2*E*)-3-(2, 4-dihydroxyphenyl)-1-(pyridin-2-yl) prop-2-en-1-one exhibit the greatest inhibition of L-DOPA oxidase activity (71.2%) of mushroom tyrosinase. These compounds are found to be more potent than the positive control, kojic acid (49.2%).

The tyrosinase inhibitory activity is found to be higher when the hydroxyl group is introduced in the *p*-position with respect to the *o*-position. Also, compound **2b** with a 2,4-substituted resorcinol structure shows threefold better tyrosinase inhibition (K_i : 3.9 μM) than kojic acid, probably because it has a molecular skeleton closely similar to that of L-tyrosine. Compound **1b** with a 2,5-dihydroxy substitution displays moderate (56.2%) tyrosinase inhibition. Further, the effect of electron withdrawing substituents on ring B is determined. The introduction of electron-withdrawing groups on ring B

increases the electrophilicity of the β -carbon, thus improving the bioactivity of the resulting compounds.

Presence of a strong electron releasing group in the ortho position (-OH) and an electron withdrawing group (-NO₂) in the para position in compound **3b** modulates the electronic structure of ring B significantly, that led to its better tyrosinase inhibitory potential (50.2%). In addition, substitution with an activating para hydroxy substituent brought about an improved tyrosinase inhibition as seen with compound **4b** (58.7%). This further affirms the significance of a *p*-hydroxy group on ring B for tyrosinase inhibition. Results indicate that electron-donating groups contribute more to the inhibitory activity of the compounds on mushroom tyrosinase than the electron-withdrawing groups.

L-DOPA is the substrate used to study the effect of potential inhibitor compounds **5b** and **2b** (diphenolase activity) on the oxidation of L-DOPA by tyrosinase (Kanade *et al* 2007). Results indicated that both compounds **5b** and **2b** inhibited the diphenolase activity of tyrosinase in a dose- dependent manner. With increasing concentrations of inhibitors, the remaining enzyme activity decreased exponentially. The inhibitor concentration leading to 50% activity lost (IC₅₀) for compounds **5b** and **2b** was estimated to be 10.22 μ M and 12.45 μ M, respectively (**Table 3**). The plots of the remaining enzyme activity versus the concentration of enzyme at different inhibitor concentrations gave a family of straight lines, which all passed through the origin. The presence of inhibitor did not reduce the amount of enzyme, but just resulted in an inhibition of enzyme activity.

Table 2 Inhibition effects and docking results of hydroxy azachalcones

Compound	Tyrosinase inhibition at 50 μ M (%) *	CDOCKER energy (kcal/mol)	Type of interactions	Donor-acceptor	Distance (\AA)
1b	56.2 \pm 0.12	-21.16	metal coordination bond	Cu401...OH-5'	2.58
			hydrophobic π - π stacking	ring B...His263	3.63
2b	64.5 \pm 0.25	-25.98	H-bonding	2'-OH...O δ_1 (Asn260)	1.95
			hydrophobic π - π stacking	ring B...His263	4.17
3b	50.2 \pm 0.22	-20.34	hydrophobic π - σ	ring B...Val283	2.71
			metal coordination bond	Cu401...O $_2$ N	2.40
			H-bonding	(His259) H ϵ_1 ... O $_2$ N	3.07
			hydrophobic π - σ	ring B...Val283	2.56
			hydrophobic π - π stacking	ring B...His263	4.56
			H-bonding	4'-OH...O=C (Met280)	1.91
4b	58.7 \pm 0.68	-23.89	H-bonding	(His61) H ϵ_1 ... O $_2$ N	2.45
			H-bonding	(His259) H ϵ_1 ... O $_2$ N	2.55
			hydrophobic π - π stacking	ring B...His263	4.32
			metal coordination bond	Cu401...OH-5'	2.56
5b	71.2 \pm 0.55	-27.00	H-bonding	3'-OH...O=C (Met280)	1.95
			hydrophobic π - π stacking	ring B...His263	3.70
			hydrophobic π - σ	ring B...Val283	2.78
			H-bonding	Val283 H α ...O	2.64
Kojic acid	49.8 \pm 0.11	-11.69	H-bonding	H...O=C (Met280)	2.84
			H-bonding	Asn260 H α ...O	2.93

* Hydroxyazachalcones were synthesized according to the details in Scheme 1; values indicate means \pm SE for three determinations.

The results indicate both the compounds **5b** and **2b** to be reversible inhibitors of mushroom tyrosinase for the oxidation of L-DOPA (**Figure 13**). The reaction rates were then measured in the presence of active inhibitors **5b** and **2b** with various concentrations of L-DOPA as a substrate. As the concentrations of inhibitors increased, K_m values gradually increased, but V_{max} values did not change, thereby indicating the inhibitors to act as competitive inhibitors of mushroom tyrosinase. The absorbance variations from these studies were used to generate Lineweaver–Burk plots to determine the inhibition type (**Figure 14**).

Table 3. Effect on mushroom tyrosinase activity and kinetic analysis of compounds

Compound	Type of inhibition ^{\$}	IC ₅₀ (μM) [*]	K _i (μM) [#]
1b	Competitive	20.27 ± 0.11	10.8
2b	Competitive	12.45 ± 0.33	3.9
3b	Competitive	22.95 ± 0.57	11.0
4b	Competitive	18.45 ± 0.22	10.5
5b	Competitive	10.22 ± 0.47	3.4
Kojic acid	-----	23.72 ± 0.45	11.2

^{*}(IC₅₀): refers to the concentration of compound that caused 50% inhibition.

[#]: Values were measured at 5 μM of active compounds and K_i is the (inhibitor constant).

^{\$}: Lineweaver- Burk plot of mushroom tyrosinase: Data are presented as mean values of 1/*V*, which is the inverse of the increase in absorbance at wavelength 492 nm/min (ΔA492/min), for three independent tests with different concentrations of L-DOPA as the substrate.

Dixon plots gave a family of straight lines passing through the same point at the second quadrant, giving the inhibition constant (K_i) (**Figure 15**). The K_i value estimated from this Dixon plot was 3.4 μM and 3.9 μM, respectively for the compounds **5b** and **2b**. A comparison of the *K_m* and *K_i* values of the compounds with that of kojic acid revealed them to possess much higher affinity to tyrosinase than kojic acid.

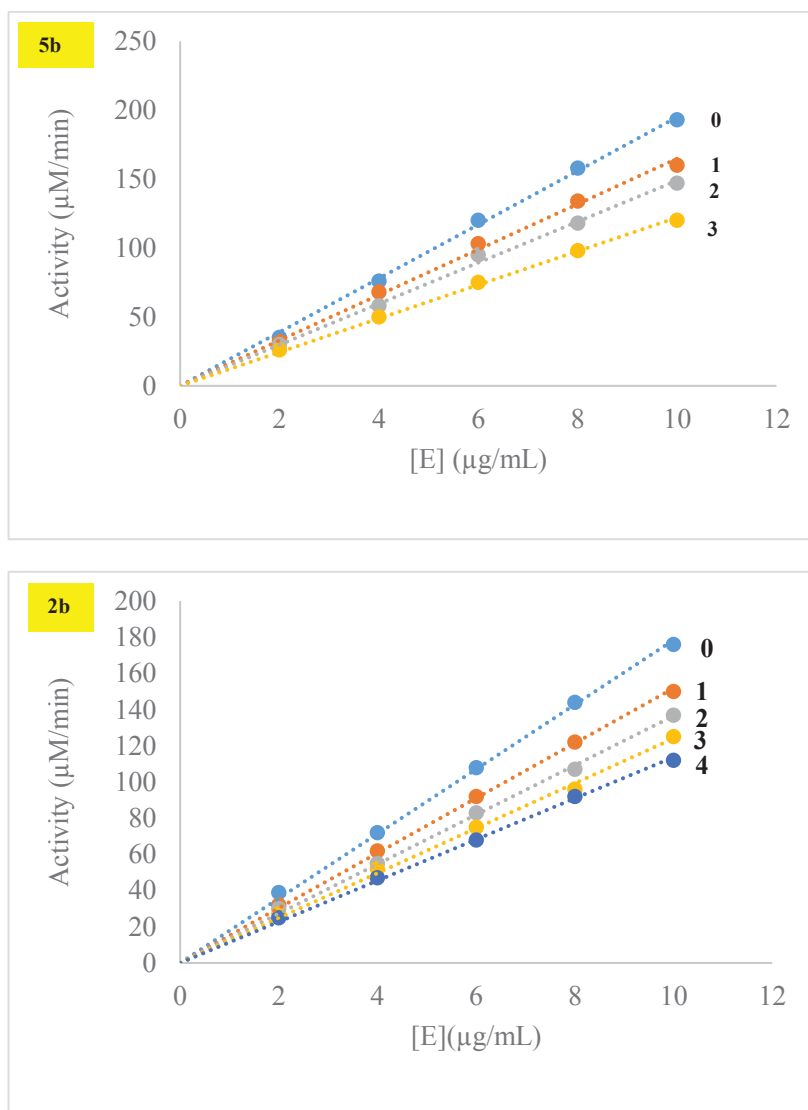


Figure 13 The inhibitory mechanism of compounds **5b** and **2b** on mushroom tyrosinase

The concentration of inhibitor used for curves 0-4 were 0, 0.25, 0.5, 1.0 and 2.0 μM, respectively.

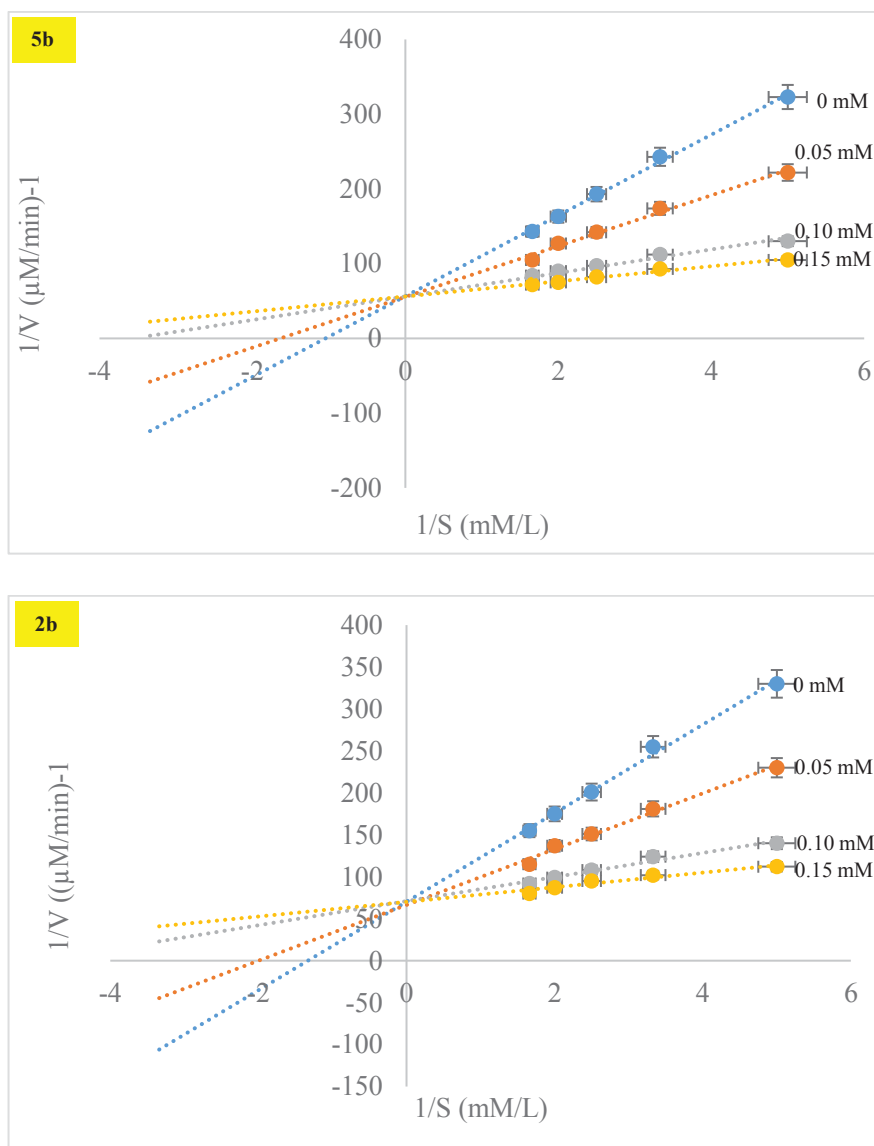


Figure 14 Lineweaver Burk plot for inhibition of compounds **5b** and **2b**

Data were obtained as mean values of $1/V$, the inverse of the absorbance increase at a wavelength of 492nm per min of three independent tests with different concentrations of L-DOPA as a substrate. The concentration of compounds **5b** and **2b** from top to bottom were 20 μM , 5 μM , 1.25 μM and 0 μM , respectively.

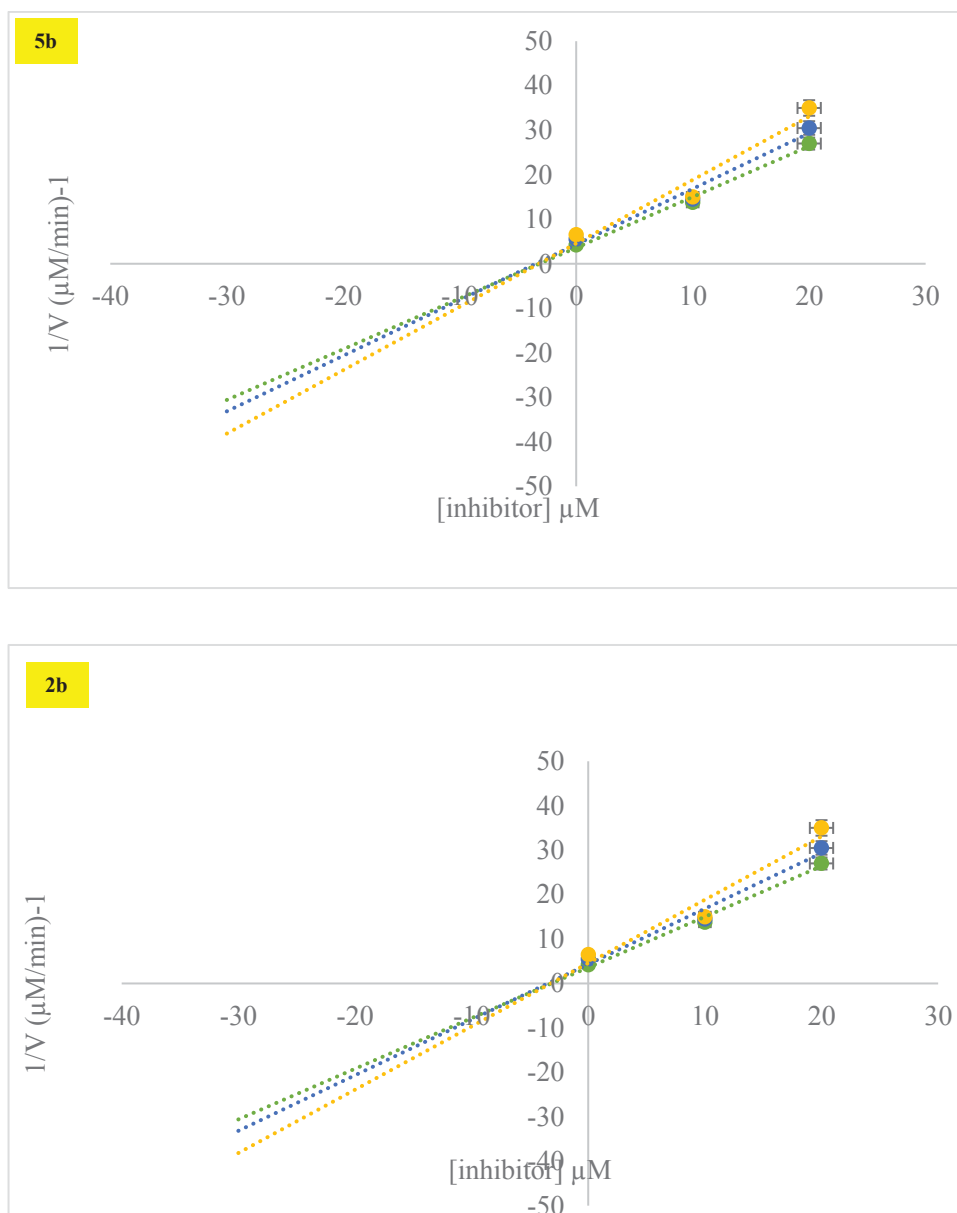


Figure 15 Dixon plot for the inhibitory effect of compounds **5b** and **2b**

The inhibitor concentrations were 0, 10 μM and 20 μM respectively. The L-DOPA concentrations were 200, 400 and 600 μM .

2.3.3. *In silico* docking studies

Accelrys Discovery Studio 4.5 suite is utilized to simulate binding between the active site of mushroom tyrosinase and substituted hydroxy azachalcone compounds. To model the tyrosinase structure, the crystal structure of *Agaricus bisporus* (**mushroom tyrosinase**) (PDB ID: 2Y9X) A chain is used. Docking procedures basically aim to identify the correct conformation of ligands in the binding pocket of a protein and to predict the affinity between the ligand and the protein. **Figure 16** shows selected docked conformations of compounds **1b–5b** along with the positive control, kojic acid in the

tyrosinase binding site. The docking simulation results support the hypothesis that the binding affinities of compounds **2b** and **5b** are higher than kojic acid, which is used as a control compound. The results of virtual screening studies indicate that the estimated CDOCKER energy of all the docked ligands range between -27.00 and -20.34 kcalmol⁻¹.

The docking score for ligand-to-receptor binding includes terms for electrostatic, van der Waals, and solvation energies. Additionally, hydrogen bonding interactions are monitored between mushroom tyrosinase and the inhibitor compounds or kojic acid (**Table 1**). The docking results indicate the positions of ligands **5b** and **2b** to be stable and depict its neighboring amino acid residues to be His85, His61, Phe292, His244, His259, Val248, His263, Asn260, Met280, Phe264, Ser282, Val283 and Ala286 which are at the most 5Å far from the compounds and which may plausibly interact with the ligands. Docking results display compound **5b** (-27.00 kcal mol⁻¹) to combine more strongly with mushroom tyrosinase than compound **2b** (-25.98 kcal mol⁻¹). Copper ion (Cu401) weakly coordinates the hydroxyl group (5'-OH) of compound **5b** at a distance of 2.56Å. Formation of a complex between a ligand and the copper ion in the active site of mushroom tyrosinase can prevent electron transfer by the metal ion. Tyrosinase substrates like L-DOPA also bind to the copper ion of tyrosinase via their hydroxy group whereas tyrosinase inhibitors like tropolone and kojic acid have been found to be competitive inhibitors by chelating the copper in the active site of the enzyme (Kahn & Andrawis 1985; Chang 2009). Compound **1b** with an IC₅₀ of 20.27µM exhibits a weak coordination with Cu401 at a distance of 2.58Å. However, the formation of a strong intramolecular hydrogen bond (2.01Å) between the 2'-OH and the carbonyl group may hamper the latter to interact with the receptor.

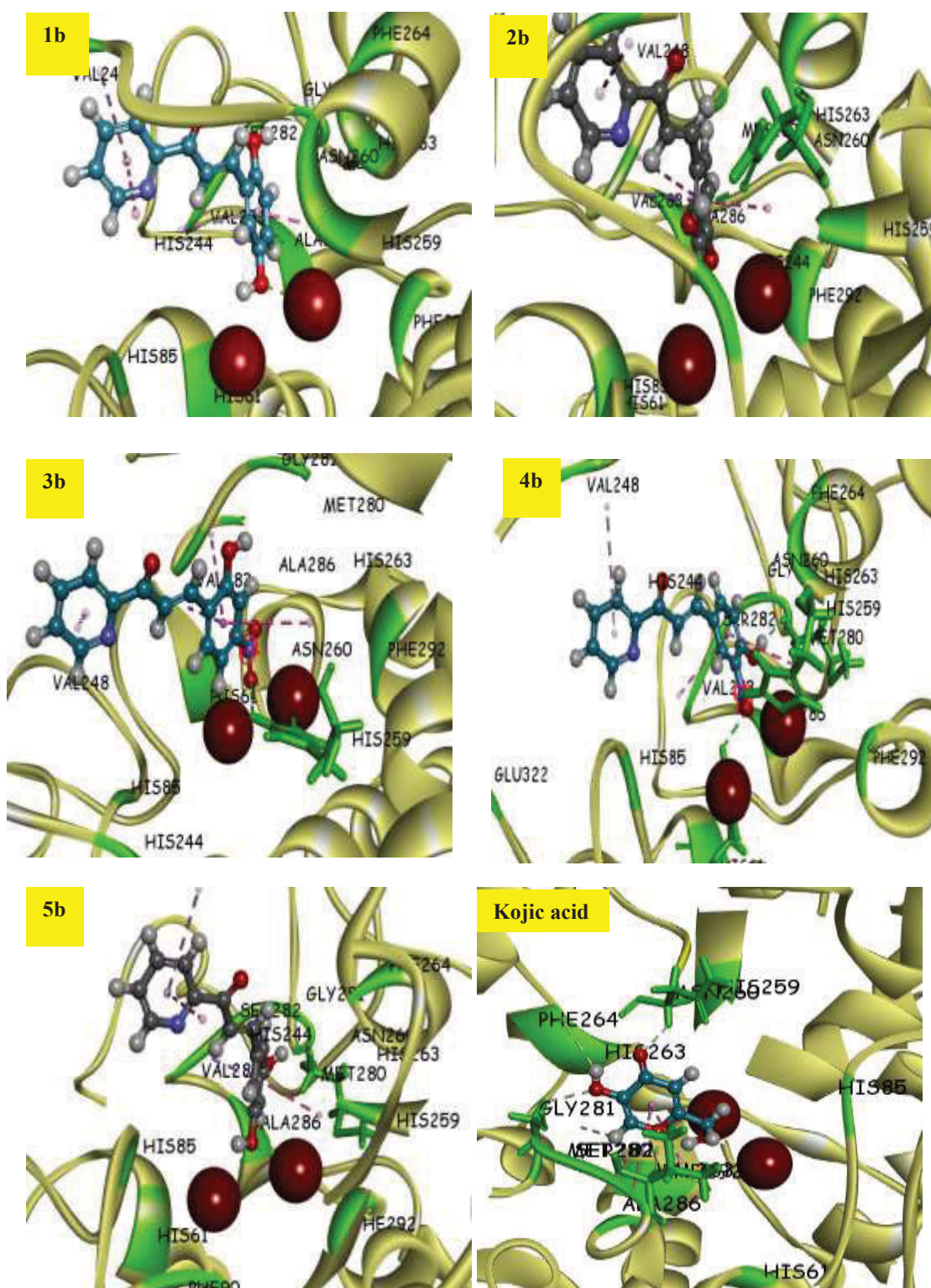
The 3'-OH group of compound **5b** forms a strong hydrogen bond (1.95Å) with the carboxylate oxygen of Met280. This helps the compound to fit into the catalytic pocket. The ligand **2b** (IC₅₀: 12.45µM) does not interact with the binuclear copper-binding site, but mainly with side chain residues in the active-site entrance. The interaction of 2'-OH of ring B in compound **2b** with Asn260 (1.95Å) emphasizes the importance of this residue located close to the entrance of the receptor. The catalytic pocket of the enzyme is hydrophobic with hydrogen bonding possibilities. Adding the ligand led to π - π interactions with the enzyme thereby enhancing drug permeability. Better intercalation of compounds **1b-5b** can be referred to their capability of forming π - π interactions that

further stabilizes its orientation in the tyrosinase catalytic pocket. It is noteworthy to mention that compounds **5b** and **2b** show π - σ interactions with Val283 while hydrophobic π - π stacking interactions are seen with His263. For kojic acid, it is observed that the compound forms hydrogen bonds with Asn260, Met280, Val283 and also a π - π interaction with His283.

2.4. Conclusion

In summary, a series of hydroxyazachalcone compounds were rigorously investigated and studied for their inhibition on the diphenolase activity of mushroom tyrosinase. Compounds **5b** and **2b** were found to be significantly more potent than kojic acid with their IC_{50} values of 10.22 μ M and 12.45 μ M, respectively. Both the compounds exhibited reversible competitive inhibition. SAR studies have identified hydroxyl as the functional group indispensable for tyrosinase inhibitory activity. Replacement of **2'-hydroxy group** resulted in a complete loss of tyrosinase inhibition. Compound **2b** with a 2,4-substituted resorcinol structure in the B-ring had structural resemblance to the substrate L-tyrosine. Moreover, the binding of the inhibitor via a coordinate bond ensured that access to the active site by the substrate was effectively blocked. This curbed the ability of the enzyme to oxidize the substrate subsequently leading to an inhibition in mushroom tyrosinase. Hence a design principle that encouraged strong coordination with the copper ions was warranted.

The soundness of the docking results and agreement with the kinetic studies suggest azachalcones to be conveniently exploited in designing inhibitors with an improved affinity for tyrosinase.



Ligands **1b–5b** are displayed as ball and stick while the core amino acid residues are displayed as stick. The green dotted lines show the hydrogen bond interactions and the purple lines show the non-bonding interactions. The ochre balls represent the copper ions.

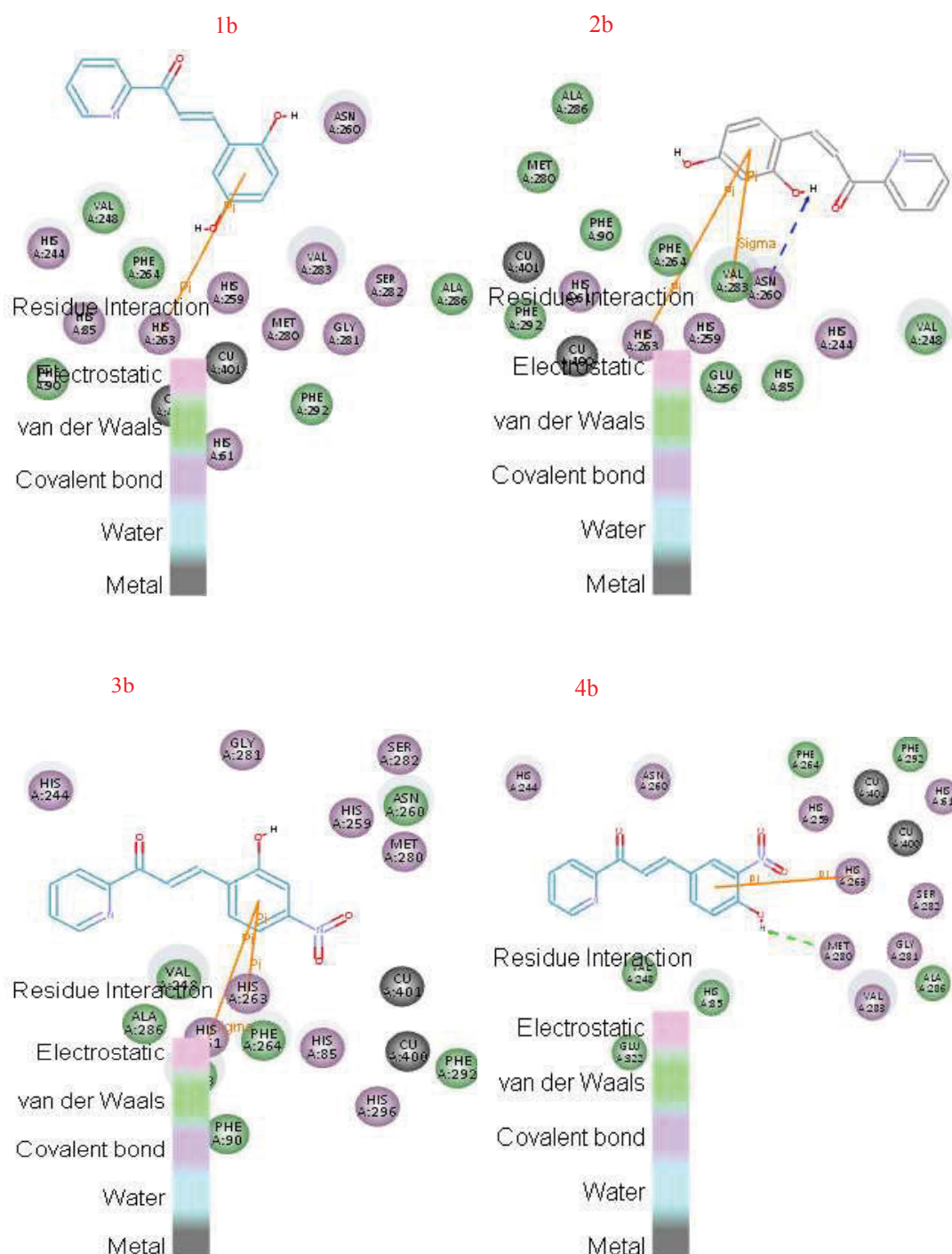


Figure 16 Docking and 2D results of compounds 1b–5b

2.5. References

Chang, TS 2009, 'An updated review of tyrosinase inhibitors', *International Journal of Molecular Sciences*, Vol 10, pp. 2440–2475.

Gao, H, Nishida, J, Saito, S, Kawabata, J 2007, 'Inhibitory effects of 5, 6, 7-trihydroxyflavones on tyrosinase', *Molecules*, Vol 12, pp. 86–97.

Kahn, V, Andrawis, A 1985, 'Inhibition of mushroom tyrosinase by tropolone', *Phytochemistry*, Vol 24, 905–908.

Kanade, SR, Suhas, VL, Chandra, N, Gowda, LR 2007, 'Functional interaction of diphenols with polyphenol oxidase. Molecular determinants of substrate/inhibitor specificity', *FEBS Journal*, Vol 274, pp. 4177–4187.

Kim, D, Park, J, Kim, J, Han, C, Yoon, J, Kim, N, Seo, J, Lee, C 2006, 'Flavonoids as mushroom tyrosinase inhibitors: a fluorescence quenching study', *Journal of Agricultural and Food Chemistry*, Vol 54, pp. 935-941.

Muñoz-Muñoz, JL, Garcia-Molina, F, Garcia-Ruíz, PA, Molina-Alarcon, M, Tudela, J, Garcia-Canovas, F, Rodriguez-Lopez, JN 2008, 'Phenolic substrates and suicide inactivation of tyrosinase: kinetics and mechanism', *Biochemical Journal*, Vol 416, pp. 431–440.

Nowakowska, Z, Wyrzykiewicz, E, Kedzia, B 2001, 'Synthesis and antimicrobial properties of N-substituted derivatives of (E)-4-azachalcones', *Farmaco*, Vol 56, pp. 325–329.

Nowakowska, Z, Wyrzykiewicz, E, Kedzia, B 2002, 'Antimicrobial activity of some N-alkyl substituted of (E)-4-azachalconium and (E)-3'-hydroxy-4-azachalconium bromides', *Farmaco*, Vol 57, pp. 657–661.

Rao, YK, Fang, SH, Tzeng, YM 2009, 'Synthesis and biological evaluation of 3', 4', 5'-trimethoxychalcone analogues as inhibitors of zinc oxide production and tumor cell proliferation', *Bioorganic and Medicinal Chemistry*, Vol 17, pp. 7909–7914.

Shiino, M, Watanabe, Y, Umezawa, K 2001, 'Synthesis of *N*-substituted *N*-nitrosohydroxylamines as inhibitors of mushroom tyrosinase', *Bioorganic and Medicinal Chemistry*, Vol 9, pp. 1233–1240.

Shiino, M, Watanabe, Y, Umezawa, K 2003, 'Synthesis of tyrosinase inhibitory activity of novel *N*-hydroxybenzyl-*N*-nitrosohydroxylamines', *Bioorganic Chemistry*, Vol 31, pp. 129–135.

Song, KK, Chen, QX, Wang, Q, Qiu, L, Huang, H 2005, 'Inhibitory effects of 4-vinylbenzaldehyde and 4-vinylbenzoic acid on the activity of mushroom tyrosinase', *Journal of Enzyme Inhibition and Medicinal Chemistry*, Vol 20, pp. 239–243.

Yamazaki, Y, Kawano, Y, Yamanaka, A, Maruyama, S 2009, 'N-[(Dihydroxyphenyl)acyl] serotoninins as potent inhibitors of tyrosinase from mouse and human melanoma cells', *Bioorganic and Medicinal Chemistry Letters*, Vol 19, pp. 4178–4182.

Yan, Q, Cao, R, Yi, W, Yu, L, Chen, Z, Ma, L, Song, H 2009, 'Synthesis and evaluation of 5-benzylidene(thio)barbiturate-beta-D-glycosides as mushroom tyrosinase inhibitors', *Bioorganic and Medicinal Chemistry Letters*, Vol 19, pp. 4055–4058.

Yayli, N, Üçüncü, O, Yaşar, A, Küçük, M, Kahriman, N, Akyuz, E, Karaoğlu, A 2006, 'Synthesis and biological activities of N-alkyl derivatives of *o*-, *m*- and *p*-nitro (E)-4-azachalcones and stereo selective photochemistry in solution, with theoretical calculations', *Turkish Journal of Chemistry*, Vol 30, pp. 505–514.

Yayli, N, Küeçüek, M, Ücüencü, O, Yaşar, A, Kahriman, N, Karaoglu, A 2007, 'Synthesis of N-alkyl derivatives and photochemistry of nitro (E)-3-azachalcones with theoretical calculations and biological activities', *Journal of Photochemistry and Photobiology A-Chemistry*, Vol 188, pp. 161–168.

CHAPTER 3

HYDROXYNAPHTHYLCHALCONES

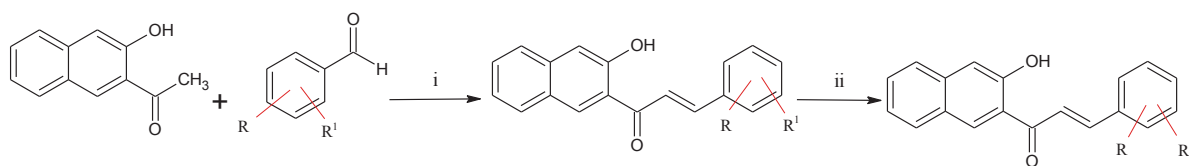
3.1. Introduction

Despite reports of a large number of tyrosinase inhibitors, only a few are used today because of their limitations with regard to cytotoxicity, selectivity, and stability (Martinez & Whitaker 1995; McEvily *et al* 1992; Kahn 1995; Fujimoto *et al* 1999; Sun *et al* 2012; Ennes, Paschoalick & Alchorne 2000).

Furthermore, several hydroxy-substituted 2-phenylnaphthalene derivatives have been reported as potent tyrosinase inhibitors. Among them, 4-(6-hydroxy-2-naphthyl)-1,3-benzendiols (HNB) and 5-(6-hydroxy-2-naphthyl)-1,2,3-benzendiols (5HNB) are found to inhibit mushroom tyrosinase activity (Song *et al* 2007; Ha *et al* 2007; Choi *et al* 2010). Docking studies have revealed better tyrosinase inhibition with the naphthyl moiety in comparison with the reference standard, kojic acid. Another structural advantage is attributed to the naphthyl ring that can exert a nucleophilic action on the dihydroxy phenyl ring. Hence, in the continuous effort to search for potential tyrosinase inhibitors and to develop a new template, a series of novel hydroxy substituted naphthylchalcone compounds are designed and synthesized for application as effective polyphenol oxidase inhibitors.

3.2. Experimental

Two step synthesis protocol as depicted in **Scheme 2** was employed for the synthesis of naphthylchalcone derivatives. The parent naphthylchalcones were synthesized by the base catalyzed Claisen-Schmidt condensation of 2'-hydroxy-1'-acetonaphthone with an appropriate aldehyde in a polar solvent like methanol. The methoxy naphthylchalcones were then successfully dealkylated to their corresponding hydroxy compounds in the presence of boron tribromide.



6a: R = 2-OMe; R¹ = 5-OMe

6b: R = 2-OH; R¹ = 5-OH

7a: R = 2-OMe; R¹ = 4-OMe

7b: R = 2-OH; R¹ = 4-OH

8a: R = 2-OMe; R¹ = 4-NO₂

8b: R = 2-OH; R¹ = 4-NO₂

9a: R = 3-NO₂; R¹ = 4-OMe

9b: R = 3-NO₂; R¹ = 4-OH

10a: R = 3-OMe; R¹ = 5-OMe

10b: R = 3-OH; R¹ = 5-OH

Scheme 2. General method for synthesis of hydroxy naphthylchalcones **6b-10b**.

Reagents and conditions: (i) MeOH, NaOH, 0° C, 24hrs; (ii) BBr₃, CH₂Cl₂

3.2.1. Method for synthesis of compound 10b

To a stirred solution of 2'-hydroxy-1'-acetonaphthone (1 mM, 186 mg) and 3, 5-dimethoxybenzaldehyde (1mM, 166mg) in 25 ml methanol, was added pulverized NaOH (2mM) and the mixture was stirred at room temperature for 24–36 h. The reaction was monitored by TLC using *n*-hexane: ethyl acetate (7:3) as mobile phase. The reaction mixture was cooled to 0°C (ice-water bath) and acidified with HCl (10 % v/v aqueous solution) to afford total precipitation of the compound. A yellowish orange precipitate was formed, which was filtered and washed with 10 % aqueous HCl solution. The product obtained was recrystallized with ethylacetate to give the pure chalcone product **10a**. A solution of BBr₃ (5.0 ml) was added to a cooled solution of the chalcone compound **10a** (1 mM, 334mg) in CH₂Cl₂ under argon. The cooling bath was removed and the dark solution was warmed to RT and stirred for 1-5hrs. The dark solution was then poured into ice water and filtered. The aqueous layer was extracted with chloroform twice. The organic extract was washed with water followed by brine and dried over anhydrous sodium sulfate. This was then rotary evaporated to give the respective hydroxy derivative **10b**.

Spectral data for parent naphthylchalcones

(6a). (2*E*)-3-(2,5-dimethoxyphenyl)-1-(3-hydroxynaphthalen-2-yl)prop-2-en-1-one. Yield: 80%; M.p 114–116°C. ¹H NMR (500 MHz, CDCl₃): δ 12.54 (s, 1H, OH), 8.12

(dd, 1H, $J=11.5, 12.5$, H-10'), 7.96 (d, 1H, $J=13.0$, H_a), 7.85 (s, 1H, H-6), 7.80 (dd, 1H, $J=8.6, 10.0$, H-5'), 7.67 (d, 1H, $J=8.5$, H-7'), 7.59 (dd, 1H, $J=8.5, 9.0$, H-8'), 7.52 (d, 1H, $J=9.5$, H-6'), 7.49 (d, 1H, $J=9.5$, H-3'), 6.92 (d, 1H, $J=13.5$, H_β), 6.57 (d, 1H, $J=10.0$, H-4), 6.49 (dd, 1H, $J=9.0, 9.5$, H-3), 3.82 (s, 3H), 3.80 (s, 3H); ¹³C NMR (125 MHz, DMSO-d₆) δ 195.2 (C=O), 116.5 (C1'), 166.2 (C2'), 123.2 (C3'), 136.1 (C4'), 130.4 (C5'), 134.0 (C6'), 128.4 (C7'), 130.0 (C8'), 122.4 (C9'), 131.2 (C10'), 142.4 (vinylic), 131.7 (vinylic), 129.2 (C1), 156.6 (C2), 112.3 (C3), 126.4 (C4), 153.2 (C5), 112.2 (C6), 56.2 (Me); IR (KBr) ν (cm⁻¹): 3022, 2992, 2773, 1682, 1550, 1425, 1046, 814, 707; MS (ESI): 335.1 ([M + H])⁺.

(7a). (2*E*)-3-(2,4-dimethoxyphenyl)-1-(3-hydroxynaphthalen-2-yl)prop-2-en-1-one. Yield: 76%; M.p 87–89°C. ¹H NMR (500 MHz, CDCl₃): δ 12.72 (s, 1H, OH), 8.19 (dd, 1H, $J=15.0$, H-10'), 7.98 (d, 1H, $J=14.5$, H_a), 7.82 (dd, 1H, $J=10.5, 12.0$, H-5'), 7.78 (dd, 1H, $J=10.0$, H-6), 7.63 (t, 1H, $J=8.5$, H-7'), 7.57 (dd, 1H, $J=8.0$, H-8'), 7.49 (dd, 1H, $J=9.0$, H-6'), 7.47 (d, 1H, $J=9.0$, H-3'), 7.09 (d, 1H, $J=15.0$, H_β), 6.53 (t, 1H, $J=16.0$, H-5), 6.44 (m, 1H, $J=9.0$, H-3), 3.86 (s, 3H), 3.88 (s, 3H); ¹³C NMR (125 MHz, DMSO-d₆) δ 194.6 (C=O), 114.1 (C1'), 165.0 (C2'), 122.2 (C3'), 137.1 (C4'), 130.4 (C5'), 132.6 (C6'), 126.1 (C7'), 128.4 (C8'), 124.4 (C9'), 133.2 (C10'), 140.8 (vinylic), 130.5 (vinylic), 119.2 (C1), 162.6 (C2), 99.3 (C3), 166.2 (C4), 107.2 (C5), 130.2 (C6), 55.6 (Me); IR (KBr) ν (cm⁻¹): 3018, 2957, 2781, 2614, 1679, 1562, 1427, 1375, 1218, 1102, 817, 717, 605; MS (ESI): 335.1 ([M + H])⁺.

(8a). (2*E*)-1-(2-hydroxyphenyl)-3-(2-methoxy-4-nitrophenyl)prop-2-en-1-one. Yield: 72%; Mp: 123–125°C; ¹H NMR (500 MHz, CDCl₃): δ 12.22 (s, 1H, OH), 8.22 (s, 1H), 7.95 (d, 1H, $J=13.5$, H_β), 7.86 (m, 1H, $J=9.5$, H-6), 7.80 (d, 1H, $J=14.0$, H_a), 7.75 (d, 1H, $J=10.5$, H-6'), 7.69 (d, 1H, $J=8.5$, H-5), 7.59 (dd, 1H, $J=7.8, 8.5$, H-4'), 7.02 (dd, 1H, $J=8.5, 9.0$, H-3'), 6.97 (m, 1H, $J=10.0$, H-5'), 3.82 (s, 3H); ¹³C NMR (125 MHz, DMSO-d₆) δ 194.2 (C=O), 130.2 (C6'), 119.3 (C1'), 118.2 (C5'), 137.0 (C4'), 118.4 (C3'), 162.9 (C2'), 128.2 (C1), 115.2 (C2), 112.2 (C3), 137.5 (C4), 122.4 (C5), 116.5 (C6), 125.5 (vinylic), 140.8 (vinylic); IR (KBr) ν (cm⁻¹): 3250, 3345, 3015, 2910, 2865, 2700, 1702, 1682, 1552, 1465, 1305, 979, 735, 680, 575; MS (ESI): 270.1 ([M + H])⁺.

9a. (2*E*)-1-(2-hydroxyphenyl)-3-(4-methoxy-3-nitrophenyl)prop-2-en-1-one. Yield: 68%; Mp: 110–112°C; ¹H NMR (500 MHz, CDCl₃): δ 12.47 (s, 1H, OH), 8.10 (s, 1H), 7.86 (d, 1H, $J=12.5$, H_β), 7.74 (d, 1H, $J=10.0$, H-6'), 7.72 (d, 1H, $J=12.0$, H_a), 7.65 (d,

1H, $J = 9.5$, H-5), 7.54 (d, 1H, $J = 8.0$, H-6), 7.49 (t, 1H, $J = 8.5$, H-4'), 6.92 (dd, 1H, $J = 9.5$, H-3'), 6.90 (dd, 1H, $J = 8.2$, 9.0, H-5'), 3.86 (s, 3H); ^{13}C NMR (125 MHz, DMSO- d_6) δ 192.22 (C=O), 130.52 (C6'), 119.25 (C1'), 118.27 (C5'), 136.77 (C4'), 118.28 (C3'), 161.92 (C2'), 126.90 (C1), 120.54 (C2), 137.22 (C3), 147.50 (C4), 112.42 (C5), 114.23 (C6), 56.67 (Me), 122.40 (vinylic), 141.83 (vinylic); IR (KBr) ν (cm^{-1}): 3200, 3070, 2914, 2864, 2720, 1686, 1578, 1550, 1468, 1349, 970, 720, 580; MS (ESI): 270.1 ($[\text{M} + \text{H}]^+$).

(10a). (2*E*)-3-(3,5-dimethoxyphenyl)-1-(3-hydroxynaphthalen-2-yl)prop-2-en-1-one. Yield: 85%; M.p 118–120°C). ^1H NMR (500 MHz, CDCl_3): δ 12.62 (s, 1H, OH), 7.92 (dd, 1H, $J = 10.0$, H-10'), 7.85 (d, 1H, $J = 10.0$, H_a), 7.82 (dd, 1H, $J = 10.5$, H-5'), 7.69 (t, 1H, $J = 9.5$, H-7'), 7.58 (dd, 1H, $J = 8.4$, 9.5, H-8'), 7.55 (m, 1H, $J = 8.5$, H-6'), 7.50 (d, 1H, $J = 9.0$, H-3'), 7.09 (dd, 2H, H-2 & H-6), 7.07 (d, 1H, $J = 10.5$, H_β), 6.75 (s, 1H, H-4), 3.90 (s, 6H); ^{13}C NMR (125 MHz, DMSO- d_6) δ 198.5 (C=O), 118.1 (C1'), 167.2 (C2'), 124.2 (C3'), 140.4 (C4'), 135.3 (C5'), 135.2 (C6'), 124.9 (C7'), 130.2 (C8'), 124.1 (C9'), 134.5 (C10'), 144.0 (vinylic), 133.2 (vinylic), 138.2 (C1), 106.6 (C2 & C6), 163.3 (C3 & C5), 106.2 (C4), 55.2 (Me); IR (KBr) ν (cm^{-1}): 3062, 2947, 2729, 2514, 1692, 1597, 1512, 1436, 1208, 1054, 871, 732; MS (ESI): 335.1 ($[\text{M} + \text{H}]^+$).

Spectral data for hydroxy derivatives of naphthylchalcones

(6b). (2*E*)-3-(2,5-dihydroxyphenyl)-1-(3-hydroxynaphthalen-2-yl)prop-2-en-1-one. Yield: 55%; M.p: 134–136°C. ^1H NMR (500 MHz, CDCl_3): δ 12.25 (s, 1H, OH), 10.60 (s, OH), 8.09 (dd, 1H, $J = 12.5$, H-10'), 7.87 (d, 1H, $J = 11.0$, H_a), 7.05 (s, 1H, H-6), 7.82 (dd, 1H, $J = 10.5$, H-5'), 7.67 (dd, 1H, $J = 7.4$, 8.0, H-7'), 7.62 (dd, 1H, $J = 8.8$, 9.5, H-8'), 7.57 (dd, 1H, $J = 8.5$, H-6'), 7.42 (d, 1H, $J = 9.5$, H-3'), 7.17 (t, 1H, $J = 10.0$, H-4), 6.91 (dd, 1H, $J = 9.0$, H-3), 6.89 (d, 1H, $J = 11.5$, H_β), 5.70 (s, OH); ^{13}C NMR (125 MHz, DMSO- d_6) δ 195.2 (C=O), 118.2 (C1'), 165.7 (C2'), 124.2 (C3'), 135.2 (C4'), 130.1 (C5'), 132.5 (C6'), 130.4 (C7'), 129.0 (C8'), 122.2 (C9'), 130.8 (C10'), 145.4 (vinylic), 130.5 (vinylic), 120.3 (C1), 155.7 (C2), 118.3 (C3), 125.6 (C4), 149.2 (C5), 118.2 (C6); IR (KBr) ν (cm^{-1}): 3285, 3032, 2965, 2873, 2755, 1750, 1662, 1627, 1561, 1431, 1377, 1210, 966, 719; HRMS m/z : 307.0963 ($[\text{M} + \text{H}]^+$); Calcd: 307.0970.

(7b). (2*E*)-3-(2,4-dihydroxyphenyl)-1-(3-hydroxynaphthalen-2-yl)prop-2-en-1-one. Yield: 47%; M.p: 164–166°C). ^1H NMR (500 MHz, CDCl_3): δ 12.45 (s, 1H, OH), 10.54 (s, OH), 9.70 (s, OH), 8.15 (dd, 1H, $J = 15.0$, H-10'), 7.92 (d, 1H, $J = 11.5$, H_a), 7.85 (dd,

1H, $J = 10.0$, H-5'), 7.78 (dd, 1H, $J = 10.5$, H-6), 7.62 (t, 1H, $J = 9.5$, H-7'), 7.55 (dd, 1H, $J = 7.4$, 8.0, H-8'), 7.51 (dd, 1H, $J = 9.0$, H-6'), 7.49 (d, 1H, $J = 8.5$, H-3'), 7.09 (d, 1H, $J = 12.0$, H $_{\beta}$), 6.59 (dd, 1H, $J = 11.0$, H-5), 6.47 (s, 1H, H-3); ^{13}C NMR (125 MHz, DMSO- d_6) δ 197.8 (C=O), 117.5 (C1'), 167.0 (C2'), 122.4 (C3'), 139.1 (C4'), 130.4 (C5'), 134.5 (C6'), 125.5 (C7'), 129.2 (C8'), 124.2 (C9'), 135.2 (C10'), 142.4 (vinyllic), 130.2 (vinyllic), 120.2 (C1), 166.7 (C2), 118.3 (C3), 169.2 (C4), 105.2 (C5), 130.2 (C6); IR (KBr) ν (cm^{-1}): 3129, 3045, 2657, 2781, 2614, 1683, 1614, 1500, 1437, 1335, 1248, 1166, 967, 662; HRMS m/z : 307.0965 ($[\text{M} + \text{H}]^+$); Calcd: 307.0970.

(8b). (2*E*)-1-(3-hydroxynaphthalen-2-yl)-3-(2-hydroxy-4-nitrophenyl)prop-2-en-1-one. Yield: 42%; M.p: 153–155°C. ^1H NMR (500 MHz, CDCl_3): δ 12.50 (s, 1H, OH), 10.55 (s, OH), 8.27 (s, 1H), 7.93 (d, 1H, $J = 12.5$, H $_{\beta}$), 7.89 (m, 1H, $J = 10.5$, H-6), 7.79 (d, 1H, $J = 12.0$, H $_{\alpha}$), 7.77 (d, 1H, $J = 9.5$, H-6'), 7.70 (d, 1H, $J = 7.5$, H-5), 7.57 (dd, 1H, $J = 7.8$, 8.5, H-4'), 7.09 (dd, 1H, $J = 8.5$, 9.5, H-3'), 6.97 (m, 1H, $J = 10.5$, H-5'); ^{13}C NMR (125 MHz, DMSO- d_6) δ 197.5 (C=O), 130.4 (C6'), 120.3 (C1'), 118.2 (C5'), 138.2 (C4'), 119.4 (C3'), 164.9 (C2'), 128.2 (C1), 165.4 (C2), 112.2 (C3), 137.5 (C4), 122.7 (C5), 118.2 (C6), 138.0 (vinyllic), 140.7 (vinyllic); IR (KBr) ν (cm^{-1}): 3370, 3254, 3085, 2960, 2869, 1697, 1682, 1532, 1479, 1365, 984, 760, 687; HRMS m/z : 336.0866 ($[\text{M} + \text{H}]^+$); Calcd: 336.0872.

(9b). (2*E*)-1-(3-hydroxynaphthalen-2-yl)-3-(4-hydroxy-3-nitrophenyl)prop-2-en-1-one. Yield: 56%; M.p: 110–112°C. ^1H NMR (500 MHz, CDCl_3): δ 12.45 (s, 1H, OH), 10.57 (s, OH), 8.15 (s, 1H), 7.89 (d, 1H, $J = 13.5$, H $_{\beta}$), 7.77 (d, 1H, $J = 10.0$, H-6'), 7.74 (d, 1H, $J = 13.0$, H $_{\alpha}$), 7.69 (d, 1H, $J = 10.0$, H-5), 7.55 (d, 1H, $J = 7.5$, H-6), 7.54 (t, 1H, $J = 8.0$, H-4'), 6.90 (dd, 1H, $J = 8.5$, 9.0, H-3'), 6.90 (dd, 1H, $J = 8.2$, 9.0, H-5'); ^{13}C NMR (125 MHz, DMSO- d_6) δ 194.2 (C=O), 130.5 (C6'), 120.5 (C1'), 118.7 (C5'), 136.7 (C4'), 117.8 (C3'), 160.2 (C2'), 125.9 (C1), 120.4 (C2), 139.2 (C3), 159.5 (C4), 112.4 (C5), 114.2 (C6), 127.4 (vinyllic), 147.3 (vinyllic); IR (KBr) ν (cm^{-1}): 3230, 3074, 2954, 2855, 1720, 1687, 1558, 1468, 1369, 1267, 1156, 920, 836, 660; HRMS m/z : 336.0864 ($[\text{M} + \text{H}]^+$); Calcd: 336.0872.

(10b). (2*E*)-3-(3,5-dihydroxyphenyl)-1-(3-hydroxynaphthalen-2-yl)prop-2-en-1-one. Yield: 44%; M.p: 148–150°C. ^1H NMR (500 MHz, CDCl_3): δ 12.20 (s, 1H, OH), 10.75 (s, OH), 7.97 (dd, 1H, $J = 10.0$, H-10'), 7.84 (d, 1H, $J = 11.0$, H $_{\alpha}$), 7.79 (dd, 1H, $J = 9.5$, H-5'), 7.73 (t, 1H, $J = 9.0$, H-7'), 7.57 (dd, 1H, $J = 7.5$, H-8'), 7.54 (dd, 1H, $J = 7.8$, 8.5, H-6'), 7.49 (d, 1H, $J = 8.0$, H-3'), 7.12 (dd, 2H, H-2 & H-6), 6.97 (d, 1H, $J = 11.5$, H $_{\beta}$),

6.74 (s, 1H, H-4), 5.95 (s, OH); ^{13}C NMR (125 MHz, DMSO- d_6) δ 200.2 (C=O), 120.1 (C1'), 168.2 (C2'), 125.3 (C3'), 139.7 (C4'), 136.2 (C5'), 137.2 (C6'), 125.2 (C7'), 132.6 (C8'), 127.1 (C9'), 135.2 (C10'), 144.7 (vinylic), 135.2 (vinylic), 137.1 (C1), 108.6 (C2 & C6), 160.3 (C3 & C5), 108.7 (C4); IR (KBr) ν (cm^{-1}): 3278, 3041, 2955, 2870, 2760, 1749, 1659, 1549, 1424, 1376, 1224, 972, 724; HRMS m/z : 307.0967 ($[\text{M} + \text{H}]^+$); Calcd: 307.0970.

3.3. Results and Discussion

All the hydroxynaphthylchalcone compounds (**6b-10b**) exhibited better tyrosinase inhibitions in comparison with the reference standard, kojic acid (**Table 4**).

3.3.1. Chemistry

The method was versatile and convenient, though yields may be variable. In terms of the structure- activity relationships, compound **10b** (*(2E)*-3-(3,5-dihydroxyphenyl)-1-(3-hydroxynaphthalen-2-yl)prop-2-en-1-one) exhibited the most potent tyrosinase inhibitory activities with inhibitions of 68.5%. Compound **10b** had a structural resemblance with resveratrol that was reported to be a powerful reversible tyrosinase inhibitor (Franco *et al* 2012). The hydroxyl groups in compounds carried out the nucleophilic attack on the copper atoms in the active site of the enzyme and were directly involved in transferring protons during catalysis, which then resulted in inactivation of the tyrosinase. Moreover, the tyrosinase inhibitory activity was higher when the hydroxyl group was introduced in the *p*-position with respect to the *o*-position. Compound **7b** (*(2E)*-3-(2, 4-dihydroxyphenyl)-1-(3-hydroxynaphthalen-2-yl)prop-2-en-1-one) with a 2,4-substituted resorcinol structure displayed threefold better tyrosinase inhibition (K_i : 4.5 μM) than kojic acid (K_i : 12.2 μM), probably because it resulted in a molecular skeleton closely similar to that of L-tyrosine. Compound **6b** with a 2,5-dihydroxy substitution showed moderate (56.2%) tyrosinase inhibition.

Table 4 Inhibition and docking results of hydroxynaphthylchalcones

Compound	Tyrosinase inhibition at 50 μ M (%) *	CDOCKER energy (kcal/mol)	Type of interactions	Donor-acceptor	Distance (\AA)
6b	56.2 \pm 0.12	-22.35	Intramolecular H-bonding	2'-OH...O=C	2.02
			metal coordination bond	Cu401...OH-5	2.53
			hydrophobic π - π stacking	ring B...His263	3.55
7b	62.5 \pm 0.45	-19.25	H-bonding	2-OH...O δ_1 (Asn260)	1.99
			hydrophobic π - π stacking	ring B...His263	4.07
			hydrophobic π - σ	ring B...Val283	2.75
8b	55.5 \pm 0.25	-16.83	Intramolecular H-bonding	2'-OH...O=C	1.97
			metal coordination bond	Cu401...O $_2$ N	2.40
			H-bonding	2-OH...O δ_1 (Asn260)	1.98
			hydrophobic π - σ	ring B...Val283	2.56
			hydrophobic π - π stacking	ring B...His263	4.40
9b	51.2 \pm 0.68	-16.23	H-bonding	Asn260 H δ_{22} ...O=C	2.59
			H-bonding	4-OH...O=C (Met280)	2.80
			H-bonding	(His85) H δ_2 ... O $_2$ N	2.52
			H-bonding	(His259) H ϵ_1 ... O $_2$ N	2.46
			π -cationic bonding	(Arg268) NH $_1$...ring A	4.02
			hydrophobic π - π stacking	ring B...His263	4.32
10b	68.5 \pm 0.22	-22.36	H-bonding	3-OH...O=C (Met280)	1.91
			metal coordination bond	Cu401...OH-5	1.95
			hydrophobic π - π stacking	ring B...His263	3.64
Kojic acid	49.5 \pm 0.66	-11.69	H-bonding	Asn260 H α ...O	2.93
			H-bonding	Val283 H α ...O	2.64
			H-bonding	H... O=C (Met280)	2.84

* Naphthylchalcone derivatives were synthesized according to the details in Scheme 1; values indicate mean \pm S.E for three determinations.

Further, the effect of electron withdrawing substituents on ring B was determined. The introduction of electron-withdrawing groups on ring B increased the electrophilicity of the β -carbon, thus improving the bioactivity of the resulting compounds. Presence of a strong electron releasing group in the ortho position (-OH) and an electron withdrawing group (-NO₂) in the para position in compound **8b** modulated the electronic structure of ring B significantly, that accounted to its better tyrosinase inhibitory potential (55.5%). However, substitution with less activating para hydroxy substituent resulted in a fall of tyrosinase inhibitory activity as seen with compound **9b** (51.2%). Results indicated that electron-donating groups contributed more to the inhibitory activity of the compounds on mushroom tyrosinase than the electron-withdrawing groups.

3.3.2. Kinetics

Results indicated that both compounds **10b** and **7b** could inhibit the diphenolase activity of tyrosinase in a dose-dependent manner. With increasing concentrations of inhibitors, the remaining enzyme activity decreased exponentially. The inhibitor concentration leading to 50% activity lost (IC₅₀) for compounds **10b** and **7b** was estimated to be 10.4 μ M and 14.4 μ M, respectively (**Figure 17**).

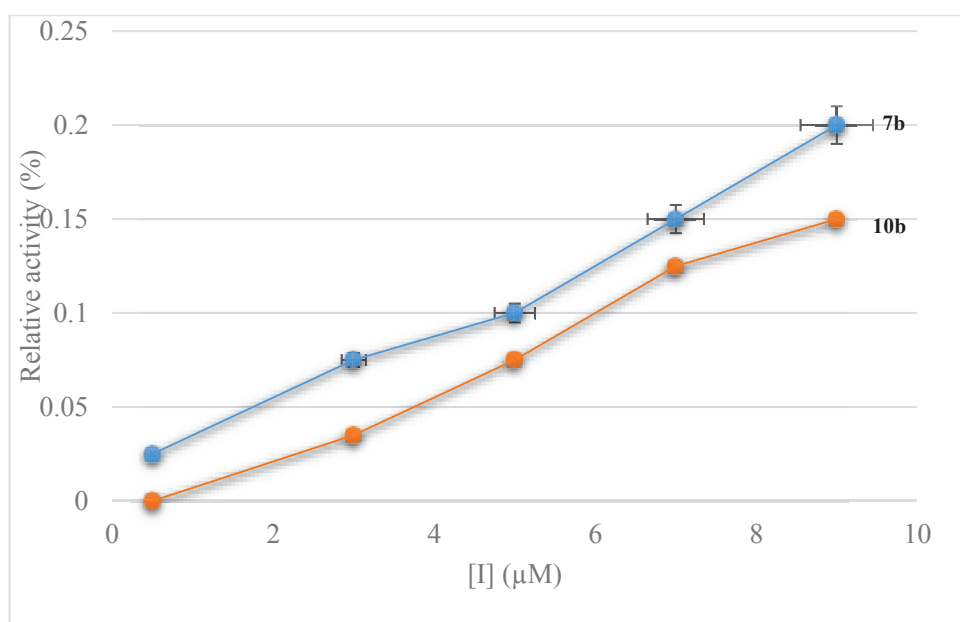


Figure 17 Inhibition effects of compounds 10b and 7b.

Data are presented as means (n = 3).

The plots of the remaining enzyme activity versus the concentration of enzyme at different inhibitor concentrations gave a family of straight lines, which all passed through the origin. The presence of inhibitor did not reduce the amount of enzyme, but just resulted in the inhibition of enzyme activity. The results showed that both the compounds **10b** and **7b** were reversible inhibitors of mushroom tyrosinase for oxidation of L-DOPA (**Figure 18**).

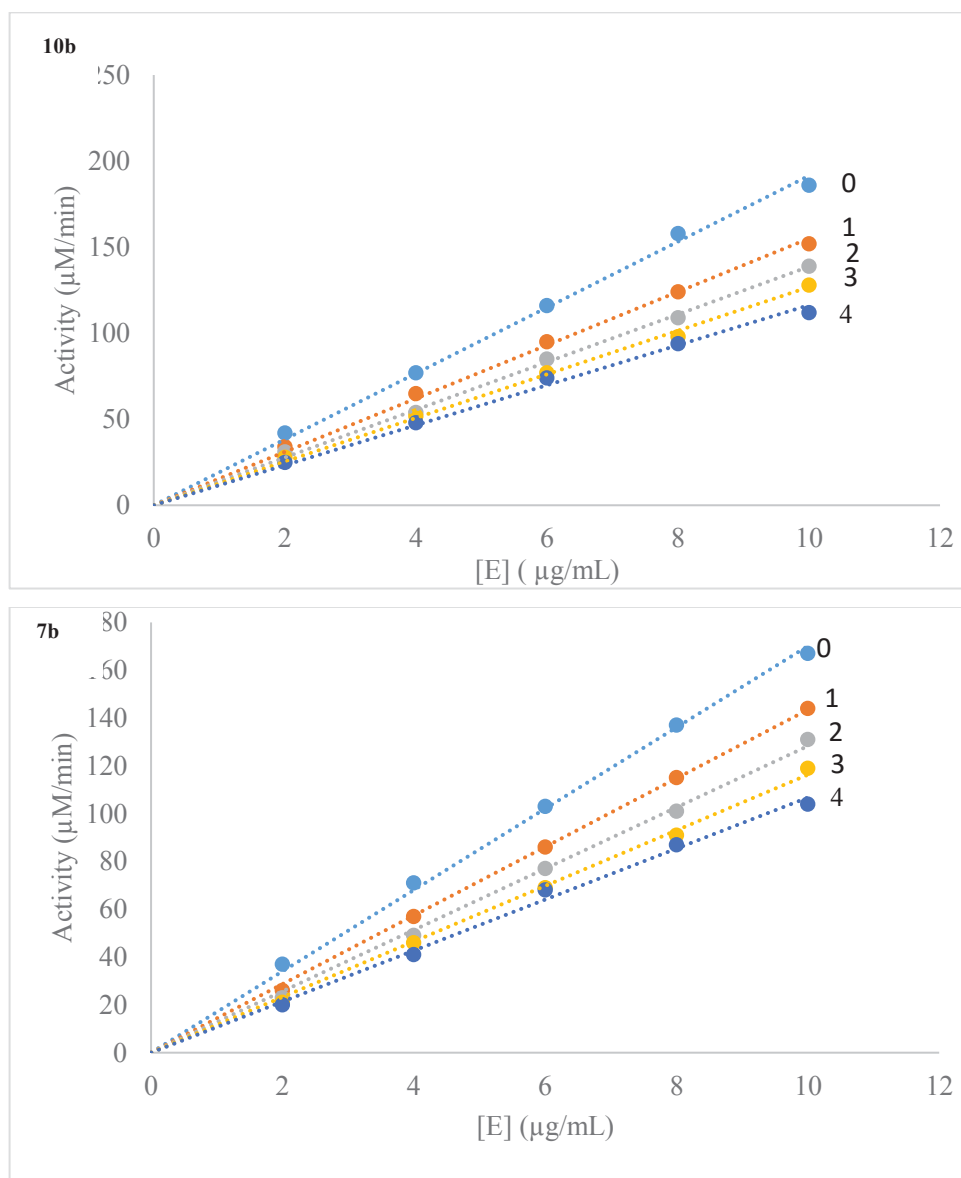


Figure 18 The inhibitory mechanism of compounds **10b** and **7b**

The concentration of inhibitor used for curves 0-4 were 0, 0.25, 0.5, 1.0 and 2.0 μM respectively.

In this study, the tyrosinase inhibitory activities of compounds **10b** and **7b** were investigated in detail. The reaction rates were measured in the presence of active

inhibitors with various concentrations of L-DOPA as a substrate. As the concentrations of active inhibitors **10b** and **7b** increased, K_m values gradually increased, but V_{max} values did not change, thereby indicating the inhibitors to act as competitive inhibitors of mushroom tyrosinase (**Figure 19**).

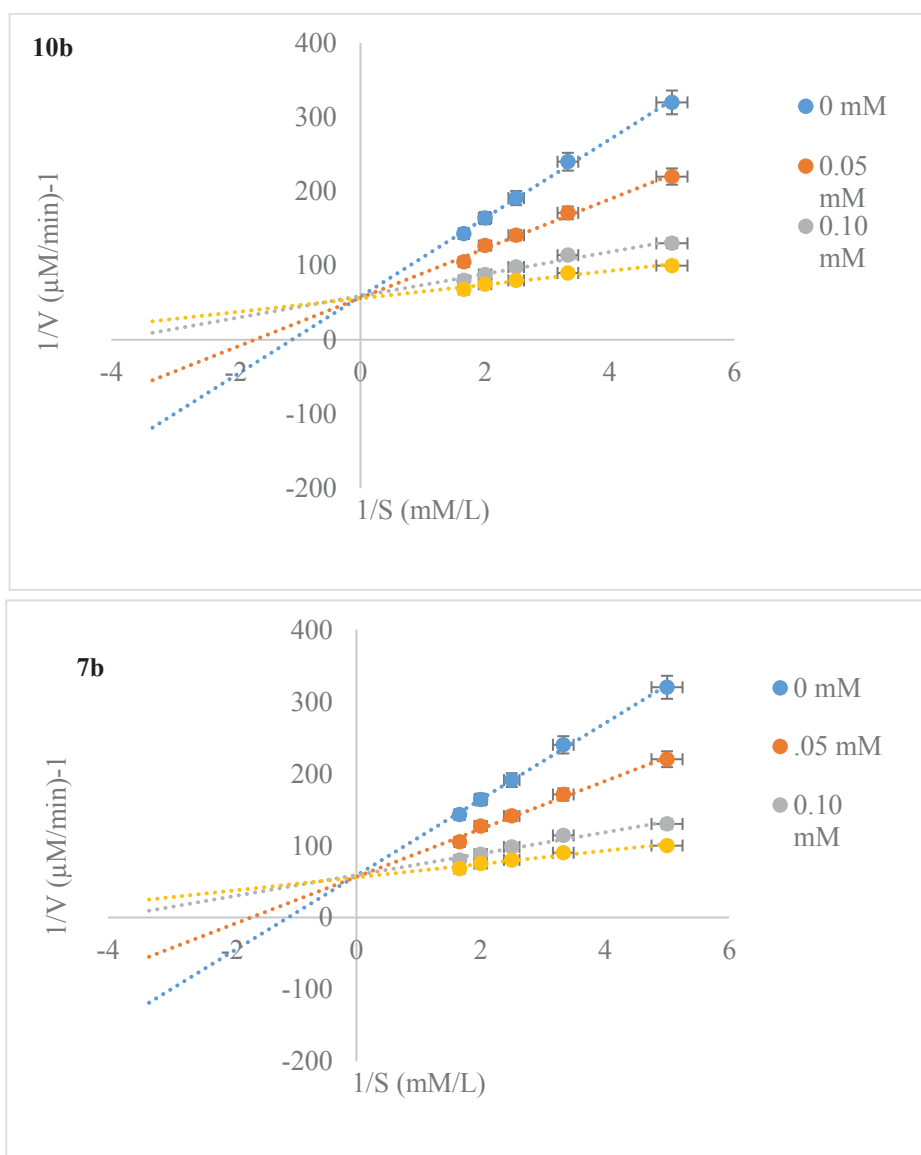


Figure 19 Lineweaver Burk plot for inhibition of compounds **10b** and **7b**.

Data were obtained as mean values of $1/V$, the inverse of the absorbance increase at a wavelength of 492nm per min of three independent tests with different concentrations of L-DOPA as a substrate. The concentration of compounds **10b** and **7b** from top to bottom were 20 μM , 5 μM , 1.25 μM and 0 μM , respectively.

The inhibition kinetics were illustrated by Dixon plots, which were obtained by plotting $1/V$ versus $[I]$ with varying concentrations of substrate. Dixon plots gave a family of straight lines passing through the same point at the second quadrant, giving the inhibition constant (K_i) (**Figure 20**). The K_i value estimated from the Dixon plot was 3.8 μM and 4.5 μM , respectively for the compounds **10b** and **7b**. A comparison of the K_i values of the compounds with that of kojic acid revealed that they possess much higher affinity to tyrosinase than kojic acid (**Table 5**).

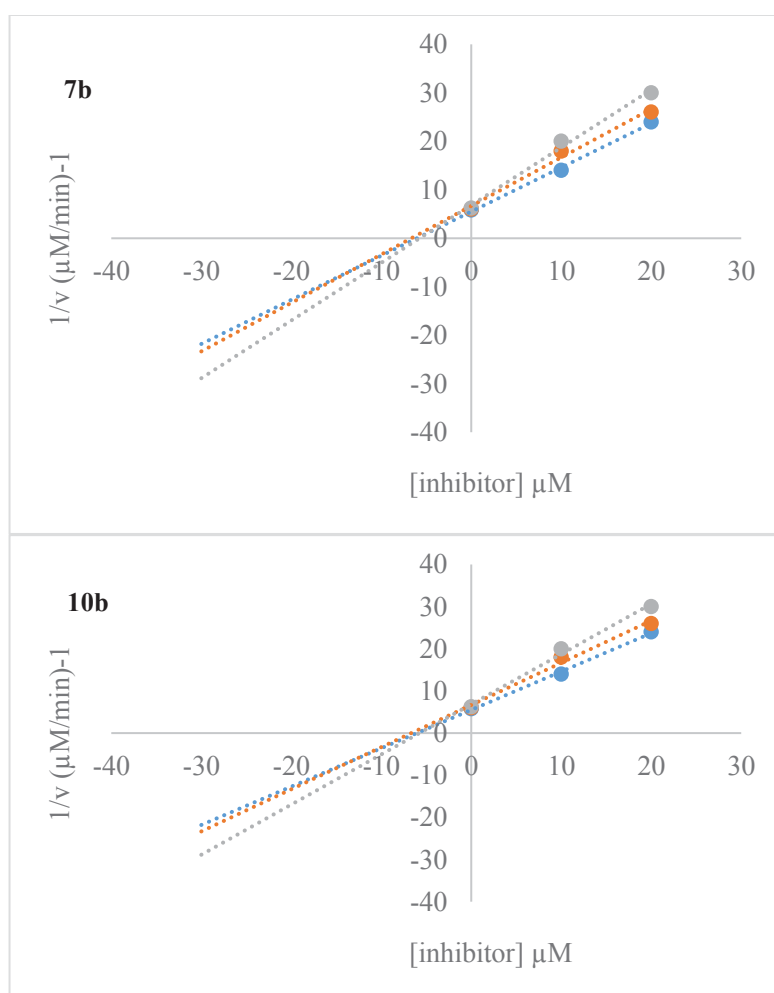


Figure 20 Dixon plot for the inhibitory effect of compounds **10b** and **7b**

The inhibitor concentrations were 0, 10 μM and 20 μM , respectively. The L-DOPA concentrations were 200, 400 and 600 μM .

Table 5 Effect on mushroom polyphenol oxidase activity and kinetic analysis of compounds.

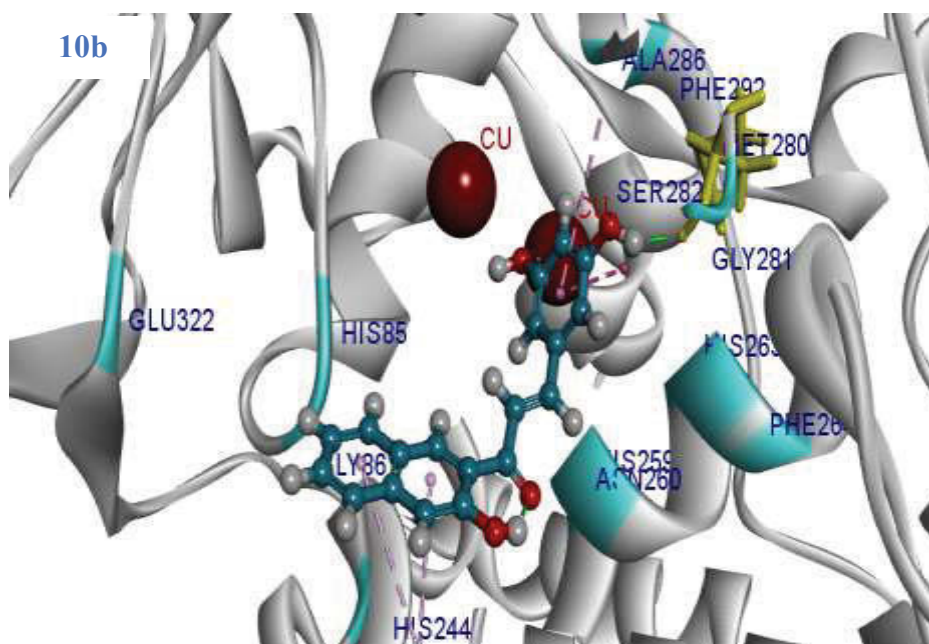
Compound	Type of inhibition ^{\$}	IC ₅₀ (μM) [*]	K _i (μM) [#]
6b	Competitive	20.4 ± 0.25	10.8
7b	Competitive	14.4 ± 0.44	4.5
8b	Competitive	22.9 ± 0.14	11.2
9b	Competitive	25.6 ± 0.11	11.9
10b	Competitive	10.4 ± 0.65	3.8
Kojic acid	-----	27.5 ± 0.56	12.2

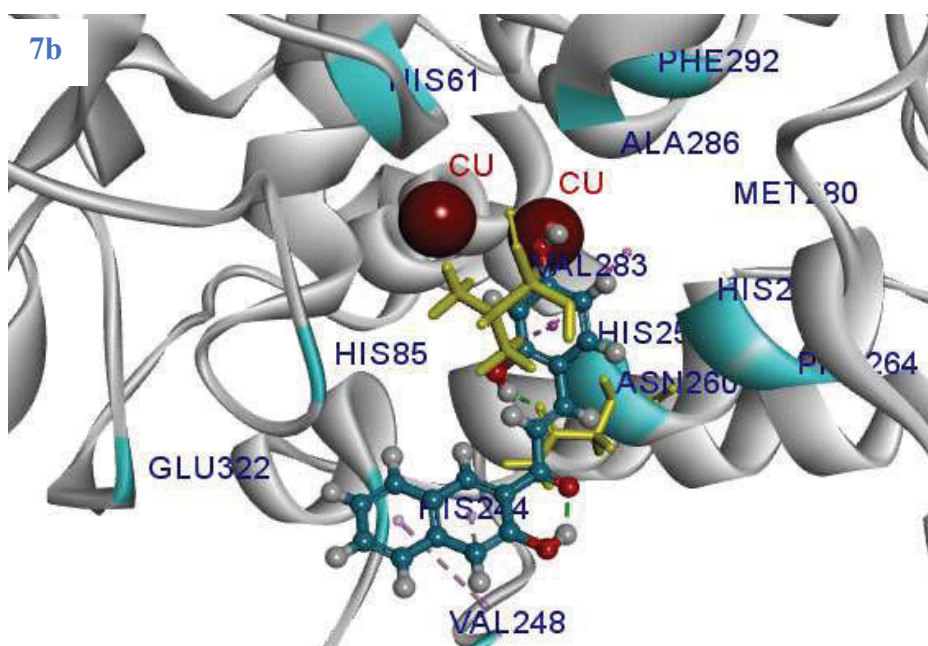
^{*}(IC₅₀): refers to the concentration of compound that caused 50% inhibition.

[#]: Values were measured at 5 μM of active compounds and K_i is the (inhibitor constant). ^{\$}: Lineweaver- Burk plot of mushroom tyrosinase: Data are presented as mean values of 1/V, which is the inverse of the increase in absorbance at wavelength 492 nm/min (ΔA492/min), for three independent tests with different concentrations of L-DOPA as the substrate.

3.3.3. Docking studies

Binding between the active site of mushroom tyrosinase and the active inhibitors **10b** and **7b** was simulated using Accelrys Discovery Studio 4.5 suite. **Figure 21** showed selected docked conformations of compounds **10b** and **7b** along with the positive control, kojic acid in the tyrosinase binding site.





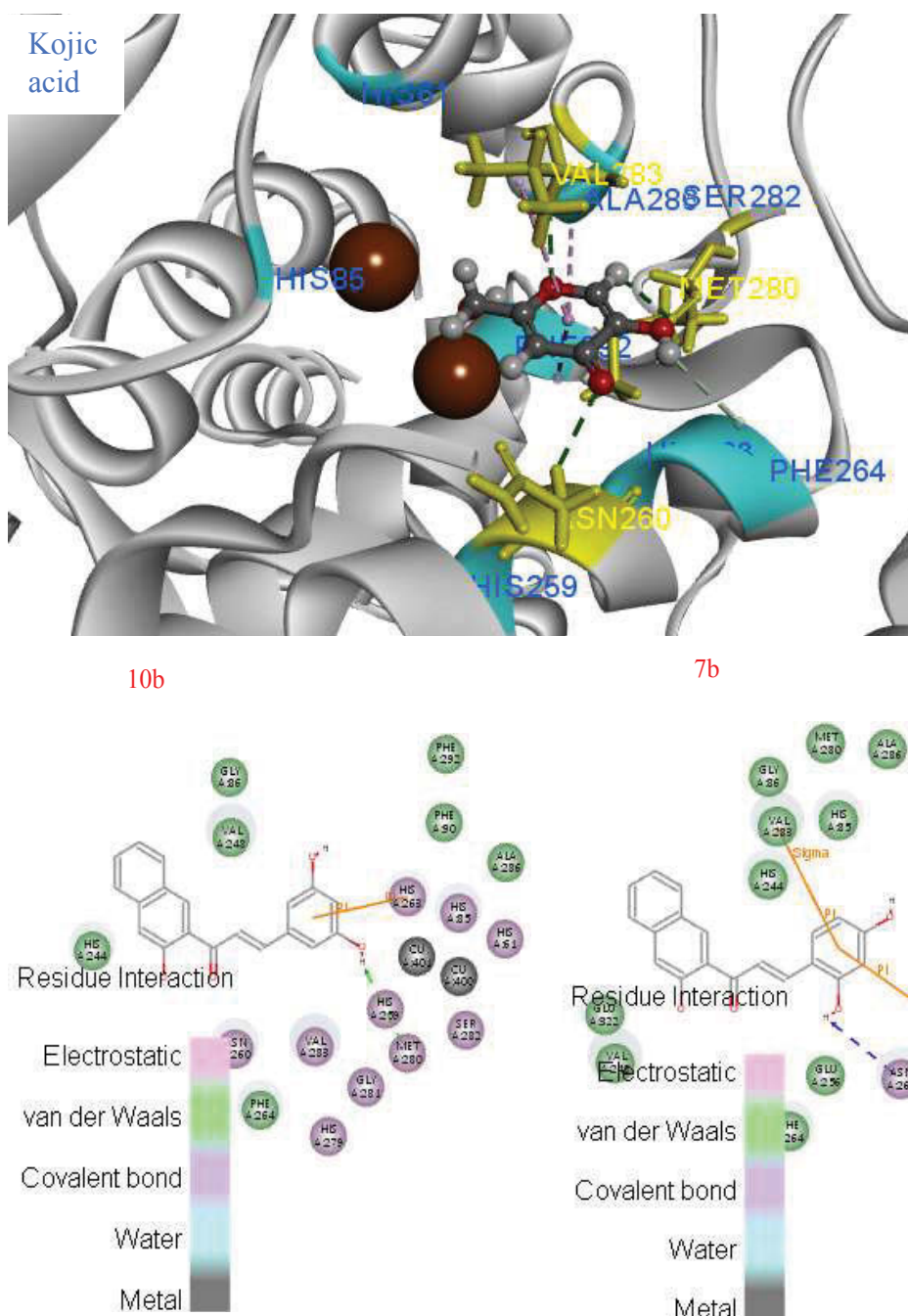


Figure 21 Docking and 2D results of compounds **10b** & **7b**

Ligands are displayed as ball and stick while the core amino acid residues are displayed as stick. The green dotted lines show the hydrogen bond interactions and the purple lines show the non-bonding interactions. The ochre balls represent the copper ions.

Additionally, hydrogen bonding interactions between mushroom tyrosinase and the inhibitor compounds or kojic acid were studied. Docking results indicated compound **10b** ($-22.36 \text{ kcal mol}^{-1}$) to be more strongly bound with mushroom tyrosinase than with compound **7b** ($-19.25 \text{ kcal mol}^{-1}$) (**Table 4**). Histidine residues in the active site had an important role in tyrosinase activity (Guo *et al* 2008). Ring B of the ligands **6b–10b**

extended deep into the hydrophobic pocket and made a π - π stacking interaction with His263 while π - σ interaction was seen with Val283. Also, weak hydrogen bonds were formed between the nitrogen atom (-NO₂) of compound **9b** with His85 and His259.

Copper ion (Cu401) was strongly bound by the hydroxyl group (3-OH) of compound **10b** at a distance of 1.95 Å. Tyrosinase substrates like L-DOPA also bind to the copper ion of tyrosinase via their OH group. According to the docking program, the 5-OH group of compound **10b** or kojic acid formed a strong hydrogen bond (1.91 Å) with the carboxylate oxygen of Met280, which indicated compound **10b** to inhibit tyrosinase activity by binding at the active site of mushroom tyrosinase.

Compound **6b** with an IC₅₀ of 20.4 μ M showed coordination with Cu401 at a distance of 2.53 Å. However, the formation of a strong intramolecular hydrogen bond (2.02 Å) between the 2'-OH and the carbonyl group hampered the latter to interact with the receptor. The ligand **7b** (IC₅₀: 14.4 μ M) does not interact with the bi-nuclear copper-binding site, but mainly with residues' side chains in the active-site entrance.

The interaction of OH-2 of ring B in compound **7b** with Asn260 (1.99 Å) emphasized the importance of this residue located close to the entrance of the receptor. For kojic acid, it was observed that the compound formed hydrogen bonds with Asn260, Met280, Val283 and also a π - π interaction with His283. This indicated the hydroxy derivatives of naphthylchalcones to inhibit tyrosinase activity by binding at the active site of mushroom tyrosinase.

3.4. Conclusion

To summarize, a series of novel hydroxy derivatives of naphthylchalcones were synthesized and studied for their inhibition on the diphenolase activity of mushroom tyrosinase. Compounds **10b** and **7b** were found to be significantly more potent than kojic acid with their IC₅₀ values of 10.4 μ M and 14.4 μ M, respectively. Experimentally the compounds exhibited a reversible inhibition of tyrosinase. Computational simulation was adopted to further explore the inhibitory action of compounds **10b** and **7b** on tyrosinase. A combination of inhibition kinetics and computational modeling was competent to probe the inhibition mechanism. Taken together, the principal results of the study suggest the following;

- a) Compounds **10b** and **7b** competitively inhibited L-DOPA oxidation and thereby prevented the further precursors from forming melanin pigment.
- b) Also, hydroxylation at 5-position in **10b** was the molecular modification that led to a strong coordination with the copper ion in the active site of tyrosinase enzyme. The 5-OH group complexed with the binuclear copper active site of tyrosinase and interacted thereby with the hydrophobic enzyme pocket, leading to enhanced inhibitor-enzyme binding affinity and improved inhibitory effects on mushroom tyrosinase. Moreover, the binding of the inhibitor via a coordinate bond ensured that access to the active site by the substrate was effectively blocked. This curbed the enzymes ability to oxidize the substrates subsequently leading to an inhibition in mushroom tyrosinase. Hence a design principle encouraging strong coordination with the copper ions was warranted as the metal centres were a key part of the enzyme machinery.
- c) SAR studies identified hydroxyl as the functional group indispensable for tyrosinase inhibitory activity. Another structural advantage was attributed to the naphthyl ring that exerted a nucleophilic action on the dihydroxy phenyl ring.
- d) Both the compounds exhibited reversible competitive inhibition. Compound **7b** with a 2,4-substituted resorcinol structure in the B-ring had structural resemblance with the substrate L-tyrosine.

These preliminary findings justified to pursue further work on hydroxy substituted naphthylchalcones that served as potential scaffolds for the future development of active tyrosinase inhibitors.

3.5. References

Choi, J, Bae, JS, Ha, MY, No, KJ, Lee, KE, Lee, SJ, Song, S, Lee, H, Suh, H, Yu, PB, Chung, YH 2010, 'A newly synthesized potent tyrosinase inhibitor: 5-(6-Hydroxy-2-naphthyl)-1,2,3-benzenetriol', *Bioorganic and Medicinal Chemistry Letters*, Vol 20, pp. 4882–4884.

Ennes, SBP, Paschoalick, R, Alchorne, MMDA 2000, 'A double-blind comparative, placebo-controlled study of the efficacy and tolerability of 4% hydroquinone as a

depigmenting agent in melasma', *Journal of Dermatological Treatment*, Vol 11, pp. 173–179.

Franco, DCZ, de Carvalho, GSG, Rocha, PR, Teixeira, RS, da Silva, AD, Raposo, NRB 2012, 'Inhibitory effects of resveratrol analogs on mushroom tyrosinase activity', *Molecules*, Vol 17, pp. 11816-11825.

Fujimoto, N, Onodera, H, Mitsumori, K, Tamura, T, Maruyama, S, Ito, A 1999, 'Changes in thyroid function during development of thyroid hyperplasia induced by kojic acid in F344 rats', *Carcinogenesis*, Vol 20, pp. 1567–1571.

Guo, L, Lu, Z.R, Park, D, Oh, SH, Shi, L, Park, SJ, Zou, F 2008, 'The effect of histidine residue modification on tyrosinase activity and conformation: Inhibition kinetics and computational prediction', *Journal of Biomolecular Structure and Dynamics*, Vol 26, pp. 395–402.

Ha, YM, Chung, SW, Song, S, Lee, H, Suh, H, Chung, HY 2007, '4-(6-Hydroxy-2-naphthyl)-1,3-benzenediol: A potent, new tyrosinase inhibitor', *Biological and Pharmaceutical Bulletin*, Vol 30, pp. 1711–1715.

Kahn, V 1995, 'Effect of kojic acid on the oxidation of DL-DOPA, Norepinephrine and Dopamine by mushroom tyrosinase', *Pigment Cell Research*, Vol 8, pp. 234–240.

Martinez, V, Whitaker, JR 1995, 'The biochemistry and control of enzymatic browning', *Trends in Food Science and Technology*, Vol 6, pp. 195–200.

Mcevely, JA, Iyengar, R, Otwell, QS 1992, 'Inhibition of enzymatic browning in foods and beverages', *Critical Reviews in Food Science and Nutrition*, Vol 32, pp. 253–273.

Song, S, Lee, H, Jin, Y, Ha, YM, Bae, S, Chung, HY, Suh, H 2007, 'Syntheses of hydroxy substituted 2-phenyl-naphthalenes as inhibitors of tyrosinase', *Bioorganic and Medicinal Chemistry Letters*, Vol 17, pp. 461–464.

Sun, LP, Gao, LX, Ma, WP, Nan, FJ, Jia, L, Piao, HR 2012, 'Synthesis and Biological Evaluation of 2,4,6-Trihydroxychalcone Derivatives as Novel Protein Tyrosine Phosphatase 1B Inhibitors', *Chemical Biology and Drug Design*, Vol 80, pp. 584–590.

CHAPTER 4

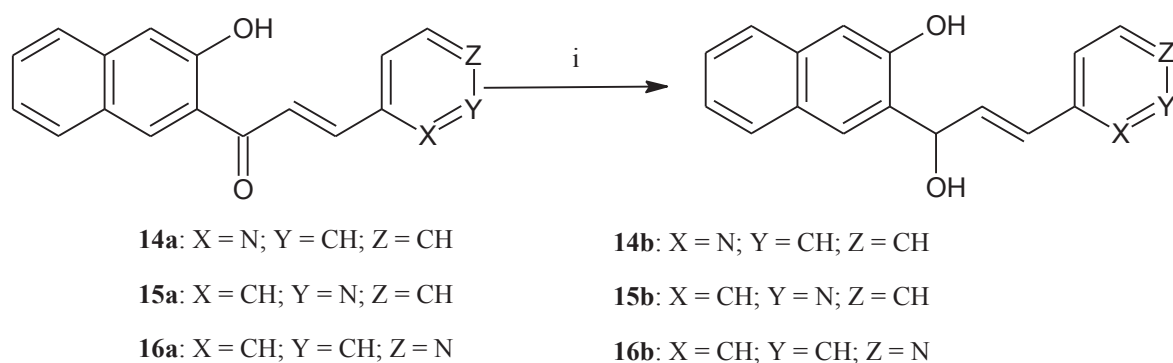
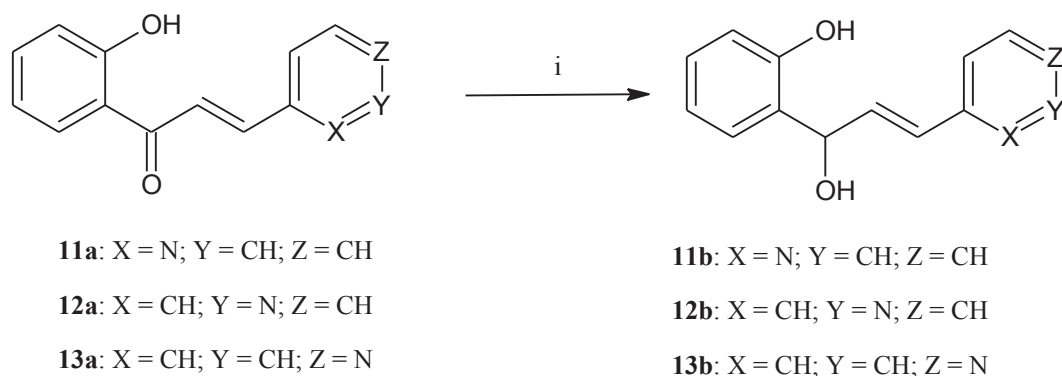
ALLYL ALCOHOLS OF AZACHALCONES

4.1. Introduction

Chapter 2 on hydroxyazachalcones and Chapter 3 on naphthylchalcones gave promising results and were published (Radhakrishnan *et al* 2015 (a); Radhakrishnan *et al* 2015) (b). These results provided an impetus to synthesize and explore hydroxyl substituted azaphenyl styryl ketone (chalcone) derivatives, in which the nitrogen heteroatom acted as a chelator of copper ions in the tyrosinase active site. Furthermore, preliminary docking calculations revealed a binding mode wherein an internal hydrogen bond was formed between the 2-hydroxy group and the carbonyl group that reduced the binding affinity and thus the biological potency. Thus an attempt was made to design new molecules eliminating the carbonyl group by Luche reduction, in order to identify its role in tyrosinase inhibition. It was presumed that this would lessen the steric hindrance by providing increased flexibility. Hence the project was directed towards synthesizing a series of hydroxy substituted azaphenyl and azanaphthyl chalcones followed by their selective reduction with a Lewis acid catalyst like cerium chloride.

4.2. Experimental

Azachalcones were readily synthesized by the base catalyzed Claisen-Schmidt condensation of an aldehyde and an appropriate ketone in a polar solvent like methanol (See 12.2). Luche reduction was employed (Scheme 3) to convert the α , β -unsaturated bond in the respective azachalcone compound to an allylic alcohol using a lanthanide metal like cerium trichloride, sodium borohydride, and an alcohol solvent (Luche 1978). Trivalent lanthanide metals like cerium (CeIII), hard Lewis acids with high oxophilicity, were employed in highly selective reactions, like Luche reduction. This procedure was adopted for the 1,2-reduction of enones where other reagents (eg., DIBAL-H, LiAlH_4 , BH_3 and NaBH_4 alone) failed to produce the allylic alcohol or gave an undesired product. The role of the cerium metal was to coordinate with the alcohol, making its proton more acidic which allowed it to be abstracted by the carbonyl oxygen of the chalcone starting material. Sodium borohydride reacted with the cerium activated alcohol to form a series of alkoxyborohydrides that favored 1,2 hydride attack on the protonated carbonyl to give the final allylic alcohol product (Gemal & Luche 1981; Kagan & Namy 1986).



Scheme 3. Reduction of azachalcones.

Reagents and conditions: (i) $\text{CeCl}_3 \cdot 7\text{H}_2\text{O}$, NaBH_4

4.2.1. Method for synthesis of compound **11b**

To a stirred solution of 2'-hydroxyacetophenone (1mM, 1.36mL) and 2-pyridinecarboxaldehyde (1mM, 1.07 mL) in 25 mL methanol, was added pulverized NaOH (2mM) and the mixture was stirred at room temperature for 24–36 h. The reaction was monitored by TLC using *n*-hexane: ethyl acetate (7:3) as mobile phase. The reaction mixture was cooled to 0°C (ice-water bath) and acidified with HCl (10 % v/v aqueous solution) to afford total precipitation of the compound. An orange oil was formed, the mixture was extracted with CH_2Cl_2 , the extracts were dried (Na_2SO_4) and the solvent was rotary evaporated to give the respective chalcone. The product obtained was recrystallized with ethylacetate to give the pure chalcone product **11a**. A solution of

the chalcone product **11a** (1mM, 225mg) in methanol (40mL) was treated with 2.5 equivalents of cerium(III) chloride heptahydrate (2.43mM, 893mg) at RT, followed by the addition of six equivalents of sodium borohydride (5.54mM, 210mg) in portions at 0° C with vigorous stirring. The reaction mixture was allowed to warm to room temperature within five hours. After monitoring the completion of the reaction with TLC, the reaction was quenched with ammonium chloride (50mL). The mixture was extracted with CHCl₃ (3 x 25ml), the organic layer was washed with brine and dried over anhydrous Na₂SO₄ to obtain the respective allylic derivative **11b**.

4.3. Results and Discussion

4.3.1. Synthesis

The parent chalcones (**11a-16a**) were readily synthesized by the base catalyzed Claisen-Schmidt condensation of an aldehyde and an appropriate ketone in a polar solvent like methanol.

11a. (2*E*)-1-(2-hydroxyphenyl)-3-(pyridin-2-yl)prop-2-en-1-one. Yield: 84%; Mp: 94–95°C; ¹H NMR (500 MHz, CDCl₃): δ 12.56 (s, 1H-OH), 7.52 (t, 1H, H-4', *J*= 8.5), 7.03 (d, 1H, H-3', *J*= 7.5), 6.96 (t, 1H, H-5', *J*= 9.0), 7.74 (d, 1H, H _{α} , *J*= 15.0), 7.90 (d, 1H, H _{β} , *J*= 16.0), 7.96 (d, 1H, H-5, *J*= 9.0), 7.91 (t, 1H, H-4, *J*= 7.5), 7.38 (t, 1H, H-3, *J*= 8.0), 8.66 (d, 1H, H-6, *J*= 9.0), 7.37 (d, 1H, H-6'); ¹³C NMR (125 MHz, DMSO-d₆) δ 195.2 (C=O), 152.6 (C6), 126.1 (C5), 137.5 (C4), 124.9 (C3), 154.2 (C2), 166.1 (C6'), 121.4 (C1'), 121.6 (C5'), 139.2 (C4'), 122.4 (C3'), 132.3 (C2'), 122.2 (vinylic), 144.6 (vinylic); IR (KBr) ν (cm⁻¹): 3421, 3047, 2361, 1715, 1592, 1559, 1347, 1311, 1233, 1209, 983, 817, 756; MS (ESI): 226.1 ([M + H])⁺.

12a. (2*E*)-1-(2-hydroxyphenyl)-3-(pyridin-3-yl)prop-2-en-1-one. Yield: 92%; Mp: 86–88°C; ¹H NMR (500 MHz, CDCl₃): δ 12.55 (s, 1H, OH), 6.99 (t, 1H, *J*= 8.5, H-3'), 7.89 (d, 1H, H _{α} , *J*= 11.0), 7.17 (d, 1H, H _{β} , *J*= 11.5), 7.50 (t, 1H, *J*= 9.0, H-4'), 7.57 (dd, 1H, *J*= 9.2, 9.5, H-5'), 7.46 (d, 1H, H-6', *J*= 8.0), 8.69 (s, 1H, H-2), 8.89 (dd, 1H, *J*= 8.2, 9.0, H-4), 7.50 (dd, 1H, *J*= 8.0, 8.5, H-5), 8.25 (dd, 1H, *J*= 9.4, 10.0, H-6); ¹³C NMR (125 MHz, DMSO-d₆) δ 195.2 (C=O), 118.9 (C1'), 130.2 (C2'), 118.2 (C3'), 136.5 (C4'), 120.2 (C5'), 162.9 (C6'), 149.2 (C2), 142.7 (C6), 124.9 (C5), 130.1 (C3), 131.7 (C4), 131.6 (C1), 125.7 (vinylic), 144.6 (vinylic); IR (KBr) ν (cm⁻¹): 3400, 1646, 1315, 1591, 1646, 1492, 825 & 689, 755 & 689; MS (ESI): 226.1 ([M + H])⁺.

13a. (2*E*)-1-(2-hydroxyphenyl)-3-(pyridin-4-yl)prop-2-en-1-one. Yield: 80%; Mp: 139–140°C; ¹H NMR (500 MHz, CDCl₃): δ 12.66 (s, 1H, OH), 6.95 (t, 1H, *J* = 8.0, H-3'), 8.88 (s, 2H, *J* = 15.5, H-3 & H-5), 7.96 (d, 1H, H_α, *J* = 10.5), 7.05 (d, 1H, H_β, *J* = 11.0), 7.44 (t, 1H, *J* = 7.5, H-6'), 7.54 (t, 1H, *J* = 9.5, H-4'), 7.71 (d, 2H, *J* = 9.0, H-2 & H-6), 7.89 (dd, 1H, *J* = 6.8, 8.0, H-5'); ¹³C NMR (125 MHz, DMSO-d₆) δ 195.7 (C=O), 153.2 (C2 & C6), 122.3 (C3 & C5), 132.3 (C2'), 121.7 (C3'), 139.6 (C4'), 121.4 (C5'), 124.8 (C1'), 166.3 (C6'), 144.5 (C4), 144.7 (vinylic), 127.2 (vinylic); IR (KBr) ν (cm⁻¹): 3445, 3034, 1710, 1583, 1568, 1376, 1349, 1318, 1216, 809, 752; MS (ESI): 226.1 ([M + H])⁺.

14 a. (2*E*)-1-(3-hydroxynaphthalen-2-yl)-3-(pyridin-2-yl)prop-2-en-1-one. Yield: 69%; Mp: 129–131°C; ¹H NMR (500 MHz, CDCl₃): δ 12.95 (s, 1H, OH), 7.92 (d, 1H, H_β, *J* = 12.5), 7.69 (d, 1H, H_α, *J* = 12.0), 8.75 (dd, 1H, *J* = 9.0, H-3), 7.59 (t, 1H, *J* = 8.5, H-4), 7.89 (dd, 1H, *J* = 7.0, 8.0, H-5), 7.92 (d, 1H, *J* = 9.0, H-6), 7.17 (dd, 1H, *J* = 9.5, H-3'), 7.82 (m, 1H, *J* = 10.5, H-5'), 7.75 (m, 1H, *J* = 10.5, H-6'), 7.35 (dd, 1H, *J* = 6.5, 7.8, H-7'), 7.57 (dd, 1H, *J* = 9.8, 10.5, H-8'), 8.02 (dd, 1H, *J* = 10.0, H-10'); ¹³C NMR (125 MHz, DMSO-d₆) δ 198.42 (C=O), 152.80 (C1), 150.07 (C3), 126.89 (C3), 126.89 (C4), 136.92 (C5), 121.67 (C6), 114.72 (C1'), 163.92 (C2'), 119.90 (C3'), 136.97 (C4'), 128.22 (C5'), 129.24 (C6'), 123.02 (C7'), 128.12 (C8'), 124.14 (C9'), 131.16 (C10'), 130.02 (vinylic), 145.20 (vinylic); IR (KBr) ν (cm⁻¹): 3853, 3420, 3054, 2923, 2361, 2337, 1652, 1635, 1621, 1595, 1508, 1458, 1370, 1234, 1105, 820, 752; MS (ESI): 276.1 ([M + H])⁺.

15 a. (2*E*)-1-(3-hydroxynaphthalen-2-yl)-3-(pyridin-3-yl)prop-2-en-1-one. Yield: 90%; M.p: 138–140 °C; ¹H NMR (500 MHz, CDCl₃): δ 13.72 (s, 1H, OH), 7.87 (d, 1H, H_β, *J* = 11.5), 7.65 (d, 1H, H_α, *J* = 11.0), 9.02 (s, 1H, H-2), 8.87 (dd, 1H, *J* = 7.4, 8.8, H-4), 7.51 (m, 1H, *J* = 9.0, H-5), 8.15 (dd, 1H, *J* = 9.5, 10.5, H-6), 7.20 (dd, 1H, *J* = 9.0, H-3'), 7.79 (dd, 1H, *J* = 10.0, H-5'), 7.79 (m, 1H, *J* = 9.5, H-6'), 7.32 (dd, 1H, *J* = 8.4, 8.8, H-7'), 7.59 (dd, 1H, *J* = 10.2, 10.6, H-8'), 8.15 (dd, 1H, *J* = 9.6, 10.5, H-10'); ¹³C NMR (125 MHz, DMSO-d₆) δ 197.5 (C=O), 131.3 (C1), 151.2 (C2), 154.1 (C4), 124.2 (C5), 135.3 (C6), 114.7 (C1'), 164.2 (C2'), 120.1 (C3'), 136.8 (C4'), 128.2 (C5'), 129.2 (C6'), 123.5 (C7'), 129.1 (C8'), 124.2 (C9'), 132.0 (C10'), 131.2 (vinylic), 144.6 (vinylic); IR (KBr) ν (cm⁻¹): 3421, 3060, 2922, 2851, 2631, 1749, 1600, 1581, 1528, 1476, 1390, 1278, 1249, 1209, 1081, 1040, 796, 726, 617, 572; MS (ESI): 276.1 ([M + H])⁺.

16 a. (2*E*)-1-(3-hydroxynaphthalen-2-yl)-3-(pyridin-4-yl)prop-2-en-1-one. Yield: 64%; M.p:132–134 °C; ¹H NMR (500 MHz, CDCl₃): δ 13.55 (s, 1H, OH), 7.89 (d, 1H, H_β, *J* = 12.5), 7.69 (d, 1H, H_α, *J* = 12.0), 7.25 (dd, 1H, *J* = 9.5, H-3'), 7.79 (dd, 1H, *J* = 9.4, 10.5, H-5'), 7.81 (m, 1H, *J* = 9.5, H-6'), 7.39 (dd, 1H, *J* = 6.7, 8.0, H-7'), 7.61 (dd, 1H, *J* = 10.0, H-8'), 8.09 (dd, 1H, *J* = 10.5, H-10') 8.90 (s, 2H, *J* = 15.0, H-3 & H-5), 7.70 (d, 2H, *J* = 9.5, H-2 & H-6); ¹³C NMR (125 MHz, DMSO-*d*₆) δ 196.4 (C=O), 113.6 (C1'), 164.2 (C2'), 121.2 (C3'), 136.8 (C4'), 128.1 (C5'), 130.1 (C6'), 123.4 (C7'), 129.1 (C8'), 124.2 (C9'), 130.9 (C10'), 131.2 (vinyllic), 145.1 (vinyllic), 140.6 (C1), 153.5 (C2 & C6), 123.5 (C3 & C5); IR (KBr) ν (cm⁻¹): 3422, 3325, 3052, 2920, 2845, 2612, 1752, 1610, 1574, 1512, 1395, 1265, 1245, 1079, 1042, 786, 722, 627, 570; MS (ESI): 276.1 ([M + H])⁺.

Reduction of the carbonyl group in compounds **11a-16a** yielded azachalcone derivatives, **11b-16b**

11b. 2-[(2*E*)-1-hydroxy-3-(pyridin-2-yl)prop-2-en-1-yl]phenol: Yield: 58%; Mp: 89–91°C; ¹H NMR (CDCl₃): δ 11.55 (s, 1H, OH), 5.45 (s, 1H, OH), 6.73 (d, 1H, *J* = 11.5, H_α), 7.72 (d, 1H, *J* = 12.0, H_β), 7.57 (t, 1H, H-4', *J* = 8.5), 7.12 (d, 1H, H-3', *J* = 7.0), 6.94 (t, 1H, H-5', *J* = 9.5), 7.39 (d, 1H, H-6, *J* = 8.5'), 7.90 (d, 1H, H-5, *J* = 9.0), 7.91 (t, 1H, H-4, *J* = 7.5), 7.39 (t, 1H, H-3, *J* = 8.5), 8.62 (d, 1H, H-6, *J* = 9.0); ¹³C NMR (125 MHz, DMSO-*d*₆) δ 152.4 (C6), 126.4 (C5), 137.5 (C4), 123.5 (C3), 154.6 (C1), 166.5 (C6'), 120.4 (C1'), 121.6 (C5'), 139.6 (C4'), 123.1 (C3'), 132.5 (C2'), 122.6 (vinyllic), 145.2 (vinyllic), 59.93 (C-OH); IR (KBr) ν (cm⁻¹): 3040, 1635, 1594, 1425, 1278, 1227, 1200, 1112, 1025, 965, 754, 710; HRMS *m/z*: 228.1031 ([M + H])⁺; Calcd: 228.1025.

12b. 2-[(2*E*)-1-hydroxy-3-(pyridin-3-yl)prop-2-en-1-yl] phenol. Mp: Yield: 60%; 82–84°C; ¹H NMR (500 MHz, CDCl₃): δ 12.50 (s, 1H, OH), 5.40 (s, 1H, OH), 6.92 (t, 1H, H-3' *J* = 7.0), 7.54 (t, 1H, H-4', *J* = 8.5), 7.52 (dd, 1H, *J* = 8.0, H-5'), 7.41 (d, 1H, H-6', *J* = 8.5), 8.7 (s, 1H, H-2), 7.89 (d, 1H, H_α, *J* = 10.0), 7.06 (d, 1H, H_β, *J* = 10.5), 8.85 (dd, 1H, *J* = 8.6, 9.7, H-4), 7.55 (t, 1H, *J* = 8.5, H-5), 8.22 (dd, 1H, *J* = 9.0, H-6); ¹³C NMR (125 MHz, DMSO-*d*₆) δ 119.7 (C1'), 129.7 (C2'), 118.8 (C3'), 136.9 (C4'), 119.0 (C5'), 163.7 (C6'), 131.2 (C1), 150.6 (C2), 142.1 (C6), 124.4 (C5), 129.7 (C3), 131.4 (C4), 123.2 (vinyllic), 144.4 (vinyllic), 59.89 (C-OH); IR (KBr) ν (cm⁻¹): 3042, 2925, 1641, 1595, 1420, 1268, 1220, 1200, 1027, 972, 760, 717; HRMS *m/z*: 228.1037 ([M + H])⁺; Calcd: 228.1025.

13b. 2-[(2*E*)-1-hydroxy-3-(pyridin-4-yl)prop-2-en-1-yl]phenol: Yield: 47%; Mp: 98–100°C; ¹H NMR 500 MHz, (CDCl₃): δ 12.25 (s, 1H, OH), 5.42 (s, 1H, OH), 6.89 (t, 1H, *J* = 8.5, H-3'), 8.95 (s, 2H, *J* = 14.0, H-3 & H-5), 7.95 (d, 1H, H_α, *J* = 11.5), 7.22 (d, 1H, H_β, *J* = 12.0), 7.47 (dd, 1H, *J* = 8.5, H-6'), 7.60 (t, 1H, *J* = 9.0, H-4'), 7.74 (m, 2H, *J* = 9.5, H-2 & H-6), 7.92 (dd, 1H, *J* = 7.4, 8.4, H-5'); ¹³C NMR (125 MHz, DMSO-d₆) δ 155.6 (C2 & C6), 122.7 (C3 & C5), 130.9 (C2'), 122.2 (C3'), 140.6 (C4'), 122.2 (C5'), 124.5 (C1'), 165.1 (C6'), 145.5 (C4), 145.3 (vinylic), 128.1 (vinylic), 60.02 (C-OH); IR (KBr) ν (cm⁻¹): 3039, 2930, 1642, 1596, 1554, 1420, 1265, 1222, 1115, 1025, 972, 767, 720; HRMS *m/z*: 228.1040 ([M + H])⁺; Calcd: 228.1025.

14b. 3-[(2*E*)-1-hydroxy-3-(pyridin-2-yl)prop-2-en-1-yl] naphthalen-2-ol. Yield: 52%; Mp: 100–102°C; ¹H NMR (500 MHz, CDCl₃): δ 13.20 (s, 1H, OH), 5.44 (s, 1H, OH), 7.97 (d, 1H, *J* = 13.5, H_β), 7.79 (d, 1H, *J* = 13.0, H_α), 8.72 (dd, 1H, *J* = 9.5, H-3), 7.56 (dd, 1H, *J* = 7.2, 8.5, H-4), 7.92 (dd, 1H, *J* = 9.0, H-5), 7.89 (dd, 1H, *J* = 9.5, H-6), 7.20 (dd, 1H, *J* = 9.4, 10.5, H-3'), 7.87 (m, 1H, *J* = 10.0, H-5'), 7.80 (dd, 1H, *J* = 11.0, H-6'), 7.36 (dd, 1H, *J* = 8.0, H-7'), 7.57 (dd, 1H, *J* = 10.5, H-8'), 8.15 (dd, 1H, *J* = 9.0, H-10'); ¹³C NMR (125 MHz, DMSO-d₆) δ 59.8 (C-OH), 150.8 (C1), 126.7 (C3), 126.2 (C4), 135.9 (C5), 122.0 (C6), 116.7 (C1'), 165.1 (C2'), 120.9 (C3'), 137.5 (C4'), 128.2 (C5'), 130.2 (C6'), 124.2 (C7'), 129.12 (C8'), 124.4 (C9'), 131.3 (C10'), 129.4 (vinylic), 143.6 (vinylic); IR (KBr) ν (cm⁻¹): 3047, 2985, 2937, 1645, 1622, 1590, 1550, 1424, 1264, 1209, 1125, 1020, 978, 762, 727; HRMS *m/z*: 278.1168 ([M + H])⁺; Calcd: 278.1181.

15b. 3-[(2*E*)-1-hydroxy-3-(pyridin-3-yl)prop-2-en-1-yl] naphthalen-2-ol. Yield: 65%; Mp: 110–112°C; ¹H NMR (500 MHz, CDCl₃): δ 12.70 (s, 1H, OH), 5.50 (s, 1H, OH), 7.92 (d, 1H, H_β, *J* = 11.0), 7.69 (d, 1H, H_α, *J* = 10.5), 8.92 (s, 1H, H-2), 8.80 (dd, 1H, *J* = 9.5, H-4), 7.49 (m, 1H, *J* = 10.0, H-5), 8.22 (dd, 1H, *J* = 9.5, H-6), 7.24 (dd, 1H, *J* = 8.8, 9.2, H-3'), 7.80 (dd, 1H, *J* = 9.5, 10.6, H-5'), 7.77 (dd, 1H, *J* = 9.5, H-6'), 7.35 (dd, 1H, *J* = 9.0, H-7'), 7.62 (dd, 1H, *J* = 9.0, 10.2, H-8'), 8.05 (dd, 1H, *J* = 6.6, 8.6, H-10'); ¹³C NMR (125 MHz, DMSO-d₆) δ 130.05 (C1), 150.95 (C2), 154.02 (C4), 127.20 (C5), 136.08 (C6), 112.74 (C1'), 165.15 (C2'), 120.52 (C3'), 137.07 (C4'), 129.50 (C5'), 130.15 (C6'), 125.45 (C7'), 59.80 (C-OH), 129.72 (C8'), 126.47 (C9'), 130.76 (C10'), 134.02 (vinylic), 145.55 (vinylic); IR (KBr) ν (cm⁻¹): 3050, 3044, 2990, 2980, 2924, 2855, 2723, 1640, 1623, 1590, 1574, 1550, 1465, 1264, 1246, 1166, 1024, 951, 822; HRMS *m/z*: 278.1177 ([M + H])⁺; Calcd: 278.1181.

16b. 3-[(2*E*)-1-hydroxy-3-(pyridin-4-yl)prop-2-en-1-yl] naphthalen-2-ol. Yield: 42%; Mp: 132–134 °C. ¹H NMR (500 MHz, CDCl₃): δ 13.20 (s, 1H, OH), 5.47 (s, 1H, OH), 7.92 (d, 1H, *J* = 13.0, H_β), 7.64 (d, 1H, *J* = 12.5, H_α), 7.27 (dd, 1H, *J* = 7.4, 9.0, H-3'), 7.82 (dd, 1H, *J* = 8.5, 10.0, H-5'), 7.85 (m, 1H, *J* = 9.5, H-6'), 7.42 (dd, 1H, *J* = 8.5, H-7'), 7.67 (dd, 1H, *J* = 9.5, 10.5, H-8'), 8.29 (dd, 1H, *J* = 10.2, 11.0, H-10') 8.87 (s, 2H, *J* = 15.0, H-3 & H-5), 7.79 (m, 2H, *J* = 10.5, H-2 & H-6); ¹³C NMR (125 MHz, DMSO-d₆) δ 63.2 (C-OH), 115.5 (C1'), 165.02 (C2'), 122.2 (C3'), 135.9 (C4'), 128.02 (C5'), 129.52 (C6'), 124.4 (C7'), 130.10 (C8'), 124.2 (C9'), 130.5 (C10'), 132.0 (vinyl), 144.2 (vinyl), 139.6 (C1), 154.2 (C2 & C6), 124.6 (C3 & C5); IR (KBr) ν (cm⁻¹): 3060, 3047, 2985, 2925, 2850, 2720, 2653, 1637, 1627, 1590, 1573, 1504, 1415, 1262, 1022, 981, 890; HRMS *m/z*: 278.1172 ([M + H])⁺; Calcd: 278.1181.

4.3.2. Chemistry

The prepared compounds were characterized by ¹H NMR, ¹³C NMR, IR and mass spectral analyses. The signals for phenolic hydroxyl protons appeared between 11–12 ppm and for naphthyl protons were seen between 12 and 13.5 ppm as indicated by the ¹H NMR spectra. The signals for aromatic hydrogens were between 6.35 and 8.45 ppm. The most noticeable feature of the structural characterization of compounds **11a–16a** was the assignment of the proton resonances of their α, β-unsaturated moiety, which was confirmed from the values of the vicinal coupling constants that established the *trans* configuration of these 2 protons. The IR spectrum of the compounds **11a–16a** showed absorption due to –OH stretching at ~ 3350 cm⁻¹, and α, β unsaturated carbonyl group at ~1700 cm⁻¹. The spectra of allyl alcohol compounds displayed singlets (δ 5.40–5.55) which integrated to one proton while no such peak existed in the starting material. This demonstrates that reduction had occurred in the carbonyl groups, yielding the alcohol products. The signal for the aromatic protons in the allyl alcohol products shifted to lower fields. ¹³C NMR showed no peaks in the characteristic carbonyl region, with the appearance of a peak at (δ 59.8–63.2) due to the carbon possessing the new hydroxyl group. No peaks appeared between 1630 cm⁻¹–1800 cm⁻¹ demonstrating the absence of carbonyl groups.

Removal of the 2'-hydroxyl group in chalcone compounds led to a dramatic loss in inhibitory activities, indicating the significance of the 2'-hydroxyl group attached to ring A of the chalcone. This was probably due to an increase in the electrophilic properties

of an α , β unsaturated ketone by hydrogen bonding between the 2'-hydroxy group and the ketone moiety. Eliminating the carbonyl group progressively increased tyrosinase inhibitory activity (**Table 6**). This demonstrated the negative effect of carbonyl group and identified the major role of selective carbonyl reduction that led to an enhancement in flexibility of the chalcone compound.

Table 6 Docking results and tyrosinase inhibition effects of allyl alcohols

Compound	Tyrosinase inhibition at 50 μ M (%) *	CDOCKER energy (kcal/mol)	Type of interactions	Donor-acceptor	Distance (\AA)
11b	80.6 \pm 0.5	-24.89	H-bonding	2'-OH...OH-C	1.95
			H-bonding	2-OH...O δ_1 (Asn260)	2.26
			H-bonding	2'-OH... HE $_{11}$ (His259)	2.25
			hydrophobic stacking	π - π ring B...His263	4.12
12b	70.2 \pm 0.12	-20.22	H-bonding	2-OH...O δ_1 (Asn260)	2.20
			hydrophobic stacking	π - π ring B...His263	4.07
			H-bonding	2'-OH... NE $_2$ (His244)	2.11
			Intramolecular bonding	H- 2'-OH...O=C	1.97
13b	75.1 \pm 0.22	-21.92	H-bonding	(His259) HE $_1$... OH..C	2.37
			H-bonding	2-OH...O δ_1 (Asn260)	2.20
			H-bonding	(His61) HE $_1$... OH-2'	3.09
			hydrophobic stacking	π - π ring B...His263	4.40
			H-bonding	2-OH...O δ_1 (Asn260)	2.90
			H-bonding	C-H... O ϵ_2 (Glu256)	2.91
			H-bonding	C-OH... NE $_2$ (His244)	2.12
			hydrophobic stacking	π - π ring B...His263	4.32
14b	48.5 \pm 0.40	-10.40	H-bonding	2'-OH... NE $_2$ (His244)	2.05
			hydrophobic stacking	π - π ring B...His263	3.64
15b	52.3 \pm 0.55	-12.09	H-bonding	2'-OH... NE $_2$ (His244)	2.21
			H-bonding	2'-OH...OH-C	1.98
16b	59.2 \pm 0.35	-12.63	H-bonding	Asn260 H α ...O	2.93
			H-bonding	Val283 H α ...O	2.64
			H-bonding	H... O=C (Met280)	2.84
Kojic acid	49.5 \pm 0.66	-11.69			

* Values indicated means \pm SE for three determinations

Among the azachalcone derivatives synthesized, compounds **11b** and **13b** exhibited the greatest inhibition of the L-DOPA oxidase activity of mushroom tyrosinase. These compounds were found to be more potent than the positive control, kojic acid. Thus the reduction of the carbonyl group brought about a substantial increase in potency.

Some possible structure–activity relationships could be inferred from tyrosinase inhibitory assay results: the nitrogen atom of substituted pyridinyl chalcone derivatives can possibly get protonated at physiological pH and might act as a positive center capable of interacting with anionic or partially anionic groups of amino acid residues existing in the tyrosinase active site. It was likely for the nitrogen atom in pyridine skeleton to coordinate with the copper atoms present in the tyrosinase active site. Replacement of the phenyl group with a naphthyl group led to a considerable decline in inhibitory activities indicating that the bulky naphthyl group in ring A might cause stereo-hindrance for the inhibitors approaching the active site.

4.3.3. Kinetics

To explore the mechanism of the most active inhibitors **11b** and **13b**, a study of the kinetic behaviour of tyrosinase activity was conducted in the presence of inhibitors. The reaction rates were measured in the presence of active inhibitors with various concentrations of L-DOPA as a substrate. As the concentrations of active inhibitors **11b** and **13b** increased, K_m values gradually increased, but V_{max} values did not change, thereby indicating that the inhibitors acted as competitive inhibitors of mushroom tyrosinase (**Figure 22**). A comparison of the K_m and K_i values of the compounds with that of kojic acid revealed that they possess much higher affinity for tyrosinase than kojic acid (**Table 7**).

Table 7 Effect on mushroom polyphenol oxidase activity and kinetic analysis of compounds.

Compound	Type of inhibition	IC ₅₀ (μM)	K _i (μM) [#]
11b	Competitive	8.70 \pm 0.57	3.82
13b	Competitive	10.25 \pm 0.40	4.56
Kojic acid	Competitive	28.79 \pm 0.85	10.23

[#]: Values were measured at 5 μM of active compounds and K_i is the (inhibitor constant).

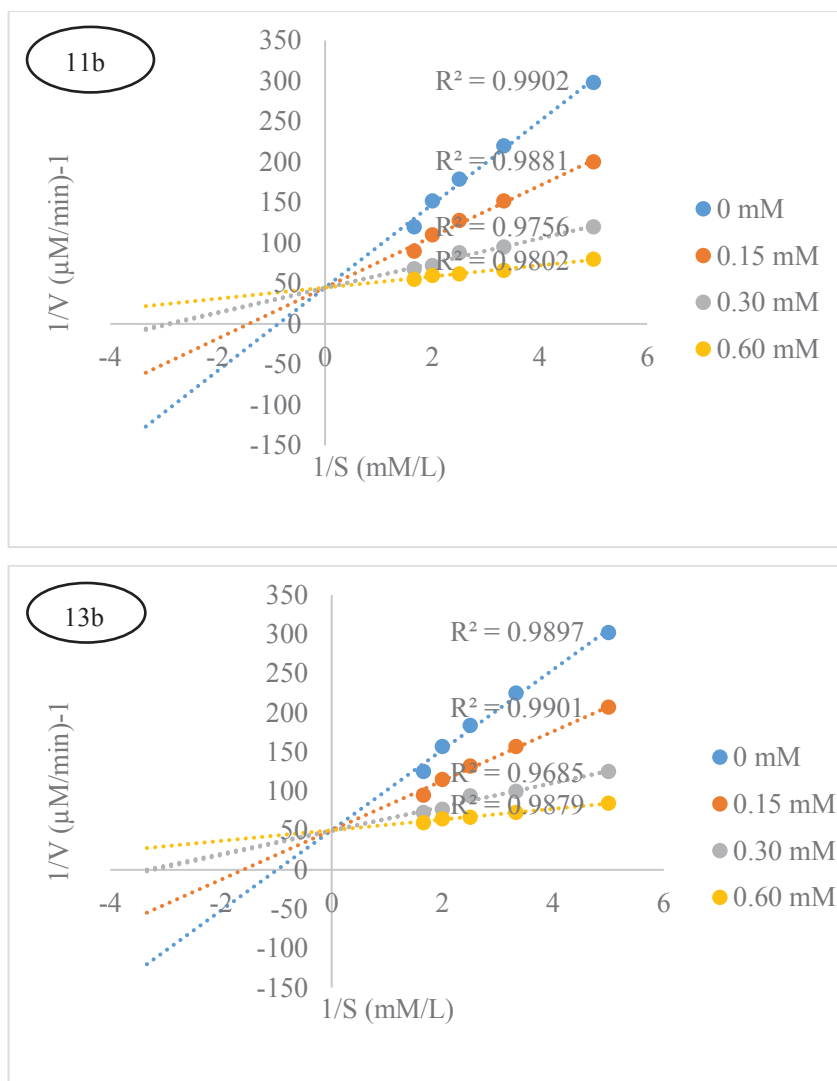


Figure 22 Lineweaver-Burk plots for inhibition of active compounds **11b** and **13b**

The inhibitor concentrations were 0, 0.15, 0.30 and 0.60 mM. The final enzyme concentration was 2.9 μg/ml.

Dixon plots gave a family of straight lines passing through the same point at the second quadrant, giving the inhibition constant (K_i) (**Figure 23**). The K_i value estimated from this Dixon plot was 3.82 μM and 4.56 μM for the compounds **11b** and **13b**, respectively.

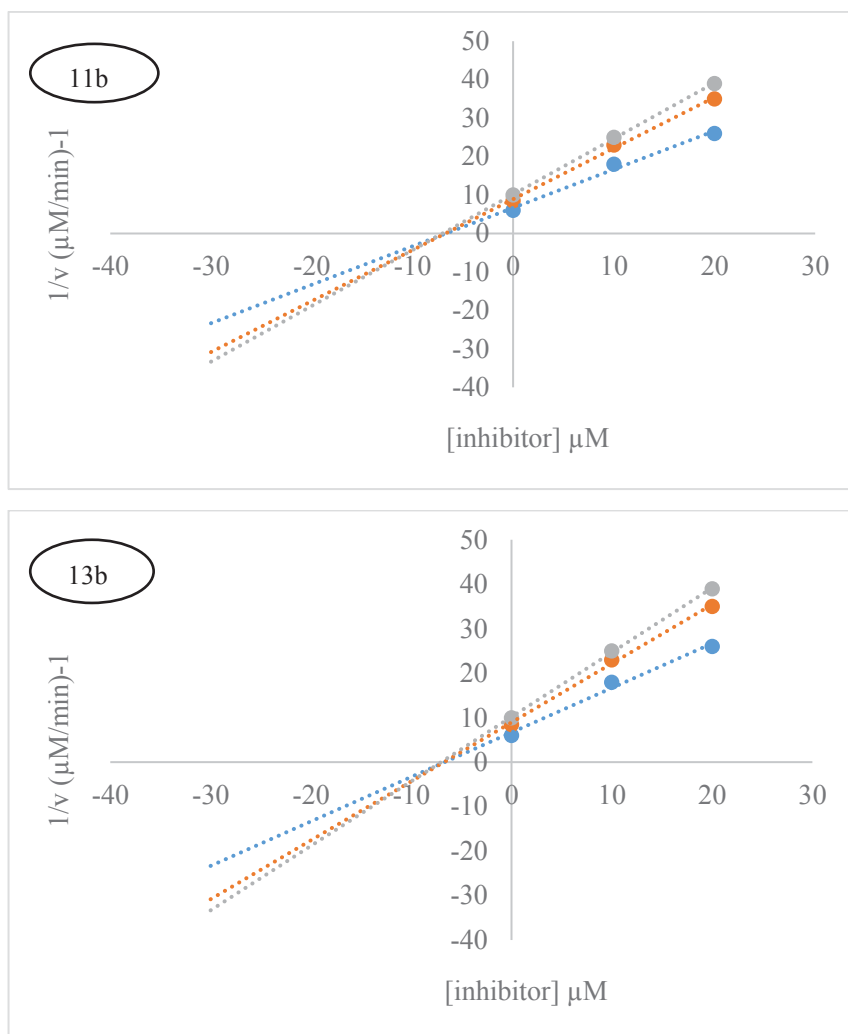


Figure 23 Dixon plot for the inhibitory effect of compounds **11b** and **13b**

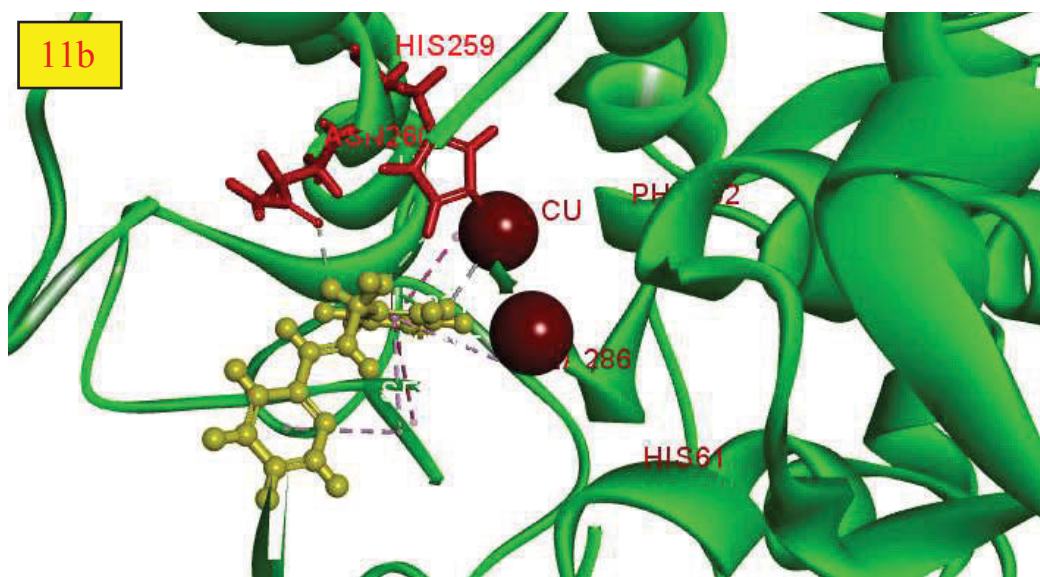
The inhibitor concentrations were 0, 10 and 20 μM . The L-DOPA concentrations were 100, 200 and 300 μM .

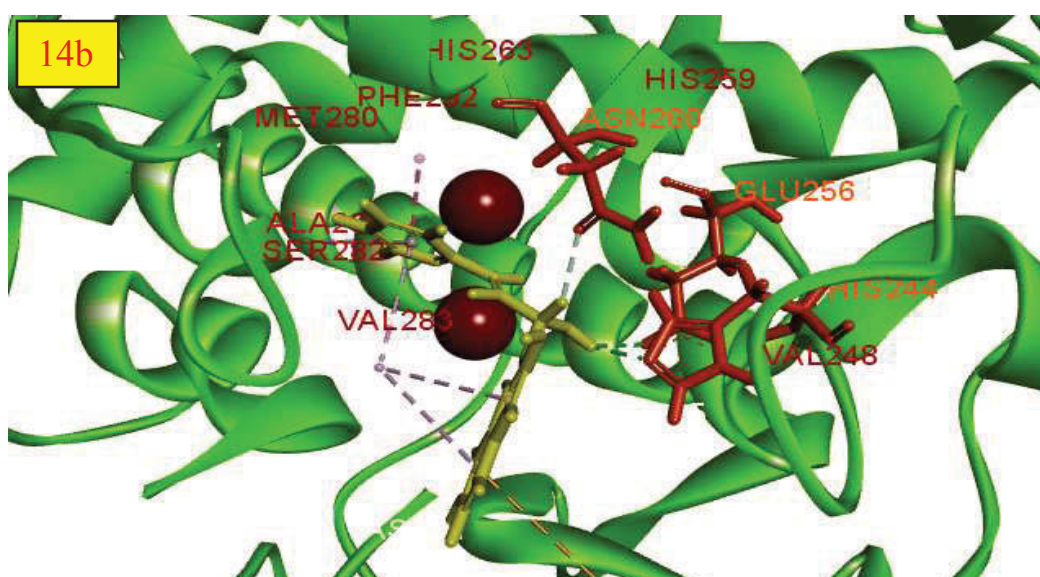
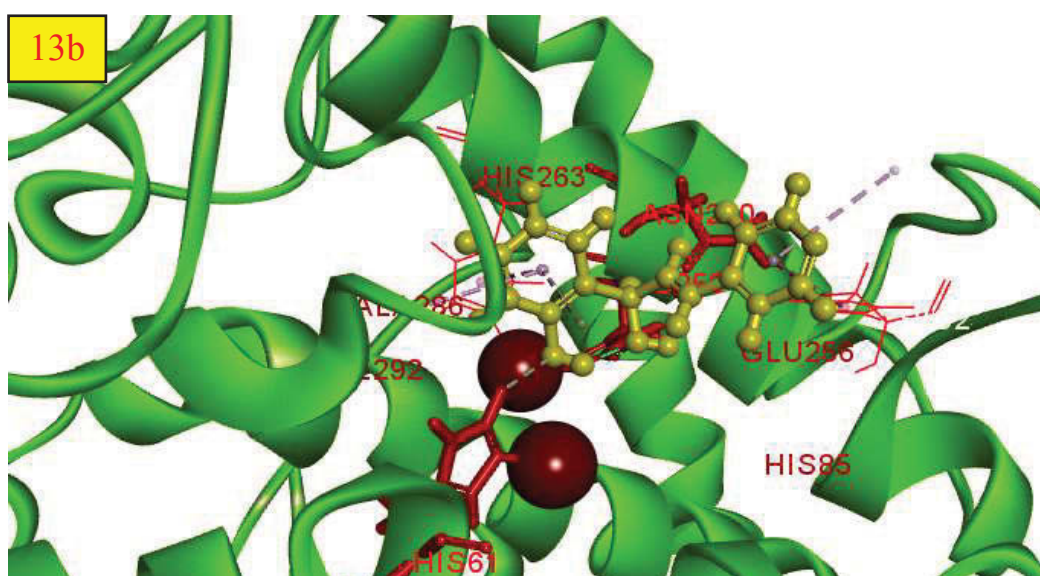
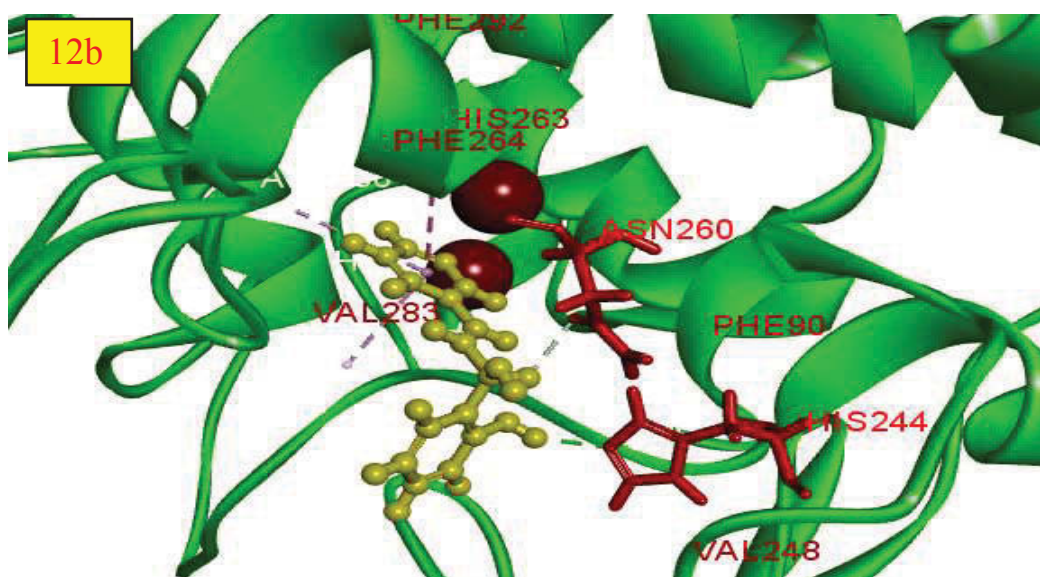
4.3.4. Docking results

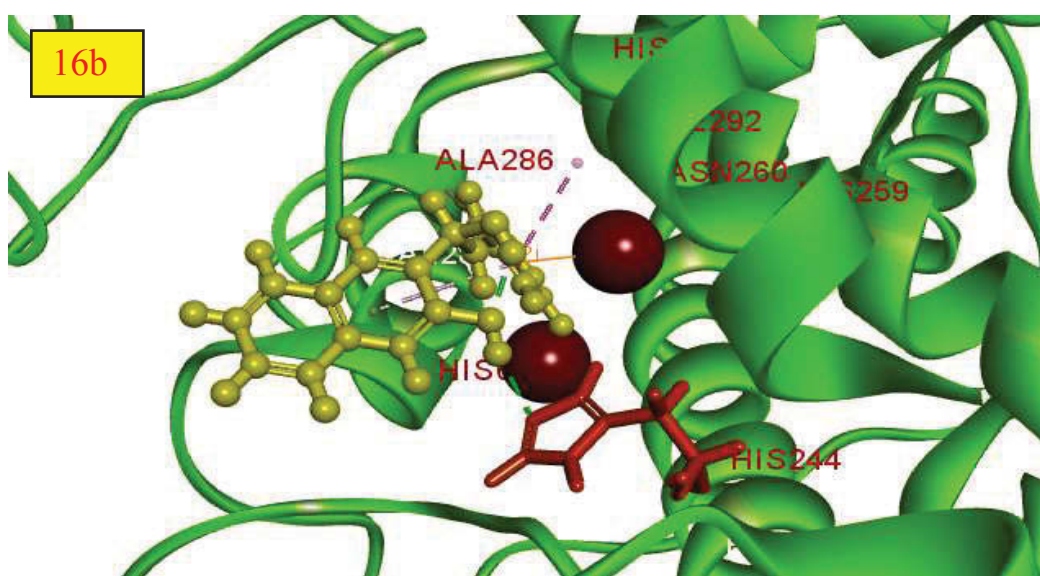
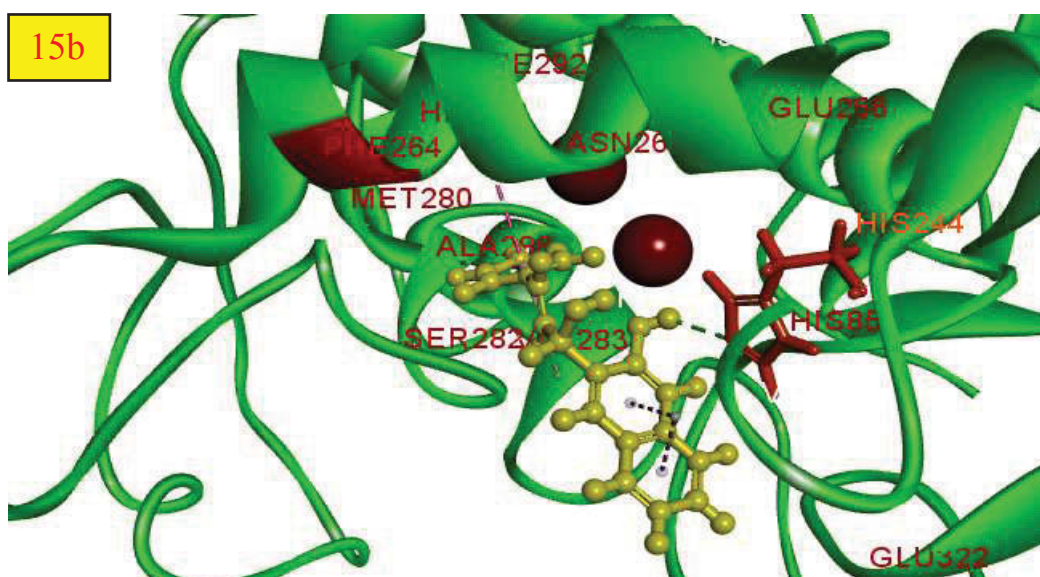
In the novel approaches of structure based drug design, docking was widely used as a computational method to determine the possible binding modes of a ligand to the active site of the receptor. Hence, the experimental results were integrated with computational simulation methods so as to obtain a relative insight into the molecular mechanisms governing the mode of inhibition. The synthesized compounds were docked on the enzyme tyrosinase. Docking procedures basically aimed to identify the correct conformation of ligands in the binding pocket of a protein and to predict the affinity between the ligand and the protein. Accelrys Discovery studio 4.5 suite was utilized to simulate binding between the active site of mushroom tyrosinase and the hydroxy substituted allyl alcoholic azachalcones. Molecular mechanics force field Charm M was

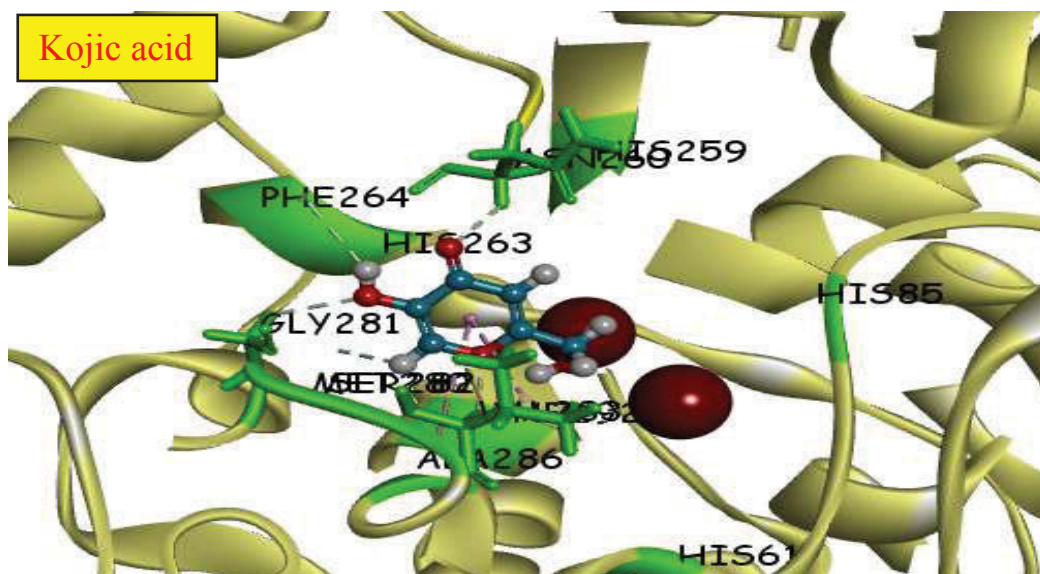
used for the estimation of binding affinity. The scoring function considered a pose as an input and returned a number indicating the likelihood for the pose to represent a favourable binding interaction. Most scoring functions were physics-based mechanics force that estimated the energy of the pose; a low (negative) energy indicated a stable system and thus a likely binding interaction (Ross & Subramanian 1981).

The results of virtual screening studies indicated that the estimated CDOCKER energy of all the docked ligands ranged between -24.89 and -10.40 kcal/mol. Among all the compounds docked, compound **11b** showed the lowest estimated free energy of binding (-24.89 kcal/mol) which correlated well with the experimental results (IC₅₀: 8.70 μ M). The most important binding residues for interaction with **11b** were found to be His259, His244, Asn260, Phe264, Val283, Ala286, His61, His85, Ser282, His263, Asn260 and Val283. The residues could have a key function and effect on binding affinity. **Figure 24** showed selected docked conformations of compounds **11b–16b** along with the positive control, kojic acid in the tyrosinase binding site.

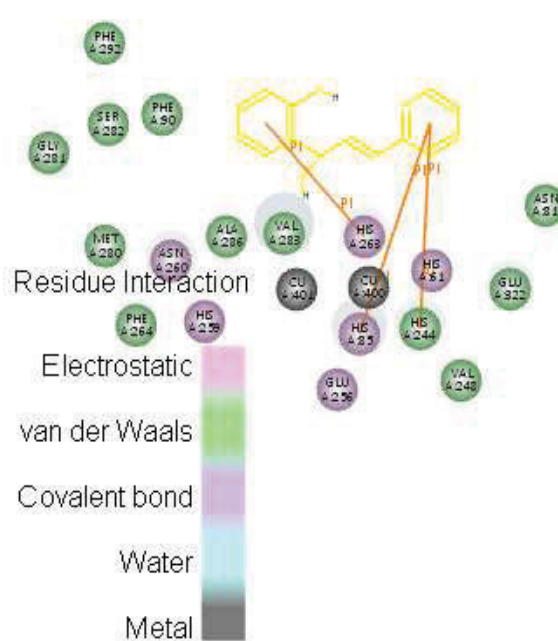




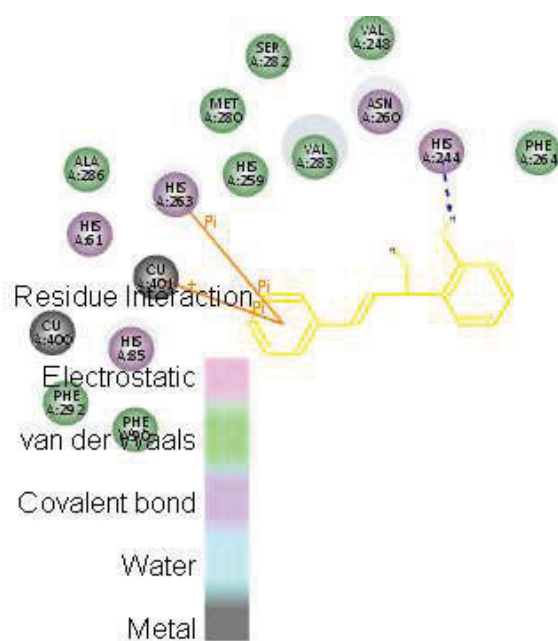




11b



12b



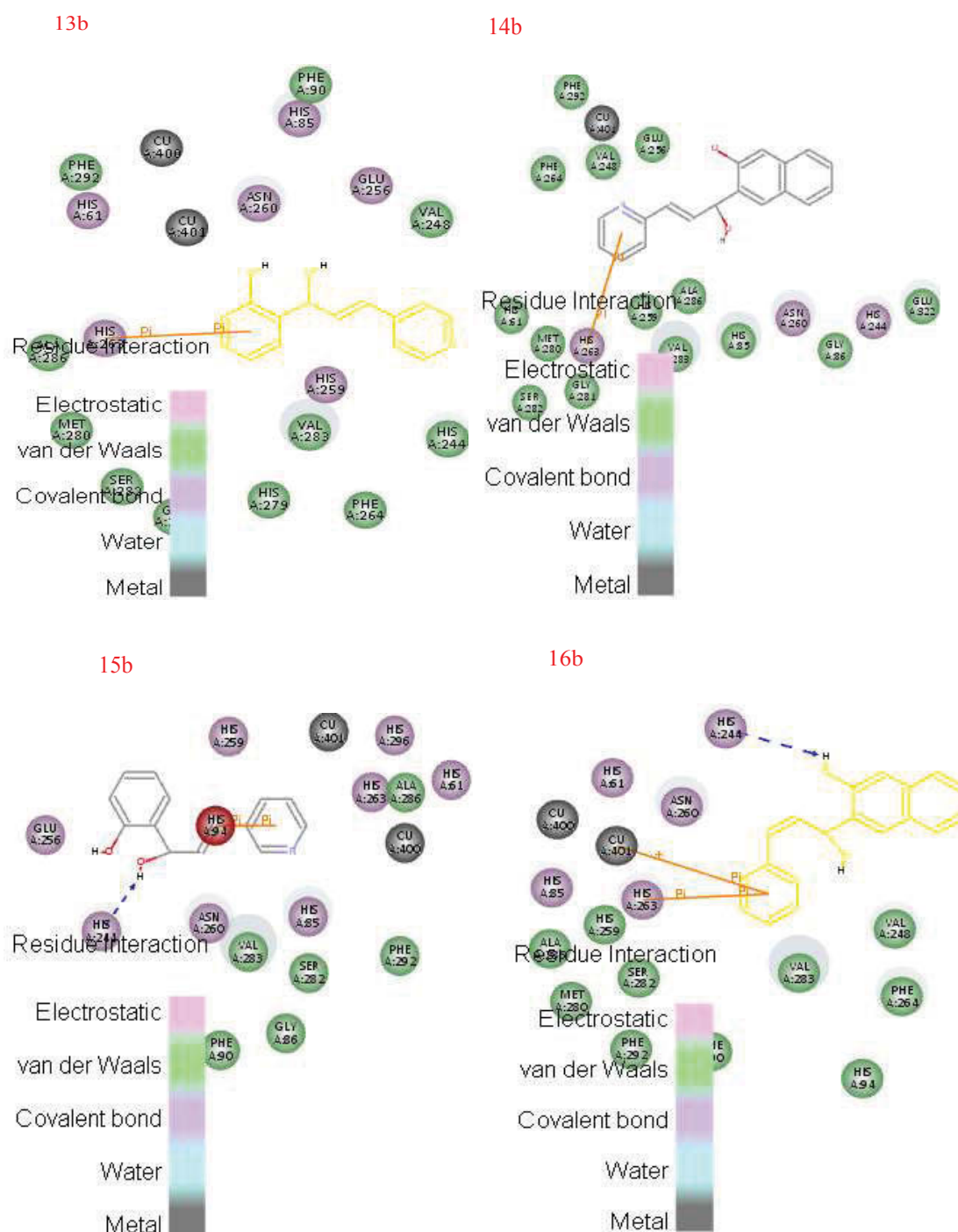


Figure 24 Docking and 2D results of compounds **11b**–**16b**

Ligands **11b**–**16b** were displayed as ball and stick in yellow while the core amino acid residues were displayed as stick in orange. The green dotted lines showed the hydrogen bond interactions and the purple lines showed the non-bonding interactions. The ochre balls represented the copper ions.

Additionally, hydrogen bonding interactions between mushroom tyrosinase and the inhibitor compounds or kojic acid were determined (**Table 6**). Coordinate bonds made a

major contribution to the binding of the inhibitor in the active site. There was a coordination between Cu401 and **the hydroxy oxygen (2') of the ligand 11b** at a distance of 3.21 Å. Tyrosinase substrates like L-DOPA also bind to the copper ion of tyrosinase via their OH group. Formation of a complex between a ligand and the copper ion in the active site of mushroom tyrosinase could prevent electron transfer by the metal ion. Compound **11b** formed one hydrogen bond at a distance of 2.25 Å where the hydrogen from His259 (HE₁) donated a hydrogen bond to the alcoholic oxygen on the alpha carbon atom. Additionally, the alpha-hydrogen atom formed a hydrogen bond (2.26 Å) with the carbonyl oxygen of Asn260. This helped the compound to fit into the catalytic pocket.

The catalytic pocket of the enzyme was hydrophobic. Adding the ligand led to π - π interactions with the enzyme thereby enhancing drug permeability (David Golan 2008). Hydrophobic π - π stacking interactions were seen with His263 whereas the N-H proton in Ser282 and in Val283 pointing directly at a phenyl ring in a hydrogen bond led to amide- π interactions. Therefore, compound **11b** inhibited tyrosinase activity by binding at the active site of mushroom tyrosinase. There appeared to be a strong intramolecular hydrogen bond (1.95 Å) in compound **11b** between the hydroxyl oxygen (2') of ring A and the alcoholic hydrogen when docked in the tyrosinase active site.

In compound **12b** (Dock score: -20.22 kcal/mol), the alpha-hydrogen atom forms a hydrogen bond (2.26 Å) with the carbonyl oxygen of Asn260. Another hydrogen bond was formed between the 2'-hydroxyl hydrogen of ring A with the imidazole nitrogen of His244 (NE₂) at a distance of 2.11 Å. Compound **13b** with a 4-pyridinyl skeleton gave a binding energy of -21.92 kcal/mol that was greater than the positive control kojic acid (-10.12 kcal/mol). The alpha-hydrogen atom formed a hydrogen bond (2.20 Å) with the carbonyl oxygen of Asn260 whereas the alpha-hydrogen atom accepted a hydrogen bond from His259 (HE₁) at a distance of 2.37 Å. Additionally, there appeared to be a strong intramolecular hydrogen bond (1.84 Å) in compound **13b** between the hydroxyl oxygen (2') of ring A and the alcoholic hydrogen. Docking results demonstrated π - π stacking interactions with His263 and T-shaped edge to face aryl-aryl interactions with His244.

The allylic alcohol products of azanaphthyl chalcones showed a considerable decrease in binding energies when compared to the azaphenyl compounds. This could be attributed to the stereo-hindrance caused by the bulky naphthyl group that could

possibly hinder the approach of the inhibitors to the active site. Compound **14b** gave a binding energy (-10.40 kcal/mol) comparable with that of kojic acid and was found to be the least active compound. The alpha-hydroxyl hydrogen atom donated a hydrogen bond to the carbonyl oxygen of Asn260 and to the oxygen atom (OE₂) of Glu322 at a distance of 2.90 Å and 2.91 Å, respectively. Ring A in compound **4a** formed electrostatic π -anion interaction with Glu322 (OE₁) while ring B of the ligand showed π - π stacking interactions with His263. Both compounds **15b** (-12.09 kcal/mol) and **16b** (-12.63 kcal/mol) formed hydrogen bonds between the 2'-hydroxyl hydrogen of ring A with the imidazole nitrogen of His244 (NE₂) at a distance of 2.05 Å and 2.21 Å, respectively. However, compound **16b** also formed a strong intramolecular hydrogen bond between the hydroxyl oxygen (2') of ring A and the alcoholic hydrogen. Histidine residues (pK value of 6.0) have an important role in enzyme activity, so the allyl compounds **11b–16b** inhibited the tyrosinase activity by forming hydrogen bonds with it. For kojic acid, it was observed that the compound formed hydrogen bonds with Asn260, Gly281, Val283 and also a π - π interaction with His283.

4.4. Conclusion

The allylic alcohol derivatives of phenyl and naphthyl chalcones were found to be more active than their parent chalcones. One possible explanation for this, based on conformational analysis, was an intramolecular hydrogen bond formed, between the carbonyl oxygen and the OH-2' (ring A) in compounds **11a–16a** that hampered the latter to interact with the receptor. Furthermore, the presence of 2'-hydroxy group in a chalcone molecule was found to be crucial for the enhancement of inhibitory activity. This was due to an increase in the electrophilic properties of an α - β unsaturated ketone by hydrogen bonding between the 2'-hydroxy group and the alcoholic hydrogen moiety. Eliminating the carbonyl group progressively increased the tyrosinase inhibitory activity. This demonstrated the negative effect of carbonyl group and identified the major role of selective carbonyl reduction that lead to an enhancement in flexibility of the chalcone compound. Compounds **11b** and **13b** were found to be significantly more potent than kojic acid with their IC₅₀ values of 8.70 μ M and 10.25 μ M, respectively. Lineweaver–Burk plots for inhibition of tyrosinase by compounds **11b** and **13b** indicated the compounds to act as competitive inhibitors of tyrosinase with respect to L-DOPA as a substrate, with their K_i values of 3.82 μ M and 4.56 μ M, respectively for **11b**

and **13b**. Experimentally the compounds exhibited a reversible inhibition of tyrosinase. Ring B of the ligands **11b–16b** extended deep into the hydrophobic pocket and made π - π stacking interactions with His263 while π - σ interactions were seen with Val283. Also, weak hydrogen bond (2.25 Å) was formed between His259 (HE₁) and the alcoholic oxygen on the alpha carbon atom. The 2'-OH group of compound **11b** coordinated weakly (3.21 Å) with the binuclear copper active site of tyrosinase and interacted thereby with the hydrophobic enzyme pocket, leading to enhanced inhibitor-enzyme binding affinity and improved inhibitory effects on mushroom tyrosinase. The information derived from computational analyses provided a tool for predicting inhibitory activities of related compounds and for guiding further structural optimization of new types of tyrosinase inhibitors. This study thus explored novel allylic alcohol derivatives of chalcones that could be targeted as effective depigmentation agents and also be employed to curb tyrosinase affected food depreciation.

4.5. References

David Golan, E 2008, 'Principles of pharmacology: The pathophysiologic basis of Drug therapy', Lipincott Williams and Wilkins, pp. 149-150.

Gemal, AL, Luche, JL 1981, 'Lanthanoids in organic synthesis. 6. Reduction of alpha-enones by sodium borohydride in the presence of lanthanoid chlorides: synthetic and mechanistic aspects', *Journal of the American Chemical Society*, Vol 103, pp. 5454-5459.

Kagan, HB, Namy, JL 1986, 'Lanthanides in organic synthesis', *Tetrahedron*, Vol 42, pp. 6573-6614.

Luche, JL 1978, 'Lanthanides in Organic Chemistry. 1. Selective 1, 2 reductions of conjugated ketones', *Journal of the American Chemical Society*, Vol 100, pp. 2226-2227.

Radhakrishnan, SK, Shimmon, R, Conn, C, Baker, AT 2015 (a), 'Azachalcones: A novel class of polyphenol oxidase inhibitors', *Bioorganic and Medicinal Chemistry Letters*, Vol 25, pp. 1753-1756.

Radhakrishnan, SK, Shimmon, R, Conn, C, Baker, AT 2015 (b), 'Development of hydroxylated naphthylchalcones as polyphenol oxidase inhibitors: Synthesis, biochemistry and molecular docking studies', *Bioorganic Chemistry*, Vol 63, pp. 116-122.

Ross, PD, Subramanian, S 1981, 'Thermodynamics of protein association reactions: forces contributing to stability', *Biochemistry*, Vol 20, pp. 3096-3102.

CHAPTER 5

METHOXYCHALCONE COMPOUNDS

5.1. Introduction

Chalcone derivatives of varied chemical designs are quite significant in anticancer drug discovery. They are known to induce apoptosis (Neves *et al* 2012), DNA and mitochondrial damage (Biradar, Sasidhar & Parveen 2010; Sharma *et al* 2010), inhibit angiogenesis (Mojzisa *et al* 2008), tubulin (Luo *et al* 2011), kinases (Li *et al* 2012) and drug efflux protein activities (Liu, Tee & Go 2008; Juvale, Pape & Wiese 2012; Aly *et al* 2012). They are also implemented in cancer diagnosis (Serra *et al* 2009). Azaphenyl, azanaphthyl and allylic derivatives of chalcones discussed in the previous chapters have shown promising results as tyrosinase inhibitors. Melanoma has been one of the most serious consequences of skin cancer where melanocytes proliferate actively with enhanced accumulation of melanin pigment, leading to pigmentation and discoloration of the skin, in addition to tumor formation (Rao *et al* 2013; Fitzpatrick *et al* 1983). Hydroquinone is one of the most common depigmenting agents for melasma treatment and exhibits clinical efficacy. It has been known to easily autooxidise *in vivo* to the quinone, which elicits cytotoxicity *per se* (Oilinger, Llopis & Cadenas 1989). However, hydroquinone has also been observed to generate reactive oxygen species (ROS) and is considered to be cytotoxic to melanocytes and potentially mutagenic to mammalian cells, causing skin irritation (Ennes, Paschoalick & Alchorne 2000; Engasser 1984; Fisher 1983; Romaguera & Grimalt 1985; Curto *et al* 1999).

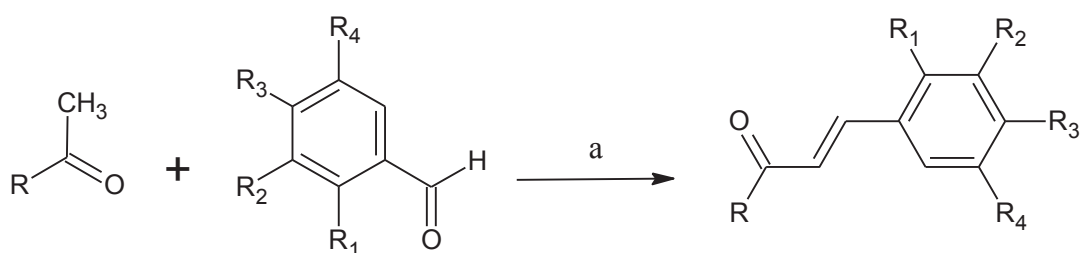
Chalcones, aromatic ketones and enones acting as the precursor for flavonoids such as quercetin, are known for their anticancer effects (Sharma, Kumar & Kumar 2013). The α - β -unsaturated carbonyl enables the chalcone to act as a Michael acceptor for nucleophilic species including glutathione (GSH) or cysteine residues on proteins and may be free from the problems of mutagenicity and carcinogenicity associated with many alkylating agents used in cancer chemotherapy (Ahn & Sok 1966; Lee *et al* 1977). Further literature revealed that structural manipulation of the aryl ring (ring B) in the chalcone skeleton could possibly explore its potential as an anticancer agent in adverse cases of melanoma (Karthikeyan *et al* 2015). Studies have shown that phenyl and naphthyl chalcones substituted with electron donating methoxy groups on ring B had significant cytotoxic activities, when tested on cancer cell lines (Bandgar *et al* 2010; Ethiraj, Aranjani & Khan 2013; Shenvi *et al* 2013).

There has been an increasing impetus to find alternative natural and synthetic pharmaceutical depigmenting agents (Franco *et al* 2012; Parvez *et al* 2006; Zhu & Gao

2008). Compounds that could inhibit melanogenesis while remaining low in cytotoxicity or devoid of toxicity towards melanocytes would be of particular interest. Methoxy substituents on the aryl rings of chalcones were reported to have a pivotal role in influencing their anticancer potential. This prompted to further investigate the effect of methoxyazachalcones and methoxynaphthylchalcones on melanin formation in murine B16F10 cells. Although few methoxychalcone derivatives were known compounds, they have not been reported yet to have an anti-melanogenesis effect.

5.2. Experimental

Simple Claisen-Schmidt condensation reaction was utilized to synthesize a series of methoxychalcone derivatives (See 12.2) in the pursuit for potential skin whitening agents (**Scheme 4**). In the current study, the tyrosinase inhibition effects and kinetic analysis were measured; in addition, docking simulations were performed on mushroom tyrosinase with active tyrosinase inhibitors.



1c: R = 2-C ₃ H ₄ N; R ₁ & R ₄ = H; R ₂ = NO ₂ ; R ₃ = OMe	7c: R = 2-C ₆ H ₄ OH; R ₁ & R ₄ = H; R ₂ = NO ₂ ; R ₃ = OMe	13c: R = naphthalen-2-yl; R ₁ & R ₄ = H; R ₂ = NO ₂ ; R ₃ = OMe
2c: R = 2-C ₃ H ₄ N; R ₁ = OMe; R ₂ & R ₄ = H; R ₃ = NO ₂	8c: R = 2-C ₆ H ₄ OH; R ₁ = OMe; R ₂ & R ₄ = H; R ₃ = NO ₂	14c: R = naphthalen-2-yl; R ₁ = OMe; R ₂ & R ₄ = H; R ₃ = NO ₂
3c: R = 2-C ₃ H ₄ N; R ₁ & R ₄ = OMe; R ₂ & R ₃ = H	9c: R = 2-C ₆ H ₄ OH; R ₁ & R ₄ = OMe; R ₂ & R ₃ = H	15c: R = naphthalen-2-yl; R ₁ & R ₄ = OMe; R ₂ & R ₃ = H
4c: R = 2-C ₃ H ₄ N; R ₂ & R ₄ = OMe; R ₁ & R ₃ = H	10c: R = 2-C ₆ H ₄ OH; R ₂ & R ₄ = OMe; R ₁ & R ₃ = H	16c: R = naphthalen-2-yl; R ₂ & R ₄ = OMe; R ₁ & R ₃ = H
5c: R = 2-C ₃ H ₄ N; R ₂ & R ₃ = OMe; R ₁ & R ₄ = H	11c: R = 2-C ₆ H ₄ OH; R ₂ & R ₃ = OMe; R ₁ & R ₄ = H	17c: R = naphthalen-2-yl; R ₂ & R ₃ = OMe; R ₁ & R ₄ = H
6c: R = 2-C ₃ H ₄ N; R ₁ & R ₃ = OMe; R ₂ & R ₄ = H	12c: R = 2-C ₆ H ₄ OH; R ₁ & R ₃ = OMe; R ₂ & R ₄ = H	18c: R = naphthalen-2-yl; R ₁ & R ₃ = OMe; R ₂ & R ₄ = H

Scheme 4. General method for synthesis of methoxychalcones.
Reagents and conditions: (a) MeOH, NaOH, 0° C, 24hrs.

5.2.1. Method for synthesis of compound 3c.

To a stirred solution of **2'-acetylpyridine** (1mM, 1.21mL) and 2, 5-dimethoxybenzaldehyde (1mM, 166mg) in 25 mL methanol, was added pulverized

NaOH (2mM) and the mixture was stirred at room temperature for 24–36 h. The reaction was monitored by TLC using *n*-hexane: ethyl acetate (7:3) as mobile phase. The reaction mixture was cooled to 0°C (ice-water bath) and acidified with HCl (10 % v/v aqueous solution) to afford total precipitation of the compound. A yellow precipitate was formed, which was filtered and washed with 10 % aqueous HCl solution. The product obtained was recrystallized with ethylacetate to give the pure chalcone product **3c**.

1c. (2*E*)-3-(4-methoxy-3-nitrophenyl)-1-(pyridin-2-yl)prop-2-en-1-one. Yield: 72%; M.p: 119–121°C). ¹H NMR(CDCl₃ δ 8.18 (s, 1H), 7.89 (1H, m, H-6', *J* = 8.5 Hz), 7.80 (1H, dd, H-5', *J* = 9.5 Hz), 8.39 (1H, dd, *J* = 10.0 Hz, H-3), 8.07 (1H, dd, *J* = 9.0 Hz, H-6), 7.85 (1H, t, *J* = 8.0 Hz, H-5), 7.94 (1H, d, *J* = 9.5 Hz, H_a), 7.53 (1H, dd, *J* = 8.4, 9.2 Hz, H-4), 6.95 (1H, d, *J* = 10.0 Hz, H_β), 3.84 (s, 3H, Me); ¹³C NMR(125 MHz, DMSO-d₆) δ 200.2 (C=O), 151.4 (C1), 146.2 (C3), 140.7 (C4), 142.4 (C5), 122.4 (C6), 137.2 (C1'), 116.2 (C2'), 142.2 (C3'), 118.2 (C4'), 126.7 (C5'), 120.2 (C6'), 132.2 (vinylic), 145.2 (vinylic); IR (KBr) ν (cm⁻¹); 3450, 2950, 2924, 2854, 1690, 1535, 1295, 1224, 1122, 877, 722; HRMS *m/z*: 285.0871 ([M + H])⁺; Calcd: 285.0875.

2c. (2*E*)-3-(2-methoxy-4-nitrophenyl)-1-(pyridin-2-yl)prop-2-en-1-one. Yield: 78%; M.p: 127–129°C). ¹H NMR (CDCl₃ δ 8.15 (s, 1H), 7.94 (1H, m, H-6', *J* = 8.5 Hz), 7.79 (1H, d, H-5', *J* = 10.5 Hz), 8.34 (1H, dd, *J* = 7.8, 9.2 Hz, H-3), 8.09 (1H, dd, *J* = 9.2, 9.5 Hz, H-6), 7.87 (1H, t, *J* = 8.0 Hz, H-5), 7.99 (1H, d, *J* = 10.0 Hz, H_a), 7.52 (1H, dd, *J* = 9.0 Hz, H-4), 6.95 (1H, d, *J* = 10.5 Hz, H_β), 3.80 (s, 3H, Me); ¹³C NMR(125 MHz, DMSO-d₆) δ 199.2 (C=O), 150.6 (C1), 145.7 (C3), 140.2 (C4), 142.2 (C5), 120.8 (C6), 137.2 (C1'), 116.2 (C2'), 112.2 (C3'), 138.2 (C4'), 125.3 (C5'), 118.2 (C6'), 130.2 (vinylic), 144.5 (vinylic); IR (KBr) ν (cm⁻¹); 3375, 2965, 2928, 2860, 1700, 1565, 1352, 1250, 1209, 1124, 872, 715; HRMS *m/z*: 285.0869 ([M + H])⁺; Calcd: 285.0875.

3c. (2*E*)-3-(2,5-dimethoxyphenyl)-1-(pyridin-2-yl)prop-2-en-1-one. Yield: 87%; M.p: 110–112°C). ¹H NMR (CDCl₃ δ 8.36 (1H, dd, *J* = 9.0 Hz, H-3), 8.02 (1H, dd, *J* = 9.0, Hz, H-6), 7.89 (1H, d, *J* = 11.5 Hz, H_a), 7.82 (1H, dd, *J* = 9.5 Hz, H-5) 7.65 (1H, dd, *J* = 10.0, 10.5 Hz, H-4'), 7.49 (1H, dd, *J* = 8.5, 10.2 Hz, H-4), 6.95 (1H, d, *J* = 12.5 Hz, H_β), 6.42 (s, 1H, H-6'), 6.47 (1H, dd, *J* = 8.5 Hz, H-3'), 3.87 (s, 3H, Me), 3.80 (s, 3H, Me); ¹³C NMR (125MHz, DMSO-d₆) δ 205.1 (C=O), 150.8 (C1), 145.9 (C3), 137.2 (C4), 135.2 (C5), 120.9 (C6), 109.2 (C5'), 125.4 (vinylic), 140.6 (vinylic), 165.8 (C4'), 160.1 (C6'), 109.1 (C3'), 129.1 (C2'), 120.5 (C1'), 59.1 (CH₃), 55.5 (CH₃); IR (KBr) ν (cm⁻¹):

3389, 3045, 2942, 2855, 1865, 1694, 1642, 1550, 1450, 1224, 1024, 722; MS (ESI): 269.2([M + H])⁺.

4c. (2*E*)-3-(3,5-dimethoxyphenyl)-1-(pyridin-2-yl)prop-2-en-1-one. Yield: 84%; M.p: 128–130°C). ¹H NMR (CDCl₃) δ 8.38 (1H, dd, *J* = 10.0 Hz, H-3), 8.02 (1H, dd, *J* = 9.0 Hz, H-6), 7.89 (1H, t, *J* = 8.0 Hz, H-5), 7.97 (1H, d, *J* = 10.5 Hz, H_α), 7.07 (s, 2H, H-2' & H-6'), 7.47 (1H, dd, *J* = 7.7, 9.2 Hz, H-4), 6.94 (1H, d, *J* = 11.0 Hz, H_β), 6.47 (1H, dd, *J* = 7.2, 8.5 Hz, H-3'), 3.84 (s, 6H, Me); ¹³C NMR (125MHz, DMSO-d₆) δ 199.2 (C=O), 152.3 (C1), 144.7 (C3), 139.2 (C4), 140.2 (C5), 122.8 (C6), 124.1 (vinylic), 144.5 (vinylic), 160.1 (C3' & C5'), 108.1 (C4'), 138.5 (C1'), 107.6 (C2' & C6'), 56.1 (CH₃); IR (KBr) ν (cm⁻¹); 3420, 3047, 2954, 2874, 1874, 1700, 1654, 1524, 1435, 1250, 1172, 1052, 975, 722; MS (ESI); 269.2([M + H])⁺.

5c. (2*E*)-3-(3,4-dimethoxyphenyl)-1-(pyridin-2-yl)prop-2-en-1-one. Yield: 75%; M.p: 132–134°C; ¹H NMR (500 MHz, CDCl₃): δ 8.32 (dd, 1H, H-3', *J* = 9.5), 8.09 (dd, 1H, H-6', *J* = 8.0), 7.87 (d, 1H, H_α, *J* = 11.5), 7.82 (dd, 1H, H-5', *J* = 10.2, 10.5), 7.47 (dd, 1H, H-4', *J* = 9.2, 9.5), 7.44 (dd, 1H, H-6, *J* = 10.2, 10.5), 7.40 (s, 1H), 6.97 (dd, 1H, H-5, *J* = 9.4, 10.0), 6.94 (d, 1H, H_β, *J* = 12.0), 6.47 (dd, 1H, H-3, *J* = 8.5), 3.89 (s, 3H, Me), 3.80 (s, 3H, Me); ¹³C NMR (125MHz, DMSO-d₆) δ 199.4 (C=O), 152.2 (C1'), 144.2 (C3'), 139.2 (C4'), 132.4 (C5'), 122.2 (C6'), 130.4 (C1), 110.6 (C2), 151.2 (C3), 150.6 (C4), 110.6 (C5), 109.5 (C6), 127.7 (vinylic), 144.6 (vinylic), 57.1 (CH₃); IR (KBr) ν (cm⁻¹); 3450, 3035, 2935, 2840, 1852, 1699, 1552, 1446, 1027, 732; MS (ESI): 270.1([M + H])⁺.

6c. (2*E*)-3-(2,4-dimethoxyphenyl)-1-(pyridin-2-yl)prop-2-en-1-one. Yield: 80%; M.p: 110–112°C; ¹H NMR (500 MHz, CDCl₃): δ 8.56 (dd, 1H, *J* = 9.5, H-3), 8.03 (dd, 1H, H-6, *J* = 8.4, 9.0), 7.97 (d, 1H, H_α, *J* = 11.0), 7.84 (t, 1H, H-5, *J* = 9.0), 7.70 (d, 1H, H-5', *J* = 10.5), 7.47 (dd, 1H, H-4, *J* = 9.2, 10.0), 6.97 (d, 1H, H_β, *J* = 11.5), 6.47 (d, 1H, H-6', *J* = 8.5), 6.40 (s, H-3', 1H), 3.89 (s, 3H, Me), 3.82 (s, 3H, Me); ¹³C NMR (125MHz, DMSO-d₆) δ 200.2 (C=O), 152.2 (C1), 147.5 (C3), 136.4 (C4), 136.7 (C5), 121.9 (C6), 109.2 (C5'), 124.9 (vinylic), 142.5 (vinylic), 165.8 (C4'), 160.1 (C6'), 109.1 (C3'), 129.1 (C2'), 120.5 (C1'), 55.1 (CH₃); IR (KBr) ν (cm⁻¹); 3375, 3055, 2924, 2865, 1871, 1695, 1659, 1568, 1465, 1255, 1186, 1020, 742; MS (ESI): 269.2([M + H])⁺.

7c. (2*E*)-1-(2-hydroxyphenyl)-3-(4-methoxy-3-nitrophenyl)prop-2-en-1-one. Yield: 72%; Mp: 110–112°C; ¹H NMR (500 MHz, CDCl₃): δ 12.47 (s, 1H, OH), 8.10 (s, 1H), 7.86 (d, 1H, H_β, *J* = 12.5), 7.74 (d, 1H, H-6', *J* = 10.0), 7.72 (d, 1H, H_α, *J* = 12.0), 7.65 (d,

1H, H-5, $J = 9.5$), 7.54 (d, 1H, H-6, $J = 8.0$), 7.49 (t, 1H, H-4', $J = 8.5$), 6.92 (dd, 1H, H-3', $J = 8.5, 9.5$), 6.90 (dd, 1H, H-5', $J = 9.0$), 3.86 (s, 3H); ^{13}C NMR (125 MHz, DMSO- d_6) δ 192.22 (C=O), 130.52 (C6'), 119.25 (C1'), 118.27 (C5'), 136.77 (C4'), 118.28 (C3'), 161.92 (C2'), 126.90 (C1), 120.54 (C2), 137.22 (C3), 147.50 (C4), 112.42 (C5), 114.23 (C6), 56.67 (Me), 122.40 (vinylic), 141.83 (vinylic); IR (KBr) ν (cm^{-1}): 3200, 3070, 2914, 2864, 2720, 1686, 1578, 1550, 1468, 1349, 970, 720, 580; MS (ESI): 270.1 ($[\text{M} + \text{H}]^+$).

8c. (2*E*)-1-(2-hydroxyphenyl)-3-(2-methoxy-4-nitrophenyl)prop-2-en-1-one. Yield: 68%; Mp: 123–125°C; IR (KBr) ν (cm^{-1}): 3250, 3345, 3015, 2910, 2865, 2700, 1702, 1682, 1552, 1465, 1305, 979, 735, 680, 575; ^1H NMR (500 MHz, CDCl_3): δ 12.22 (s, 1H, OH), 8.22 (s, 1H), 7.95 (d, 1H, H_β , $J = 14.0$), 7.86 (m, 1H, H-6, $J = 9.5$), 7.80 (d, 1H, H_α , $J = 13.5$), 7.75 (d, 1H, H-6', $J = 10.5$), 7.69 (d, 1H, H-5, $J = 8.5$), 7.59 (dd, 1H, H-4', $J = 8.5$), 7.02 (dd, 1H, H-3', $J = 7.7, 9.4$), 6.97 (m, 1H, H-5', $J = 10.0$), 3.82 (s, 3H); ^{13}C NMR (125 MHz, DMSO- d_6) δ 194.25 (C=O), 130.24 (C6'), 119.33 (C1'), 118.20 (C5'), 137.07 (C4'), 118.48 (C3'), 162.90 (C2'), 128.22 (C1), 115.24 (C2), 112.22 (C3), 137.50 (C4), 122.47 (C5), 116.55 (C6), 125.50 (vinylic), 140.87 (vinylic); MS (ESI): 270.1 ($[\text{M} + \text{H}]^+$).

9c. (2*E*)-3-(2,5-dimethoxyphenyl)-1-(2-hydroxyphenyl)prop-2-en-1-one. Yield: 67%; M.p: 132–134°C; ^1H NMR (500 MHz, CDCl_3): δ 12.50 (s, 1H, OH), 7.87 (d, 1H, H_β , $J = 12.5$), 7.81 (dd, 1H, H-3, $J = 8.2, 9.5$), 7.79 (d, 1H, $J = 12.0$, H_α), 7.70 (d, 1H, $J = 9.0$, H-6'), 7.59 (dd, 1H, H-4', $J = 7.5, 8.5$), 7.14 (dd, 1H, H-3', $J = 9.4, 10.0$), 6.94 (dd, 1H, H-5', $J = 10.8, 11.5$), 6.67 (dd, 1H, H-4, $J = 7.4, 8.5$), 6.49 (s, 1H), 3.89 (s, 3H), 3.86 (s, 3H); ^{13}C NMR (125 MHz, DMSO- d_6) δ 200.4 (C=O), 129.7 (C6'), 119.7 (C1'), 118.7 (C5'), 132.9 (C4'), 120.1 (C3'), 160.2 (C2'), 120.2 (C1), 160.7 (C2), 102.5 (C3), 110.1 (C4), 164.7 (C5), 128.5 (C6), 125.7 (vinylic), 140.5 (vinylic); IR (KBr) ν (cm^{-1}): 3255, 3099, 2965, 2875, 1677, 1585, 1505, 1471, 1407, 1225, 1153, 799, 630; MS (ESI): 285.1 ($[\text{M} + \text{H}]^+$).

10c. (2*E*)-3-(3,5-dimethoxyphenyl)-1-(2-hydroxyphenyl)prop-2-en-1-one. Yield: 77%; M.p: 137–139°C; ^1H NMR (500 MHz, CDCl_3): δ 12.57 (s, 1H, OH), 7.92 (d, 1H, H_β , $J = 11.0$), 7.68 (d, 1H, H_α , $J = 10.5$), 7.70 (d, 1H, H-6', $J = 9.5$), 7.59 (dd, 1H, H-4', $J = 8.5$), 7.15 (dd, 1H, H-3', $J = 10.0$), 7.09 (dd, 1H, H-5', $J = 10.5$), 7.00 (dd, 2H, H-2 & H-6, $J = 10.5$), 6.70 (s, 1H), 3.84 (s, 6H); ^{13}C NMR (125 MHz, DMSO- d_6) δ 200.7 (C=O), 131.6 (C6'), 119.1 (C1'), 120.4 (C5'), 135.2 (C4'), 118.7 (C3'), 160.3 (C2'), 120.2

(C1), 163.2 (C2), 161.2 (C3 & C5), 167.1 (C4), 130.2 (C6), 129.2 (vinylic), 140.7 (vinylic); IR (KBr) ν (cm⁻¹): 3255, 3065, 2955, 2850, 2730, 1698, 1592, 1502, 1495, 1395, 1205, 1190, 950, 873; MS (ESI): 285.1 ([M + H])⁺.

11c. (2*E*)-3-(3,4-dimethoxyphenyl)-1-(2-hydroxyphenyl)prop-2-en-1-one. Yield: 82%; M.p: 123–125°C; ¹H NMR (500 MHz, CDCl₃): δ 12.45 (s, 1H, OH), 7.97 (d, 1H, H _{β} , *J* = 13.0), 7.92 (d, 1H, H _{α} , *J* = 11.0), 7.75 (d, 1H, H-6', *J* = 9.0), 7.47 (dd, 1H, *J* = 8.5, 9.5, H-6), 7.41 (s, 1H), 7.58 (dd, 1H, H-4', *J* = 7.4, 8.0), 7.17 (dd, 1H, H-3', *J* = 9.5, 10.5), 6.98 (dd, 1H, H-5, *J* = 9.0), 6.94 (dd, 1H, H-5', *J* = 10.2, 11.2), 3.87 (s, 3H), 3.82 (s, 3H); ¹³C NMR (125 MHz, DMSO-d₆) δ 199.7 (C=O), 129.7 (C6'), 119.1 (C1'), 118.7 (C5'), 130.9 (C4'), 119.5 (C3'), 160.8 (C2'), 130.2 (C1), 110.2 (C2), 149.2 (C3), 154.1 (C4), 109.7 (C5), 110.5 (C6), 129.7 (vinylic), 145.6 (vinylic); IR (KBr) ν (cm⁻¹): 3435, 3000, 2947, 2840, 2726, 1685, 1587, 1512, 1468, 1467, 1269, 1190, 1042, 672; MS (ESI): 285.1 ([M + H])⁺.

12c. (2*E*)-3-(2,4-dimethoxyphenyl)-1-(2-hydroxyphenyl)prop-2-en-1-one. Yield: 85%; M.p: 128–130°C; ¹H NMR (500 MHz, CDCl₃): δ 12.25 (s, 1H, OH), 7.97 (d, 1H, H _{β} , *J* = 13.0), 7.82 (d, 1H, H _{α} , *J* = 12.5), 7.74 (dd, 1H, H-6, *J* = 4.5, 9.0), 7.72 (d, 1H, H-6', *J* = 9.5), 7.62 (dd, 1H, *J* = 5.6, 8.0, H-4'), 7.10 (d, 1H, *J* = 9.5, H-3'), 6.99 (dd, 1H, H-5', *J* = 4.5, 10.5), 6.60 (dd, 1H, H-5, *J* = 7.5), 6.44 (s, 1H), 3.82 (s, 3H), 3.87 (s, 3H); ¹³C NMR (125 MHz, DMSO-d₆) δ 199.2 (C=O), 130.2 (C6'), 120.1 (C1'), 119.4 (C5'), 134.7 (C4'), 118.1 (C3'), 159.8 (C2'), 120.2 (C1), 163.2 (C2), 100.2 (C3), 167.1 (C4), 107.7 (C5), 130.5 (C6), 127.2 (vinylic), 142.7 (vinylic); IR (KBr) ν (cm⁻¹): 3245, 3017, 2955, 2615, 1669, 1582, 1502, 1468, 1427, 1285, 1025, 942, 642; MS (ESI): 285.1 ([M + H])⁺.

13c. (2*E*)-1-(2-hydroxyphenyl)-3-(4-methoxy-3-nitrophenyl)prop-2-en-1-one. Yield: 68%; M.p: 110–112°C; ¹H NMR (500 MHz, CDCl₃): δ 12.47 (s, 1H, OH), 8.10 (s, 1H), 7.86 (d, 1H, *J* = 12.5, H _{β}), 7.74 (d, 1H, *J* = 10.0, H-6'), 7.72 (d, 1H, *J* = 12.0, H _{α}), 7.65 (d, 1H, *J* = 9.5, H-5), 7.54 (d, 1H, *J* = 8.0, H-6), 7.49 (t, 1H, *J* = 8.5, H-4'), 6.92 (dd, 1H, *J* = 9.5, H-3'), 6.90 (dd, 1H, *J* = 9.0, H-5'), 3.86 (s, 3H); ¹³C NMR (125 MHz, DMSO-d₆) δ 192.22 (C=O), 130.52 (C6'), 119.25 (C1'), 118.27 (C5'), 136.77 (C4'), 118.28 (C3'), 161.92 (C2'), 126.90 (C1), 120.54 (C2), 137.22 (C3), 147.50 (C4), 112.42 (C5), 114.23 (C6), 56.67 (Me), 122.40 (vinylic), 141.83 (vinylic); IR (KBr) ν (cm⁻¹): 3200, 3070, 2914, 2864, 2720, 1686, 1578, 1550, 1468, 1349, 970, 720, 580; MS (ESI): 270.1 ([M + H])⁺.

14c. (2*E*)-1-(2-hydroxyphenyl)-3-(2-methoxy-4-nitrophenyl)prop-2-en-1-one. Yield: 72%; Mp: 123–125°C; ¹H NMR (500 MHz, CDCl₃): δ 12.22 (s, 1H, OH), 8.22 (s, 1H), 7.95 (d, 1H, *J* = 14.0, H_β), 7.86 (m, 1H, *J* = 9.5, H-6), 7.80 (d, 1H, *J* = 14.0, H_α), 7.75 (d, 1H, *J* = 10.5, H-6'), 7.69 (d, 1H, *J* = 8.5, H-5), 7.59 (dd, 1H, *J* = 8.5, H-4'), 7.02 (dd, 1H, *J* = 9.0, H-3'), 6.97 (m, 1H, *J* = 10.0, H-5'), 3.82 (s, 3H); ¹³C NMR (125 MHz, DMSO-*d*₆) δ 194.2 (C=O), 130.2 (C6'), 119.3 (C1'), 118.2 (C5'), 137.0 (C4'), 118.4 (C3'), 162.9 (C2'), 128.2 (C1), 115.2 (C2), 112.2 (C3), 137.5 (C4), 122.4 (C5), 116.5 (C6), 125.5 (vinylic), 140.8 (vinylic); IR (KBr) ν (cm⁻¹): 3250, 3345, 3015, 2910, 2865, 2700, 1702, 1682, 1552, 1465, 1305, 979, 735, 680, 575; MS (ESI): 270.1 ([M + H])⁺.

15c. (2*E*)-3-(2,5-dimethoxyphenyl)-1-(3-hydroxynaphthalen-2-yl)prop-2-en-1-one. Yield: 80%; M.p 114–116°C. ¹H NMR (500 MHz, CDCl₃): δ 12.54 (s, 1H, OH), 8.12 (dd, 1H, *J* = 12.5, H-10'), 7.96 (d, 1H, *J* = 13.0, H_α), 7.85 (s, 1H, H-6), 7.80 (dd, 1H, *J* = 10.0, H-5'), 7.67 (dd, 1H, *J* = 8.5, H-7'), 7.59 (dd, 1H, *J* = 9.0, H-8'), 7.52 (dd, 1H, *J* = 9.5, H-6'), 7.49 (d, 1H, *J* = 9.5, H-3'), 6.92 (d, 1H, *J* = 13.5, H_β), 6.57 (dd, 1H, *J* = 10.0, H-4), 6.49 (dd, 1H, *J* = 9.5, H-3), 3.82 (s, 3H), 3.80 (s, 3H); ¹³C NMR (125 MHz, DMSO-*d*₆) δ 195.2 (C=O), 116.5 (C1'), 166.2 (C2'), 123.2 (C3'), 136.1 (C4'), 130.4 (C5'), 134.0 (C6'), 128.4 (C7'), 130.0 (C8'), 122.4 (C9'), 131.2 (C10'), 142.4 (vinylic), 131.7 (vinylic), 129.2 (C1), 156.6 (C2), 112.3 (C3), 126.4 (C4), 153.2 (C5), 112.2 (C6), 56.2 (Me); IR (KBr) ν (cm⁻¹): 3022, 2992, 2773, 1682, 1550, 1425, 1046, 814, 707; MS (ESI): 335.1 ([M + H])⁺.

16c. (2*E*)-3-(3,5-dimethoxyphenyl)-1-(3-hydroxynaphthalen-2-yl)prop-2-en-1-one. Yield: 85%; M.p 118–120°C. ¹H NMR (500 MHz, CDCl₃): δ 12.62 (s, 1H, OH), 7.92 (dd, 1H, *J* = 10.0, H-10'), 7.85 (d, 1H, *J* = 10.0, H_α), 7.82 (dd, 1H, *J* = 10.5, H-5'), 7.69 (t, 1H, *J* = 9.5, H-7'), 7.58 (dd, 1H, *J* = 6.5, 9.5, H-8'), 7.55 (m, 1H, *J* = 8.5, H-6'), 7.50 (d, 1H, *J* = 9.0, H-3'), 7.09 (d, 2H, H-2 & H-6), 7.07 (d, 1H, *J* = 10.5, H_β), 6.75 (s, 1H, H-4), 3.90 (s, 6H); ¹³C NMR (125 MHz, DMSO-*d*₆) δ 198.5 (C=O), 118.1 (C1'), 167.2 (C2'), 124.2 (C3'), 140.4 (C4'), 135.3 (C5'), 135.2 (C6'), 124.9 (C7'), 130.2 (C8'), 124.1 (C9'), 134.5 (C10'), 144.0 (vinylic), 133.2 (vinylic), 138.2 (C1), 106.6 (C2 & C6), 163.3 (C3 & C5), 106.2 (C4), 55.2 (Me); IR (KBr) ν (cm⁻¹): 3062, 2947, 2729, 2514, 1692, 1597, 1512, 1436, 1208, 1054, 871, 732; MS (ESI): 335.1 ([M + H])⁺.

17c. (2*E*)-3-(3,4-dimethoxyphenyl)-1-(3-hydroxynaphthalen-2-yl)prop-2-en-1-one. Yield: 62%; M.p: 108–110°C; ¹H NMR (500 MHz, CDCl₃): δ 12.65 (s, 1H, OH), 8.20 (dd, 1H, H-10', *J* = 12.5), 7.96 (d, 1H, *J* = 13.0, H_α), 7.80 (dd, 1H, *J* = 10.0, H-5'), 7.48

(dd, 1H, $J = 7.2, 10.5$, H-6), 7.65 (t, 1H, $J = 8.0$, H-7'), 7.59 (dd, 1H, $J = 8.5$, H-8'), 7.54 (dd, 1H, $J = 9.0$, H-6'), 7.48 (d, 1H, $J = 8.0$, H-3'), 7.39 (s, 1H), 7.14 (d, 1H, $J = 13.5$, H $_{\beta}$), 6.93 (dd, 1H, $J = 11.5$, H-5), 3.80 (s, 3H), 3.84 (s, 3H); ^{13}C NMR (125 MHz, DMSO- d_6) δ 196.2 (C=O), 116.4 (C1'), 162.2 (C2'), 127.2 (C3'), 139.4 (C4'), 129.4 (C5'), 130.5 (C6'), 127.4 (C7'), 129.2 (C8'), 125.2 (C9'), 136.0 (C10'), 144.1 (vinylic), 130.2 (vinylic), 129.6 (C1), 110.6 (C2), 150.3 (C3), 156.2 (C4), 107.7 (C5), 110.2 (C6), 55.6 (Me); IR (KBr) ν (cm^{-1}): 3475, 3007, 2957, 2781, 2614, 1679, 1562, 1447, 1382, 1218, 1102, 817, 737, 605; HRMS m/z : 335.1274 ($[\text{M} + \text{H}]^+$); Calcd: 335.1283.

18c. (2*E*)-3-(2,4-dimethoxyphenyl)-1-(3-hydroxynaphthalen-2-yl)prop-2-en-1-one. Yield: 79%; M.p 87–89°C; ^1H NMR (500 MHz, CDCl_3): δ 12.72 (s, 1H, OH), 8.19 (dd, 1H, H-10', $J = 15.0$), 7.98 (d, 1H, H $_{\alpha}$, $J = 14.5$), 7.82 (dd, 1H, H-5', $J = 12.0$), 7.78 (dd, 1H, H-6, $J = 7.0, 10.0$), 7.63 (t, 1H, H-7', $J = 8.5$), 7.57 (dd, 1H, H-8', $J = 7.2, 8.0$), 7.49 (dd, 1H, H-6', $J = 6.8, 9.0$), 7.47 (d, 1H, H-3', $J = 9.0$), 7.09 (d, 1H, H $_{\beta}$, $J = 15.0$), 6.53 (t, 1H, H-5, $J = 16.0$), 6.44 (m, 1H, H-3, $J = 9.0$), 3.86 (s, 3H), 3.88 (s, 3H); ^{13}C NMR (125 MHz, DMSO- d_6) δ 194.6 (C=O), 114.1 (C1'), 165.0 (C2'), 122.2 (C3'), 137.1 (C4'), 130.4 (C5'), 132.6 (C6'), 126.1 (C7'), 128.4 (C8'), 124.4 (C9'), 133.2 (C10'), 140.8 (vinylic), 130.5 (vinylic), 119.2 (C1), 162.6 (C2), 99.3 (C3), 166.2 (C4), 107.2 (C5), 130.2 (C6), 55.6 (Me); IR (KBr) ν (cm^{-1}): 3018, 2957, 2781, 2614, 1679, 1562, 1427, 1375, 1218, 1102, 817, 717, 605; MS (ESI): 335.1 ($[\text{M} + \text{H}]^+$).

5.3. Results and Discussion

5.3.1. Chemistry & inhibition kinetics

Results showed that compounds **3c** and **1c** were found to be twice as active as kojic acid with their IC_{50} values of 10.6 μM and 12.5 μM , respectively in the overall structure activity relationship study, as shown in **Table 8**. This was consistent with the docking results where the electron-donating groups increased the electron density of ring B through a resonance donating effect and higher electron density bonded the copper ions more effectively in the active site of enzyme. Replacement of the phenyl group with a naphthyl group led to a decline in inhibitory activities indicating that the bulky naphthyl group in ring A might cause stereo-hindrance for the inhibitors approaching the active site. However, substituting the naphthylchalcones with electron withdrawing nitro group on ring B gave compound **14c** and **13c** with inhibitory potentials that were still more

effective than kojic acid (IC_{50} : 23.72 μ M). However, the introduction of a pyridinyl ring brought about an increase in tyrosinase inhibition.

The nitrogen atom of substituted pyridinyl chalcone derivatives can possibly get protonated at physiological pH and might act as a positive center capable of interacting with anionic or partially anionic groups of amino acid residues existing in the tyrosinase active site. It was likely for the nitrogen atom in pyridine skeleton to coordinate with the copper atoms present in the tyrosinase active site.

The bioactivities of compounds **3c** and **1c**, which had more potent activity than kojic acid were investigated in greater detail. The reaction rates were measured, in the presence of active inhibitors, with various concentrations of L-DOPA as a substrate.

Table 8 Docking results, tyrosinase inhibition and cytotoxic effects of methoxychalcones

Compound	Yield (%)	IC_{50} (μ M) *		CDOCKER energy (kcal/mol)
		Tyrosinase activity	Cytotoxic activity	
1c	74.8	12.5 \pm 0.22	4.7 \pm 0.12	-19.23
2c	92.5	14.1 \pm 0.45	10.5 \pm 0.56	-18.48
3c	88.2	10.6 \pm 0.66	4.2 \pm 0.32	-21.32
4c	84.5	20.8 \pm 0.15	20.3 \pm 0.45	-12.25
5c	90.2	20.2 \pm 0.36	16.2 \pm 0.63	-14.20
6c	72.3	19.6 \pm 0.36	14.3 \pm 0.66	-17.26
7c	45.7	15.4 \pm 0.11	12.2 \pm 0.42	-20.51
8c	74.8	19.8 \pm 0.33	18.2 \pm 0.34	-16.75
9c	70.2	22.9 \pm 0.57	19.1 \pm 0.27	-17.95
10c	68.5	22.1 \pm 0.22	20.5 \pm 0.22	-14.56
11c	37.8	23.2 \pm 0.47	22.1 \pm 0.20	-12.50
12c	55.5	17.2 \pm 0.47	15.5 \pm 0.20	-18.59
13c	77.9	22.9 \pm 0.13	19.3 \pm 0.14	-14.22
14c	80.5	23.0 \pm 0.47	24.7 \pm 1.22	-14.88
15c	72.5	23.6 \pm 0.50	18.2 \pm 0.90	-11.80
16c	80.2	37.2 \pm 0.44	30.3 \pm 0.77	-8.17
17c	74.1	35.9 \pm 0.27	29.7 \pm 0.15	-8.49
18c	68.5	24.1 \pm 0.27	34.7 \pm 0.27	-10.18
Kojic acid		23.72 \pm 0.45	----	-10.59
Adriamycin		-----	0.1	

* 50% inhibitory concentration (IC_{50}).

As the concentrations of active inhibitors **3c** and **1c** increased, K_m values gradually increased, but V_{max} values did not change, thereby indicating that the inhibitors acted as

competitive inhibitors of mushroom tyrosinase (**Figure 25**). Tyrosinase was a copper-containing enzyme and most tyrosinase inhibitors that chelated the copper in the active site of the enzyme showed competitive inhibition; examples were tropolone and kojic acid (LoPachin, Barber & Gavin 2008; Son, Moon & Lee 2000). On the basis of these kinetic results, **3c** and **1c** showed inhibition by binding to the copper-containing active site of mushroom tyrosinase.

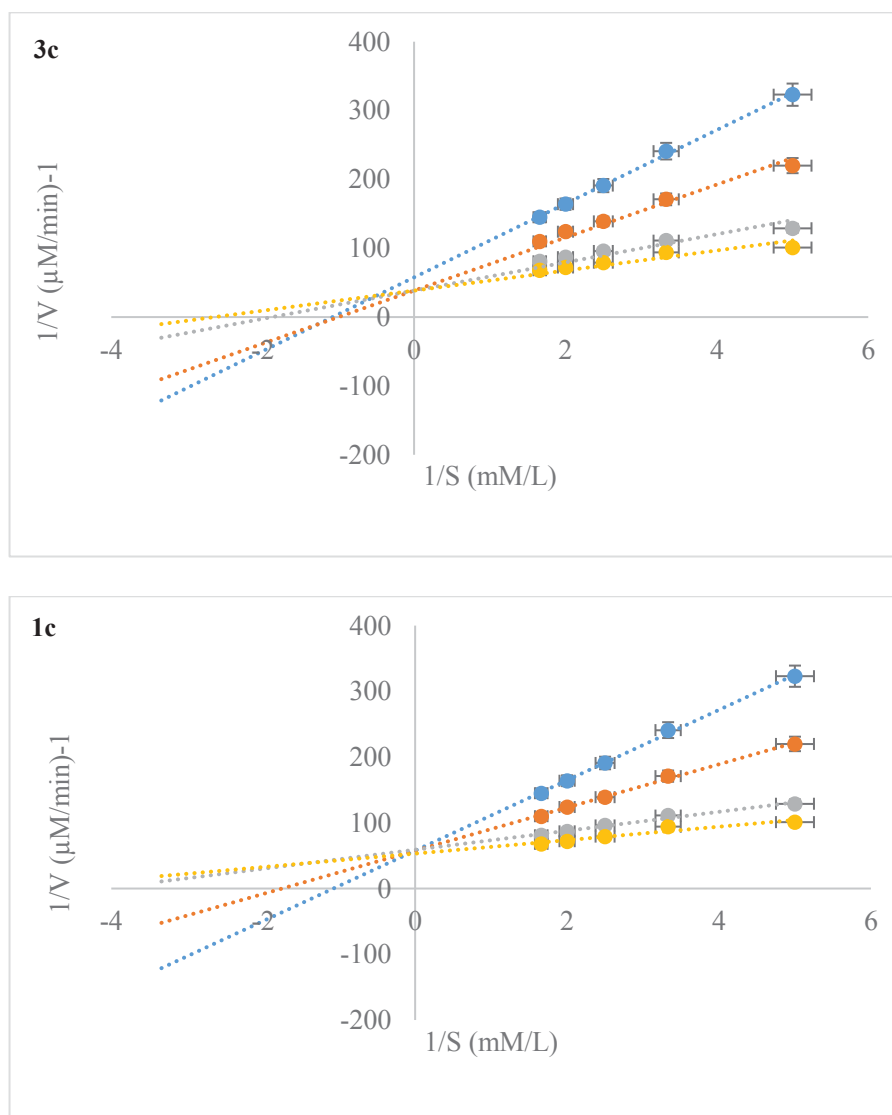


Figure 25 Lineweaver Burk plot for inhibition of compounds **3c** and **1c**

Data were obtained as mean values of $1/V$, the inverse of the absorbance increase at a wavelength of 492 nm per min of three independent tests with different concentrations of L-DOPA as a substrate. The concentration of compounds **3a** and **1a** from top to bottom were 20 μM , 5 μM , 1.25 μM and 0 μM , respectively.

5.3.2. Effect on melanogenesis

An initial evaluation of compounds for potential anticancer agents involved elaborate screening tests with B16F10 murine cancer cell lines. In this study cytotoxicity of chalcones and reference compound, adriamycin was determined by the MTT (3-(4, 5-dimethylthiazol-2-yl) 2, 5-diphenyltetrazolium bromide) assay. The results for compounds synthesized are shown as IC₅₀ values in **Table 8**. The antimelanogenic properties of chalcones are mainly influenced by the substitutions on the two aryl rings of chalcone molecule and their substitution patterns. Compounds, where toxicity could be related to that mechanism, require electron-deficient sites susceptible to accept an electron pair from electron-rich biomolecules.

Experimental data indicated that the α , β -unsaturated carbonyl chemicals as an electrophiles evoked cytotoxicity due to Michael-type adducts with sulfhydryl groups on specific cysteine residues. Chalcone molecule had three reactive sites where a nucleophile was prone to attack; carbon of the carbonyl group and each hydrogen of α and β carbons. As long as the ring A remained most electron-rich region of the compound, the chalcone would show higher cytotoxic activity. This could be achieved by placement of electron donating substituents, such as OH in ring A. Also placement of strongly electron-withdrawing groups such as NO₂ in ring B (compound **7c**) correlated with increase of cytotoxic activity. The presence of strongly electron-withdrawing NO₂ group provided high electrophilicity.

Studies on these methoxylated chalcones suggested that the position of the methoxy group on the B-ring had great importance; position 4 was favourable, while position 3 was unfavourable for cytotoxic activity. Replacement of the phenyl ring with a naphthyl ring led to compounds with moderate cytotoxicity. The extended aromatic rings or the heteroatoms increased the binding of these compounds to appropriate receptors through a van der Waals force or hydrogen bonding. From the structure-activity relationships, it was observed that the introduction of pyridinyl group in chalcone was associated with enhanced cytotoxic activity.

Further, the cytotoxic effects of **3c** and **1c** were estimated by measuring cell viability on B16F10 melanoma cell lines, where no significant cytotoxic effect was found at any of the concentrations tested. At doses of 1.0, 10.0, 50.0 and 100.0 μ M of compounds **3c** or **1c** for 48 h, cell viability was 82%, 78.5%, 72.4%, and 61.3%, for compound **3c**, and 125%, 102.5%, 87.5% and 74.7% for compound **1c**, respectively, compared with the

control (**Figure 26**). Thus, neither compound **3c** nor **1c** were cytotoxic to B16 cells in the concentration range of 1.0–100.0 μM .

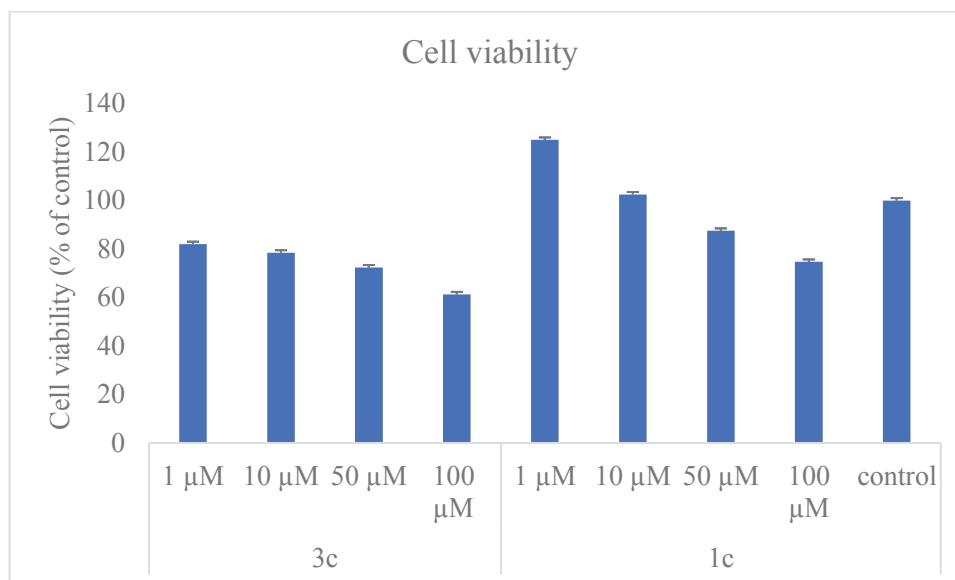


Figure 26 Effect of compounds **3c** and **1c** on B16 cell viability

Cells were treated with varying doses of compounds **3a** and **1a** (1–100 μM) and examined using an MTT assay. Data are expressed as a percentage of the control.

Later, the inhibitory effects of compounds **3c** and **1c** on melanogenesis was ascertained by quantifying the melanin content of B16 cells treated with compounds **3c** and **1c** (**Fig. 27**). The melanin content of B16 cells after treatment with compound **3c** in the presence of 100 nM α -melanocyte-stimulating hormone (α -MSH) decreased dose-dependently, showing 217% at 1.0 μM , 168.5% at 5.0 μM and 108% at 10.0 μM , compared with the 100 nM α -MSH-only treated group (235%) and the control group (100%). Similarly, cells treated with compound **1c**, exhibited melanin contents of 225% at 1.0 μM , 185% at 5.0 μM , and 117% at 10.0 μM compared with 100 nM α -MSH-only-treated group (235%) and the control group (100%).

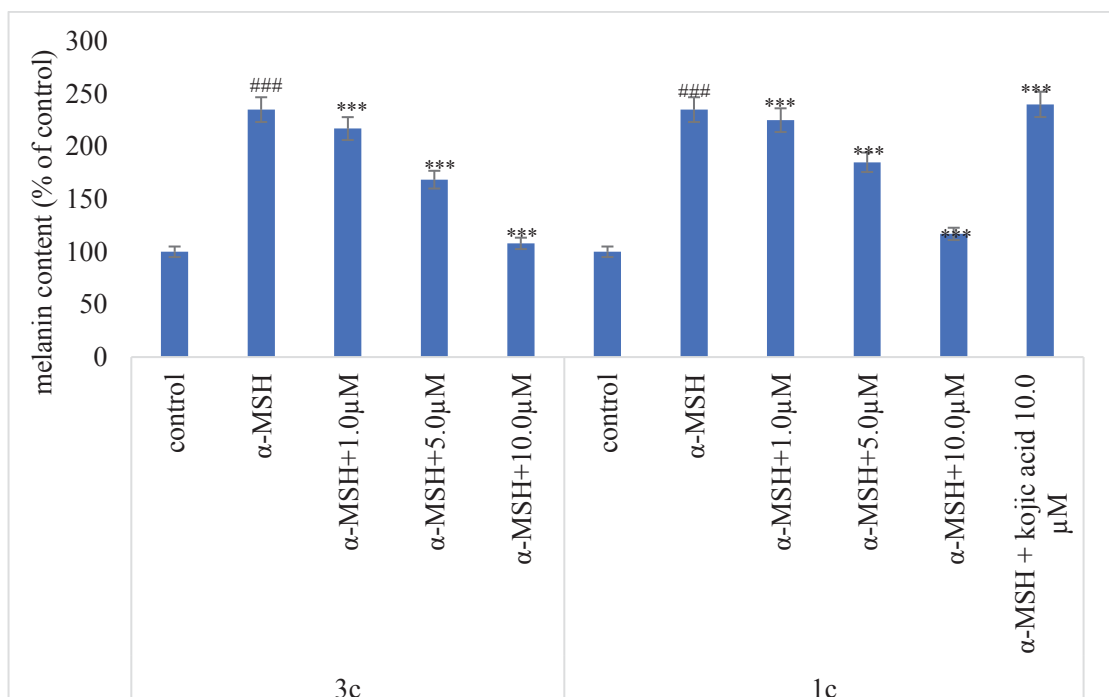


Figure 27 Inhibitory effect of compounds **3c** and **1c** after treatment with 100 nM α-MSH

Melanin contents were measured at 405 nm. Values represent the mean \pm S.E. of three experiments. Data are expressed as a percentage of the control. *** $p < 0.001$ compared to the group treated with 100nm α-MSH and ### $p < 0.001$, compared with the untreated control.

Furthermore, the inhibitory effects of compounds **3c** and **1c** on tyrosinase activity of B16 cells treated with 100 nm α-MSH was determined. After 24h incubation with **3c** and **1c**, tyrosinase activities were 135.6% at 1.0μM, 102.6% at 5.0 μM and 99.5% at 10.0 μM of **3c** (**Figure 28**), compared with the 100 nM α-MSH-only treated group (235%) and the control group (100%). Similarly, cells treated with compound **1c**, exhibited melanin contents of 175.2% at 1.0μM, 120.5% at 5.0 μM, and 112.5% at 10.0 μM compared with 100 nM α-MSH-only-treated group (235%) and the control group (100%). The inhibition of compounds **3** on murine tyrosinase activity was greater than the reference compound kojic acid. The results established that compounds **3c** and **1c** suppressed melanin biosynthesis through the inhibition of tyrosinase. These results supported the hypothesis that the inhibitory effect of compounds **3c** and **1c** on melanin biosynthesis should be attributed to inhibition of tyrosinase activity.

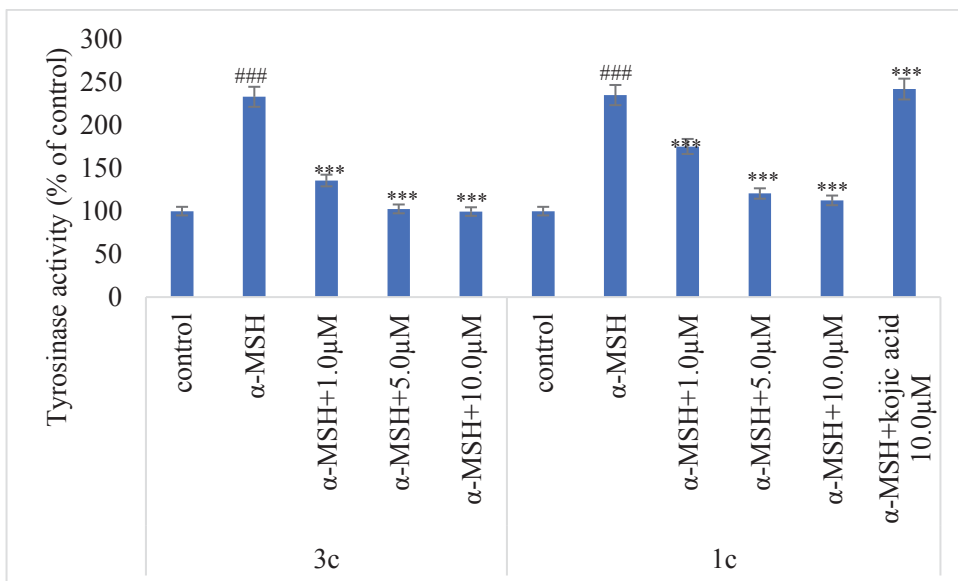
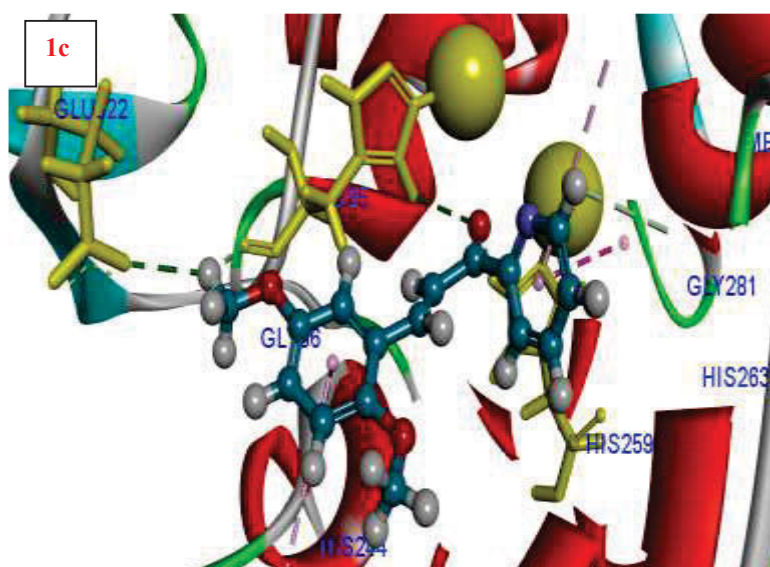
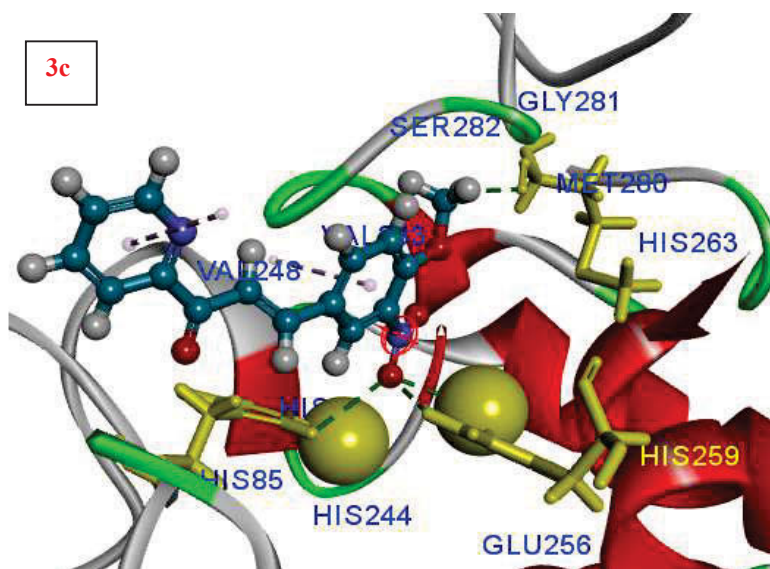


Figure 28 Inhibitory effect of compounds **3c** and **1c** on B16 cells tyrosinase

Values represent the mean \pm S.E. of three experiments. Data are expressed as a percentage of the control. *** $p < 0.001$ compared to the group treated with 100nm α -MSH and ### $p < 0.001$, compared with the untreated control.

5.3.3. Docking studies

To confirm these results, binding between the active site of mushroom tyrosinase and the active inhibitors **3c** and **1c** was simulated using Accelrys Discovery studio 4.5 suite. **Figure 29** showed selected docked conformations of active inhibitors **3c** and **1c** in the tyrosinase binding site. Docking results showed that compound **3c** ($-21.32 \text{ kcal mol}^{-1}$) combined more strongly with mushroom tyrosinase than compound **1c** ($-19.23 \text{ kcal mol}^{-1}$) (**Table 7**). Strong hydrogen bonding with His259, His85 and Met280 was seen for compound **3c** while compound **1c** exhibited hydrogen bonding interactions with His85, Glu322 and His259. The catalytic pocket of the enzyme was hydrophobic. Both the active compounds showed hydrophobic π - π stacking interactions with His263 and T-shaped edge to face aryl-aryl interactions with Phe264 and His244. Copper ion (Cu401) was weakly coordinated by the oxygen of the nitro group of compound **3c** at a distance of 2.92 \AA . Compound **7c** with an IC_{50} of $20.4 \text{ }\mu\text{M}$ showed a weak coordination with Cu401 at a distance of 3.08 \AA . However, the formation of a strong intramolecular hydrogen bond (1.90 \AA) between the 2'-OH and the carbonyl group hampered the latter to interact with the receptor. The ligand **1c** (IC_{50} : $12.5 \text{ }\mu\text{M}$) did not interact with the binuclear copper-binding site, but mainly with side chain residues in the active-site entrance.



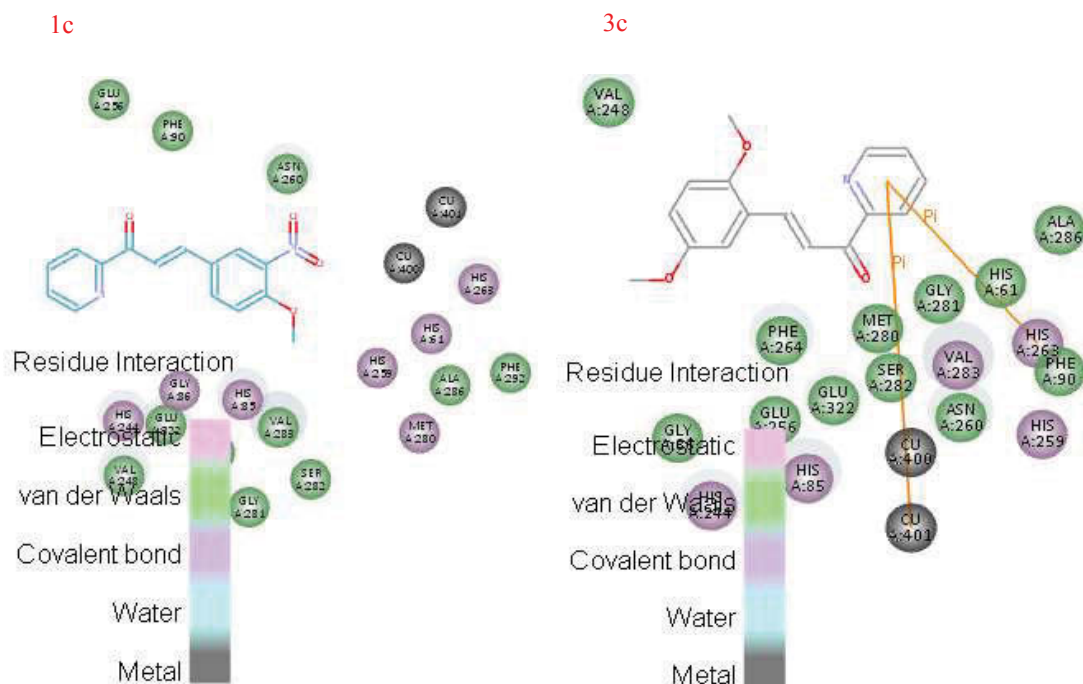


Figure 29 Docking and 2D results of compounds **3c** and **1c** in the tyrosinase catalytic pocket

Ligands **3c** and **1c** are displayed as ball and stick while the core amino acid residues are displayed as stick. The green dotted lines show the hydrogen bond interactions and the purple lines show the non-bonding interactions. The ochre balls represent the copper ions.

5.4. Conclusion

In summary, a series of methoxychalcone compounds were synthesized. Amongst the synthesized compounds, compounds **3c** [(*2E*)-3-(2,5-dimethoxyphenyl)-1-(pyridin-2-yl)prop-2-en-1-one] and **1c** [(*2E*)-3-(4-methoxy-3-nitrophenyl)-1-(pyridin-2-yl)prop-2-en-1-one] were found to be the most active tyrosinase inhibitors with their IC₅₀ values of 10.6 μ M and 12.5 μ M, respectively indicating them to be more potent than the reference compound, kojic acid (23.72 μ M). Both **3c** and **1c** were identified as competitive inhibitors of mushroom tyrosinase in a kinetic study.

Studies on these methoxylated chalcones suggested that the number and position of methoxy substituents on the aromatic rings appeared to be critical for cytotoxicity. Position 4 was favourable, while position 3 was unfavourable for cytotoxic activity. Replacement of the phenyl ring with a naphthyl ring led to compounds with moderate cytotoxicity. The extended aromatic rings or the heteroatoms increased the binding of these compounds to appropriate receptors through a van der Waals force or hydrogen

bonding. Compounds **3c** and **1c** showed very effective inhibitions of both melanin production and tyrosinase activity on B16F10 melanoma cell lines.

From the structure-activity relationships, it was inferred that the introduction of pyridinyl group in chalcone was associated with enhanced cytotoxic activity. Also placement of strongly electron-withdrawing groups such as NO₂ in ring B (compound **7c**) correlated with increase of cytotoxic activity. The presence of strongly electron-withdrawing NO₂ group provided high electrophilicity. This was consistent with the docking results where the electron-donating groups increased the electron density of ring B through a resonance donating effect and higher electron density bonded copper ions more effectively in the active site of enzyme. Copper ion (Cu401) was weakly coordinated by the oxygen of the nitro group of compound **1a** at a distance of 2.92Å. Strong hydrogen bonding with His259, His85 and Met280 was seen for compound **3c** while compound **1c** exhibited hydrogen bonding interactions with His85, Glu322 and His259.

This study provided valuable information in utilizing methoxychalcone as a lead compound for the further design and development of potential tyrosinase inhibitors with antimelanogenic effects.

5.5. References

Ahn, BZ, Sok, DE 1966, 'Michael acceptors as a tool for anticancer drug design', *Current Pharmaceutical Design*, Vol 2, pp. 247–262.

Aly, MRE, Ibrahim, EI, El Shahed, FA, Soliman, HA, Ibrahim, ZS, El-Shazly, SAM 2012, 'Synthesis of some quinolinyl chalcone analogues and investigation of their anticancer and synergistic anticancer effect with doxorubicin', *Russian Journal of Bioorganic Chemistry*, Vol 38, pp. 428–434.

Bandgar, BP, Gawande, SS, Bodade, RG, Totre, JV, Khobragade, CN 2010, 'Synthesis and biological evaluation of simple methoxylated chalcones as anticancer, anti-inflammatory and antioxidant agents', *Bioorganic and Medicinal Chemistry*, Vol 18, pp. 1364–1370.

Biradar, JS, Sasidhar, BS, Parveen, R 2010, 'Synthesis, antioxidant and DNA cleavage activities of novel indole derivatives', *European Journal of Medicinal Chemistry*, Vol 45, pp. 4074–4078.

Curto, EV, Kwong, C, Hermersdorfer, H, Glatt, H, Santis, C, Virador, V, Hearing, VJ, Dooley, TP 1999, 'Inhibitors of mammalian melanocyte tyrosinase; in vitro comparisons of alkyl esters of gentisic acid with other putative inhibitors', *Biochemical Pharmacology*, Vol 57, pp. 663–672.

Engasser, PG 1984, 'Ochronosis caused by bleaching creams', *Journal of the American Academy of Dermatology*, Vol 10, pp. 1072–1073.

Ennes, SBP, Paschoalick, R, Alchorne, MMDA 2000, 'A double-blind comparative, placebo-controlled study of the efficacy and tolerability of 4% hydroquinone as a depigmenting agent in melasma', *Journal of Dermatological Treatment*, Vol 11, pp. 173–179.

Ethiraj, KR, Aranjani, JM, Khan, FR 2013, 'Synthesis of methoxy-substituted chalcones and in vitro evaluation of their anticancer potential', *Chemical Biology and Drug Design*, Vol 82, pp. 732–742.

Fisher, AA 1983, 'Current contact news. Hydroquinone uses and abnormal reactions', *Cutis*, Vol 31, pp. 240–244, 250.

Fitzpatrick, TB, Eisen, AZ, Wolff, K, Freedberg, IM, Austen, KF 1983, 'Updates: dermatology in general medicine', In: Mosher, DB, Pathak, MA, Fitzpatrick, TB (eds) *Vitiligo: ethology, pathogenesis, diagnosis and treatment*. McGraw-Hill, New York.

Franco, DCZ, de Carvalho, GSG, Rocha, PR, Teixeira, R, da Silva, AD, Raposo, NRB 2012, 'Inhibitory effects of resveratrol analogs on mushroom tyrosinase activity', *Molecules*, Vol 17, pp. 11816–11825.

Juvala, K, Pape, VFS, Wiese, M 2012, 'Investigation of chalcones and benzochalcones as inhibitors of breast cancer resistance protein', *Bioorganic and Medicinal Chemistry*, Vol 20, pp. 346–355.

Karthikeyan, C, Moorthy, NS, Ramasamy, S, Vanam, U, Manivannan, E, Karunakaran, D, Trivedi, P 2015, 'Advances in chalcones with anticancer activities', *Recent patents on Anti-Cancer Drug Discovery*, Vol 10, pp. 97–115.

Lee, KH, Hall, IH, Starness, CD, Elgebaly, SA, Waddell, TG, Hadgraft, RT, Ruffler, CG, Weidner, I 1977, 'Sesquiterpene antitumor agents: inhibitors of cellular metabolism', *Science*, Vol 196, pp. 533–536.

Li, QS, Li, CY, Lu, X, Zhang, H, Zhu, HL 2012, 'Design, synthesis and biological evaluation of novel (E)- α -benzylsulfonylchalcone derivatives as potential BRAF inhibitors', *European Journal of Medicinal Chemistry*, Vol 50, pp. 288–295.

Liu, XL, Tee, HW, Go, ML 2008, 'Functionalized chalcones as selective inhibitors of P-glycoprotein and breast cancer resistance protein', *Bioorganic and Medicinal Chemistry*, Vol 16, pp. 171–180.

LoPachin, RM, Barber, DS, Gavin, T 2008, 'Molecular mechanisms of the conjugated alpha, beta-unsaturated carbonyl derivatives: relevance to neurotoxicity and neurodegenerative diseases', *Toxicological Sciences*, Vol 104, pp. 235–249.

Luo, Y, Qiu, KM, Lu, X, Liu, K, Fu, J, Zhu, HL 2011, 'Synthesis, biological evaluation and molecular modeling of cinnamic acyl sulfonamide derivatives as novel antitubulin agents', *Bioorganic and Medicinal Chemistry*, Vol 19, pp. 4730–4738.

Mojzisa, J, Varinskaa, L, Mojzisovab, G, Kostovac, I, Mirossaya, L 2008, 'Anti-angiogenic effects of flavonoids and chalcones', *Pharmaceutical Research*, Vol 57, pp. 259–265.

Neves, MP, Cravo, S, Lima, RT, Vasconcelos, MH, Nascimento, MSJ, Silva, AMS, Pinto, M, Cidade, H, Corrêa, AG 2012, 'Solid-phase synthesis of 2'-hydroxychalcones. Effects on cell growth inhibition, cell cycle and apoptosis of human tumor cell lines', *Bioorganic and Medicinal Chemistry*, Vol 20, pp. 25–33.

Oilinger, K, Llopis, J, Cadenas, E 1989, 'Study of the redox properties of naphthazarin (5, 8-dihydroxy-1, 4-naphthoquinone) and its glutathionyl conjugate in biological reactions: one and two electron enzymatic reduction', *Archives of Biochemistry and Biophysics*, Vol 275, pp. 514–530.

Parvez, S, Kang, M, Chung, HS, Cho, C, Hong, MC, Shin, MK, Bae, H 2006, 'Survey and mechanism of skin depigmenting and lightening agents', *Phytotherapy Research*, Vol 20, pp. 921–934.

Rao, AR, Sindhuja, HN, Dharmesh, SM, Sankar, KU, Sarada, R, Ravishankar, GA 2013, 'Effective inhibition of skin cancer, tyrosinase and antioxidative properties by astaxanthin and astaxanthin esters from the green alga *Haemotococcus pluvialis*', *Journal of Agricultural and Food Chemistry*, Vol 61, pp. 3842–3851.

Romaguera, C, Grimalt, F 1985, 'Leukoderma from hydroquinone', *Contact Dermatitis* Vol 12, pp. 183.

Serra, VV, Camões, F, Vieira, SI, Faustino, MAF, Tomé, JPC, Pinto, DCGA, Neves, MGPMS, Tomé, AC, Silva, AMS, Silva, EFDE, Cavaleiro, JAS 2009, 'Synthesis and biological evaluation of novel chalcone-porphyrin conjugates', *Acta Chimica Slovenica*, Vol 56, pp. 603–611.

Sharma, A, Chakravarti, B, Gupt, MP, Siddiqui, JA, Konwar, R, Tripathi, RP 2010, 'Synthesis and anti-breast cancer activity of biphenyl based chalcones', *Bioorganic and Medicinal Chemistry*, Vol 18, pp. 471147–20.

Sharma, V, Kumar, V, Kumar, P 2013, 'Heterocyclic chalcone analogues as potential anticancer agents', *Anticancer agents in Medicinal Chemistry*, Vol 13, pp. 422–432.

Shenvi, S, Kumar, K, Hatti, KS, Rijesh, K, Diwakar, L, Reddy, GC 2013, 'Synthesis, anticancer and antioxidant activities of 2, 4, 5-trimethoxy chalcones and analogues from asaronaldehyde: structure-activity relationship', *European Journal of Medicinal Chemistry*, Vol 62, pp. 435–442.

Son, SM, Moon, KD, Lee, CY 2000, 'Kinetic study of oxalic acid inhibition on enzymatic browning', *Journal of Agricultural and Food Chemistry*, Vol 48, pp. 2071–2074.

Zhu, W, Gao, J 2008, 'The use of botanical extracts as topical skin-lightening agents for the improvement of skin pigmentation disorders', *Journal of Investigative Dermatology Symposium Proceedings*, Vol 13, pp. 20–24.

CHAPTER 6

CHALCONE OXIMES

(Phenyl & naphthyl derivatives)

6.1. Introduction

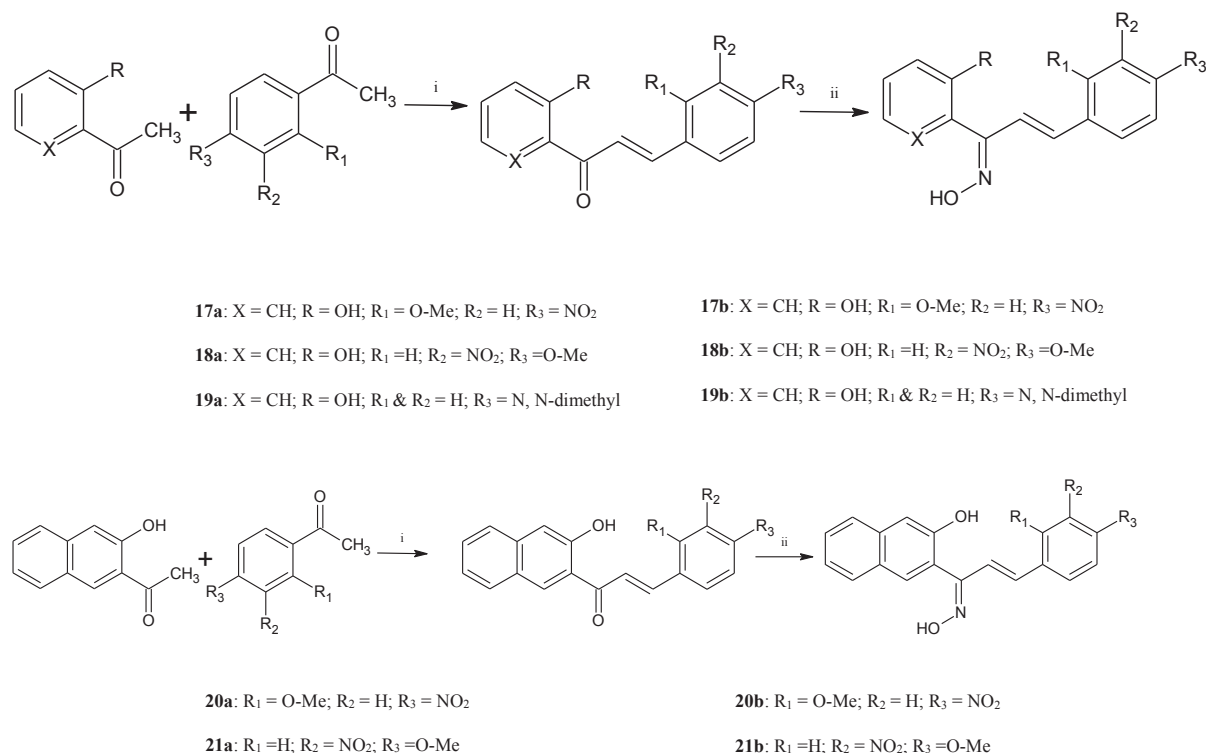
Most melanin biosynthesis inhibitors were phenol or catechol analogues, which were structurally similar to the tyrosinase substrates, tyrosine or L-DOPA (Passi & Nazzaro 1981). Hydroxamate molecules, one of the major classes of naturally occurring metal complexing agents, had been thoroughly studied as ligands for different metal ions such as Fe(III), Zn(II), and Cu(II) (Criton & Mellay-Hamon 2008; Baek *et al* 2008). The chelation involved the oxygen belonging to the =N-OH group (Lindner & Goettlicher 1969). Many compounds with oxime groups displayed potent biological activities and low toxicities (Adamkova *et al* 2001). Hydroxyphenylchalcones and hydroxynaphthylchalcones had shown promising results and preliminary docking calculations prompted to synthesize a whole new template of chalconeoximes and explore their potential as depigmentation agents and on melanin formation in murine B16F10 melanoma cell lines.

In the last few years, knowledge of melanocyte biology and the processes underlying melanin synthesis underwent remarkable progress, opening new paths in the identification of melanogenesis inhibitors and novel approaches to treat diseases caused by melanocyte dysfunction. The presence in chalcones of a conjugated double bond and a completely delocalized π electron system reduced their redox potentials and made them susceptible to electron transfer reactions. The α - β unsaturated bond enabled the chalcone to act as a Michael acceptor for nucleophilic species including glutathione (GSH) or cysteine residues on proteins (Meng *et al* 2007). Previous studies have indicated the use of chalcone oximes as anticancer agents (Yan *et al* 2014). The lack of tumor cells selectivity of anti-cancer drugs and the development of multidrug resistance were the key factors that played role in the search of new class of target-specific cytotoxic compounds that may be able to overcome multidrug resistance (Raj *et al* 2011; Yap *et al* 2011). Thus the research study was further extended to investigate the effect of chalcone oximes on melanin formation in murine B16F10 cells.

6.2. Experimental

A series of hydroxy substituted chalcone compounds were synthesized by base catalyzed Claisen-Schmidt condensation of an aldehyde and an appropriate ketone in a polar solvent like methanol. These compounds were then subsequently converted to their oxime derivatives by reaction with hydroxylamine hydrochloride (**Scheme 5**).

Assays were performed with L-DOPA as the substrate, using kojic acid, a well-known effective tyrosinase inhibitor as the positive control.



Scheme 5. General method for synthesis of hydroxy substituted chalconeoximes
Reagents and conditions: (i) MeOH, NaOH, 0° C, 24hrs; (ii) NH₂ OH. HCl

6.2.1. Method for the synthesis of compound **17b**.

To a stirred solution of 2'-hydroxyacetophenone (1 mM, 136 mg) and 2-methoxy-4-nitrobenzaldehyde (1mM, 181mg) in 25 ml methanol, was added pulverized NaOH (2mM) and the mixture was stirred at room temperature for 24–36 h. The reaction was monitored by TLC using *n*-hexane: ethyl acetate (7:3) as mobile phase. The reaction mixture was cooled to 0°C (ice-water bath) and acidified with HCl (10 % v/v aqueous solution) to afford total precipitation of the compound. A yellow precipitate was formed, which was filtered and washed with 10 % aqueous HCl solution. The product obtained was recrystallized with ethylacetate to give the pure chalcone product **17a**.

A mixture of chalcone **17a** (1 mM, 299mg), hydroxylamine hydrochloride (1.5 mmol, 104mg), and anhydrous sodium sulfate (1 mmol, 140mg) was refluxed in ethanol (5 mL) under stirring for the period (the reaction was followed by TLC). After completion of the reaction, the mixture was filtered, and the solvent was evaporated under reduced pressure. Then distilled water (10 mL) was added, and ethyl acetate (10 mL×3) was

added to extract organic compounds. The combined organic layers were dried over anhydrous sodium sulfate and filtered. Evaporation of the solvent in reduced pressure gave the crude product, which was purified by column chromatography on silica (200-300 mesh), eluted with petroleum ether (60–90 °C) or a mixture of petroleum ether and ethyl acetate (v/v = 1:4) to yield the pure oxime product **17b**.

6.2.2. Spectral data

17a. (2*E*)-1-(2-hydroxyphenyl)-3-(2-methoxy-4-nitrophenyl)prop-2-en-1-one. Yield: 68%; Mp: 123–125°C; IR (KBr) ν (cm⁻¹): 3250, 3345, 3015, 2910, 2865, 2700, 1702, 1682, 1552, 1465, 1305, 979, 735, 680, 575; ¹H NMR (500 MHz, CDCl₃): δ 12.22 (s, 1H, OH), 8.22 (s, 1H), 7.95 (d, 1H, H _{β} , J = 14.0), 7.86 (m, 1H, H-6, J = 9.5), 7.80 (d, 1H, H _{α} , J = 13.5), 7.75 (d, 1H, H-6', J = 10.5), 7.69 (d, 1H, H-5, J = 8.5), 7.59 (dd, 1H, H-4', J = 6.8, 8.5), 7.02 (dd, 1H, H-3', J = 7.3, 9.0), 6.97 (m, 1H, H-5', J = 10.0), 3.82 (s, 3H); ¹³C NMR (125 MHz, DMSO-*d*₆) δ 194.25 (C=O), 130.24 (C6'), 119.33 (C1'), 118.20 (C5'), 137.07 (C4'), 118.48 (C3'), 162.90 (C2'), 128.22 (C1), 115.24 (C2), 112.22 (C3), 137.50 (C4), 122.47 (C5), 116.55 (C6), 125.50 (vinylic), 140.87 (vinylic); MS (ESI): 270.1 ([M + H])⁺.

18a. (2*E*)-1-(2-hydroxyphenyl)-3-(4-methoxy-3-nitrophenyl)prop-2-en-1-one. Yield: 72%; Mp: 110–112°C; ¹H NMR (500 MHz, CDCl₃): δ 12.47 (s, 1H, OH), 8.10 (s, 1H), 7.86 (d, 1H, H _{β} , J = 12.5), 7.74 (d, 1H, H-6', J = 10.0), 7.72 (d, 1H, H _{α} , J = 12.0), 7.65 (d, 1H, H-5, J = 9.5), 7.54 (d, 1H, H-6, J = 8.0), 7.49 (t, 1H, H-4', J = 8.5), 6.92 (dd, 1H, H-3', J = 9.5), 6.90 (dd, 1H, H-5', J = 8.5, 9.0), 3.86 (s, 3H); ¹³C NMR (125 MHz, DMSO-*d*₆) δ 192.22 (C=O), 130.52 (C6'), 119.25 (C1'), 118.27 (C5'), 136.77 (C4'), 118.28 (C3'), 161.92 (C2'), 126.90 (C1), 120.54 (C2), 137.22 (C3), 147.50 (C4), 112.42 (C5), 114.23 (C6), 56.67 (Me), 122.40 (vinylic), 141.83 (vinylic); IR (KBr) ν (cm⁻¹): 3200, 3070, 2914, 2864, 2720, 1686, 1578, 1550, 1468, 1349, 970, 720, 580; MS (ESI): 270.1 ([M + H])⁺.

19a. (2*E*)-3-[4-(dimethyl amino) phenyl]-1-(2-hydroxyphenyl)prop-2-en-1-one. Yield: 87%; M.p: 108–110°C; ¹H NMR (500 MHz CDCl₃): δ 12.26 (s, 1H, OH), 8.06 (d, 1H, J = 11.5, H _{β}), 7.85 (d, 1H, J = 11.0, H _{α}), 7.72 (d, 1H, J = 5.5, H-6), 7.68 (dd, 2H, J = 8.0, H-2' & H-6'), 7.49 (dd, 1H, J = 8.5, H-4), 6.92 (t, 1H, J = 9.0, H-3), 6.89 (dd, 1H, J = 10.5, 15.0, H-5), 6.64 (dd, 2H, J = 9.0, H-3' & H-5'); ¹³C NMR (100 MHz, DMSO-*d*₆) δ 190.3 (C=O), 125.1 (C1), 131.9 (C2 & C6), 110.9 (C5 & C3), 154.3 (C4), 40.0 (N-

CH₃), 145.3 (vinylic), 125.1 (vinylic), 119.7 (C1'), 162.3 (C2'), 118.1 (C3'), 118.3 (C4'), 136.4 (C5'), 130.9 (C6'); IR (KBr) ν (cm⁻¹): 3420, 1710, 1640, 1335, 813, 680, 757, 680; MS (ESI): 268.2 ([M + H])⁺.

20a. (2*E*)-1-(2-hydroxyphenyl)-3-(2-methoxy-4-nitrophenyl)prop-2-en-1-one. Yield: 72%; Mp: 123–125°C; ¹H NMR (500 MHz, CDCl₃): δ 12.22 (s, 1H, OH), 8.22 (s, 1H), 7.95 (d, 1H, *J* = 14.0, H _{β}), 7.86 (m, 1H, *J* = 9.5, H-6), 7.80 (d, 1H, *J* = 13.5, H _{α}), 7.75 (d, 1H, *J* = 10.5, H-6'), 7.69 (d, 1H, *J* = 8.5, H-5), 7.59 (dd, 1H, *J* = 7.0, 8.5, H-4'), 7.02 (dd, 1H, *J* = 7.4, 9.0, H-3'), 6.97 (m, 1H, *J* = 10.0, H-5'), 3.82 (s, 3H); ¹³C NMR (125 MHz, DMSO-d₆) δ 194.2 (C=O), 130.2 (C6'), 119.3 (C1'), 118.2 (C5'), 137.0 (C4'), 118.4 (C3'), 162.9 (C2'), 128.2 (C1), 115.2 (C2), 112.2 (C3), 137.5 (C4), 122.4 (C5), 116.5 (C6), 125.5 (vinylic), 140.8 (vinylic); IR (KBr) ν (cm⁻¹): 3250, 3345, 3015, 2910, 2865, 2700, 1702, 1682, 1552, 1465, 1305, 979, 735, 680, 575; MS (ESI): 270.1 ([M + H])⁺.

21a. (2*E*)-1-(2-hydroxyphenyl)-3-(4-methoxy-3-nitrophenyl)prop-2-en-1-one. Yield: 68%; Mp: 110–112°C; ¹H NMR (500 MHz, CDCl₃): δ 12.47 (s, 1H, OH), 8.10 (s, 1H), 7.86 (d, 1H, *J* = 12.5, H _{β}), 7.74 (d, 1H, *J* = 10.0, H-6'), 7.72 (d, 1H, *J* = 12.0, H _{α}), 7.65 (d, 1H, *J* = 9.5, H-5), 7.54 (d, 1H, *J* = 8.0, H-6), 7.49 (t, 1H, *J* = 8.5, H-4'), 6.92 (dd, 1H, *J* = 9.5, H-3'), 6.90 (dd, 1H, *J* = 7.2, 9.0, H-5'), 3.86 (s, 3H); ¹³C NMR (125 MHz, DMSO-d₆) δ 192.22 (C=O), 130.52 (C6'), 119.25 (C1'), 118.27 (C5'), 136.77 (C4'), 118.28 (C3'), 161.92 (C2'), 126.90 (C1), 120.54 (C2), 137.22 (C3), 147.50 (C4), 112.42 (C5), 114.23 (C6), 56.67 (Me), 122.40 (vinylic), 141.83 (vinylic); IR (KBr) ν (cm⁻¹): 3200, 3070, 2914, 2864, 2720, 1686, 1578, 1550, 1468, 1349, 970, 720, 580; MS (ESI): 270.1 ([M + H])⁺.

17b. (1*E*, 2*E*)-*N*-hydroxy-3-(2-methoxy-4-nitrophenyl)-1-(pyridin-2-yl)prop-2-en-1-imine. Yield: 58%; Mp: 178–180°C; ¹H NMR (500 MHz, CDCl₃): δ 9.42 (s, 1H), 8.77 (dd, 1H, H-3, *J* = 10.5), 8.47 (dd, 1H, H-6, *J* = 6.8, 8.0), 8.20 (s, 1H), 7.88 (m, 1H, *J* = 8.0, H-6'), 7.85 (d, 1H, *J* = 11.0, H _{α}), 7.80 (t, 1H, H-5, *J* = 9.5), 7.75 (d, 1H, *J* = 9.5, H-5'), 7.44 (dd, 1H, *J* = 11.0, H-4), 6.94 (d, 1H, *J* = 11.5, H _{β}), 3.88 (s, 3H); ¹³C NMR (125 MHz, DMSO-d₆) δ 162.5 (C=N), 153.5 (C1), 118.9 (C6), 134.4 (C5), 130.4 (C4), 150.2 (C3), 136.4 (C1'), 118.2 (C2'), 114.2 (C3'), 139.7 (C4'), 125.3 (C5'), 120.2 (C6'), 144.2 (vinylic), 133.2 (vinylic); IR (KBr) ν (cm⁻¹): 3645, 3548, 2652, 1635, 1425, 1302, 1225, 805, 672; HRMS *m/z*: 300.0978 ([M + H])⁺; Calcd: 300.0984.

18b. 2-[(1*E*,2*E*)-*N*-hydroxy-3-(4-methoxy-3-nitrophenyl)prop-2-enimidoyl]phenol
Yield: 54%; Mp: 165–167°C; ¹H NMR (500 MHz, CDCl₃): δ 12.50 (s, 1H, OH), 9.39 (s, 1H), 8.22 (s, 1H), 7.92 (d, 1H, *J* = 11.0, H_a), 7.82 (d, 1H, *J* = 10.0, H-6'), 7.64 (d, 1H, *J* = 9.0, H-5), 7.57 (d, 1H, *J* = 8.0, H-6), 7.44 (t, 1H, *J* = 8.0, H-4'), 7.35 (d, 1H, H_β, *J* = 11.5), 7.02 (dd, 1H, *J* = 9.5, H-5'), 6.94 (dd, 1H, *J* = 10.0, 10.5, H-3'), 3.92 (s, 3H); ¹³C NMR (125 MHz, DMSO-d₆) δ 160.2 (C=N), 129.9 (C6'), 120.2 (C1'), 118.1 (C5'), 137.7 (C4'), 118.2 (C3'), 162.9 (C2'), 124.9 (C1), 118.4 (C2), 137.2 (C3), 148.5 (C4), 114.2 (C5), 116.3 (C6), 55.8 (Me), 123.2 (vinylic), 140.9 (vinylic); IR (KBr) ν (cm⁻¹): 3659, 3545, 2650, 1625, 1400, 1312, 1234, 875, 632; HRMS *m/z*: 315.0975 ([M + H])⁺; Calcd: 315.0981.

19b. 2- {(1*E*, 2*E*)-3-[4-(dimethylamino) phenyl]-*N*-hydroxyprop-2-enimidoyl} phenol.
Yield: 49%; M.p: 158–160°C. ¹H NMR (500 MHz CDCl₃): δ 12.35 (s, 1H, OH), 9.52 (s, 1H), 7.04 (dd, 2H, *J* = 10.5, H-3' & H-5'), 7.89 (d, 1H, *J* = 12.0, H_a), 7.79 (d, 1H, *J* = 7.5, H-6), 7.72 (dd, 2H, *J* = 10.0, H-2' & H-6'), 7.46 (dd, 1H, *J* = 6.5, 8.0, H-4), 6.97 (t, 1H, *J* = 9.5, H-3), 6.92 (d, 1H, *J* = 12.5, H_β), 6.82 (dd, 1H, *J* = 13.5, H-5); ¹³C NMR (100 MHz, DMSO-d₆) δ 160.3 (C=N), 127.2 (C1), 131.9 (C2 & C6), 110.97 (C5 & C3), 154.3 (C4), 40.5 (N-CH₃), 147.1 (vinylic), 127.2 (vinylic), 121.8 (C1'), 160.5 (C2'), 122.6 (C3'), 119.7 (C4'), 137.4 (C5'), 134.7 (C6'); IR (KBr) ν (cm⁻¹): 3620, 3528, 2342, 1620, 1415, 1300, 1222, 817, 632; HRMS *m/z*: 283.1439 ([M + H])⁺; Calcd: 283.1447.

20b. 3-[(1*E*, 2*E*)-*N*-hydroxy-3-(2-methoxy-4-nitrophenyl)prop-2-enimidoyl] naphthalen-2-ol. Yield: 53%; Mp: 145–147°C; ¹H NMR (500 MHz, CDCl₃): δ 12.55 (s, 1H, OH), 9.70 (s, 1H), 8.17 (s, 1H), 8.09 (dd, 1H, *J* = 9.2, 10.5, H-4'), 7.85 (dd, 1H, *J* = 9.0, H-8'), 7.74 (dd, 1H, *J* = 8.0, H-7'), 7.58 (t, 1H, *J* = 10.0, H-5'), 7.57 (d, 1H, *J* = 12.0, H_β), 7.52 (d, 1H, *J* = 11.5, H_a), 7.35 (dd, 1H, *J* = 8.5, H-6'), 7.24 (dd, 1H, *J* = 9.5, H-3'), 7.12 (d, 1H, *J* = 7.5, H-3'), 3.72 (s, 3H); ¹³C NMR (125 MHz, DMSO-d₆) δ 162.5 (C=N), 126.1 (C1'), 160.8 (C2'), 120.1 (C3'), 130.4 (C4'), 126.4 (C5'), 130.5 (C6'), 127.2 (C7'), 130.4 (C8'), 129.9 (C9'), 140.2 (C10'), 132.2 (vinylic), 144.6 (vinylic), 58.6 (Me), 130.2 (C1), 120.8 (C2), 118.4 (C3), 129.4 (C4), 122.6 (C5), 120.2 (C6); IR (KBr) ν (cm⁻¹): 3650, 3255, 3024, 2842, 1692, 1600, 1557, 1443, 934, 720, 655, 538; HRMS *m/z*: 365.1131 ([M + H])⁺; Calcd: 365.1137.

21b. 3-[(1*E*, 2*E*)-*N*-hydroxy-3-(4-methoxy-3-nitrophenyl)prop-2-enimidoyl] naphthalen-2-ol. Yield: 47%; Mp: 132–134°C; ¹H NMR (500 MHz, CDCl₃): δ 12.05 (s,

¹H, OH), 9.42 (s, 1H, OH), 8.20 (s, 1H), 7.89 (dd, 1H, *J* = 10.5, H-5), 7.84 (dd, 1H, *J* = 9.5, H-8'), 7.82 (dd, 1H, *J* = 9.5, H-6), 7.74 (dd, 1H, *J* = 8.0, H-7'), 7.62 (d, 1H, *J* = 13.0, H_β), 7.52 (t, 1H, *J* = 10.0, H-5'), 7.51 (dd, 1H, *J* = 6.5, 9.0, H-4'), 7.49 (d, 1H, *J* = 12.5, H_α), 7.24 (dd, 1H, *J* = 9.5, H-3'), 6.62 (dd, 1H, *J* = 6.4, 8.5, H-6'), 3.72 (s, 3H); ¹³C NMR (125 MHz, DMSO-d₆) δ 159.8 (C=N), 119.2 (C1'), 120.4 (C2'), 148.4 (C3'), 150.2 (C4'), 123.4 (C5'), 128.8 (C6'), 122.4 (C7'), 129.4 (C8'), 130.4 (C9'), 140.25 (C10'), 126.9 (vinylic), 140.5 (vinylic), 122.8 (C1), 124.5 (C2), 140.2 (C3), 140.4 (C4), 116.82 (C5), 118.2 (C6), 58.7 (Me); IR (KBr) ν (cm⁻¹): 3685, 3250, 2850, 2565, 2320, 1670, 1550, 1434, 1250, 935, 712, 535; HRMS *m/z*: 365.1130 ([M + H])⁺; Calcd: 365.1137.

6.3. Results and Discussion

6.3.1. Chemistry & inhibition kinetics

In the current study, the successful identification of several hydroxy substituted chalcone oxime compounds with improved tyrosinase inhibition has been reported. The structures of the compounds synthesized were confirmed by ¹H NMR, ¹³C NMR, FTIR and HRMS. The signals for phenolic hydroxyl protons appeared between 11 and 13 ppm and were indicated by ¹H NMR spectra. The signals for aromatic hydrogens were seen between 6.5 and 9.0 ppm. The coupling constants for vinylic protons appeared between 9 and 13 Hz which confirms their *trans* conformations. Chemical shift values further confirm *anti* isomer conformation of the oximes. The inhibitory activities of the synthesized oxime compounds **17b–21b** were compared with the reference compound kojic acid (**Figure 30**).

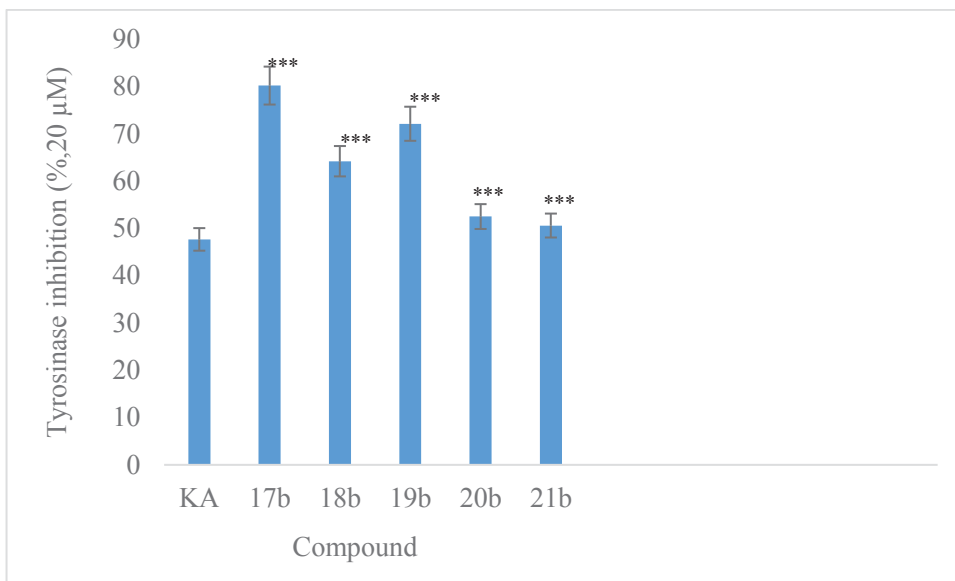


Figure 30 Inhibitory effects of chalcone oximes on mushroom tyrosinase activity

Values represent means \pm S.E of three determinations. Inhibitory concentration is 20 μ M. * $p < 0.05$ and *** $p < 0.001$ compared to kojic acid. KA: kojic acid.

In terms of the structure- activity relationships, compound **17b** (2- [(1*E*, 2*E*)-*N*-hydroxy-3-(2-methoxy-4-nitrophenyl)prop-2-enimidoyl] phenol) exhibited the most potent tyrosinase inhibitory activity with inhibition of 80.19%. This could be accounted to the presence of a strongly activating ortho-methoxy substituent and a meta directing nitro substituent. Presence of a strong electron releasing group in the ortho position (O-Me) and an electron withdrawing group (O-NO₂) in the para position modulated the electronic structure of ring B significantly. It was equally likely for the oxime moiety to coordinate with the copper atoms present in the tyrosinase active site. Compound **19b** with an electron donating para-dimethyl amino group on ring B showed an inhibition of 72.12% at 20 μ M.

The inhibition of both compounds **17b** and **19b** was seen to be greater than the positive control kojic acid which exhibited 47.67% inhibition at 20 μ M. Compound **20b** showed significant tyrosinase inhibition. Replacement of phenyl ring with a naphthyl ring gave compound **20b** with moderate tyrosinase inhibition while compound **21b** showed low inhibitory activity (50.6%) against mushroom tyrosinase. In particular, compounds **17b** and **19b** exhibited the greatest inhibition of L-DOPA oxidase activity of mushroom tyrosinase. These compounds were found to be more potent than the positive control, kojic acid. In this study, we investigated in depth the tyrosinase inhibitory activities of

compounds **18b** and **21b**. As shown in **Table 9**, compounds **17b** and **19b** and kojic acid inhibited mushroom tyrosinase activity in a concentration dependent manner.

Table 9 Inhibitory effects of kojic acid, 17b and 19b on mushroom tyrosinase

Sample	Concentration (μM)	Inhibition (%)				Average inhibition (%)	of IC ₅₀ (μM) ^a
Kojic acid	1.25	2.19	3.90	2.65	2.91		22.25 ± 0.22
	5.00	29.22	28.53	30.22	29.32		
	20.00	49.26	47.54	46.23	47.67		
17b	1.25	43.20	44.17	42.65	43.34		4.77 ± 0.35
	5.00	49.60	50.25	57.44	52.43		
	20.00	80.60	78.77	81.22	80.19		
19b	1.25	39.36	34.25	35.50	36.37		7.89 ± 0.15
	5.00	45.22	47.21	44.65	45.69		
	20.00	72.50	70.23	73.65	72.12		

a: 50% inhibitory concentration (IC₅₀).

Table 10 Kinetic analysis of compounds 17b and 19b

Compound	Type of inhibition	V _{max} (mM/min)	K _i (μM) ^c
17b	Competitive	0.045	5.25
19b	Competitive	0.023	8.33

c: Data were represented as mean values of three independent tests. K_i was the (inhibitor constant). V_{max} was the maximum reaction velocity.

Both the compounds **17b** and **19b** had better inhibitory activities with IC₅₀ values of 4.77 μM and 7.89 μM, respectively than the reference compound kojic acid (IC₅₀: 22.25 μM). To explore the mechanism, the kinetics of tyrosinase inhibition were examined in the presence of the most active compounds **17b** and **19b**. The data are shown in **Table 10**. As the concentrations of active inhibitors **17b** and **19b** increased, K_m values gradually increased, but V_{max} values did not change, thereby indicating that the inhibitors act as competitive inhibitors of mushroom tyrosinase (**Figure 31**).

Dixon plots gave a family of straight lines passing through the same point at the second quadrant, giving the inhibition constant (K_i) (**Figure 32**). The K_i value estimated from this Dixon plot was 5.25 μM and 8.33 μM for the compounds **17b** and **19b**, respectively. Kinetic results indicate that compounds **17b** and **19b** inhibited the tyrosinase activity by binding to the copper containing active site region. To confirm

this, further docking simulation studies were carried on the active compounds with mushroom tyrosinase.

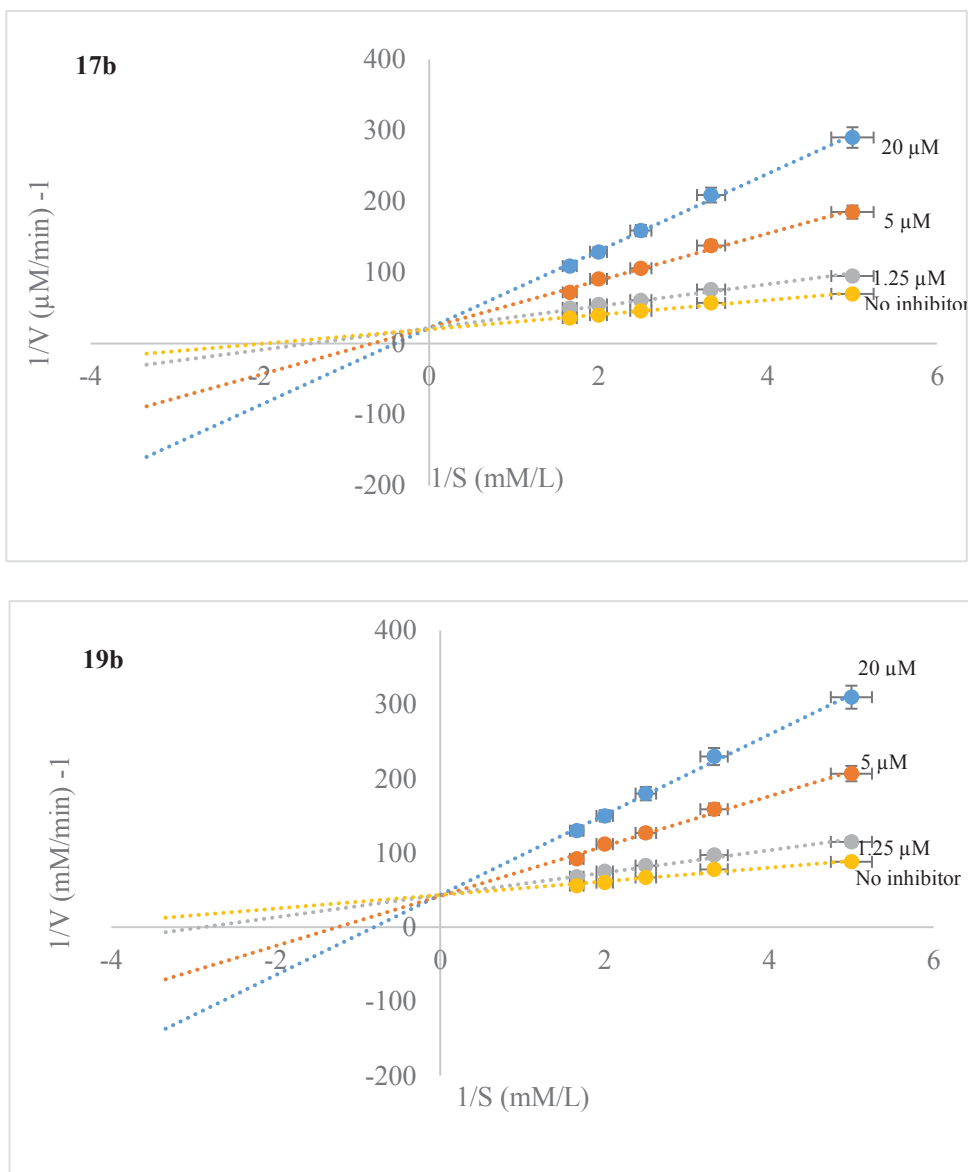


Figure 31 Lineweaver Burk plot for inhibition of compounds **17b** and **19b**

Data were obtained as mean values of $1/V$, the inverse of the absorbance increase at a wavelength of 492nm per min of three independent tests with different concentrations of L-DOPA as a substrate. The concentration of compounds **17b** and **19b** from top to bottom were 20 μM , 5 μM , 1.25 μM and 0 μM , respectively.

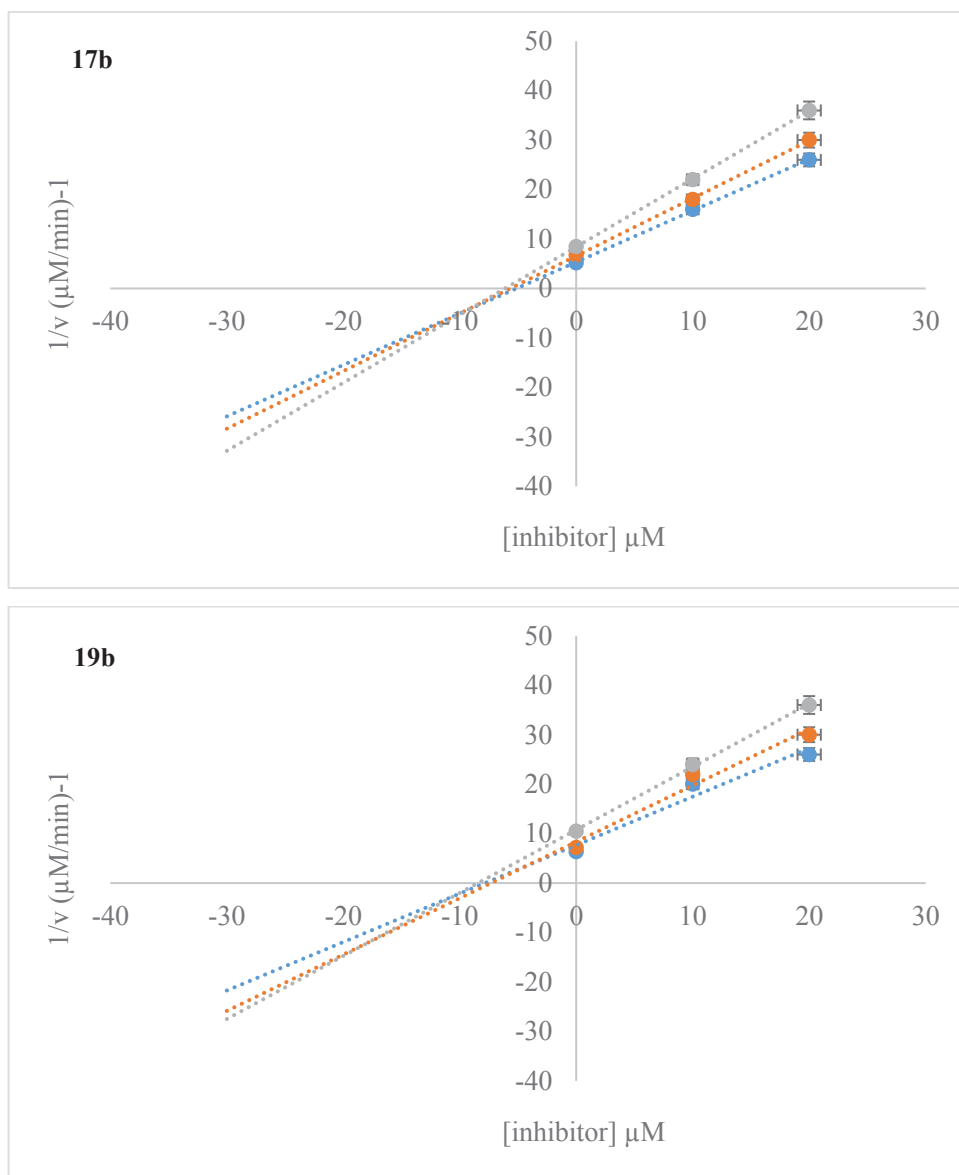


Figure 32 Dixon plot for the inhibitory effect of compounds **17b** and **19b**

The inhibitor concentrations were 0, 10 μM and 20 μM respectively. The L-DOPA concentrations were 200, 400 and 600 μM .

6.3.2. Docking studies

Accelrys Discovery Studio 4.5 suite was utilized to simulate binding between mushroom tyrosinase and active tyrosinase inhibitors **17b** and **19b**. Amongst all the compounds synthesized, compounds **17b** and **19b** had the highest docking scores when compared with the standard, kojic acid (dock score: $-10.29 \text{ kcal mol}^{-1}$).

The greater inhibitory efficacy of compound **17b** was attributed to the coordination of the oxime oxygen atom with copper ion ($\text{Cu}401$) in the active site of mushroom tyrosinase (2.29 \AA). Tyrosinase substrates like L-DOPA also bonded to the copper ion of tyrosinase via their OH group. Formation of a complex between a ligand and the copper ion in the active site of mushroom tyrosinase could prevent electron transfer by

the metal ion. Results showed that the most important binding residues for interaction were His65, His85, Val248, Ala286, His244, Asn260, Val 283, Met280, Ser282, His259, Phe292 and Glu322 for both compounds **17b** and **19b**. Strong hydrogen bonding with His61, His85 and Val283 was seen for compound **17b** while compound **19b** exhibited hydrogen bonding interactions with Asn260, Glu322 and His259 (**Table 11**).

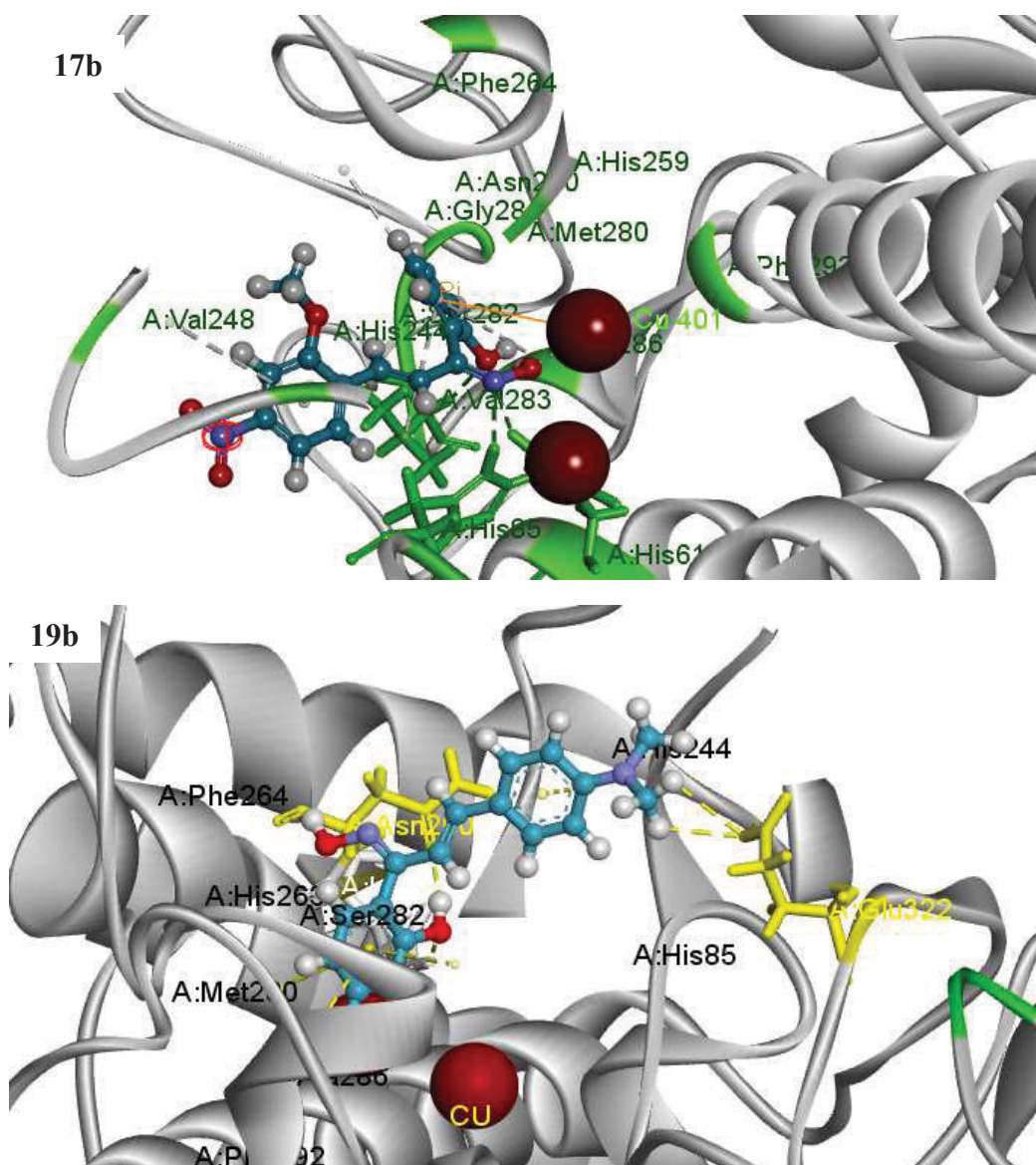
Table 11 Inhibition effects and docking results of chalconeoximes

Compound	Tyrosinase Inhibition at 50 μ M (%) [*]	CDOCKER energy (kcal/mol)	Type of interactions	Donor-acceptor	Distance (Å)
17b	80.6 \pm 0.25	-28.94	H-bonding	(His61) HE ₁ ... 2'-OH	2.70
				(His85) H δ_2 ...N (oxime)	2.77
				(Val283) H α ... 2'-OH	2.29
			Metal coordination	Cu401...O (oxime)	2.02
			hydrophobic stacking	π - π ring B...His263	3.85
18b	62.7 \pm 0.44	-20.87	H-bonding	H (oxime)... O δ_1 Asn260)	1.98
				(His61) HE ₁ ... 2'-OH	2.80
			hydrophobic stacking	(His259) H ϵ_1 ...N (oxime)	2.37
				π - π ring B...His263	3.64
19b	71.5 \pm 0.22	-28.14	H-bonding	2'-OH ... O δ_1 Asn260)	1.97
				H (oxime)... O δ_1 Asn260)	2.42
				2-OH...O δ_1 (Asn260)	2.14
				(His259) HE ₁ ...HO-2'	2.35
				H...O δ_1 (Glu322)	2.69
			hydrophobic stacking	H...O δ_1 (Glu322)	2.87
				π - π ring B...His263	3.69
			Intramolecular bonding	H- 2'-OH...O (Me)	2.77
20b	52.6 \pm 0.58	-12.85	H-bonding	(His61) HE ₁ ... 2'-OH	2.75
				(His259) HE ₁ ...HO-2'	2.93
				(His259) HE ₁ ... O ₂ N	2.46
				2'-OH ... O δ_1 Asn260)	2.53
			hydrophobic	π - π ring B...His263	4.60

21b	50.8 ± 0.22	-7.56	stacking hydrophobic stacking	π - π	ring B...His263	3.64
Kojic acid	49.5 ± 0.66	-11.69	H-bonding		Asn260 H α ...O	2.93
					Val283 H α ...O	2.64
					H... O=C (Met280)	2.84

*Chalconeoximes were synthesized according to the details in Scheme 1; Values indicate means \pm SE for three determinations.

Docking results showed that compound **17b** had better binding capability (CDOCKER energy: -28.94 kcal mol⁻¹) with mushroom tyrosinase as compared to compound **19b** (CDOCKER energy: -25.89 kcal mol⁻¹).



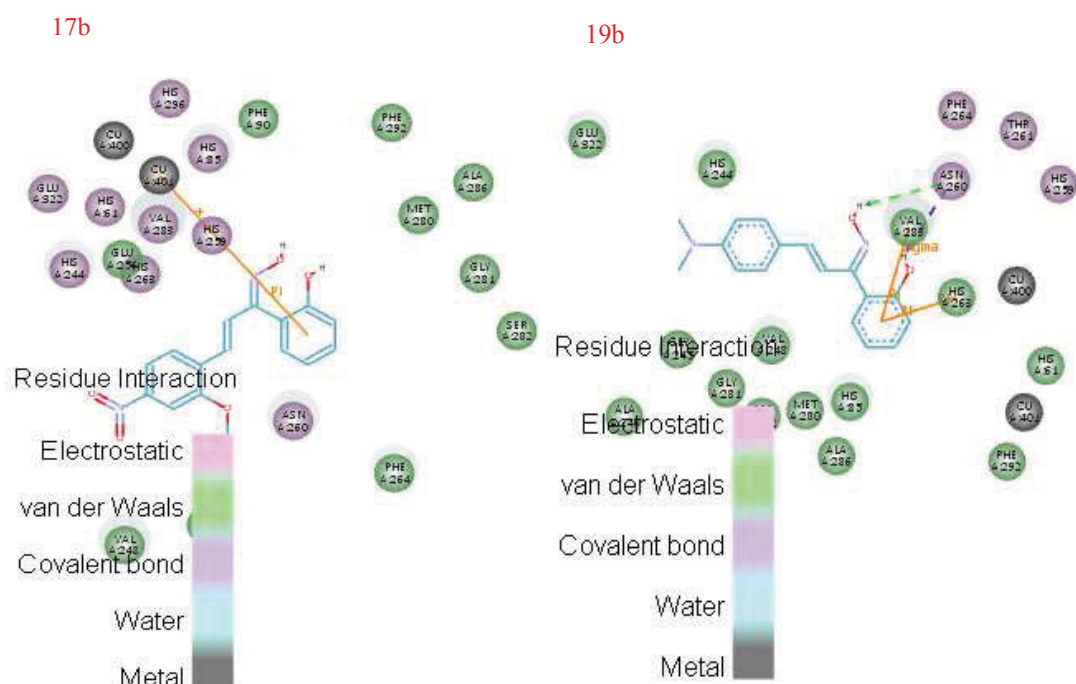


Figure 33 Docking and 2D results of compounds **17b** and **19b** in the tyrosinase pocket

Ligands **17b** and **19b** are displayed as ball and stick while the core amino acid residues are displayed as stick. The green dotted lines show the hydrogen bond interactions and the yellow lines show the non-bonding interactions. The ochre balls represent the copper ions.

The residues had a key function and effect on binding affinity. **Figure 33** showed selected docked conformations of compounds **17b** and **19b** in the tyrosinase binding site. The 2'-OH oxygen atom in ring A of compound **17b** accepted a hydrogen bond each from Val283 and from His61 at a distance of 2.29 Å and 2.70 Å, respectively. Another hydrogen bond was formed between the nitrogen atom of the oxime with the hydrogen atom of His85 at a distance of 2.77 Å. The oxime hydrogen atom (N-OH) in ligand **19b** formed a moderately strong hydrogen bond (2.14 Å) with the carboxylate oxygen atom of Asn260 while a weak hydrogen bond (2.42 Å) was seen between the oxygen atom of Asn260 and the 2'-hydroxyl hydrogen atom. Another weak hydrogen bond was formed between the 2'-hydroxyl oxygen atom of ring A with the hydrogen atom of His244 (HE₁) at a distance of 2.35 Å.

Adding the ligand to the catalytic pocket of the enzyme led to π - π interactions with the enzyme thereby enhancing drug permeability (David Golan 2008). The ligand **19b** (IC₅₀: 12.5 µM) did not interact with the binuclear copper-binding site, but mainly with side chain residues in the active-site entrance. Both the active compounds showed

hydrophobic π - π stacking interactions with His263 and T-shaped edge to face aryl-aryl interactions with Phe264 and His244.

6.3.3. Effect on melanogenesis

The study was further extended to investigate the effect of novel chalcone oxime compounds **17b** and **19b** on the tyrosinase activity and melanin levels in B16F10 melanoma cells. The cytotoxic effects of **17b** and **19b** were estimated by measuring cell viability, where no significant cytotoxic effect was found at any of the concentrations tested. At doses of 1.0, 10.0, 50.0 and 100.0 μ M of compounds **17b** or **19b** for 48 h, cell viability was 118%, 92.2%, 78.4%, and 72.6%, for compound **17b**, and 89%, 82%, 76.4% and 64% for compound **19b**, respectively, compared with the control (**Figure 34**). Thus, neither compound **17b** nor **19b** were cytotoxic to B16 cells in the concentration range of 1.0–100.0 μ M.

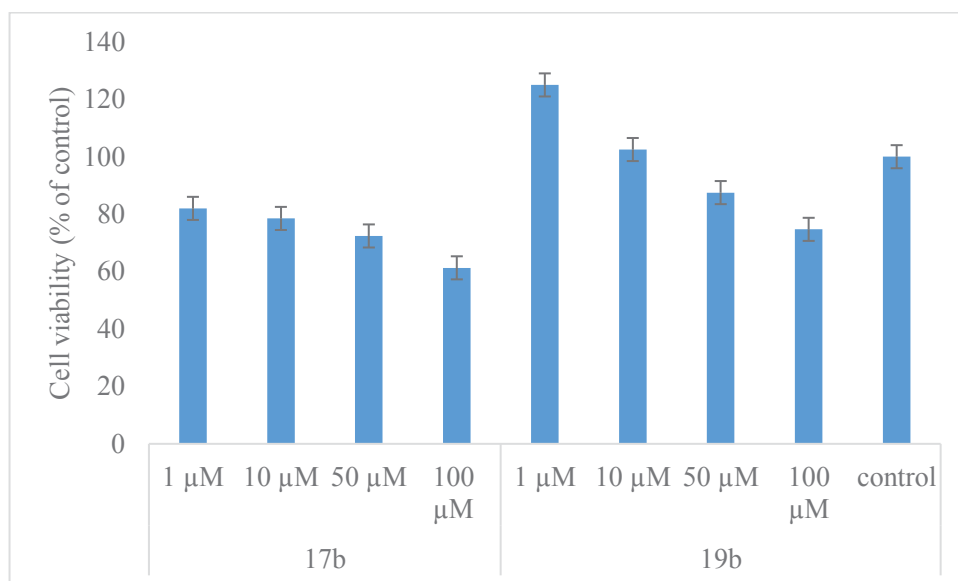


Figure 34 Effect of compounds **17b** and **19b** on cell viability

Data are expressed as a percentage of the control.

The inhibitory effects of compounds **17b** and **19b** were then ascertained on melanogenesis by quantifying the melanin content of B16 cells treated with compounds **17b** and **19b** (**Figure 35**).

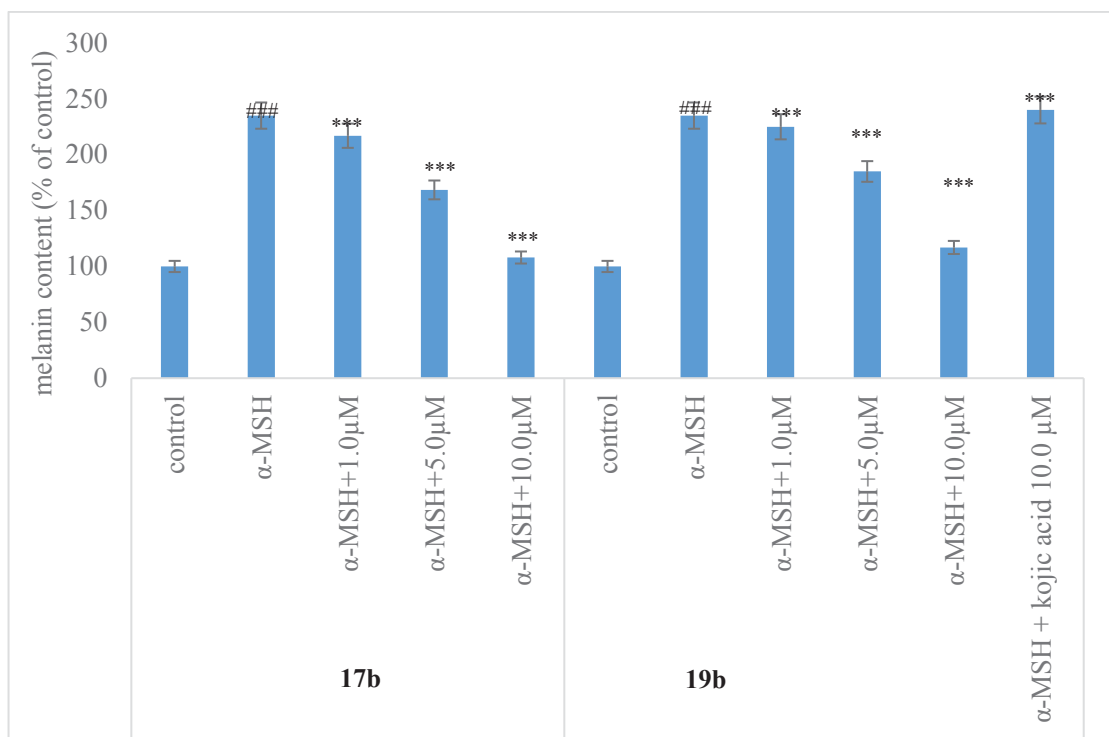


Figure 35 Inhibitory effect of compounds **17b** and **19b** after treatment with 100 nM α -MSH in B16 cells

Melanin contents were measured at 405 nm. Values represent the mean \pm S.E. of three experiments. Data are expressed as a percentage of the control. *** $p < 0.001$ compared to the group treated with 100nm α -MSH and ### $p < 0.001$, compared with the untreated control.

The melanin content of B16 cells after treatment with compound **17b** in the presence of 100 nM α -melanocyte-stimulating hormone (α -MSH) decreased dose-dependently, showing 215.25% at 1.0 μ M, 175.16% at 5.0 μ M and 112.0% at 10.0 μ M, compared with the 100 nM α -MSH-only treated group (225.22%) and the control group (100%). Similarly, cells treated with compound **19b**, exhibited melanin contents of 235.17% at 1.0 μ M, 215.55% at 5.0 μ M, and 165.35% at 10.0 μ M compared with 100 nM α -MSH-only-treated group (225.22%) and the control group (100%).

Finally, the inhibitory effects of compounds **17b** and **19b** were determined on tyrosinase activity of B16 cells treated with 100 nm α -MSH. After 24h incubation with **17b** and **19b**, tyrosinase activities were 145.91% at 1.0 μ M, 114.52% at 5.0 μ M and 108.77% at 10.0 μ M of **17b** (**Figure 36**), compared with the 100 nM α -MSH-only treated group (225.25%) and the control group (100%).

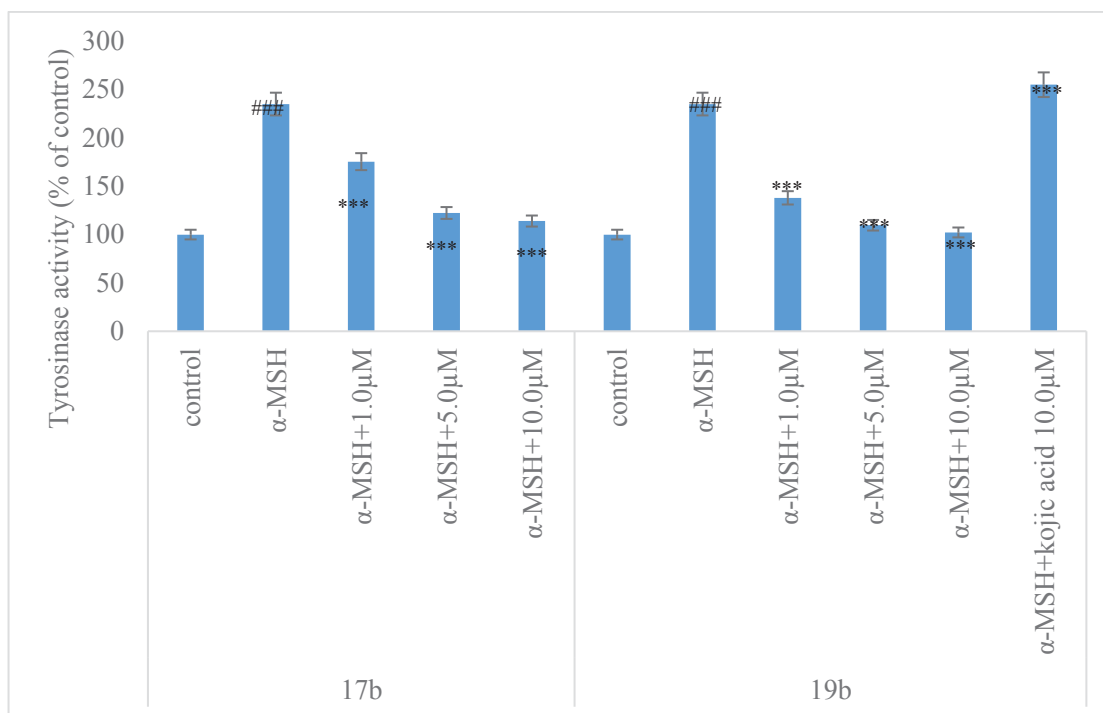


Figure 36 Inhibitory effect of compounds **17b** and **19b** on B16 cells tyrosinase

Values represent the mean \pm S.E. of three experiments. Data are expressed as a percentage of the control. *** $p < 0.001$ compared to the group treated with 100nm α -MSH and ### $p < 0.001$, compared with the untreated control.

Similarly, cells treated with compound **17b**, exhibited melanin contents of 160.45% at 1.0μM, 126.5% at 5.0μM, and 111.22% at 10.0μM compared with 100 nM α -MSH-only-treated group (225.25%) and the control group (100%). The inhibition of compounds **17b** and **19b** on murine tyrosinase activity was greater than the reference compound kojic acid. The results established that compounds **17b** and **19b** suppressed melanin biosynthesis through the inhibition of tyrosinase.

6.4. Conclusion

In a nutshell, amongst hydroxy substituted chalcone oxime compounds, compounds **17b** and **19b** were found to be more potent than the positive reference compound kojic acid. Kinetic studies identified both the compounds to be competitive inhibitors of mushroom tyrosinase. Docking simulation studies determined the possible residues of tyrosinase that played a key role in binding the inhibitor molecules. In the B16 cell culture system, tyrosinase activity and melanin levels were significantly reduced in the presence of compounds **17b** and **19b**, suggesting therefore inhibition of melanin biosynthesis to be attributed to tyrosinase inhibition. The structures of the non-cyclic moieties of the

molecules synthesized had similar features to those of hydroxamic acids and hydroxamates which were good chelating agents. Tyrosinase inhibition of compounds **17b** and **19b** depended on the competency of the inhibitor compounds to block access by any substrate molecule in the active site of enzyme. Strong co-ordination with the copper metal, significant hydrophobic and π - π stacking interactions contributed to effective tyrosinase inhibition. Also placement of strongly electron-withdrawing groups such as NO₂ in ring B (compound **17b**) correlated with increase of cytotoxic activity. The presence of strongly electron-withdrawing NO₂ group provided high electrophilicity. Also, oximes, popular in supramolecular chemistry as strong hydrogen bond donors, were involved in hydrogen bond interactions with the amino acid residues of the enzyme. This in turn, helped the compound to have a better fit to the catalytic pocket of the enzyme tyrosinase. The current study portrayed chalcone oximes as promising candidates to be explored as depigmentation agents.

6.5. References

- Adamkova, S, Frebort, I, Sebel, M, Pec, PJ 2001, 'Probing the active site of pea seedlings amine oxidase with optical antipodes of sedamine alkaloids', *Journal of enzyme inhibition*, Vol 16, pp. 367–372.
- Baek, HS, Rho, HS, Yoo, JW, Ahn, SM, Lee, JY, Lee, J, Kim, MK, Kim, DK, Chang, IS 2008, 'The inhibitory effect of new hydroxamic acid derivatives on melanogenesis', *Bulletin of the Korean Chemical Society*, Vol 29, pp. 43–46.
- Criton, M, Le Mellay-Hamon, V 2008, 'Analogues of *N*-hydroxy-*N'*-phenylthiourea and *N*-hydroxy-*N'*-phenyl urea as inhibitors of tyrosinase and melanin formation', *Bioorganic and Medicinal Chemistry Letters*, Vol 18, pp. 3607–3610.
- Lindner, HJ, Goettlicher, S 1969, 'Crystal and molecular structure of iron(III) benzhydroxamate trihydrate', *Acta Crystallographica*, Sect. B, Vol 25, pp. 832-842.
- Meng, CQ, Ni, L, Worsencroft, KJ, Ye, Z, Weingarten, MD, Simpson, JE, Skudlarek, JW, Marino, EM, Suen, KL, Kunsch, C, Souder, A, Howard, RB, Sundell, CL, 162

Wasserman, MA, Sikorski, JA 2007, 'Carboxylated, heteroaryl-substituted chalcones as inhibitors of vascular cell adhesion molecule-1 expression for use in chronic inflammatory diseases', *Journal of Medicinal Chemistry*, Vol 50, pp. 1304–1315.

Passi, S, Nazzaro, PM 1981, 'Molecular basis of substrate and inhibitory specificity of tyrosinase: phenolic compounds', *British Journal of Dermatology*, Vol 104, pp. 659–665.

Raj, L, Ide, T, Gurkar, AU, Foley, M, Schenone, M, Li, XY, Tolliday, NJ, Golub, TR, Carr, SA, Shamji, AF, Stern, AM, Mandinova, A, Schreiber, SL, Lee, SW 2011, 'Selective killing of cancer cells by a small molecule targeting the stress response to ROS', *Nature*, Vol 475, pp. 231–234.

Yan, TW, Ya, JQ, Ya, LZ, Yu, J, Li, Bing, R, Yan, QZ, Meng, RY, Ai, QJ, Jin, L, Qi, Hai, LZ 2014, 'Synthesis, biological evaluation and molecular docking studies of novel chalcone oxime derivatives as potential tubulin polymerization inhibitors', *RSC Advances*, Vol 61, pp. 32263–32275.

Yap, TA, Sandhu, SK, Carden, CP, de Bono, JS 2011, 'Poly(ADP-ribose) polymerase (PARP) inhibitors. Exploiting a synthetic lethal strategy in the clinic', *CA-A cancer journal for clinicians*, Vol 61, pp. 31-49.

CHAPTER 7

SOLID STATE SYNTHESIS

of

CHALCONEOXIMES

7.1. Introduction

Oximes were widely used as intermediates in fine organic synthesis and the oxime functionality was an important structural feature in several biologically active compound (Jin *et al* 2010; Flick *et al* 2010; Ghiaci *et al* 2009). The classical method for preparing them was the reaction of an aldehyde or ketone with hydroxylamine hydrochloride (Hajipour & Mahboubghah 1998). Several methods for their preparation had been reported in the literature including the use of formic acid (Olah & Keumi 1979), pyridine-chloroform (Sosnovsky, Krogh & Umhoefer 1979), ethanol-pyridine (Miller & Kaufman 2000), sulfuric acid (Weissermer & Arpe 1978), and NaOH with or without solvent (Ramón *et al* 2010; Abele *et al* 2003; Damljjanovic, Vukicevic & Vukicevic 2006; Osadchenko & Tomilov 2002). However, the hazardous nature of these reagents results in many limitations. The excessive use of organic solvents, long reaction times, high temperatures, and extensive work-up procedures, made this solution-based synthetic method environmentally stressful and expensive. In order to circumvent these limitations, many alternative strategies had been developed using solid catalysts such as alumina (Ley & Bertram 2001), silica gel (Shen & Sigman 1991), basic Al₂O₃ (Kad *et al* 2001), resin (Amberlyst) in ethanol (Ballini, Barboni & Filippone 1997), CaO (Sharjhi & Sarvari 2000), FeCl₃ (Eshghi & Hassankhani 2005), TiO₂ /SO₄²⁻ without solvent (Guo *et al* 2001), supported-POM (Kukushkin & Pombeiro 1999), and Na₂SO₄ under ultrasound irradiation (Li, Li & Li 2006; Luo *et al* 2005; Mehrabi 2008).

Reports had shown that many reactions could be conducted with good yields by just grinding solids (or liquid and solids) together (Toda, Yagi & Kiyoshige 1988). Therefore, the goal was to carry out the synthesis of novel chalcone compounds under green chemistry approach. Green chemistry was the utilization of a set of principle that reduced or eliminated the use or generation of hazardous substances in the design, manufacture, and application of chemical products (Redasani *et al* 2010). Green chemistry aimed to prevent waste and generate substances with little or no toxicity to humans and the environment, thereby maximizing atom economy (**Figure 37**). This was achieved by assuring that the final product contained the greatest possible proportion of the starting materials and avoided the use of harmful solvents, or even better, any solvents at all.

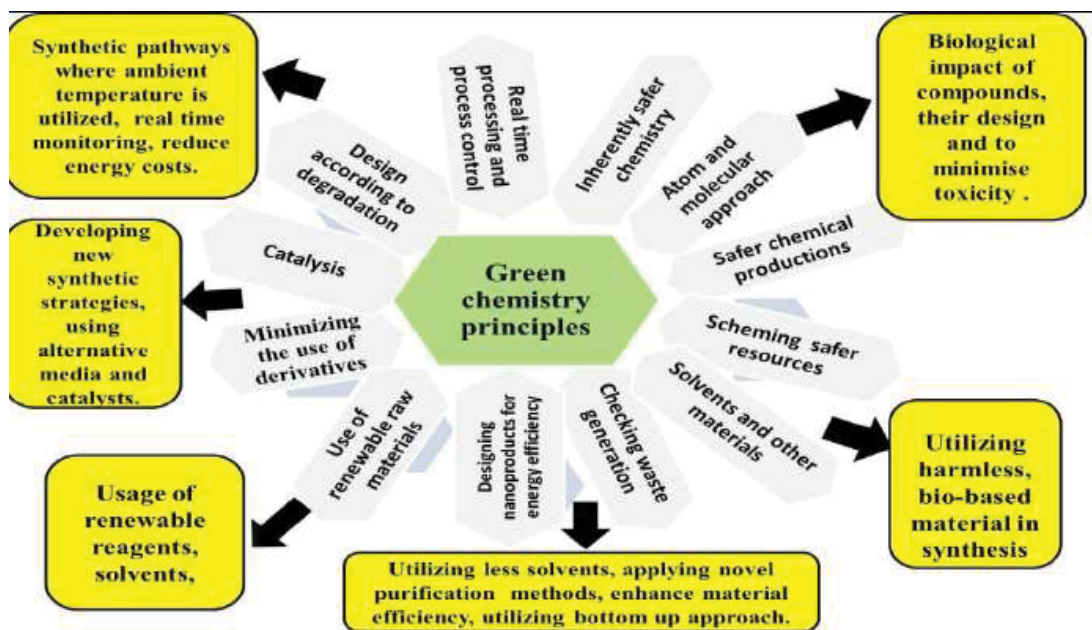


Figure 37 Principles of green chemistry

Because green chemistry had attracted great attention in recent years, an attempt was made in this direction for the preparation of chalcone derivatives. The method reported here for the synthesis of chalcones was simple and effective in terms of short reaction time, excellent yields, and the formation of one product as measured by thin-layer chromatography (TLC). It was also consistent with the green chemistry approach because it did not require heating or microwave irradiation. It occurred at room temperature and was completely free from organic solvents during both the reaction and separation of the product (except for recrystallization). Solvent free synthesis of chalcones thus generated an environmentally benign protocol through optimal waste minimization (Bose *et al* 2004; Anastas & Warner 1998). Taking inspiration from the number of reported biological activities associated with the previous library of azachalcones, the research study was directed towards the synthesis of some novel azachalconeoxime derivatives under the green chemistry approach.

7.2. Experimental

The current study employed the use of green chemistry where the desired azachalcones were prepared by grinding together equivalent amounts of the appropriate ketones and different aldehydes in the presence of solid pulverized sodium hydroxide at room

temperature. Focusing on green chemistry, the use of calcium oxide for the synthesis of oximes of azachalcones was examined and it was found that the reaction proceeded smoothly to give oximes in quantitative yields. Thus a novel, quick, environmentally safe, and clean method was developed for the synthesis of oximes of azachalcones (**Scheme 7**) utilizing pestle and mortar under solvent-free conditions. The method made use of local heat generated by simply grinding the reactants and was catalyzed by cheap and commercially available calcium oxide for driving the chemical reaction at room temperature. Most importantly, this method minimized waste disposal problems and provided a rather benign protocol for the synthesis of potent tyrosinase inhibitors to be targeted for their use as anti-browning food additives.



22a: R = C₆H₅OH; R¹ = 2-pyridinyl

23a: R = C₆H₅OH; R¹ = 3-pyridinyl

24a: R = C₆H₅OH; R¹ = 4-pyridinyl

25a: R = naphthalen-2-ol; R¹ = 2-pyridinyl

26a: R = naphthalen-2-ol; R¹ = 2-pyridinyl

27a: R = naphthalen-2-ol; R¹ = 2-pyridinyl

28a: R = C₆H₅N; R¹ = 4-N, N-dimethylamino

22b: R = C₆H₅OH; R¹ = 2-pyridinyl

23b: R = C₆H₅OH; R¹ = 3-pyridinyl

24b: R = C₆H₅OH; R¹ = 4-pyridinyl

25b: R = naphthalen-2-ol; R¹ = 2-pyridinyl

26b: R = naphthalen-2-ol; R¹ = 2-pyridinyl

27b: R = naphthalen-2-ol; R¹ = 2-pyridinyl

28b: R = C₆H₅N; R¹ = 4-N, N-dimethylamino

Scheme 6. Method for synthesis of azachalconeoximes.

7.2.1. Method for synthesis of **23b**

A mixture of 2'-hydroxyacetophenone (2 mmol, 2.7ml), 3-pyridinecarboxaldehyde (2 mmol, 2.14ml), and sodium hydroxide (7 mmol) was thoroughly ground with a pestle in an open mortar at room temperature for 2–3 min until the mixture turned into a melt. The initial syrupy reaction mixture solidified within 3–5 min. Grinding continued for 5–10 min more, and the reaction was monitored by TLC. The solid was washed with cold

water to remove the sodium hydroxide and recrystallized from methanol to give the corresponding chalcone derivative **23a**.

A mixture of azachalcone (1 mmol, 225mg), hydroxylamine hydrochloride (1.2 mmol, 85mg) and calcium oxide (0.6 mmol) was ground in a mortar with a pestle. On completion of the reaction as monitored by TLC, ethylacetate (2x10 mL) was added to the reaction mixture and filtered to separate the CaO. The filtrate was concentrated down to approximately 6mL and then poured into crushed ice to obtain the product as a precipitate. The precipitate was filtered and dried in high vacuum to yield the pure oxime **23b**.

7.2.2. Spectral data

22a. (2*E*)-1-(2-hydroxyphenyl)-3-(pyridin-2-yl)prop-2-en-1-one. Yield: 84%; Mp: 94–95°C; ¹H NMR (500 MHz, CDCl₃): δ 12.56 (s, 1H-OH), 7.52 (t, 1H, H-4', *J*= 8.5), 7.03 (d, 1H, H-3', *J*= 7.5), 6.96 (t, 1H, H-5', *J*= 9.0), 7.74 (d, 1H, H_α, *J*= 15.0), 7.90 (d, 1H, H_β, *J*= 16.0), 7.96 (d, 1H, H-5, *J*= 9.0), 7.91 (t, 1H, H-4, *J*= 7.5), 7.38 (t, 1H, H-3, *J*= 8.0), 8.66 (d, 1H, H-6, *J*= 9.0), 7.37 (d, 1H, H-6'); ¹³C NMR (125 MHz, DMSO-d₆) δ 195.2 (C=O), 152.6 (C6), 126.1 (C5), 137.5 (C4), 124.9 (C3), 154.2 (C2), 166.1 (C6'), 121.4 (C1'), 121.6 (C5'), 139.2 (C4'), 122.4 (C3'), 132.3 (C2'), 122.2 (vinylic), 144.6 (vinylic); IR (KBr) ν (cm⁻¹): 3421, 3047, 2361, 1715, 1592, 1559, 1347, 1311, 1233, 1209, 983, 817, 756; MS (ESI): 226.1 ([M + H])⁺.

23a. (2*E*)-1-(2-hydroxyphenyl)-3-(pyridin-3-yl)prop-2-en-1-one. Yield: 92%; Mp: 86–88°C; ¹H NMR (500 MHz, CDCl₃): δ 12.55 (s, 1H, OH), 6.99 (t, 1H, *J*= 8.5, H-3'), 7.89 (d, 1H, H_α, *J*= 11.0), 7.17 (d, 1H, H_β, *J*= 11.5), 7.50 (t, 1H, *J*= 9.0, H-4'), 7.57 (dd, 1H, *J*= 9.5, H-5'), 7.46 (d, 1H, H-6', *J*= 8.0), 8.69 (s, 1H, H-2), 8.89 (dd, 1H, *J*= 7.4, 9.0, H-4), 7.50 (dd, 1H, *J*= 6.2, 8.5, H-5), 8.25 (dd, 1H, *J*= 7.8, 10.0, H-6); ¹³C NMR (125 MHz, DMSO-d₆) δ 195.2 (C=O), 118.9 (C1'), 130.2 (C2'), 118.2 (C3'), 136.5 (C4'), 120.2 (C5'), 162.9 (C6'), 149.2 (C2), 142.7 (C6), 124.9 (C5), 130.1 (C3), 131.7 (C4), 131.6 (C1), 125.7 (vinylic), 144.6 (vinylic); IR (KBr) ν (cm⁻¹): 3400, 1646, 1315, 1591, 1646, 1492, 825 & 689, 755 & 689; MS (ESI): 226.1 ([M + H])⁺.

24a. (2*E*)-1-(2-hydroxyphenyl)-3-(pyridin-4-yl)prop-2-en-1-one. Yield: 80%; Mp: 139–140°C; ¹H NMR (500 MHz, CDCl₃): δ 12.66 (s, 1H, OH), 6.95 (t, 1H, *J*= 8.0, H-3'), 8.88 (s, 2H, *J*= 15.5, H-3 & H-5), 7.96 (d, 1H, H_α, *J*= 10.5), 7.05 (d, 1H, H_β, *J*= 11.0), 7.44 (t, 1H, *J*= 7.5, H-6'), 7.54 (t, 1H, *J*= 9.5, H-4'), 7.71 (d, 2H, *J*= 9.0, H-2 & H-6),

7.89 (dd, 1H, J = 8.0, H-5'); ^{13}C NMR (125 MHz, DMSO- d_6) δ 195.7 (C=O), 153.2 (C2 & C6), 122.3 (C3 & C5), 132.3 (C2'), 121.7 (C3'), 139.6 (C4'), 121.4 (C5'), 124.8 (C1'), 166.3 (C6'), 144.5 (C4), 144.7 (vinylic), 127.2 (vinylic); IR (KBr) ν (cm^{-1}): 3445, 3034, 1710, 1583, 1568, 1376, 1349, 1318, 1216, 809, 752; MS (ESI): 226.1 ($[\text{M} + \text{H}]$)

25a. (2*E*)-1-(3-hydroxynaphthalen-2-yl)-3-(pyridin-2-yl)prop-2-en-1-one. Yield: 69%; Mp: 129–131 °C; ^1H NMR (500 MHz, CDCl_3): δ 12.95 (s, 1H, OH), 7.92 (d, 1H, H_β , J = 12.5), 7.69 (d, 1H, H_α , J = 12.5), 8.75 (dd, 1H, J = 9.0, H-3), 7.59 (t, 1H, J = 8.5, H-4), 7.89 (dd, 1H, J = 7.7, 8.0, H-5), 7.92 (d, 1H, J = 9.0, H-6), 7.17 (dd, 1H, J = 9.5, H-3'), 7.82 (m, 1H, J = 10.5, H-5'), 7.75 (m, 1H, J = 10.5, H-6'), 7.35 (dd, 1H, J = 6.5, 8.0, H-7'), 7.57 (dd, 1H, J = 6.8, 10.5, H-8'), 8.02 (dd, 1H, J = 10.0, H-10'); ^{13}C NMR (125 MHz, DMSO- d_6) δ 198.42 (C=O), 152.80 (C1), 150.07 (C3), 126.89 (C3), 126.89 (C4), 136.92 (C5), 121.67 (C6), 114.72 (C1'), 163.92 (C2'), 119.90 (C3'), 136.97 (C4'), 128.22 (C5'), 129.24 (C6'), 123.02 (C7'), 128.12 (C8'), 124.14 (C9'), 131.16 (C10'), 130.02 (vinylic), 145.20 (vinylic); IR (KBr) ν (cm^{-1}): 3853, 3420, 3054, 2923, 2361, 2337, 1652, 1635, 1621, 1595, 1508, 1458, 1370, 1234, 1105, 820, 752; MS (ESI): 276.1 ($[\text{M} + \text{H}]$) $^+$.

26a. (2*E*)-1-(3-hydroxynaphthalen-2-yl)-3-(pyridin-3-yl)prop-2-en-1-one. Yield: 90%; M.p: 138–140 °C; ^1H NMR (500 MHz, CDCl_3): δ 13.72 (s, 1H, OH), 7.87 (d, 1H, H_β , J = 11.5), 7.65 (d, 1H, H_α , J = 11.0), 9.02 (s, 1H, H-2), 8.87 (dd, 1H, J = 7.4, 8.5, H-4), 7.51 (m, 1H, J = 9.0, H-5), 8.15 (dd, 1H, J = 10.5, H-6), 7.20 (dd, 1H, J = 9.0, H-3'), 7.79 (dd, 1H, J = 10.0, H-5'), 7.79 (m, 1H, J = 9.5, H-6'), 7.32 (dd, 1H, J = 8.5, H-7'), 7.59 (dd, 1H, J = 10.5, H-8'), 8.15 (dd, 1H, J = 10.5, H-10'); ^{13}C NMR (125 MHz, DMSO- d_6) δ 197.5 (C=O), 131.3 (C1), 151.2 (C2), 154.1 (C4), 124.2 (C5), 135.3 (C6), 114.7 (C1'), 164.2 (C2'), 120.1 (C3'), 136.8 (C4'), 128.2 (C5'), 129.2 (C6'), 123.5 (C7'), 129.1 (C8'), 124.2 (C9'), 132.0 (C10'), 131.2 (vinylic), 144.6 (vinylic); IR (KBr) ν (cm^{-1}): 3421, 3060, 2922, 2851, 2631, 1749, 1600, 1581, 1528, 1476, 1390, 1278, 1249, 1209, 1081, 1040, 796, 726, 617, 572; MS (ESI): 276.1 ($[\text{M} + \text{H}]$) $^+$.

27a. (2*E*)-1-(3-hydroxynaphthalen-2-yl)-3-(pyridin-4-yl)prop-2-en-1-one. Yield: 64%; M.p: 132–134 °C; ^1H NMR (500 MHz, CDCl_3): δ 13.55 (s, 1H, OH), 7.89 (d, 1H, H_β , J = 12.5), 7.69 (d, 1H, H_α , J = 12.0), 7.25 (dd, 1H, J = 7.9, 9.5, H-3'), 7.79 (dd, 1H, J = 8.5, 10.5, H-5'), 7.81 (m, 1H, J = 9.5, H-6'), 7.39 (dd, 1H, J = 6.5, 8.0, H-7'), 7.61 (dd, 1H, J = 10.0, H-8'), 8.09 (dd, 1H, J = 7.7, 10.5, H-10') 8.90 (s, 2H, J = 15.0, H-3 & H-5), 7.70 (d, 2H, J = 9.5, H-2 & H-6); ^{13}C NMR (125 MHz, DMSO- d_6) δ 196.4 (C=O), 113.6

(C1'), 164.2 (C2'), 121.2 (C3'), 136.8 (C4'), 128.1 (C5'), 130.1 (C6'), 123.4 (C7'), 129.1 (C8'), 124.2 (C9'), 130.9 (C10'), 131.2 (vinyl), 145.1 (vinyl), 140.6 (C1), 153.5 (C2 & C6), 123.5 (C3 & C5); IR (KBr) ν (cm⁻¹): 3422, 3325, 3052, 2920, 2845, 2612, 1752, 1610, 1574, 1512, 1395, 1265, 1245, 1079, 1042, 786, 722, 627, 570; MS (ESI): 276.1 ([M + H])⁺.

22b. 2-[(1E, 2E)-N-hydroxy-3-(pyridin-2-yl)prop-2-enimidoyl] phenol. Yield: 58%; Mp: 139–140°C; ¹H NMR (500 MHz, CDCl₃): δ 12.65 (s, 1H-OH), 8.78 (s, 1H), 7.96 (t, 1H, H-5, *J* = 9.0), 7.91 (t, 1H, H-4, *J* = 8.5), 7.89 (m, 2H, H-4' and H-5', *J* = 8.5), 7.87 (d, 1H, H_β, *J* = 16.0), 7.74 (d, 1H, H_α, *J* = 15.0), 7.66 (dd, 1H, H-6, *J* = 7.7, 9.4), 7.48 (dd, 1H, H-3, *J* = 7.5), 7.37 (d, 1H, H-6', *J* = 9.5), 6.98 (dd, 1H, H-3', *J* = 6.2, 8.0); ¹³C NMR (125 MHz, DMSO-d₆) δ 159.8 (C=N), 152.3 (C6), 126.2 (C5), 137.3 (C4), 124.4 (C3), 165.6 (C6'), 121.4 (C1'), 121.6 (C5'), 139.2 (C4'), 122.4 (C3'), 132.3 (C2'), 122.5 (vinyl), 144.7 (vinyl); IR (KBr) ν (cm⁻¹): 3440, 3325, 3047, 2361, 1685, 1592, 1559, 1347, 1309, 1233, 1209, 992, 789, 756; HRMS *m/z*: 241.0952 ([M + H])⁺; Calcd: 241.0977.

23b. 2-[(1E, 2E)-N-hydroxy-3-(pyridin-3-yl)prop-2-enimidoyl] phenol. Yield: 68%; Mp: 144–146°C; ¹H NMR (500 MHz, CDCl₃): δ 12.20 (s, 1H, OH), 9.38 (s, 1H), 8.79 (s, 2H, H-3' & H-5', *J* = 15.0), 7.89 (d, 1H, H_α, *J* = 12.5), 7.75 (d, 2H, H-2' & H-6', *J* = 6.8, 9.5), 7.52 (t, 1H, H-4', *J* = 9.0), 7.42 (t, 1H, H-6, *J* = 7.5), 7.26 (d, 1H, H-4, *J* = 10.0), 7.05 (d, 1H, H_β, *J* = 13.0), 6.82 (dd, 1H, H-5, *J* = 7.2, 8.5), 6.55 (t, 1H, H-3, *J* = 8.5); ¹³C NMR (125 MHz, DMSO-d₆) δ 160.2 (C=N), 152.5 (C2&C6), 121.4 (C3&C5), 132.3 (C2'), 120.6 (C3'), 140.6 (C4'), 121.4 (C5'), 125.7 (C1'), 162.3 (C6'), 144.5 (C4), 144.4 (vinyl), 128.2 (vinyl); IR (KBr) ν (cm⁻¹): 3445, 3320, 3247, 1660, 1580, 1528, 1355, 1309, 1318, 1216, 786, 771; HRMS *m/z*: 241.0992 ([M + H])⁺; Calcd: 241.0977.

24b 2-[(1E, 2E)-N-hydroxy-3-(pyridin-4-yl)prop-2-enimidoyl]phenol. Yield: 42%; Mp: 137–139°C; ¹H NMR (500 MHz, CDCl₃): δ 12.25 (s, 1H-OH), 8.78 (dd, 2H, H-3 & H-5, *J* = 15.5), 8.70 (s, 1H), 7.99 (d, 1H, H_α, *J* = 11.5), 7.74 (dd, 2H, H-2 & H-6, *J* = 9.0), 7.59 (t, 1H, H-4', *J* = 10.5), 7.51 (dd, 1H, H-6', *J* = 7.5); 7.10 (d, 1H, H_β, *J* = 11.5), 6.97 (dd, 1H, H-3', *J* = 9.0), 6.89 (dd, 1H, H-5', *J* = 8.0); ¹³C NMR (125 MHz, DMSO-d₆) δ 159.9 (C=N), 153.4 (C2 & C6), 122.41 (C3 & C5), 132.3 (C2'), 121.8 (C3'), 139.8 (C4'), 121.4 (C5'), 124.8 (C1'), 166.4 (C6'), 144.5 (C4), 144.7 (vinyl), 127.2 (vinyl); IR (KBr) ν (cm⁻¹): 3425, 3340, 3035, 2347, 1652, 1590, 1552, 1345, 1300, 1222, 1210, 991, 783, 751; HRMS *m/z*: 241.0933 ([M + H])⁺; Calcd: 241.0977.

25b. 3-[(1*E*, 2*E*)-*N*-hydroxy-3-(pyridin-2-yl)prop-2-enimidoyl] naphthalen-2-ol. Yield: 45%; Mp: 149–151°C; ¹H NMR (500 MHz, CDCl₃) δ 13.52 (s, 1H, OH), 9.31 (s, 1H), 8.81 (dd, 1H, H-3, *J* = 9.5), 8.07 (dd, 1H, H-9', *J* = 6.3, 9.4), 7.94 (dd, 1H, H-6, *J* = 10.5), 7.85 (d, 1H, H_α, *J* = 10.0), 7.82 (dd, 1H, H-4', *J* = 7.0), 7.80 (dd, 1H, H-5, *J* = 9.5), 7.75 (m, 1H, H-6', *J* = 10.5), 7.54 (d, 1H, H-4, *J* = 8.5), 7.52 (dd, 1H, H-8', *J* = 8.5), 7.23 (d, 1H, H-3', *J* = 15.0), 7.32 (t, 1H, H-7', *J* = 7.5), 7.10 (d, 1H, H_β, *J* = 10.5); ¹³C NMR (125 MHz, DMSO-*d*₆) δ 163.5 (C=N), 114.1 (C1'), 164.0 (C2'), 120.1 (C3'), 136.7 (C4'), 128.6 (C5'), 130.2 (C6'), 123.6 (C7'), 128.3 (C8'), 124.0 (C9'), 131.7 (C10'), 142.1 (vinylic), 128.1 (vinylic), 151.3 (C1), 150.2 (C3), 124.6 (C4), 137.9 (C5), 122.0 (C6); IR (KBr) ν (cm⁻¹): 3360, 3322, 3248, 1652, 1629, 1342, 1276, 1215, 782, 751; HRMS *m/z*: 291.1132 ([*M* + *H*])⁺; Calcd: 291.1133.

26b. 3-[(1*E*, 2*E*)-*N*-hydroxy-3-(pyridin-3-yl)prop-2-enimidoyl] naphthalen-2-ol. Yield: 57%; Mp: 154–156°C; ¹H NMR (500 MHz, CDCl₃) δ 13.72 (s, 1H, OH), 9.35 (s, 1H), 9.11 (s, 1H, H-2), 8.85 (d, 1H, H-4, *J* = 8.0), 8.20 (d, 1H, H-6, *J* = 11.5), 8.01 (dd, 1H, H-9', *J* = 8.0), 7.99 (dd, 1H, H-4', *J* = 7.75), 7.85 (d, 1H, H_α, *J* = 12.0), 7.79 (m, 1H, H-6', *J* = 12.0), 7.54 (dd, 1H, H-8', *J* = 6.5, 8.0), 7.52 (dd, 1H, H-5, *J* = 9.0), 7.38 (t, 1H, H-7', *J* = 7.5), 7.28 (d, 1H, *J* = 15.5, H-3'), 7.12 (d, 1H, H_β, *J* = 12.5); ¹³C NMR (125 MHz, DMSO-*d*₆) δ 162.1 (C=N), 114.5 (C1'), 163.9 (C2'), 119.9 (C3'), 136.9 (C4'), 128.2 (C5'), 129.7 (C6'), 123.5 (C7'), 128.2 (C8'), 123.9 (C9'), 131.9 (C10'), 142.27 (vinylic), 128.05 (vinylic), 131.6 (C1), 151.2 (C2), 154.6 (C4), 124.9 (C5), 136.0 (C6); IR (KBr) ν (cm⁻¹): 3400, 3320, 3250, 1655, 1690, 1352, 1280, 1215, 790, 751; HRMS *m/z*: 291.1149 ([*M* + *H*])⁺; Calcd: 291.1133.

27b. 3-[(1*E*, 2*E*)-*N*-hydroxy-3-(pyridin-4-yl)prop-2-enimidoyl] naphthalen-2-ol. Yield: 68%; Mp: 132–134°C; ¹H NMR (500 MHz, CDCl₃) δ 13.59 (s, 1H, OH), 9.30 (s, 1H), 8.89 (m, 2H, H-3 & H-5, *J* = 10.5), 8.09 (dd, 1H, H-9', *J* = 7.2, 7.5), 7.92 (dd, 1H, H-4', *J* = 6.5, 7.5), 7.81 (d, 1H, H_α, *J* = 11.0), 7.74 (m, 2H, H-2 & H-6, *J* = 9.0), 7.72 (m, 1H, H-6', *J* = 9.5), 7.52 (dd, 1H, H-8', *J* = 9.0), 7.35 (t, 1H, H-7', *J* = 8.5), 7.22 (d, 1H, H-3', *J* = 11.5), 7.15 (d, 1H, H_β, *J* = 11.5); ¹³C NMR (125 MHz, DMSO-*d*₆) δ 164.1 (C=N), 114.0 (C1'), 163.4 (C2'), 119.2 (C3'), 136.9 (C4'), 128.0 (C5'), 129.6 (C6'), 123.5 (C7'), 128.0 (C8'), 122.9 (C9'), 131.7 (C10'), 142.1 (vinylic), 126.2 (vinylic), 141.6 (C1), 122.2 (C2 & C6), 151.6 (C3 & C5); IR (KBr) ν (cm⁻¹): 3462, 3350, 3310, 3249, 1625, 1690, 1322, 1276, 1225, 1215, 769, 742; HRMS *m/z*: 291.1142 ([*M* + *H*])⁺; Calcd: 291.1133.

28b. 4-[(1E, 3E)-3-(hydroxyimino)-3-(pyridin-2-yl)prop-1-en-1-yl]-N, N- dimethyl aniline. Yield: 64%; Mp: 104–106°C; IR (KBr) ν (cm⁻¹): 3465, 3369, 3042, 2965, 2452, 1640, 1252, 1164, 1090, 862, 651; ¹H NMR (500 MHz, CDCl₃): δ 8.77 (dd, 1H, H-3, J = 8.5), 8.07 (dd, 1H, H-6, J =6.3, 9.5), 7.92 (dd, 2H, H-2' & H-4', J = 9.7, 10.8), 7.89 (t, 1H, H-5, J = 9.0), 7.82 (d, 1H, H _{α} , J = 11.5), 7.51 (m, 1H, H-4, J = 11.5), 7.20 (d, 1H, H _{β} , J = 12.0), 6.72 (m, 2H, H-3' & H-5', J = 15.5); ¹³C NMR (125 MHz, DMSO-d₆) δ 169.5 (C=N), 150.6 (C1), 127.5 (C6), 136.2 (C5), 128.3 (C4), 145.0 (C3), 42.2 (-Me), 125.2 (C1'), 111.3 (C3' & C5'), 135.9 (C2 & C6'), 159.6 (C4'), 140.9 (vinylic), 129.4 (vinylic); HRMS m/z : 268.1412 ([M + H]⁺); Calcd: 268.1450.

7.3. Results and Discussion

7.3.1. Effect of compounds on tyrosinase activity: inhibition kinetics

The present work was targeted towards the synthesis of tyrosinase inhibitors by solid-state synthesis. In the first step, simple grindstone chemistry was utilized to synthesize azachalcones. The parent azachalcones were prepared by grinding together equivalent amounts of the appropriate ketones and different aldehydes in the presence of solid pulverized sodium hydroxide at room temperature. In the second step, the azachalcones on reaction with hydroxylamine hydrochloride and calcium oxide got converted into corresponding oximes which were isolated and recrystallized from ethylacetate. This method emphasized the effectiveness of CaO in oxime synthesis under grinding conditions without any rearrangement of α , β - double bond. All the synthesized compounds were characterized by spectroscopic data. The parent azachalcones synthesized exhibited moderate tyrosinase inhibitory activities. This indicated that a 2'-hydroxyl group substituted on ring A appeared to be an important design element in achieving enhanced tyrosinase inhibition. The presence of a pyridinyl skeleton resulted in an improved tyrosinase effect. The pyridinyl nitrogen atom of substituted azachalcone derivatives could get protonated at physiological pH or might be available to coordinate the copper atom existing in the tyrosinase active site. Replacement of the phenyl group in ring A with a naphthyl group brought about a decrease in tyrosinase inhibitory activity. This could be due to steric hindrance caused by the presence of the bulky naphthyl group that could hinder the binding of the ligand with the active site of the enzyme.

Briefly, all the synthesized compounds were screened for the diphenolase inhibitory activity of mushroom tyrosinase inhibition activity using L-DOPA as substrate (Fisher 1983). It was interesting to note that all of the oxime derivatives synthesized (**22b–28b**) had good tyrosinase inhibitory activities when compared with the positive control, kojic acid. In particular, compounds **22b** and **23b** exhibited the greatest inhibition of the L-DOPA oxidase activity of mushroom tyrosinase. These compounds were found to be more potent than the positive control, kojic acid (IC_{50} : 37.3 μ M).

The structures of the non-cyclic moieties of our molecules had similar features to those of hydroxamic acids and hydroxamates which were good chelating agents. Tyrosinase inhibition of compounds **22b–28b** depended on the competency of the hydroxamate moiety to chelate with the dinuclear copper active site in the active site of enzyme (Romaguera & Grimalt 1985). The oxime moiety was seen to coordinate with the copper metal at the active site of mushroom tyrosinase thereby preventing electron transfer by the metal ion. This decreased the ability of the enzyme to oxidize the substrate subsequently leading to an inhibition in mushroom tyrosinase activity. Also, oximes, popular in supramolecular chemistry as strong hydrogen bond donors, could therefore be involved in hydrogen bond interactions with the amino acid residues of the enzyme (Gerdemann, Eicken & Krebs 2002). This in turn, helped the compound to have a better fit to the catalytic pocket of the enzyme tyrosinase. Compound **34b** with a para-dimethyl substituent showed moderate tyrosinase inhibition of 50.6 %. The inhibitory activities of these newly synthesized compounds were compared to that of kojic acid as a reference standard and the results are shown in **Table 12**.

7.3.2. Inhibition mechanism of the selected compounds on mushroom tyrosinase

To explore the mechanism of active inhibitors, the kinetic behaviour of tyrosinase activity was studied in the presence of active inhibitors **22b** and **23b**. L-DOPA was used as substrate for the effect of inhibitor compounds on the oxidation of L-DOPA by tyrosinase (diphenolase activity). The result showed that both compounds could inhibit the diphenolase activity of tyrosinase in a dose-dependent manner. With increasing concentrations of inhibitors, the remaining enzyme activity decreased exponentially. The inhibitor concentration leading to 50% activity lost (IC_{50}) for compounds **22b** and **23b** was estimated to be 15.3 μ M and 12.7 μ M, respectively.

Table 12 Inhibition effects and docking results of chalconeoximes

Compound	Tyrosinase Inhibition at 50 μ M (%) *	CDOCKER energy (kcal/mol)	Type of interactions	Donor-acceptor	Distance (Å)
22b	77.5 \pm 1.1	-27.93	H-bonding	N-OH...O δ_1 (Asn260)	2.03
				(His61) HE ₁ ... OH	2.86
				(His259) HE ₁ ...N	2.40
			hydrophobic stacking	π - π ring B...His263	3.73
23b	80.6 \pm 0.5	-27.05	H-bonding	N-OH...N ϵ_2 (His244)	2.01
			hydrophobic stacking	π - π ring B...His263	3.69
24b	69.8 \pm 1.2	-24.00	H-bonding	(His85) δ_2 ... N- OH	2.40
				(Val283) H α ..OH	2.28
			Intramolecular bonding	H- OH (oxime)...N	1.98
			hydrophobic stacking	π - π ring B...His263	3.94
25b	58.2 \pm 1.2	-13.37	H-bonding	N-OH...N ϵ_2 (His244)	2.09
				N-OH...O ϵ_2 (Glu256)	1.95
				(His244) δ_2 ... N- OH	2.85
			hydrophobic stacking	π - π ring B...His263	3.78
26b	62.6 \pm 0.3	-18.78	H-bonding	N-OH...N ϵ_2 (His244)	2.03
			hydrophobic stacking	π - π ring B...His263	3.72
27b	57.5 \pm 0.7	-13.64	hydrophobic stacking	π - π ring B...His263	3.78
28b	52.5 \pm 1.5	-14.52	H-bonding	N-OH...O (Met280)	2.58
Kojic acid	49.8 \pm 0.2	-11.69	H-bonding	Val283 H α ...O	2.64
				H...O=C (Met280)	2.84
				Asn260 H α ...O	2.93

* Hydroxy azachalcones were synthesized according to the details in Scheme 1; Values indicated means \pm SE for three determinations.

The plots of the remaining enzyme activity versus the concentration of enzyme at different inhibitor concentrations gave a family of straight lines, which all passed

through the origin. The presence of inhibitor did not reduce the amount of enzyme, but just resulted in the inhibition of enzyme activity. The results showed that both the compounds **22b** and **23b** were reversible inhibitors of mushroom tyrosinase for oxidation of L-DOPA (**Figure 38**).

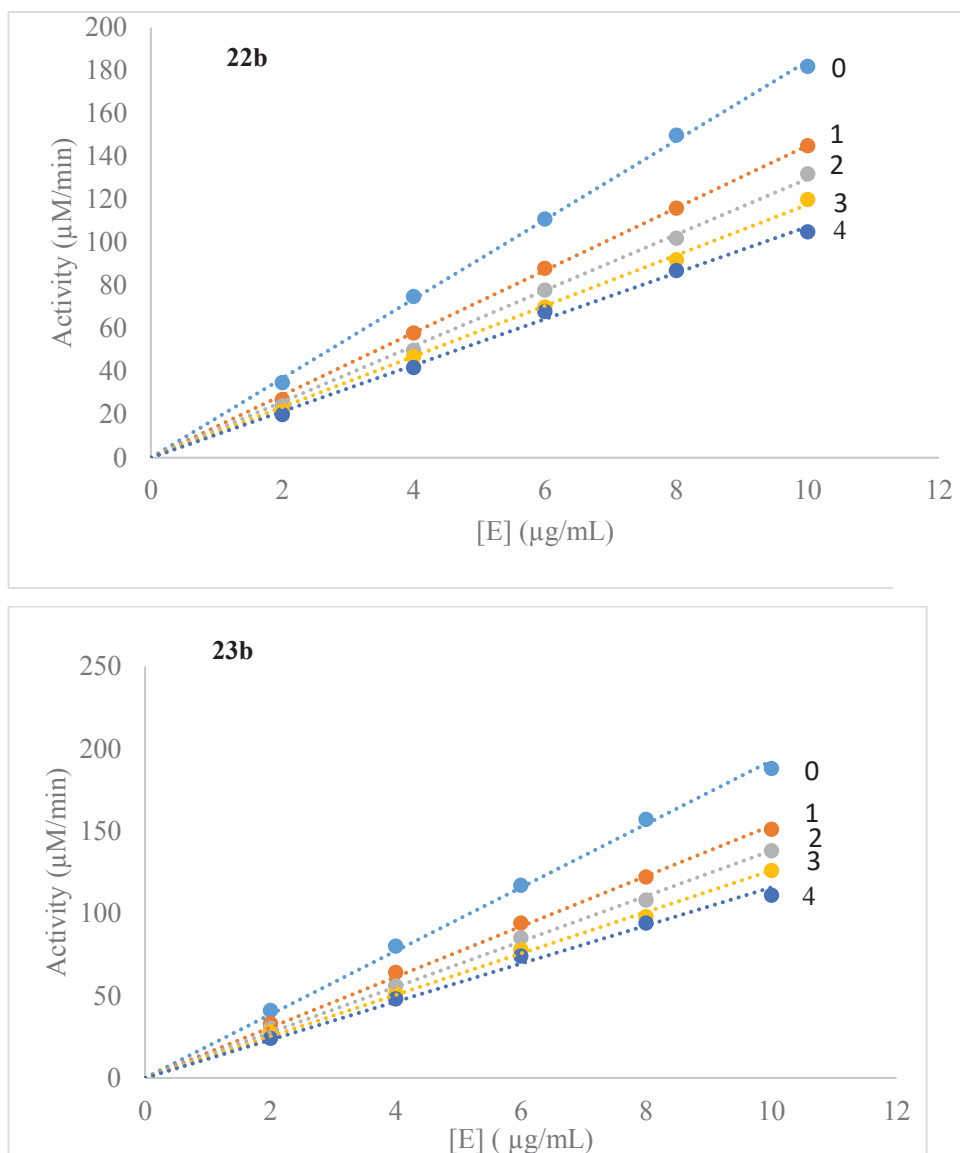


Figure 38 The inhibitory mechanism of compounds **22b** and **23b**

The concentration of inhibitor used for curves 0-4 were 0, 0.25, 0.5, 1.0 and 2.0 μM respectively.

7.3.3. Lineweaver–Burk analysis of tyrosinase inhibition by compounds **22b** and **23b**

The reaction rates were measured in the presence of active inhibitors with various concentrations of L-DOPA as a substrate. As the concentrations of active inhibitors **22b**

and **23b** increased, K_m values gradually increased, but V_{max} values did not change, thereby indicating the inhibitors act as competitive inhibitors of mushroom tyrosinase (**Figure 39**).

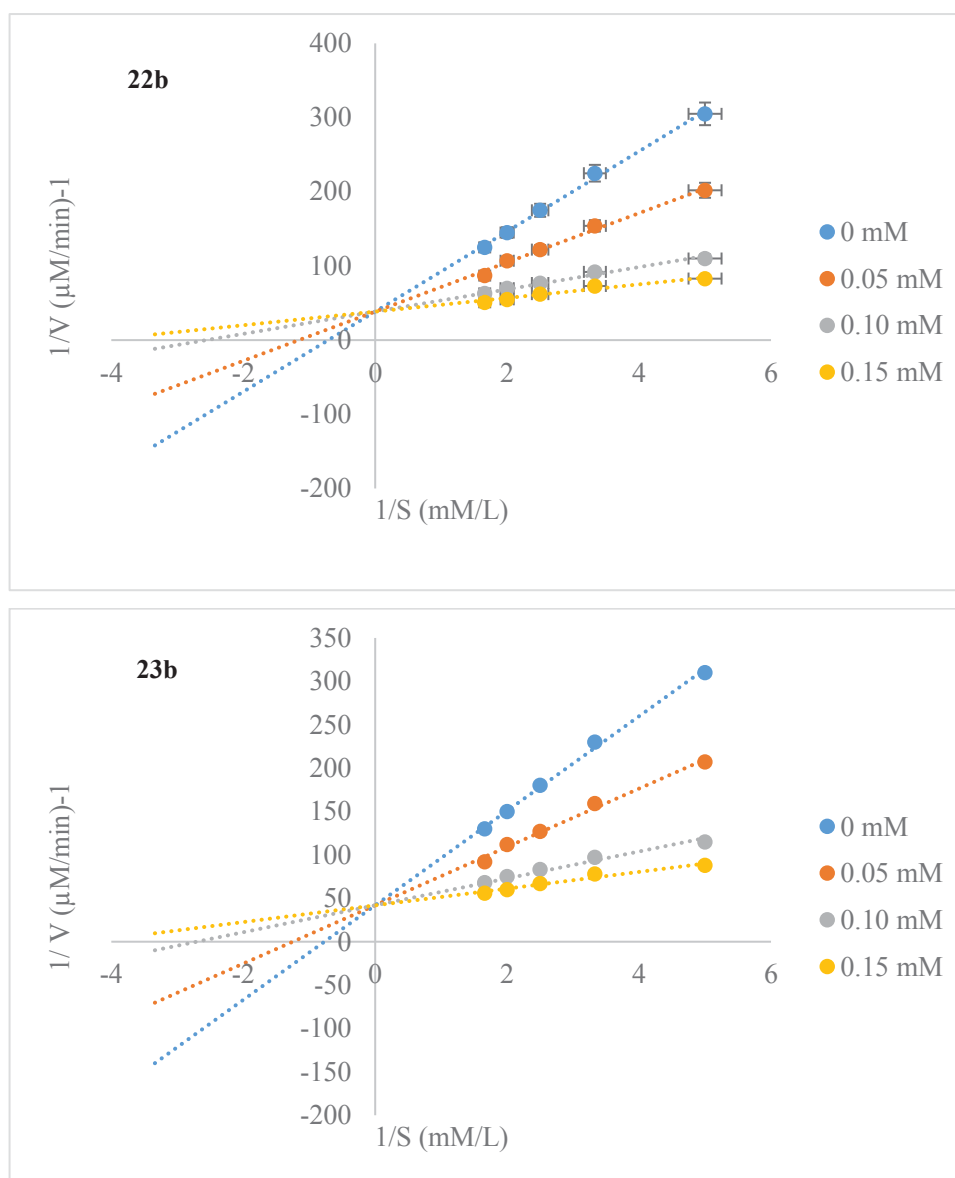


Figure 39 Lineweaver-Burk plots for inhibition of compounds **22b** and **23b**

The inhibitor concentrations were 0, 0.05, 0.10 and 0.15 mM. The final enzyme concentration was 2.9 $\mu\text{g}/\text{ml}$.

The inhibition kinetics were illustrated by Dixon plots, which were obtained by plotting $1/V$ versus $[I]$ with varying concentrations of substrate. Dixon plots gave a family of straight lines passing through the same point at the second quadrant, giving the inhibition constant (K_i) (**Figure 40**).

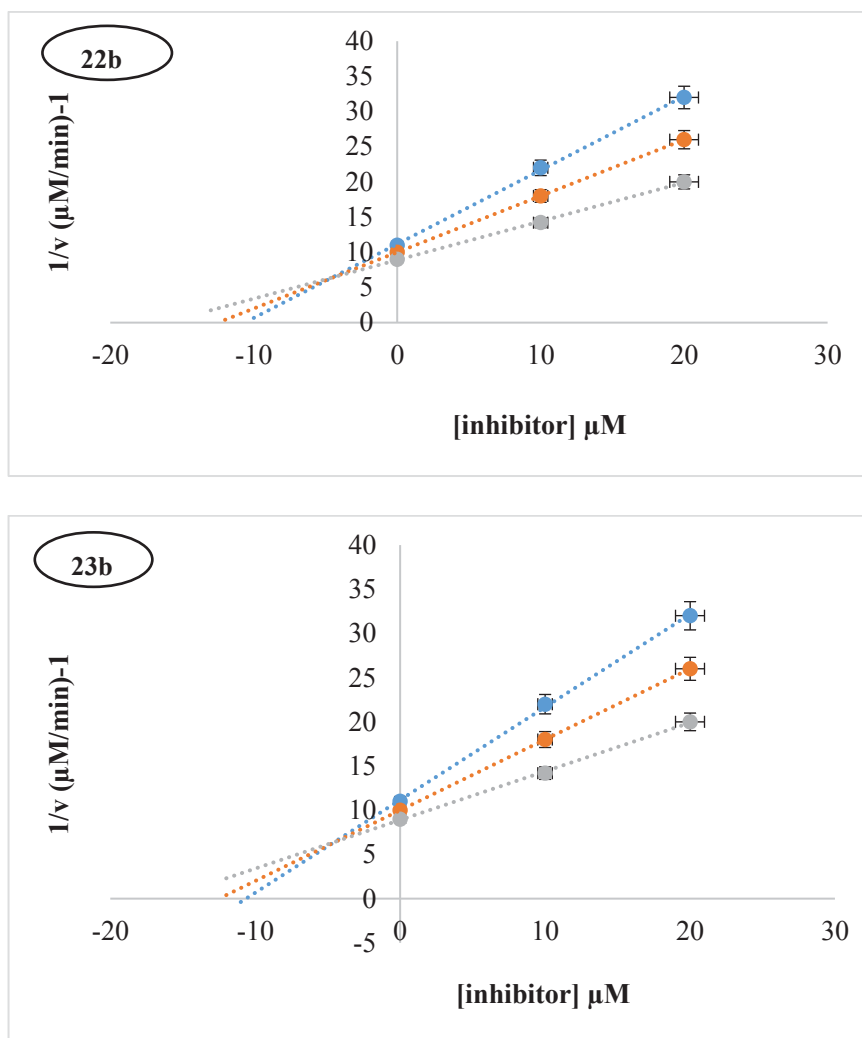


Figure 40 Dixon plot for the inhibitory effect of compounds **22b** and **23b**

The inhibitor concentrations were 0, 0.5 and 2.0 μM , respectively. The L-DOPA concentrations were 100, 200 and 300 μM .

The K_i value estimated from this Dixon plot was 5.1 μM and 2.5 μM , respectively for the compounds **22b** and **23b**. A comparison of the K_m and K_i values of the compounds with that of kojic acid revealed that they possess much higher affinity to tyrosinase than kojic acid (**Table 13**).

Table 13 Effect on mushroom tyrosinase activity and kinetic analysis

Compound	Type of inhibition	IC ₅₀ (μM)	K _i (μM) ^c
22b	Competitive	15.3 ± 1.0	5.1
23b	Competitive	12.7 ± 0.8	2.5
Kojic acid	Competitive	37.3 ± 0.3	8.8

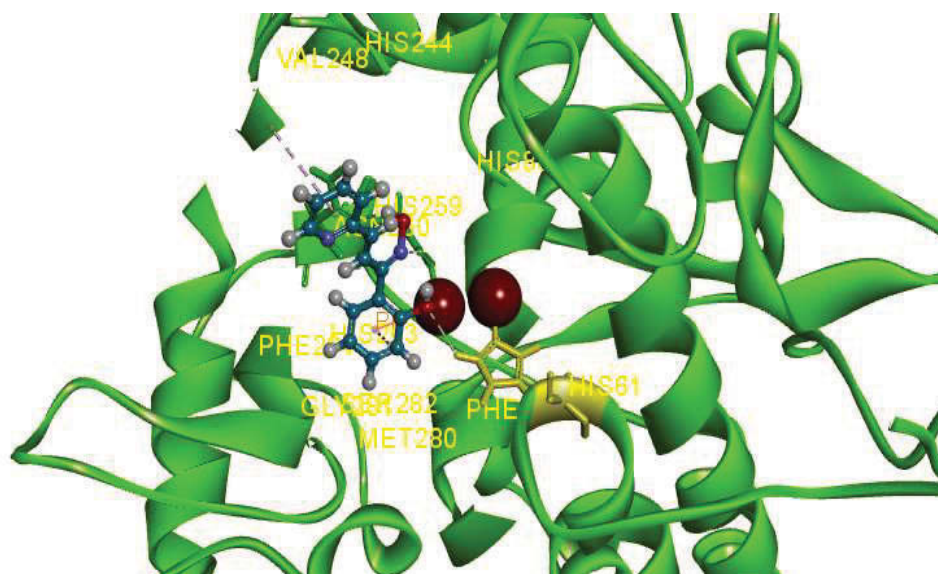
c: Values were measured at 5 μM of active compounds and *K_i* is the (inhibitor constant).

7.3.4. Docking studies

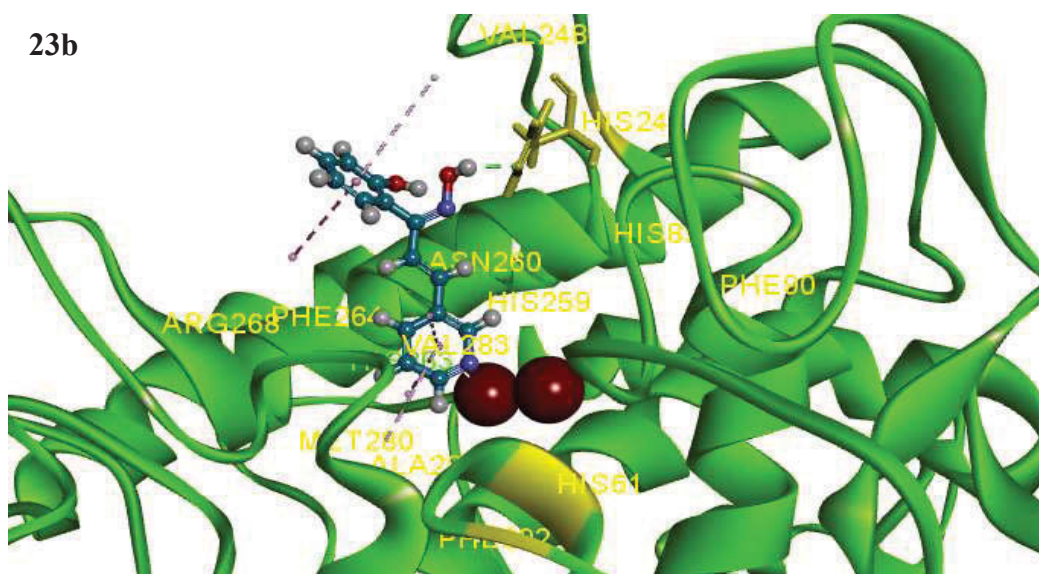
The results of kinetic studies were correlated with the docking results. Accelrys Discovery Studio 4.5 suite was utilized to simulate binding between the active site of mushroom tyrosinase and substituted azachalcone oxime compounds. The results of virtual screening studies indicated that the estimated CDOCKER energy of all the docked ligands ranged between -27.93 and -11.69 kcal/mol. **Figure 41** showed selected docked conformations of active inhibitors **22b** and **23b** in the tyrosinase binding site. Docking results showed that compound **22b** had the highest docking score (-27.93 kcal mol⁻¹) that correlated well with the experimental results (**Table 12**). In the case of most of the oxime chalcones reported here, the oxime OH group was actively involved in hydrogen bonding interactions with amino acid residues of the tyrosinase. This in turn, helped the compounds to have a better fit to the catalytic pocket of the enzyme tyrosinase.

Compound **22b** formed 3 hydrogen bonds with amino-acid residues in the tyrosinase catalytic pocket. Hydrogen bonding with Asn260, His61 and His259 was seen for compound **22b** while compound **23b** formed a strong hydrogen bonding with His244 at a distance of 2.0 Å. The heterocyclic nitrogen atom in ring B of compound **22b** formed a weak hydrogen bond (2.40 Å) with the hydrogen of His259. Another weak hydrogen bond (2.86 Å) was seen between the oxime oxygen of **22b** and the hydrogen in His61. The residues had a key function and effect on binding affinity. Both the active compounds showed hydrophobic π - π stacking interactions with His263. According to the docking program, the binding residues interacting with kojic acid were Met280, Val283, Asn260 and Gly281 of tyrosinase. This indicated that the oxime derivatives of azachalcones inhibited tyrosinase activity by binding at the active site of mushroom tyrosinase.

22b



23b



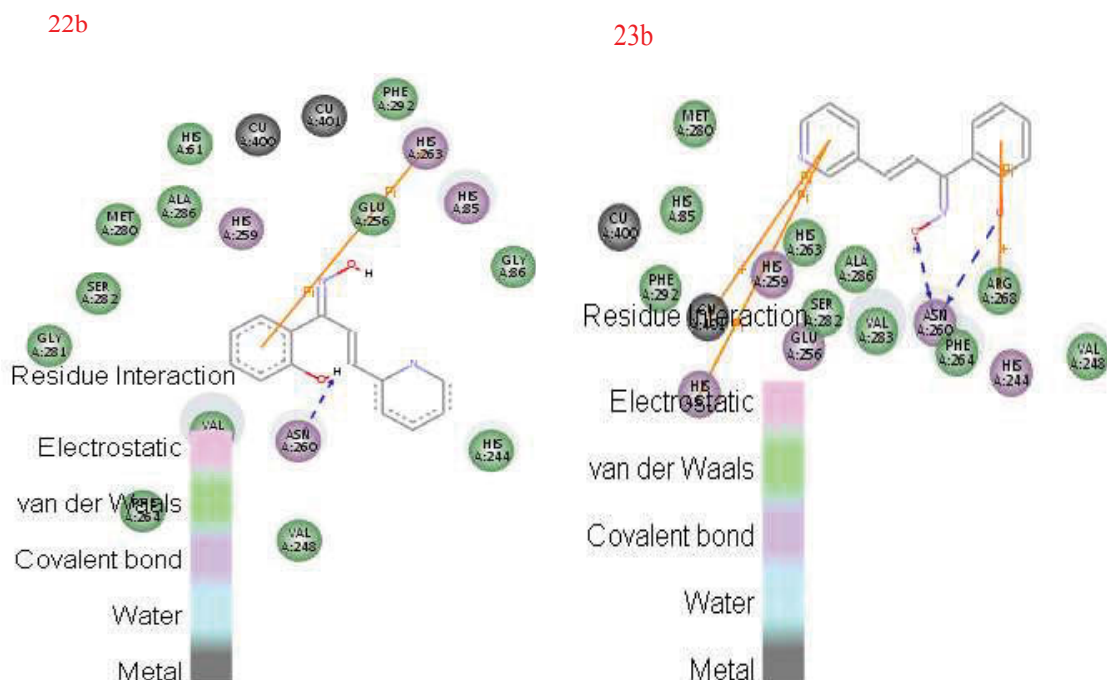


Figure 41 Docking and 2D results of compounds **22b** and **23b** in the tyrosinase pocket

Ligands **22b** and **23b** were displayed as ball and stick while the core amino acid residues were displayed as stick. The green dotted lines showed the hydrogen bond interactions and the purple lines showed the non-bonding interactions. The ochre balls represented the copper ions.

7.4. Conclusion

To summarize, novel azachalcone oxime compounds were synthesized and studied for their inhibition on the diphenolase activity of mushroom tyrosinase. The solvent-free synthesis was particularly attractive because it incorporated the principles of green chemistry. Green chemistry was “the utilization of a set of principle that reduced or eliminated the use or generation of hazardous substances in the design, manufacture, and application of chemical products”. Green chemistry aimed to prevent waste and generate substances with little or no toxicity to humans and the environment, thereby maximizing atom economy.

Azachalcone oxime compounds **22b** and **23b** were found to be significantly more potent than kojic acid with their IC_{50} values of 15.3 μ M and 12.7 μ M, respectively. Both the compounds exhibited reversible competitive inhibition. *In silico* studies revealed that the formation of a strong intramolecular hydrogen bond formed between the pyridinyl nitrogen and the oxygen atom of oxime group brought about a substantial decline in tyrosinase inhibitory potential. Replacement of phenyl ring with a naphthyl ring led to a substantial decline in tyrosinase inhibition. In a nutshell, the present study established a

versatile and robust mechanochemical route to the facile synthesis of chalconeoxime compounds via a simple mortar–pestle grinding method.

7.5. References

Abele, E, Abele, R, Dzenitis, O, Lukevics, E 2003, 'Indole and isatin oximes: Synthesis, reactions and biological activity', *Chemistry of Heterocyclic Compounds*, Vol 39, pp. 3–35.

Anastas, P, Warner, J 1998, 'Principles of green chemistry', *Green Chemistry*, New York, Oxford University Press, p.30.

Ballini, R, Barboni, L, Filippone, P 1997, 'Amberlyst A-21 an excellent heterogeneous catalyst for the conversion of carbonyl compounds to oximes', *Chemistry Letters*, pp. 475–476.

Bose, AK, Pednekar, S, Ganguly, SN, Chakraborty, G, Manhas, MS 2004, 'A simplified green chemistry approach to the Biginelli reaction using grindstone chemistry', *Tetrahedron Letters*, Vol 45, pp. 8351–8353.

Damljanovic, I, Vukicevic, M, Vukicevic, RD 2006, 'A simple synthesis of oximes', *Monatshefte für Chemie*, Vol 137, pp. 301–305.

Eshghi, H, Hassankhani, A 2005, 'Regioselective synthesis of E-oximes catalyzed by ferric chloride under solvent-free conditions', *Organic Preparations and Procedures International*, Vol 37, pp. 575–579.

Fisher, AA 1983, 'Current contact news. Hydroquinone uses and abnormal reactions', *Cutis*, Vol 31, pp. 240–244, 250.

Flick, AC, Caballero, MJA, Lee, HI, Padwa, A 2010, '2, 3-Bis (phenylsulfonyl)-1, 3-butadiene as a reagent for the synthesis of the azatricyclic core of (+/-)-halichlorine', *Journal of Organic Chemistry*, Vol 75, pp. 1992–1996.

Gerdemann, C, Eicken, C, Krebs, B 2002, 'The crystal structure of catechol oxidase: new insight into the function of type-3 copper proteins', *Accounts of Chemical Research*, Vol 35, pp. 183–191.

Ghiaci, M, Aghaei, H, Oroojeni, M, Aghabarari, B, Rives, V, Vicente, MA, Sobrados, I, Sanz, J 2009, 'Synthesis of paracetamol by liquid phase Beckmann rearrangement of 4-hydroxyacetophenone oxime over H₃PO₄/Al-MCM-41', *Catalysis Communications*, Vol 10, pp. 1486–1492.

Guo, JJ, Jin, TS, Zhang, SL, Li, TS 2001, 'TiO₂/SO₄²⁻ : an efficient and convenient catalyst for preparation of aromatic oximes', *Green Chemistry*, Vol 3, pp. 193–195.

Hajipour, AR, Mahboubghah, N 1998, 'A rapid and convenient synthesis of oximes in dry media under microwave irradiation', *Journal of Chemical Research*, pp. 122–123.

Jin, J, Li, Y, Wang, ZJ, Qian, WX, Bao, WL 2010, 'A concise, metal-free approach to the synthesis of oxime ethers from cross-dehydrogenative-coupling of sp³ C-H bonds with oximes', *European Journal of Organic Chemistry*, pp. 1235–1238.

Kad, GL, Bhandari, M, Kaur, J, Rathee, R, Singh, J 2001, 'Solventless preparation of oximes in the solid state and via microwave irradiation', *Green Chemistry*; Vol 3, pp. 275–277.

Khan, MTH 2007, 'Heterocyclic Compounds against the Enzyme Tyrosinase Essential for Melanin Production: Biochemical Features of Inhibition', *Heterocyclic Chemistry*, Vol 9, 119–138.

Kukushkin, VY, Pombeiro, AJL 1999, 'Oxime and oximate metal complexes: unconventional synthesis and reactivity', *Coordination Chemistry Reviews*, Vol 181, pp.147–157.

Ley, JP, Bertram, HJ 2001, 'Hydroxy or methoxy-substituted benzaldoximes and Benzaldehyde-O-alkyloximes as tyrosinase inhibitors', *Bioorganic & Medicinal Chemistry*, Vol 9, pp.1879–1885.

Li, JT, Li, XL, Li, TS 2006, 'Synthesis of oximes under ultrasound irradiation', *Ultrasonics Sonochemistry*, Vol 13, pp. 200–202.

Luo, HM, Li, YQ, Zheng, WJ 2005, 'A novel ionic liquid/water biphasic system for the preparation of oximes', *Chinese Chemical Letters*, Vol 16, pp. 906–908.

Mehrabi, H 2008, 'Synthesis of α -oximinoketones under ultrasound irradiation', *Ultrasonics Sonochemistry*, Vol 15, pp. 279–282.

Miller, P, Kaufman, DH 2000, 'Mild and efficient dehydration of oximes to nitriles mediated by the Burgess reagent', *Synlett*, pp. 1169–1171.

Olah, GA, Keumi, T 1979, 'Synthetic methods and reactions: Improved one-step conversion of aldehydes into nitriles with hydroxylamine in formic acid solution', *Synthesis*, pp. 112–113.

Osadchenko, IM, Tomilov, AP 2002, 'Phase-transfer catalysis in synthesis of oximes', *Russian Journal of Applied Chemistry*, Vol 75, pp. 511–512.

Ramón, RS, Bosson, J, Díez-González, S, Marion, N, Nolan, SP 2010, 'Au/ag-Cocatalyzed aldoximes to amides rearrangement under solvent and acid-free conditions', *Journal of Organic Chemistry*, Vol 75, pp.1197–1202.

Redasani, VK, Kumawat, VS, Kabra, RP, Kanagara, P, Surana, SJ 2010, 'Applications of green chemistry in organic synthesis', *International Journal of ChemTech Research*, Vol 2, pp. 1856–1859.

Romaguera, C, Grimalt, F 1985, 'Leukoderma from hydroquinone', *Contact Dermatitis* Vol 12, pp. 183.

Sharjhi, H, Sarvari, MH 2000, 'A mild and versatile method for the preparation of oximes by the use of calcium oxide', *Journal of Chemical Research*, Vol 1, pp. 24–25.

Shen, C, Sigman, DS 1991, 'New inhibitors of aldose reductase: anti-oximes of aromatic aldehydes', *Archives of Biochemistry and Biophysics*, Vol 286, pp. 596–603.

Sosnovsky, G, Krogh, JA, Umhoefer, SG 1979, 'A one-flask conversion of aldehydes to nitriles using hydroxylamine hydrochloride and selenium dioxide', *Synthesis*, pp. 722–724.

Toda, F, Yagi, M, Kiyoshige, K 1988, 'Baeyer-Villiger reaction in the solid state', *Journal of the Chemical Society, Chemical Communications*, pp. 958–959.

Weissermer, K, Arpe, H 1978, 'Industrial organic chemistry', Berlin: Springer Verlag, pp. 225–228.

CHAPTER 8

AMINOCHALCONES

8.1. Introduction

Amino chalcones have been reported to have promising biological activities (Zhu *et al* 2010; Chen *et al* 2005). It was interesting to note that the amino chalcone skeleton had few structural features that were quite similar to the substrate L-DOPA. In addition, naphthalene derivatives of oxyresveratrol have served to be a favourable scaffold with potent tyrosinase inhibition (Xia *et al* 2000). On the basis of these findings, a series of hydroxyphenyl and hydroxynaphthyl substituted aminochalcone compounds were designed and synthesized for use as depigmentation agents and as anti-browning food additives.

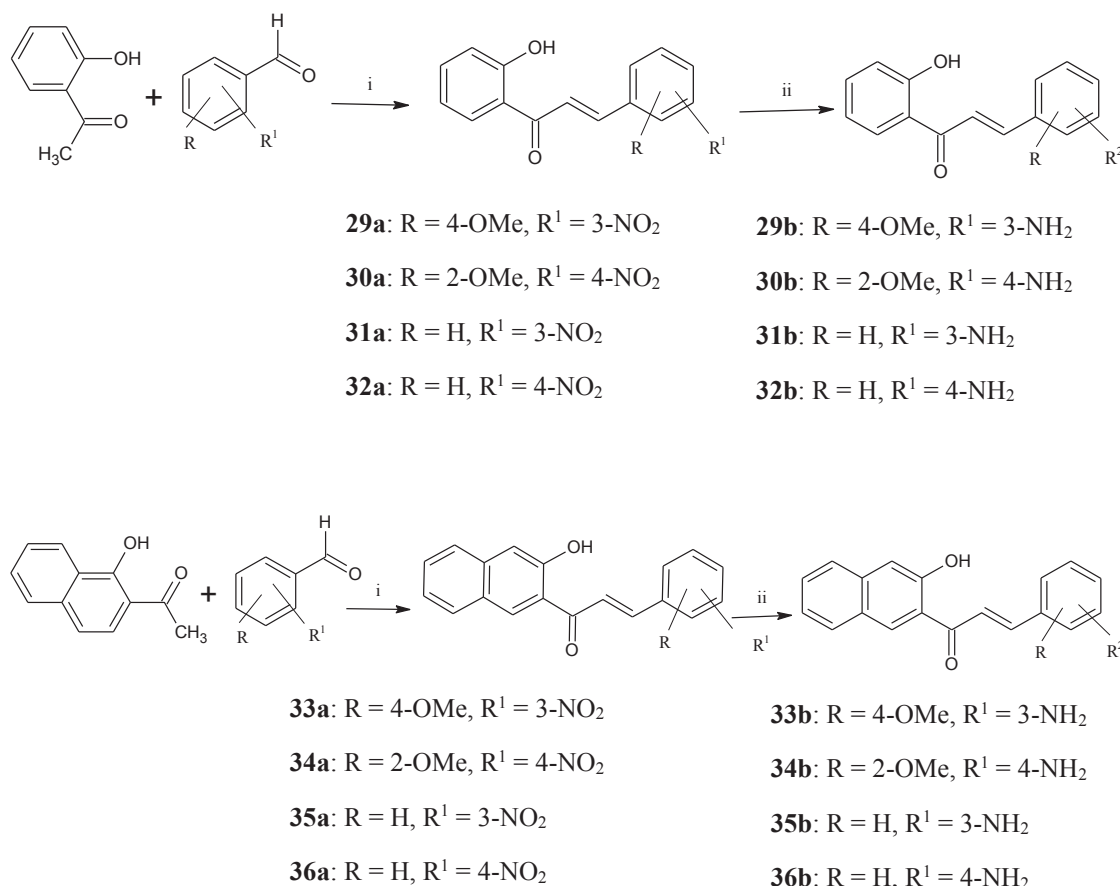
A number of α , β -unsaturated ketones have demonstrated preferential reactivity toward thiols (Prasad, Rao & Rambabu 2009; Song *et al* 2007). Alkylation with a cellular thiol such as glutathione (GSH) may also occur with chalcones, leading to adducts at the β -position (Lee *et al* 1971; Dimmock *et al* 1983). Hence, these α , β -unsaturated ketones may be free from the problems of mutagenicity and carcinogenicity that are associated with many alkylating agents used in cancer chemotherapy. There has been an increasing impetus to find alternative natural and synthetic pharmaceutical depigmenting agents (Franco *et al* 2012; Parvez *et al* 2006; Zhu & Gao 2008). Compounds that could inhibit melanogenesis while remaining low in cytotoxicity or devoid of toxicity towards melanocytes would be of particular interest. Studies have shown that chalcones substituted with electron donating methoxy groups on ring B had significant cytotoxic activities, when tested on cancer cell lines (Bandgar *et al* 2010; Ethiraj, Aranjani & Khan 2013; Shenvi *et al* 2013). Studies have also indicated 2'-aminochalcones to elicit significant cytotoxic activity against a panel of human tumor cell lines (Xia *et al* 2000).

Moreover, the synthesis of amino chalcones for cytotoxic and anticancer properties appears to be an unexplored field. This prompted to further investigate the effect of aminochalcones on melanin formation in murine B16F10 cells.

8.2. Experimental

In the first step, nitro chalcones were synthesized by the base-catalyzed Claisen-Schmidt condensation of an aldehyde and an appropriate ketone in a polar solvent like methanol. These nitro chalcones were then successfully reduced to their corresponding primary amines in the presence of palladium/carbon, using ammonium formate as the hydrogen source (Benvenuto *et al* 1993) (**Scheme 7**). The reaction was based on a facile

mechanism of catalytic hydrogen transfer hydrogenation, an extension of the ‘Leuckart reaction’. Further investigations were conducted to determine the effect of aminochalcone compounds on melanin formation in murine B16F10 cells.



Scheme 7. General method for the synthesis of aminochalcones **29b–36b**.

Reagents and conditions: (i) MeOH, NaOH, 0°C, 24 hrs. (ii) Ammonium formate, palladium on carbon, MeOH, RT.

8.2.1. Method for the synthesis of compound **30b**.

To a stirred solution of 2'-hydroxyacetophenone (1 mM, 1.36 mL) and 2-methoxy-4-nitrobenzaldehyde (1mM, 181mg) in 25 mL methanol, was added pulverized NaOH (2mM) and the mixture was stirred at room temperature for 24–36 h. The reaction was monitored by TLC using *n*-hexane: ethyl acetate (7:3) as mobile phase. The reaction mixture was cooled to 0°C (ice-water bath) and acidified with HCl (10 % v/v aqueous solution) to afford total precipitation of the compound. An orange precipitate was formed, which was filtered and washed with 10 % aqueous HCl solution. The product obtained was recrystallized with ethylacetate to give the pure chalcone product **30a**.

To a stirred suspension of the nitrochalcone compound **30a** (5mmol), 0.25 g 10% palladium on charcoal in 10 cm³ dry methanol at room temperature, was added anhydrous ammonium formate (23 mmol), in a single portion under N₂. The resulting mixture was stirred at room temperature for 3 h. The catalyst was removed by filtration through celite and washed with 2x10 cm³ methanol. The filtrate was evaporated under reduced pressure and the residue was taken up in CHCl₃ and washed with 3 x 25 cm³ H₂O. The organic layer was dried (Na₂SO₄) and evaporated to dryness to give the aminochalcone product **30b**.

8.2.2. Spectral data

29a. (2*E*)-1-(2-hydroxyphenyl)-3-(4-methoxy-3-nitrophenyl)prop-2-en-1-one. Yield: 72%; Mp: 110–112°C; ¹H NMR (500 MHz, CDCl₃): δ 12.47 (s, 1H, OH), 8.10 (s, 1H), 7.86 (d, 1H, H_β, *J* = 12.5), 7.74 (d, 1H, H-6', *J* = 10.0), 7.72 (d, 1H, H_α, *J* = 12.0), 7.65 (d, 1H, H-5, *J* = 9.5), 7.54 (d, 1H, H-6, *J* = 8.0), 7.49 (t, 1H, H-4', *J* = 8.5), 6.92 (dd, 1H, H-3', *J* = 8.0, 9.5), 6.90 (dd, 1H, H-5', *J* = 7.4, 9.0), 3.86 (s, 3H); ¹³C NMR (125 MHz, DMSO-*d*₆) δ 192.22 (C=O), 130.52 (C6'), 119.25 (C1'), 118.27 (C5'), 136.77 (C4'), 118.28 (C3'), 161.92 (C2'), 126.90 (C1), 120.54 (C2), 137.22 (C3), 147.50 (C4), 112.42 (C5), 114.23 (C6), 56.67 (Me), 122.40 (vinylic), 141.83 (vinylic); IR (KBr) ν (cm⁻¹): 3200, 3070, 2914, 2864, 2720, 1686, 1578, 1550, 1468, 1349, 970, 720, 580; MS (ESI): 270.1 ([M + H])⁺.

30a. (2*E*)-1-(2-hydroxyphenyl)-3-(2-methoxy-4-nitrophenyl)prop-2-en-1-one. Yield: 68%; Mp: 123–125°C; IR (KBr) ν (cm⁻¹): 3250, 3345, 3015, 2910, 2865, 2700, 1702, 1682, 1552, 1465, 1305, 979, 735, 680, 575; ¹H NMR (500 MHz, CDCl₃): δ 12.22 (s, 1H, OH), 8.22 (s, 1H), 7.95 (d, 1H, H_β, *J* = 14.0), 7.86 (m, 1H, H-6, *J* = 9.5), 7.80 (d, 1H, H_α, *J* = 13.0), 7.75 (d, 1H, H-6', *J* = 10.5), 7.69 (d, 1H, H-5, *J* = 8.5), 7.59 (dd, 1H, H-4', *J* = 8.5), 7.02 (dd, 1H, H-3', *J* = 7.9, 9.0), 6.97 (m, 1H, H-5', *J* = 10.0), 3.82 (s, 3H); ¹³C NMR (125 MHz, DMSO-*d*₆) δ 194.25 (C=O), 130.24 (C6'), 119.33 (C1'), 118.20 (C5'), 137.07 (C4'), 118.48 (C3'), 162.90 (C2'), 128.22 (C1), 115.24 (C2), 112.22 (C3), 137.50 (C4), 122.47 (C5), 116.55 (C6), 125.50 (vinylic), 140.87 (vinylic); MS (ESI): 270.1 ([M + H])⁺.

31a. (2*E*)-1-(2-hydroxyphenyl)-3-(3-nitrophenyl)prop-2-en-1-one. Yield: 92%; Mp: 97–98°C; ¹H NMR (500 MHz, CDCl₃): δ 12.61 (s, 1H, OH), 8.54 (s, 1H, H-2'), 8.26 (d, 1H, *J* = 16.0, H-4'), 8.24 (d, 1H, *J* = 8.0, H-6'), 7.95 (t, 1H, *J* = 8.5, H-6), 7.92 (d, 1H, H_β,

$J = 15.5$), 7.79 (d, 1H, H_a , $J = 15.0$), 7.52 (t, 1H, $J = 7.5$, H-5'), 7.04 (d, 1H, $J = 9.0$, H-4), 6.97 (t, 1H, $J = 8.0$, H-3), 6.89 (d, 1H, $J = 8.5$, H-5); ^{13}C NMR (125 MHz, DMSO- d_6) δ 193.3 (C=O), 204.7 (C6'), 119.4 (C1'), 118.8 (C5'), 136.34 (C4'), 118.7 (C3'), 130.1 (C2'), 124.9 (C6), 137.2 (C1), 134.5 (C2), 129.9 (C3), 129.6 (C4), 148.76 (C5), 122.4 (vinylic), 142.2 (vinylic); IR (KBr) ν (cm^{-1}): 3530, 3085, 1752, 1589, 1439, 1357, 1289, 1265, 1210, 998, 830, 730, 659; MS (ESI): 270.1 ($[\text{M} + \text{H}]^+$).

32a. (2*E*)-1-(2-hydroxyphenyl)-3-(4-nitrophenyl)prop-2-en-1-one. Yield: 85%; Mp: 92–94°C; ^1H NMR (500 MHz, CDCl_3): δ 12.22 (s, 1H, OH), 8.41 (dd, 2H, $J = 11.5$), 8.10 (dd, 2H, $J = 6.5, 9.5$, H-2 & H-6), 7.92 (d, 1H, H_β , $J = 15.5$), 7.76 (d, 1H, H_a , $J = 15.0$), 7.71 (d, 1H, $J = 8.0$, H-6'), 7.46 (dd, 1H, $J = 16.0$, H-4'), 6.94 (dd, 1H, $J = 8.5$, H-3'), 6.88 (t, 1H, $J = 7.5$, H-5'); ^{13}C NMR (125 MHz, DMSO- d_6) δ 199.2 (C=O), 162.3 (C2'), 119.7 (C1'), 118.3 (C3'), 118.9 (C4'), 130.6 (C5'), 140.9 (C1), 130.2 (C2 & C6), 124.5 (C3 & C5), 122.4 (vinylic), 142.2 (vinylic); IR (KBr) ν (cm^{-1}): 3533, 3079, 1755, 1582, 1436, 1355, 1288, 1265, 1215, 992, 830, 737; MS (ESI): 270.1 ($[\text{M} + \text{H}]^+$).

33a. (2*E*)-1-(2-hydroxyphenyl)-3-(4-methoxy-3-nitrophenyl)prop-2-en-1-one. Yield: 68%; Mp: 110–112°C; ^1H NMR (500 MHz, CDCl_3): δ 12.47 (s, 1H, OH), 8.10 (s, 1H), 7.86 (d, 1H, $J = 12.5$, H_β), 7.74 (d, 1H, $J = 10.0$, H-6'), 7.72 (d, 1H, $J = 12.0$, H_a), 7.65 (d, 1H, $J = 9.5$, H-5), 7.54 (d, 1H, $J = 8.0$, H-6), 7.49 (t, 1H, $J = 8.5$, H-4'), 6.92 (dd, 1H, $J = 9.5$, H-3'), 6.90 (dd, 1H, $J = 6.3, 9.4$, H-5'), 3.86 (s, 3H); ^{13}C NMR (125 MHz, DMSO- d_6) δ 192.22 (C=O), 130.52 (C6'), 119.25 (C1'), 118.27 (C5'), 136.77 (C4'), 118.28 (C3'), 161.92 (C2'), 126.90 (C1), 120.54 (C2), 137.22 (C3), 147.50 (C4), 112.42 (C5), 114.23 (C6), 56.67 (Me), 122.40 (vinylic), 141.83 (vinylic); IR (KBr) ν (cm^{-1}): 3200, 3070, 2914, 2864, 2720, 1686, 1578, 1550, 1468, 1349, 970, 720, 580; MS (ESI): 270.1 ($[\text{M} + \text{H}]^+$).

34a. (2*E*)-1-(2-hydroxyphenyl)-3-(2-methoxy-4-nitrophenyl)prop-2-en-1-one. Yield: 72%; Mp: 123–125°C; ^1H NMR (500 MHz, CDCl_3): δ 12.22 (s, 1H, OH), 8.22 (s, 1H), 7.95 (d, 1H, $J = 14.0$, H_β), 7.86 (m, 1H, $J = 9.5$, H-6), 7.80 (d, 1H, $J = 13.5$, H_a), 7.75 (d, 1H, $J = 10.5$, H-6'), 7.69 (d, 1H, $J = 8.5$, H-5), 7.59 (dd, 1H, $J = 7.6, 8.5$, H-4'), 7.02 (dd, 1H, $J = 9.0$, H-3'), 6.97 (m, 1H, $J = 10.0$, H-5'), 3.82 (s, 3H); ^{13}C NMR (125 MHz, DMSO- d_6) δ 194.2 (C=O), 130.2 (C6'), 119.3 (C1'), 118.2 (C5'), 137.0 (C4'), 118.4 (C3'), 162.9 (C2'), 128.2 (C1), 115.2 (C2), 112.2 (C3), 137.5 (C4), 122.4 (C5), 116.5 (C6), 125.5 (vinylic), 140.8 (vinylic); IR (KBr) ν (cm^{-1}): 3250, 3345, 3015, 2910, 2865, 2700, 1702, 1682, 1552, 1465, 1305, 979, 735, 680, 575; MS (ESI): 270.1 ($[\text{M} + \text{H}]^+$).

35a. (2*E*)-1-(3-hydroxynaphthalen-2-yl)-3-(3-nitrophenyl) prop-2-en-1-one Yield: 79%; Mp: 125–127°C; ¹H NMR (500 MHz, CDCl₃): δ 11.97 (s, 1H, OH), 8.72 (s, 1H), 8.49 (dd, 1H, *J* = 10.5, H-4), 8.25 (d, 1H, *J* = 8.0, H-6), 8.10 (dd, 1H, *J* = 9.5, H-10'), 8.05 (dd, 1H, *J* = 9.0, H-5'), 7.85 (d, 1H, *J* = 11.5, H_β), 7.80 (dd, 1H, *J* = 6.8, 9.5, H-5), 7.75 (dd, 1H, *J* = 9.0, H-8'), 7.54 (t, 1H, *J* = 8.5, H-6'), 7.52 (d, 1H, *J* = 11.0, H_α), 7.37 (m, 1H, *J* = 10.0, H-7'), 7.11 (dd, 1H, *J* = 6.0, 7.5, H-3'); ¹³C NMR (125 MHz, DMSO-d₆) δ 202.4 (C=O), 136.4 (C1), 124.4 (C2), 149.8 (C3), 124.1 (C4), 130.4 (C5), 128.9 (C6), 115.2 (C1'), 165.4 (C2'), 119.9 (C3'), 131.1 (C4'), 124.2 (C5'), 128.1 (C6'), 122.9 (C7'), 129.4 (C8'), 128.51 (C9'), 139.2 (C10'), 127.6 (vinylic), 143.2 (vinylic); IR (KBr) ν (cm⁻¹): 3080, 1710, 1561, 1526, 1426, 1340, 1291, 1253, 1158, 988, 973, 827, 728; MS (ESI): 320.1 ([M + H])⁺.

36a. (2*E*)-1-(3-hydroxynaphthalen-2-yl)-3-(4-nitrophenyl)prop-2-en-1-one. Yield: 60%; Mp: 114–116°C; ¹H NMR (500 MHz, CDCl₃): δ 12.17 (s, 1H, OH), 8.32 (dd, 1H, *J* = 10.0, H-5'), 8.19 (dd, 2H, *J* = 9.0, H-2 & H-6), 8.15 (dd, 1H, *J* = 8.0, H-10'), 7.92 (d, 1H, *J* = 12.5, H_β), 7.75 (dd, 1H, *J* = 8.8, 9.5, H-8'), 7.59 (d, 1H, *J* = 12.0, H_α), 7.57 (dd, 1H, *J* = 8.5, 9.5, H-6'), 7.42 (m, 1H, *J* = 10.5, H-7'), 7.29 (dd, 1H, *J* = 8.5, H-3'), 6.92 (dd, 2H, *J* = 11.5, H-3 & H-5); ¹³C NMR (125 MHz, DMSO-d₆) δ 197.47 (C=O), 139.49 (C1), 134.45 (C2 & C6), 129.82 (C3 & C5), 150.02 (C4), 119.27 (C1'), 160.21 (C2'), 119.92 (C3'), 130.92 (C4'), 126.27 (C5'), 129.12 (C6'), 124.90 (C7'), 130.45 (C8'), 129.22 (C9'), 140.20 (C10'), 129.62 (vinylic), 146.20 (vinylic); IR (KBr) ν (cm⁻¹): 3075, 1685, 1652, 1586, 1439, 13450, 1285, 1249, 1155, 1025, 970, 835, 732; MS (ESI): 320.1 ([M + H])⁺.

29b. (2*E*)-3-(3-amino-4-methoxyphenyl)-1-(2-hydroxyphenyl)prop-2-en-1-one. Yield: 92%; Mp: 202–204°C; ¹H NMR (500 MHz, CDCl₃): δ 11.97 (s, 1H, OH), 8.27 (s, 1H), 7.55 (d, 1H, *J* = 9.0, H-5), 7.92 (d, 1H, *J* = 14.5, H_β), 7.72 (d, 1H, *J* = 9.5, H-6'), 7.49 (d, 1H, *J* = 8.0, H-6), 7.40 (t, 1H, *J* = 8.5, H-4'), 7.32 (d, 1H, *J* = 14.0, H_α), 6.87 (dd, 1H, *J* = 7.4, 8.5, H-5'), 6.85 (dd, 1H, *J* = 7.5, H-3'), 5.52 (s, 2H), 3.89 (s, 3H); ¹³C NMR (125 MHz, DMSO-d₆) δ 190.96 (C=O), 129.4 (C6'), 119.2 (C1'), 117.6 (C5'), 136.7 (C4'), 118.2 (C3'), 158.9 (C2'), 126.6 (C1), 119.5 (C2), 145.8 (C3), 147.5 (C4), 112.4 (C5), 114.22 (C6), 123.2 (vinylic), 140.8 (vinylic); IR (KBr) ν (cm⁻¹): 3225, 3100, 2955, 2860, 2680, 2015, 1690, 1580, 1550, 1440, 1350, 972, 727, 582; HRMS *m/z*: 270.1118 ([M + H])⁺; Calcd: 270.1124.

30b. (2*E*)-3-(4-amino-2-methoxyphenyl)-1-(2-hydroxyphenyl) prop-2-en-1-one. Yield: 57%; 235–237°C; ¹H NMR (500 MHz, CDCl₃): δ 11.95 (s, 1H, OH), 8.27 (s, 1H), 8.05 (d, 1H, *J* = 12.0, H_β), 7.95 (d, 1H, *J* = 9.5, H-6'), 7.92 (d, 1H, *J* = 11.5, H_a), 7.89 (m, 1H, *J* = 9.5, H-6), 7.75 (d, 1H, *J* = 9.0, H-5), 7.62 (dd, 1H, *J* = 8.0, H-4'), 7.20 (dd, 1H, *J* = 9.5, H-3'), 6.99 (dd, 1H, *J* = 9.5, 10.5, H-5'), 5.68 (s, 2H), 3.69 (s, 3H); ¹³C NMR (125 MHz, DMSO-d₆) δ 195.5 (C=O), 132.4 (C6'), 120.3 (C1'), 119.2 (C5'), 139.1 (C4'), 118.4 (C3'), 160.9 (C2'), 129.2 (C1), 117.6 (C2), 112.20 (C3), 149.5 (C4), 125.4 (C5), 119.4 (C6), 126.4 (vinylic), 145.2 (vinylic); IR (KBr) ν (cm⁻¹): 3350, 3325, 3224, 3019, 2922, 2850, 2685, 1700, 1656, 1550, 1425, 1329, 1015, 970, 728, 572; HRMS *m/z*: 270.1114 ([M + H])⁺; Calcd: 270.1124.

31b. (2*E*)-3-(3-aminophenyl)-1-(2-hydroxyphenyl)prop-2-en-1-one: Yield: 48%; Mp: 102–103°C; ¹H NMR (500 MHz, CDCl₃): δ 11.95 (s, 1H, OH), 8.34 (s, 1H, H-2), 8.19 (d, 1H, *J* = 8.5 Hz, H_β), 8.17 (dd, 1H, *J* = 7.0, H-4), 8.05 (dd, 1H, *J* = 7.5, H-6), 7.96 (t, 1H, *J* = 9.0, H-5), 7.69 (d, 1H, *J* = 7.0, H-6'), 7.49 (t, 1H, *J* = 7.5, H-4'), 7.03 (d, 1H, *J* = 8.0 Hz, H_a), 6.96 (dd, 1H, *J* = 6.2, 8.0, H-3'), 6.89 (t, 1H, *J* = 7.0, H-5'), 5.48 (s, 2H); ¹³C NMR (125 MHz, DMSO-d₆) δ 193.3 (C=O), 204.7 (C6'), 119.7 (C1'), 118.80 (C5'), 136.34 (C4'), 118.78 (C3'), 130.1 (C2'), 137.9 (C1), 124.5 (C2), 148.5 (C3), 128.2 (C4), 120.4 (vinylic), 142.5 (vinylic), 130.5 (C5), 134.8 (C6); IR (KBr) ν (cm⁻¹): 3367, 3085, 2925, 1680, 1752, 1590, 1420, 1289, 1255, 1210, 998, 830, 730, 667; HRMS *m/z*: 240.1026 ([M + H])⁺; Calcd: 240.1024.

32b. (2*E*)-3-(4-aminophenyl)-1-(2-hydroxyphenyl)prop-2-en-1-one. Yield: 47%; Mp: 106–108°C; ¹H NMR (500 MHz, CDCl₃): δ 12.50 (s, 1H, OH), 7.90 (d, 1H, H_β, *J* = 15.5), 7.70 (d, 1H, *J* = 8.5, H-6'), 7.74 (d, 1H, H_a, *J* = 15.0), 7.69 (dd, 2H, *J* = 6.8, 9.5, H-2 & H-6), 7.49 (dd, 1H, *J* = 15.0, H-4'), 6.90 (dd, 1H, *J* = 8.0, H-3'), 6.82 (t, 1H, *J* = 7.5, H-5'), 6.80 (dd, 2H, *J* = 15.5, H-3 & H-5), 5.36 (s, 2H); ¹³C NMR (100 MHz, DMSO-d₆) δ 193.3 (C=O), 204.5 (C6'), 119.7 (C1'), 118.8 (C5'), 136.3 (C4'), 118.8 (C3'), 130.4 (C2'), 154.9 (C4), 132.5 3 (C2 & C6), 124.5 2 (C3 & C5), 141.2 9 (C1), 120.2 (vinylic), 142.5 (vinylic); IR (KBr) ν (cm⁻¹): 3467, 31085, 2955, 1685, 1752, 1422, 1256, 1210, 996, 832, 748, 660; HRMS *m/z*: 240.1049 ([M + H])⁺; Calcd: 240.1024.

33b. (2*E*)-3-(3-aminophenyl)-1-(3-hydroxynaphthalen-2-yl) prop-2-en-1-one. Yield: 53%; Mp: 228–230°C; ¹H NMR (500 MHz, CDCl₃): δ 12.25 (s, 1H, OH), 8.69 (s, 1H), 8.57 (dd, 1H, *J* = 9.5, H-4), 8.27 (d, 1H, *J* = 8.5, H-6), 8.22 (dd, 1H, *J* = 9.5, H-5'), 8.17 (dd, 1H, *J* = 9.0, H-10'), 7.91 (d, 1H, *J* = 10.0, H_β), 7.89 (dd, 1H, *J* = 9.5, H-5), 7.82 (d,

1H, $J = 9.5$, H_a), 7.79 (dd, 1H, $J = 7.9$, 9.4, H-8'), 7.57 (dd, 1H, $J = 8.2$, 9.5, H-6'), 7.40 (m, 1H, $J = 11.5$, H-7'), 7.20 (dd, 1H, $J = 6.8$, 8.5, H-3'), 5.98 (s, 2H); ^{13}C NMR (125 MHz, DMSO- d_6) δ 198.9 (C=O), 134.2 (C1), 125.2 (C2), 152.6 (C3), 125.2 (C4), 130.2 (C5), 127.6 (C6), 116.2 (C1'), 162.5 (C2'), 120.1 (C3'), 134.3 (C4'), 124.2 (C5'), 128.7 (C6'), 122.5 (C7'), 129.2 (C8'), 128.5 (C9'), 140.5 (C10'), 129.2 (vinyl), 145.2 (vinyl); IR (KBr) ν (cm^{-1}): 3345, 3328, 3060, 2600, 1717, 1650, 1567, 1535, 1420, 1335, 1228, 980, 935, 820, 752; HRMS m/z : 320.1149 ($[\text{M} + \text{H}]^+$); Calcd: 320.1175

34b. (2E)-3-(4-aminophenyl)-1-(3-hydroxynaphthalen-2-yl) prop-2-en-1-one. Yield: 59%; Mp: 240–242°C; ^1H NMR (500 MHz, CDCl_3): δ 12.25 (s, 1H, OH), 8.27 (dd, 1H, $J = 9.0$, H-5'), 8.07 (d, 1H, $J = 9.5$, H_β), 8.05 (dd, 1H, $J = 6.2$, 8.0, H-10'), 7.85 (d, 1H, $J = 9.0$, H_a), 7.80 (m, 1H, $J = 10.5$, H-8'), 7.75 (dd, 2H, $J = 7.7$, 10.2, H-2 & H-6), 7.55 (dd, 1H, $J = 9.0$, H-6'), 7.47 (dd, 1H, $J = 8.5$, 10.5, H-7'), 7.35 (dd, 1H, $J = 8.0$, H-3'), 6.87 (dd, 2H, $J = 15.0$, H-3 & H-5), 5.97 (s, 2H); ^{13}C NMR (125 MHz, DMSO- d_6) δ 192.4 (C=O), 139.25 (C1), 125.68 (C3 & C5), 155.25 (C4), 132.23 (C2 & C6), 120.20 (C1'), 164.66 (C2'), 119.2 (C3'), 133.8 (C4'), 122.9 (C5'), 128.6 (C6'), 122.4 (C7'), 130.1 (C8'), 129.2 (C9'), 140.2 (C10'), 132.1 (vinyl), 144.2 (vinyl); IR (KBr) ν (cm^{-1}): 3425, 3345, 3312, 3026, 2559, 1712, 1648, 1525, 1508, 1415, 1329, 1209, 905, 817, 762; HRMS m/z : 320.1155 ($[\text{M} + \text{H}]^+$); Calcd: 320.1175.

35b. (2E)-3-(3-aminophenyl)-1-(3-hydroxynaphthalen-2-yl) prop-2-en-1-one. Yield: 49%; Mp: 228–230°C; ^1H NMR (500 MHz, CDCl_3): δ 12.25 (s, 1H, OH), 8.69 (s, 1H), 8.57 (dd, 1H, $J = 9.5$, H-4), 8.27 (d, 1H, $J = 8.5$, H-6), 8.22 (dd, 1H, $J = 9.5$, H-5'), 8.17 (dd, 1H, $J = 9.0$, H-10'), 7.91 (d, 1H, $J = 10.0$, H_β), 7.89 (dd, 1H, $J = 9.5$, H-5), 7.82 (d, 1H, $J = 9.5$, H_a), 7.79 (dd, 1H, $J = 7.9$, 9.0, H-8'), 7.57 (dd, 1H, $J = 9.5$, H-6'), 7.40 (m, 1H, $J = 11.5$, H-7'), 7.20 (dd, 1H, $J = 6.2$, 8.5, H-3'), 5.98 (s, 2H); ^{13}C NMR (125 MHz, DMSO- d_6) δ 198.98 (C=O), 134.2 (C1), 125.2 (C2), 152.6 (C3), 125.2 (C4), 130.2 (C5), 127.62 (C6), 116.2 (C1'), 162.5 (C2'), 120.1 (C3'), 134.3 (C4'), 124.2 (C5'), 128.7 (C6'), 122.5 (C7'), 129.2 (C8'), 128.5 (C9'), 140.5 (C10'), 129.2 (vinyl), 145.2 (vinyl); IR (KBr) ν (cm^{-1}): 3345, 3328, 3060, 2600, 1717, 1650, 1567, 1535, 1420, 1335, 1228, 980, 935, 820, 752; HRMS m/z : 320.1149 ($[\text{M} + \text{H}]^+$); Calcd: 320.1175

36b. (2E)-3-(4-aminophenyl)-1-(3-hydroxynaphthalen-2-yl) prop-2-en-1-one. Yield: 43%; Mp: 240–242°C; ^1H NMR (500 MHz, CDCl_3): δ 12.25 (s, 1H, OH), 8.27 (dd, 1H, $J = 7.9$, 9.6, H-5'), 8.07 (d, 1H, $J = 9.5$, H_β), 8.05 (dd, 1H, $J = 8.0$, H-10'), 7.85 (d, 1H, $J = 9.0$, H_a), 7.80 (m, 1H, $J = 10.5$, H-8'), 7.75 (dd, 2H, $J = 10.0$, H-2 & H-6), 7.55 (dd,

1H, $J = 9.0$, H-6'), 7.47 (dd, 1H, $J = 6.5, 10.5$, H-7'), 7.35 (dd, 1H, $J = 8.0$, H-3'), 6.87 (dd, 2H, $J = 15.0$, H-3 & H-5), 5.97 (s, 2H); ^{13}C NMR (125 MHz, DMSO- d_6) δ 192.4 (C=O), 139.2 (C1), 125.6 (C3 & C5), 155.2 (C4), 132.2 (C2 & C6), 120.2 (C1'), 164.6 (C2'), 119.2 (C3'), 133.8 (C4'), 122.9 (C5'), 128.6 (C6'), 122.4 (C7'), 130.1 (C8'), 129.2 (C9'), 140.2 (C10'), 132.1 (vinyllic), 144.2 (vinyllic); IR (KBr) ν (cm^{-1}): 3425, 3345, 3312, 3026, 2559, 1712, 1648, 1525, 1508, 1415, 1329, 1209, 905, 817, 762; HRMS m/z : 320.1155 ($[\text{M} + \text{H}]^+$; Calcd: 320.1175.

8.3. Results and Discussion

8.3.1. Chemistry

A series of substituted nitrochalcone compounds were synthesized by simple base catalyzed Claisen-Schmidt condensation reaction. The nitro-chalcones were subsequently reduced to their respective amino derivatives by transfer hydrogenation reaction using ammonium formate catalyzed by palladium on carbon. The prepared compounds were characterized by ^1H NMR, IR and mass spectral analyses. The signals for phenolic hydroxyl protons appeared between 11–12 ppm and were indicated by ^1H NMR spectra. The signals for aromatic hydrogens are between 6.35 and 8.45 ppm. In the infrared spectra of active compounds **29b-36b**, it was possible to observe the absorptions between 3200 and 3450 cm^{-1} relating to -NH stretch, absorptions in 1600–1660 cm^{-1} from α, β -unsaturated carbonyl moiety stretch and absorptions in 1650–1745 cm^{-1} from carbonyl moiety stretching. ^1H NMR spectrum showed typical singlets between 5.5–6.5 Hz (-NH) and typical ^1H - ^1H coupling constants between 12 and 15 Hz indicating *trans* stereochemistry of the double bond

In terms of the structure-activity relationships, compound **30b** (*2E*)-3-(4-amino-2-methoxyphenyl)-1-(2-hydroxyphenyl) prop-2-en-1-one) exhibited the most potent tyrosinase inhibitory activity with inhibition of 75.51% (**Table 14**). This could be accounted for the presence of strong ortho-para activating substituents on ring B. Presence of strong electron releasing groups in the ortho position (-OMe) and a strongly activating para amino substituent modulates the electronic structure of ring B significantly. This was consistent with the docking results where the electron-donating groups increased the electron density of ring B through a resonance donating effect and

higher electron density bonded copper ions more effectively in the active site of enzyme. Amongst all the investigated compounds, the amino chalcone compound **30b** showed better inhibitory potential (IC_{50} : 7.82 μ M) than kojic acid (IC_{50} : 22.83 μ M). Removal of electron donating substituents on ring B brought about a slight decrease in tyrosinase inhibition as seen with compound **29b** that had an IC_{50} of 9.75 μ M. The fact that the activity was markedly affected by altering the substituents on the aminophenyl ring, suggested that the aromatic ring made a specific contribution to the binding via an aromatic ring orientation. Substitution of the para amino group with a less activating meta amino substituent gave compound **31b** with a slight decline in its tyrosinase inhibitory activity. (IC_{50} :16.75 μ M). However, the para-amino substituted chalcone compound **32b** bearing a hydroxyl group at position-2' of the phenyl ring A exhibited more potent tyrosinase inhibitory activity (IC_{50} : 12.75 μ M) when compared with the positive control, kojic acid (IC_{50} : 27.3 μ M).

Replacement of the phenyl group with a naphthyl group led to a slight decline in inhibitory activities (compounds **33b** and **34b**) indicating that the bulky naphthyl group in ring A might cause stereo-hindrance for the inhibitors approaching the active site. However, substituting the naphthyl amino chalcone with a para activating group on ring B gave compound **35b** with an inhibitory potential ($58.5 \pm 1.62\%$) that was still more effective than kojic acid ($42.6 \pm 0.32\%$) while substitution with an ortho directing methoxy group gave compound **36b** that showed a considerable decline in tyrosinase inhibition ($39.6 \pm 0.66\%$).

8.3.2. Kinetics

The bioactivities of compounds **29b** and **30b**, that had more potent activity than kojic acid were subjected for a detailed investigation. Compounds **29b**, **30b** and kojic acid were found to inhibit mushroom tyrosinase activity in a concentration-dependent manner (**Table 15**).

Table 14 Docking results and tyrosinase inhibition effects of amino chalcones

Compound	Dock Score (kcal/mol)	Tyrosinase inhibition* (%)	Type of interactions	Donor-acceptor	Distance (Å)
29b	-25.86	63.2 ± 0.12	H-bonding	(His61) HE ₁ ...OH	2.79
				(His85) H δ ₂ ...O=C	2.36
				(His259) HE ₁ ...O=C	2.26
			Hydrophobic	ring B...His263	3.88
			π-π stacking		
			Intramolecular bonding	H- OH... O=C	1.95
				(His61) HE ₁ ...OH	2.97
30b	-26.74	75.5 ± 1.12	H-bonding	(His85) H δ ₂ ...O=C	2.53
				(His259) HE ₁ ...O=C	2.30
			Metal coordination bond	Cu401...OH	3.15
			Hydrophobic	ring B...His263	3.79
			π-π stacking		
			Intramolecular bonding	H- OH... O=C	1.97
31b	-23.77	59.5 ± 0.12	H-bonding	H...O (His85)	2.65
				(His85) H δ ₂ ...O=C	2.47
				(His259) HE ₁ ...O=C	2.26
			Hydrophobic	ring B...His263	4.01
			π-π stacking		
			Intramolecular bonding	H- OH... O=C	1.90
				(His61) HE ₁ ...OH	2.96
32b	-24.54	60.5 ± 0.65	H-bonding	(His85) H δ ₂ ...O=C	2.57
				(His259) HE ₁ ...O=C	2.30
			Metal coordination bond	Cu401...OH	3.08
			hydrophobic stacking	π-π ring B...His263	3.60
			Intramolecular bonding	H- OH... O=C	1.91
				(Arg268) H...OH	2.07
33b	-13.90	49.3 ± 0.45	H-bonding	(His259) HE ₁ ...O=C	2.48

34b	-11.39	54.3 ± 0.24	H-bonding	HO...NE ₂ (His244)	2.67
35b	-12.13	58.5 ± 1.62	Intramolecular bonding	H- OH... O=C	1.96
			Hydrophobic	ring B...His263	3.78
			π - π stacking		
36b	-7.67	39.6 ± 0.66	Intramolecular bonding	H- OH... O=C	1.99
			hydrophobic	ring B...His263	3.88
			π - π stacking		
Kojic acid	-10.59	49.4 ± 0.32	H-bonding	Asn260 H α ...O	2.93
				Val283 H α ...O	2.64
				H... O=C (Met280)	2.84

* Values indicate means ± S.E for three determinations

Table 15 Inhibitory effects of kojic acid, 29b and 30b on mushroom tyrosinase

Sample	Concentration (μM)	Inhibition (%)				Average of IC ₅₀ (μM) ^a		Ki (μM) [#]
Kojic acid	1.25	3.62	3.60	3.65	3.62			
	5.00	16.45	16.52	16.42	16.46	22.83	±	9.23
	20.00	49.07	48.05	48.25	48.45	0.66		
29b	1.25	23.55	25.20	21.25	23.25			
	5.00	44.60	42.20	40.25	42.35	7.82 ± 0.42		1.89
	20.00	77.60	73.75	75.20	75.51			
30b	1.25	39.36	34.25	35.50	22.95			
	5.00	46.45	44.25	44.65	45.11	9.75 ± 1.22		4.82
	20.00	72.50	70.23	73.65	63.25			

^a 50% inhibitory concentration (IC₅₀). [#]: Values were measured at 5 μM of active compounds and *K_i* is the (inhibitor constant).

The reaction rates were measured in the presence of active inhibitors with various concentrations of L-DOPA as a substrate. As the concentrations of active inhibitors **29b** and **30b** increased, *K_m* values gradually increased, but *V_{max}* values did not change, thereby indicating that the inhibitors act as competitive inhibitors of mushroom tyrosinase (**Figure 42**).

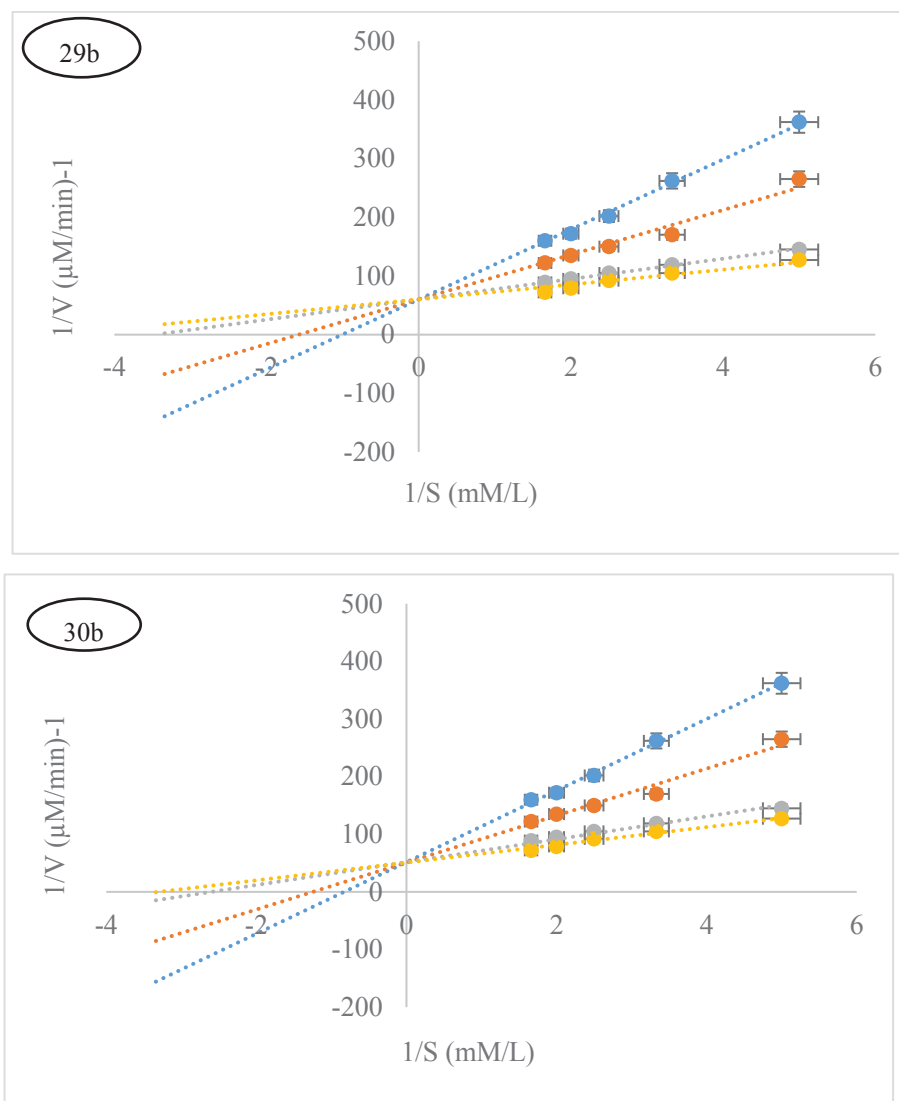


Figure 42 Lineweaver Burk plot for inhibition of compounds **29b** and **30b**

Data were obtained as mean values of $1/V$, the inverse of the absorbance increase at a wavelength of 492nm per min of three independent tests with different concentrations of L-DOPA as a substrate. The concentration of compounds **29b** and **30b** from top to bottom is 20 μM , 5 μM , 1.25 μM and 0 μM respectively.

The inhibition kinetics were illustrated by Dixon plots, which were obtained by plotting $1/V$ versus $[I]$ with varying concentrations of substrate. Dixon plots gave a family of straight lines passing through the same point at the second quadrant, giving the inhibition constant (K_i) (**Figure 43**).

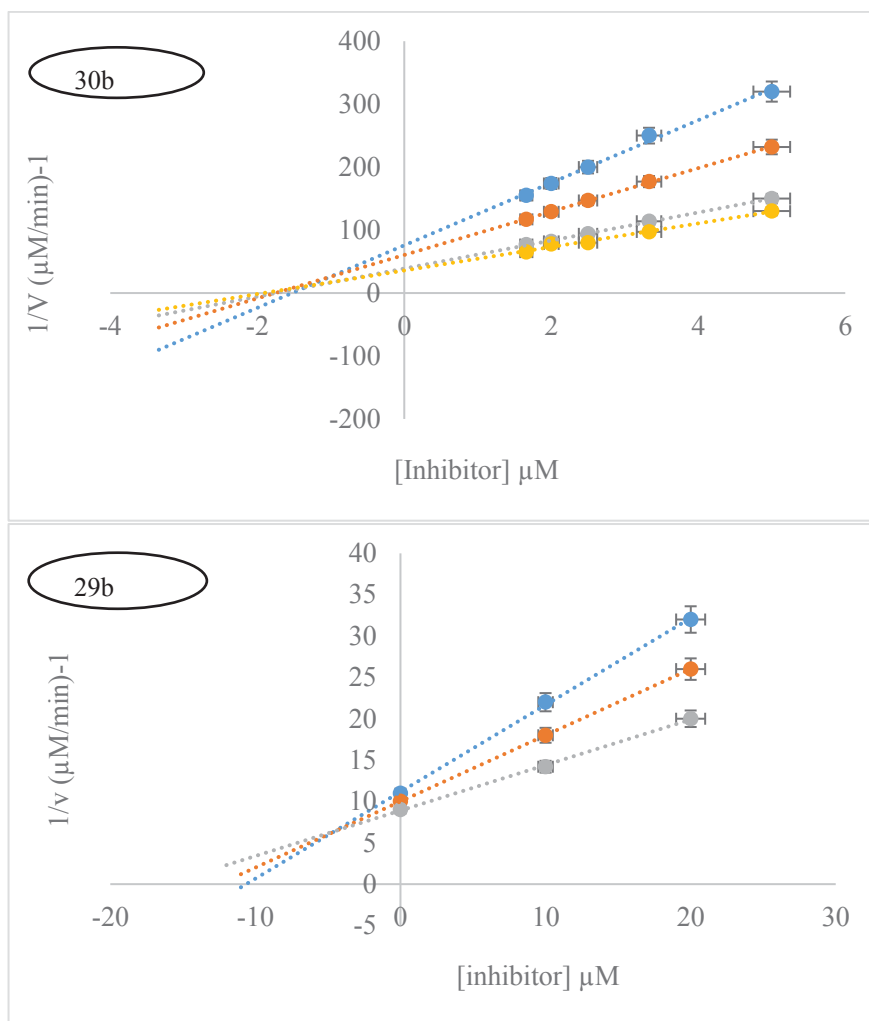


Figure 43 Dixon plot for the inhibitory effect of compounds **30b** and **29b**

The inhibitor concentrations were 0, 10 μM and 20 μM respectively. The L-DOPA concentrations were 200, 400 and 600 μM .

The K_i value estimated from this Dixon plot was 6.75 μM and 5.80 μM for the compounds **29b** and **30b**, respectively. A comparison of the K_m and K_i values of the compounds with that of kojic acid revealed that they possess much higher affinity to tyrosinase than kojic acid.

8.3.3. Docking studies

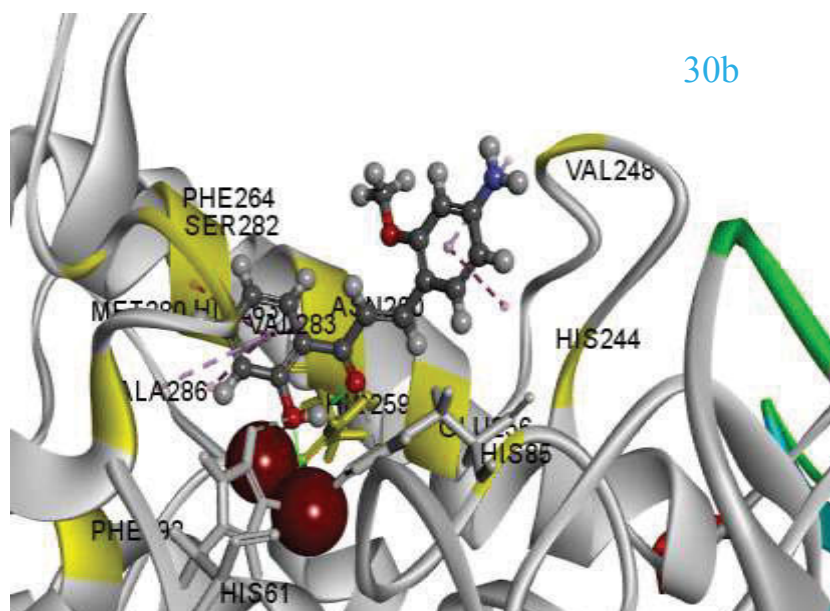
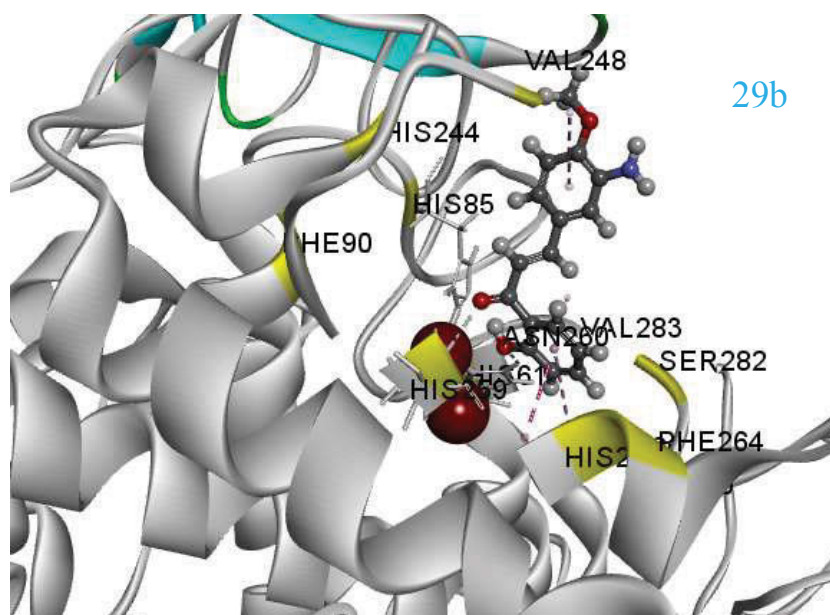
The synthesized compounds were docked on the enzyme tyrosinase. Docking procedures basically aim to identify the correct conformation of ligands in the binding pocket of a protein and to predict the affinity between the ligand and the protein.

Therefore, the tertiary structure of mushroom tyrosinase was used to simulate docking with the active inhibitors. (Ross and Subramanian 1981).

Simulation studies were conducted between the active site of mushroom tyrosinase and the active inhibitors **29b** and **30b** using Accelrys Discovery studio 4.5 suite. Compounds **29b** and **30b** exhibited hydrogen bonding interactions with His259, His85 and His61 (**Table 16**). Both the active compounds showed hydrophobic π - π stacking interactions with His263 and T-shaped edge to face aryl-aryl interactions with Phe264 and His244 (**Figure 44**).

The binding energies for compounds **31b** and **32b** were -23.77 kcal/mol and -24.54 kcal/mol, respectively which were found to be significantly greater than kojic acid that had a binding energy of -10.48 kcal/mol. The docking score for ligand-to-receptor binding included terms for electrostatic, van der Waals, and solvation energies. Docking results showed that compound **30b** (-25.75 kcal mol⁻¹) combined with mushroom tyrosinase more strongly than compound **29b** (-24.86 kcal mol⁻¹) (**Table 10**). The lower tyrosinase inhibition of compound **29b** could be accounted for the formation of a strong intramolecular hydrogen bond (1.95 Å) formed between the 2'-hydroxyl hydrogen with the carbonyl oxygen.

Copper ion (Cu400) was strongly bound by the hydroxyl group (2') of compound **30b** at a distance of 1.95 Å. There was also a coordination between Cu401 and the hydroxy oxygen (2') of the ligand **30b** at a distance of 3.15 Å. Formation of a complex between a ligand and the copper ion in the active site of mushroom tyrosinase could prevent electron transfer by the metal ion. Moreover, the binding of the inhibitor via a coordinate bond ensured that access to the active site by the substrate was effectively blocked. This could curb the enzymes ability to oxidize the substrates subsequently leading to an inhibition in mushroom tyrosinase. Docking results demonstrated π - π stacking interactions between ring A of compound **30b** with the imidazole ring of His263 and T-shaped edge to face aryl-aryl interactions with Phe264 whereas amide- π interactions were observed with Ser282 and Val283. This study indicated the possibility of the amine group acting as a pharmacophore for tyrosinase inhibition. For kojic acid, it was observed that the compound formed hydrogen bonds with Asn260 and also a π - π interaction with His283.



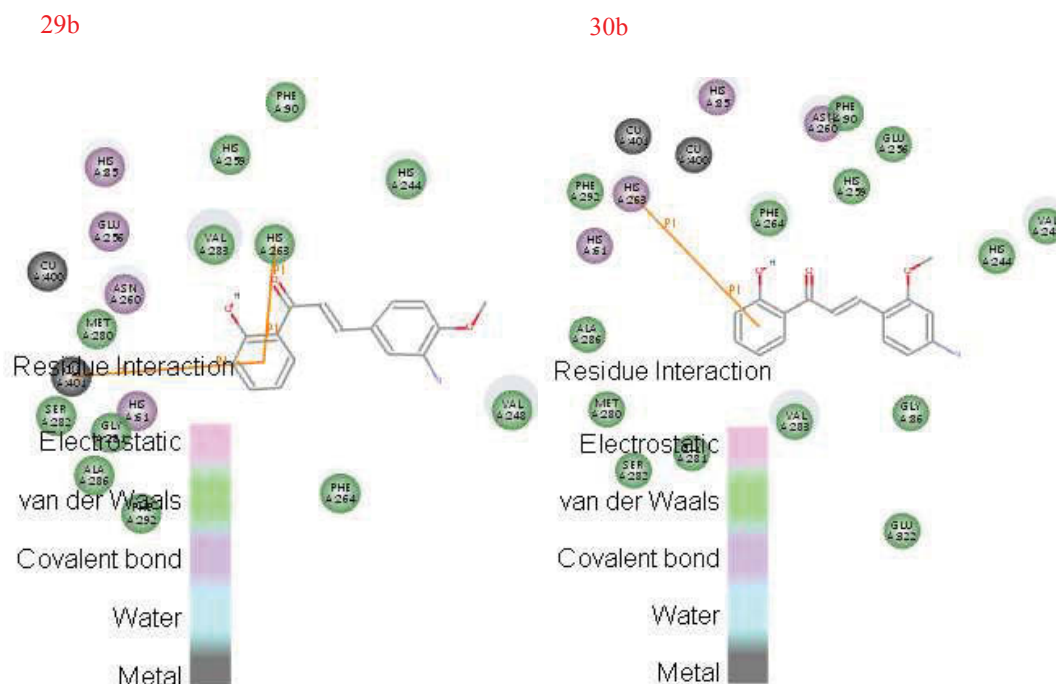


Figure 44 Docking and 2D results of compounds **29b** and **30b** in the tyrosinase catalytic pocket

Ligands **29b** and **30b** were displayed as ball and stick while the core amino acid residues were displayed as stick. The green dotted lines showed the hydrogen bond interactions and the purple lines showed the non-bonding interactions. The ochre balls represented the copper ions.

8.3.4. Effect on melanogenesis

Further studies were done to explore if the compounds **29b** and **30b** that showed good tyrosinase inhibition activity were cytotoxic to B16F10 melanoma cells. The cytotoxicity of these active compounds was estimated by using the MTT assay and the results implied that these compounds were not cytotoxic up to 10 μ M but showed little cytotoxicity at 100 μ M (**Figure 45**).

The melanin content of B16 cells after treatment with compound **29b** in the presence of 100 nM α -melanocyte-stimulating hormone (α -MSH) decreased dose-dependently, showing 215.22% at 1.0 μ M, 182.56% at 5.0 μ M and 123.55% at 10.0 μ M.

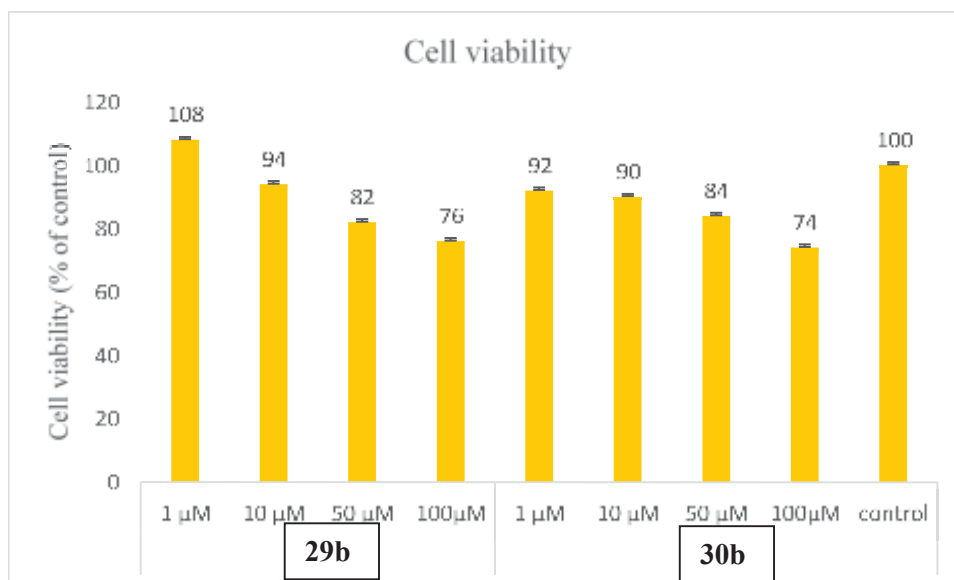


Figure 45 Effect of compounds **29b** and **30b** on cell viability

Data are expressed as a percentage of the control.

Similarly, cells treated with compound **29b**, exhibited melanin contents of 270.18% at 5.0 μ M, 244.11% at 5.0 μ M and 200.05% at 10.0 μ M (**Figure 46**) as compared with 100 nM α -MSH-only-treated group (280.24%) and the control group (100%).

Finally, to examine the mechanisms by which compounds **29b** and **30b** inhibit melanin production, the effect of these compounds on cellular tyrosinase activity in B16F10 melanoma cells treated with 100 nM α -MSH was examined. These compounds effectively diminished tyrosinase activity in a dose-dependent pattern compared to the control (**Figure 47**).

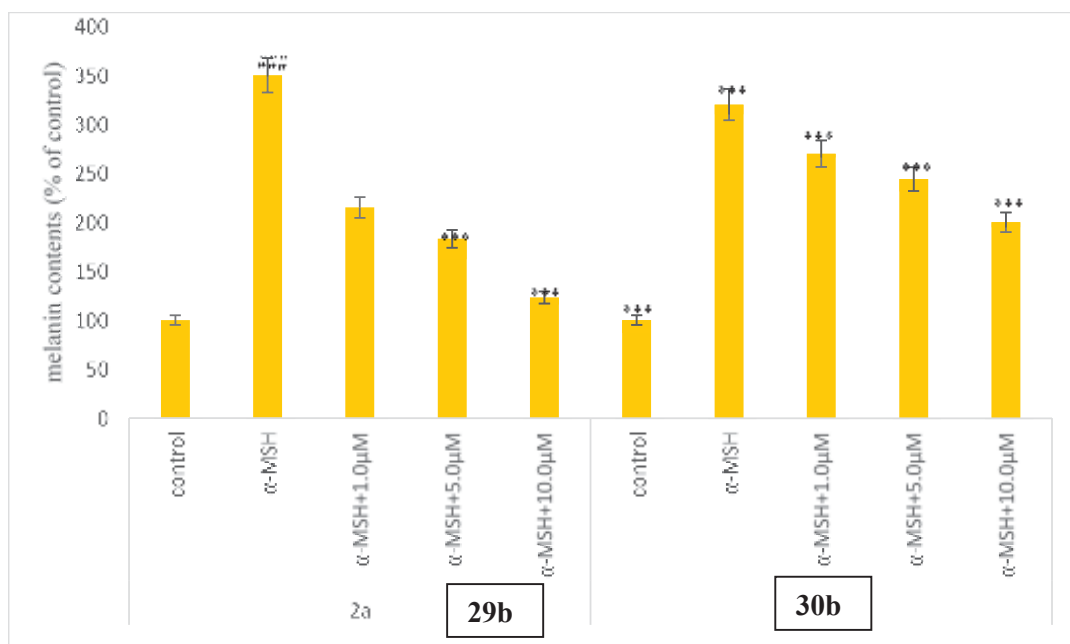


Figure 46 Inhibitory effect of **29b** and **30b** after treatment with 100 nM α-MSH

Melanin contents were measured at 405 nm. Values represent the mean \pm S.E. of three experiments. Data are expressed as a percentage of the control. *** p < 0.001 compared to the group treated with 100nm α-MSH and ### p < 0.001, compared with the untreated control.

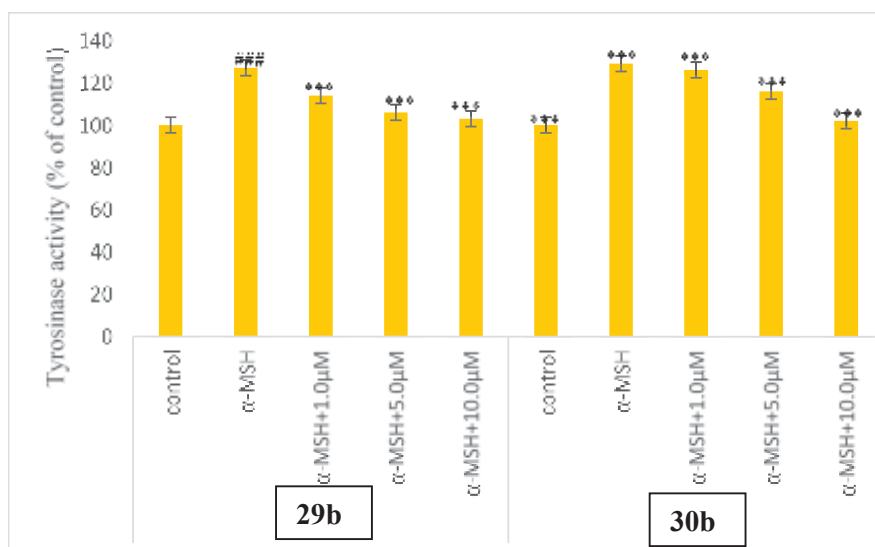


Figure 47 Inhibitory effect of compounds **29b** and **30b** on B16 cells of tyrosinase

Values represented the mean \pm S.E. of three experiments. Data were expressed as a percentage of the control. *** p < 0.001 compared to the group treated with 100nm α-MSH and ### p < 0.001, compared with the untreated control.

These results supported the hypothesis that the inhibitory effect of compounds **29b** and **30b** on melanin biosynthesis should be attributed to inhibition of tyrosinase activity.

8.4. Conclusion

A series of substituted nitrochalcone compounds were synthesized by simple base catalyzed Claisen-Schmidt condensation reaction. The nitro-chalcones were subsequently reduced to their respective amino derivatives by transfer hydrogenation reaction using ammonium formate catalyzed by palladium on carbon. Amongst substituted amino chalcone compounds, compounds **29b** [(2*E*)-3-(3-amino-4-methoxyphenyl)-1-(2-hydroxyphenyl) prop-2-en-1-one] and **30b** [(2*E*)-3-(4-amino-2-methoxyphenyl)-1-(2-hydroxyphenyl) prop-2-en-1-one] were found to be the most active tyrosinase inhibitors with their IC₅₀ values of $9.75 \pm 1.22 \mu\text{M}$ and $7.82 \pm 0.42 \mu\text{M}$, respectively indicating them to be more potent than the reference compound, kojic acid ($22.83 \pm 0.66 \mu\text{M}$). Both **29b** and **30b** were identified as competitive inhibitors of mushroom tyrosinase in a kinetic study.

Docking simulation identified the ligand binding residues that acted as the key determinants to enhance the binding affinity between the inhibitor compounds and the enzyme tyrosinase. *In silico* studies revealed that the formation of a strong intramolecular hydrogen bond formed between the carbonyl oxygen and the hydroxyl hydrogen atom of ring A brought about a substantial decline in tyrosinase inhibitory potential. Thus reduction of nitro compounds to their amino derivatives brought about an increase in hydrogen bonding interactions with the active site of enzyme tyrosinase. In cell based experiments both the compounds **29b** and **30b** showed very effective inhibitions of both melanin production and tyrosinase activity, suggesting amino chalcones to be a promising candidate for use as depigmentation agents in the field of cosmetics or as anti-browning food additives in the field of agriculture.

8.5. References

Benvenuto, JA, Connor, TH, Monteith, DK, Laid-law, JL, Adams, SC, Matney, TS, Theiss, JC 1993, 'Degradation and inactivation of antitumor drugs', *Journal of Pharmaceutical Sciences*, Vol 82, pp. 988–991.

Chen, QX, Song, KK, Qiu, L, Liu, XD, Huang, H, Guo, HY 2005, 'Inhibitory effects on mushroom tyrosinase by p-alkoxybenzoic acids', *Food Chemistry*, Vol 91, pp. 269–274.

Dimmock, J'R, Raghavan, SK, Logan, BM, Bigam, GE 1983, 'Antileukemic evaluation of some Mannich bases derived from 2-arylidene-1, 3-diketones', *European Journal of Medicinal Chemistry*, Vol 18, pp. 248–254.

Lee, KH, Huang, ES, Piantadosi, C, Pagano, J, Geissman, TA 1971, 'Cytotoxicity of sesquiterpene lactones', *Cancer Research*, Vol 31, pp. 1649–1654.

Prasad, YR, Rao, AS, Rambabu, R 2009, 'Synthesis of some 4'-amino chalcones and their anti-inflammatory and antimicrobial activity', *Asian Journal of Chemistry*, Vol 21, pp. 907–914.

Ross, PD, Subramanian, S 1981, 'Thermodynamics of protein association reactions: forces contributing to stability', *Biochemistry*, Vol 20, pp. 3096–3102.

Song, S, Lee, H, Jin, Y, Ha, YM, Bae, S, Chung, HY, Suh, H 2007, 'Syntheses of hydroxy substituted 2-phenyl-naphthalenes as inhibitors of tyrosinase', *Bioorganic and Medicinal Chemistry Letters*, Vol 17, pp. 461–464.

Xia, Y, Yang, ZY, Xia, P, Bastow, KF, Nakanishi, Y, Lee, KH 2000, 'Antitumor agents. Part 202: novel 2'-amino chalcones: design, synthesis and biological evaluation', *Bioorganic and Medicinal Chemistry Letters*, Vol 10, pp. 699–701.

Zhu, YJ, Qiu, L, Zhou, JJ, Guo, HY, Hu, YH, Li, ZC, Wang, Q, Chen, QX, Liu, B 2010, 'Inhibitory effects of hinokitiol on tyrosinase activity and melanin biosynthesis and its antimicrobial activities', *Journal of Enzyme Inhibition and Medicinal Chemistry*, Vol 25, pp. 798–803.

CHAPTER 9

2,3-DIHYDRO-1H-INDEN-1-ONE (1-INDANONE)

CHALCONE -LIKE DERIVATIVES

9.1. Introduction

Indanones are bioactive molecules that are frequently used as precursors in the synthesis of pharmaceutical and natural product substances. Previously, indanone based curcumin analogs were reported to have strong inhibitory effects on tyrosinase (Lee *et al* 1977; Sugimoto 1999). Another indanone derivative, tetrahydrocurcumin, was recommended to be used in cosmetics as a lighting agent (Asawanonda & Klahan 2010).

Although indole and its derivatives were popular medicinal agents, the related heterocycles like indene and their derivatives like substituted 1-indanones (2,3-dihydro-1*H*-inden-1-one) had much less been exploited for their biological potential. Previously the tyrosinase inhibitions of hydroxyazachalcone compounds and hydroxyaminochalcone compounds were studied. Preliminary docking calculations were instrumental to identify the correct conformation of ligands in the binding pocket of a protein and to predict the affinity between the ligand and the protein. The pursuit for a novel template that could possibly act as a potential lead molecule was the impetus to consider synthesizing a series of novel 2,3-dihydro-1*H*-inden-1-one chalcone-like compounds and their hydroxyl derivatives for use as depigmentation agents and as anti-browning food additives.

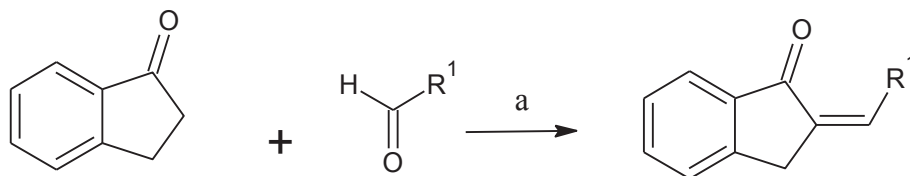
9.2. Experimental

In the first step, 2,3-dihydro-1*H*-inden-1-one chalcone-like compounds were synthesized by the base catalyzed Claisen-Schmidt condensation of 1-indanone and an appropriate ketone in a polar solvent like methanol (**Scheme 8**). Some selected methoxy chalcones were then successfully dealkylated to their corresponding hydroxy compounds in the presence of boron tribromide (BBR₃) (**Scheme 9**).

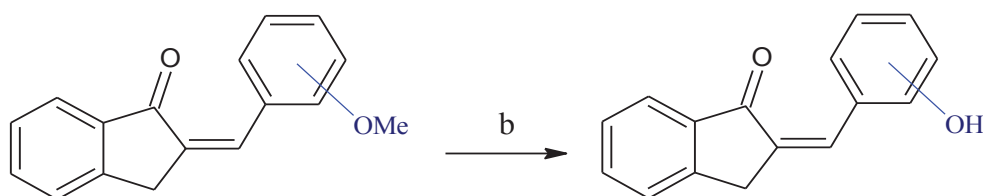
9.2.1. Method for the synthesis of compound **41b**

To a stirred solution of 1-indanone (1 mM, 132 mg) and 2, 4-dimethoxybenzaldehyde (1mM, 166mg) in 25 ml methanol, was added pulverized NaOH (2mM) and the mixture was stirred at room temperature for 4–6 h. The reaction was monitored by TLC using *n*-hexane: ethyl acetate (7:3) as mobile phase. The reaction mixture was cooled to 0°C (ice-water bath) and acidified with HCl (10 % v/v aqueous solution) to afford total precipitation of the compound. A pinkish cream precipitate was formed, which was

filtered and washed with 10 % aqueous HCl solution. The product obtained was recrystallized with ethylacetate to give the pure chalcone product **41a**.



Scheme 8. (General method for synthesis of 2, 3-dihydro-1*H*-inden-1-one chalcones. Reagents and conditions: (a) MeOH, NaOH, 0° C, 24hrs.



Scheme 9. Dealkylation of methoxy chalcones.

Reagents and conditions: (b) BBr₃, CH₂Cl₂

A solution of BBr₃ (5.0 ml) was added to a cooled solution of the chalcone compound **41a** (1mmol, 280mg) in CH₂Cl₂ under argon. The cooling bath was removed and the dark solution was warmed to RT and stirred for 1-5hrs. The dark solution was then poured into ice water and filtered. The aqueous layer was extracted with chloroform twice. The organic extract was washed with water followed by brine and dried over anhydrous sodium sulphate. This was then rotary evaporated to give the respective hydroxy derivative **41b**.

9.2.2. Spectral data

37a. (2*Z*)-2-(3-nitrobenzylidene)-2,3-dihydro-1*H*-inden-1-one. Yield: 92%; Mp: 118–120°C; ¹H NMR (500 MHz, CDCl₃): δ 8.54 (s, 1H, H-2'), 8.26 (d, 1H, H-4', *J*=16.0), 8.24 (d, 1H, H-6', *J*=8.0), 7.94 (d, 1H, *J* = 11.0), 7.69 (dd, 1H, H-3, *J* = 9.5), 7.61 (t, 1H, H-4, *J* = 10.0), 7.52 (t, 1H, H-5', *J*=7.5), 7.48 (dd, 1H, H-6, *J* = 9.0), 7.46 (dd, 1H, H-5, *J* = 6.8, 8.5), 4.12 (s, 2H, H-8); ¹³C NMR (125 MHz, DMSO-*d*₆) δ 208.1 (C=O), 138.9 (C2), 123.4 (C3), 126.8 (C4), 133.5 (C5), 126.2 (C6), 155.2 (C7), 26.2 (C8), 36.8 (C9), 122.4 (vinylic), 137.5 (C1'), 123.8 (C2'), 149.3 (C3'), 128.2 (C4'), 130.4 (C5'),

134.6 (C6'); IR (KBr) ν (cm⁻¹): 2962, 2935, 1700, 1596, 1521, 1357, 1244, 1205, 1210, 1146, 829; MS (ESI): 266.1 ([M + H])⁺.

38a. (2Z)-2-(4-nitrobenzylidene)-2,3-dihydro-1*H*-inden-1-one. Yield: 79%; M.p: 133–135°C). ¹H NMR (500 MHz, CDCl₃); δ 8.39 (dd, 2H, H-3' & H-5', *J* = 10.5), 8.10 (dd, 2H, *J* = 7.5, 9.5, H-2' & H-6'), 7.92 (d, 1H, *J* = 10.5), 7.64 (dd, 1H, H-4, *J* = 7.4, 9.5), 7.62 (dd, 1H, H-3, *J* = 6.8, 9.5), 7.49 (dd, 1H, H-6, *J* = 7.0, 9.5), 7.46 (dd, 1H, H-5, *J* = 6.3, 8.0), 3.89 (s, 2H, H-8); ¹³C NMR (125 MHz, DMSO-d₆) δ 206.4 (C=O), 138.3 (C2), 125.2 (C3), 128.8 (C4), 135.7 (C5), 122.2 (C6), 154.3 (C7), 28.2 (C8), 37.3 (C9), 127.6 (vinylic), 140.2 (C1'), 130.2 (C2' & C6'), 124.5 (C3' & C5'), 151.2 (C4'), 127.4 (vinylic); IR (KBr) ν (cm⁻¹): 2981, 2931, 1702, 1589, 1354, 1239, 1205, 1209, 1134, 832, 702; MS (ESI): 266.1 ([M + H])⁺.

39a. (2Z)-2-(2-methoxy-4-nitrobenzylidene)-2, 3-dihydro-1*H*-inden-1-one. Yield: 74%; M.p: 113–115°C). ¹H NMR (500 MHz, CDCl₃); δ 8.17 (s, 1H), 7.96 (d, 1H, *J* = 11.5), 7.94 (m, 1H, H-6', *J* = 8.0), 7.79 (d, 1H, H-5', *J* = 10.5), 7.70 (dd, 1H, H-4, *J* = 7.2, 9.5), 7.68 (dd, 1H, H-3, *J* = 6.9, 8.5), 7.54 (dd, 1H, H-6, *J* = 10.0, 10.5), 7.52 (dd, 1H, H-5, *J* = 7.7, 8.0), 3.86 (s, 2H, H-8); ¹³C NMR (125 MHz, DMSO-d₆) δ 202.6 (C=O), 140.4 (C2), 125.7 (C3), 128.2 (C4), 136.7 (C5), 124.2 (C6), 150.5 (C7), 30.2 (C8), 36.8 (C9), 134.0 (C1'), 116.2 (C2'), 112.2 (C3'), 138.2 (C4'), 125.3 (C5'), 118.2 (C6'), 129.2 (vinylic); IR (KBr) ν (cm⁻¹): 2965, 2928, 2860, 1700, 1565, 1352, 1250, 1209, 1124, 872, 715; HRMS *m/z*: 296.0917 ([M + H])⁺; Calcd: 296.0923.

40a. (2Z)-2-(4-methoxy-3-nitrobenzylidene)-2, 3-dihydro-1*H*-inden-1-one. Yield: 68%; M.p: 123–125°C). ¹H NMR (500 MHz, CDCl₃); δ 8.10 (s, 1H), 7.92 (d, 1H, *J* = 12.5), 7.72 (dd, 1H, H-4, *J* = 9.0), 7.65 (d, 1H, H-5', *J* = 9.5), 7.64 (dd, 1H, H-3, *J* = 7.6, 9.5), 7.57 (dd, 1H, H-5, *J* = 8.0, 8.5), 7.54 (dd, 1H, H-6, *J* = 8.2, 10.0), 7.50 (d, 1H, H-6', *J* = 8.0), 3.86 (s, 3H), 3.84 (s, 2H, H-8); ¹³C NMR (125 MHz, DMSO-d₆) δ 199.8 (C=O), 140.2 (C2), 127.1 (C3), 128.2 (C4), 136.5 (C5), 124.0 (C6), 150.1 (C7), 34.1 (C8), 36.5 (C9), 126.9 (C1'), 120.5 (C2'), 137.2 (C3'), 147.5 (C4'), 112.4 (C5'), 114.2 (C6'), 56.6 (Me), 122.4 (vinylic); IR (KBr) ν (cm⁻¹): 2971, 2918, 2860, 1702, 1555, 1364, 1250, 1210, 1134, 802; HRMS *m/z*: 296.0914 ([M + H])⁺; Calcd: 296.0923.

41a. (2Z)-2-(2,4-dimethoxybenzylidene)-2, 3-dihydro-1*H*-inden-1-one. Yield: 62%; M.p: 80–82°C). ¹H NMR (500 MHz, CDCl₃); δ 7.97 (d, 1H, *J* = 12.0), 7.74 (d, 1H, *J* = 8.5), 7.72 (d, 1H, *J* = 15.5, H-5'), 7.70 (dd, 1H, H-4, *J* = 8.0, 10.0), 7.59 (dd, 1H, H-6, *J* = 7.4, 9.5), 7.56 (dd, 1H, H-3, *J* = 6.9, 9.0), 7.54 (dd, 1H, H-5, *J* = 6.2, 8.5), 6.46 (d,

1H, H-6', $J=7.5$), 6.42 (s, 1H, H-3'), 3.86 (s, 2H, H-8), 3.90 (s, 3H, Me), 3.82 (s, 3H, Me); ^{13}C NMR (125MHz, DMSO- d_6) δ 200.6 (C=O), 142.2 (C2), 127.5 (C3), 130.4 (C4), 136.4 (C5), 124.9 (C6), 149.7 (C7), 36.2 (C8), 36.6 (C9), (C5'), 122.9 (vinylic), 144.5 (vinylic), 165.88 (C4'), 163.1 (C6'), 108.1 (C3'), 129.1 (C2'), 120.9 (C1'), 58.1 (O-CH₃); IR (KBr) ν (cm⁻¹); 3017, 2954, 2925, 2855, 1695, 1669, 1504, 1265, 1245, 1176, 819, 712; MS (ESI): 281.1([M + H])⁺.

42a. (2*Z*)-2-(3,4-dimethoxybenzylidene)-2, 3-dihydro-1*H*-inden-1-one. Yield: 59%; M.p: 109–111°C). ^1H NMR(500 MHz, CDCl₃); δ 7.94 (d, 1H, $J=11.0$), 7.74 (dd, 1H, H-4, $J=9.0$), 7.60 (dd, 1H, H-6, $J=8.5$), 7.54 (dd, 1H, H-5, $J=6.0, 8.5$), 7.49 (dd, 1H, H-3, $J=7.4, 8.0$), 7.46 (dd, 1H, H-6', $J=7.7, 9.5$), 7.39 (s, 1H, H-2'), 6.99 (d, 1H, H-5', $J=8.5$), 3.98 (s, 3H), 3.95 (s, 3H), 3.89 (s, 2H, H-8); ^{13}C NMR (125 MHz, DMSO- d_6) δ 204.2 (C=O), 144.5 (vinylic), 140.6 (C2), 124.5 (C3), 129.4 (C4), 136.2 (C5), 122.6 (C6), 147.7 (C7), 37.6 (C8), 36.5 (C9), 130.2 (C1'), 112.6 (C2'), 148.3 (C3'), 156.2 (C4'), 107.2 (C5'), 128.6 (C6'); IR (KBr) ν (cm⁻¹); 3024, 2957, 2920, 2834, 1700, 1650, 1535, 1268, 1150, 824, 715; MS (ESI): 281.1([M + H])⁺.

43a. (2*Z*)-2-(3,5-dimethoxybenzylidene)-2, 3-dihydro-1*H*-inden-1-one. Yield: 68%; M.p: 128–130°C). ^1H NMR (500 MHz, CDCl₃); δ 7.89 (d, 1H, $J=12.5$), 7.79 (dd, 1H, H-4, $J=10.0$), 7.64 (dd, 1H, H-6, $J=6.9, 8.0$), 7.57 (dd, 1H, H-5, $J=8.0, 9.5$), 7.52 (dd, 1H, H-3, $J=6.4, 8.5$), 7.06 (dd, 2H, H-2' & H-6', $J=7.4, 9.0$), 6.79 (d, 1H, H-4', $J=7.5$), 3.88 (s, 3H), 3.90 (s, 3H), 3.80 (s, 2H, H-8); ^{13}C NMR (125 MHz, DMSO- d_6) δ 207.1 (C=O), 140.2 (vinylic), 140.6 (C2), 124.5 (C3), 139.4 (C4), 129.2 (C5), 120.4 (C6), 145.2 (C7), 35.2 (C8), 36.2 (C9), 130.2 (C1'), 112.6 (C2'), 148.3 (C3'), 106.2 (C4'), 147.2 (C5'), 128.6 (C6'); IR (KBr) ν (cm⁻¹); 3064, 3017, 2954, 2749, 2729, 1678, 1652, 1522, 1265, 835, 722; MS (ESI): 281.1([M + H])⁺.

41b. (2*Z*)-2-(2,4-dihydroxybenzylidene)-2, 3-dihydro-1*H*-inden-1-one. Yield: 59%; M.p: 162–164°C). ^1H NMR (500 MHz, CDCl₃); δ 10.54 (s, OH), 9.70 (s, OH), 7.92 (d, 1H, $J=11.5$), 7.72 (dd, 1H, H-4, $J=9.0$), 7.65 (dd, 1H, H-6, $J=8.0$), 7.49 (dd, 1H, H-5, $J=6.4, 8.0$), 7.47 (dd, 1H, H-3, $J=8.5$), 7.32 (dd, 1H, H-6', $J=7.9, 10.0$), 7.22 (s, 1H, H-3'), 6.95 (d, 1H, H-5', $J=7.5$), 3.80 (s, 2H, H-8); ^{13}C NMR (125 MHz, DMSO- d_6) δ 206.2 (C=O), 142.6 (vinylic), 138.6 (C2), 126.5 (C3), 132.4 (C4), 130.2 (C5), 122.2 (C6), 145.6 (C7), 38.1 (C8), 36.9 (C9), 130.6 (C1'), 149.4 (C2'), 125.3 (C3'), 154.2 (C4'), 105.2 (C5'), 130.6 (C6'); IR (KBr) ν (cm⁻¹); 3600, 3330, 2657, 2824, 2764, 1655, 1596, 1505, 1248, 780, 631; HRMS m/z : 253.0865 ([M + H])⁺; Calcd: 253.0861.

42b. (2*Z*)-2-(3,4-dihydroxybenzylidene)-2, 3-dihydro-1*H*-inden-1-one. Yield: 56%; M.p: 149–151°C). ¹H NMR (500 MHz, CDCl₃); δ 10.45 (s, OH), 9.76 (s, OH), 7.89 (d, 1H, *J* = 10.0), 7.70 (dd, 1H, H-4, *J* = 6.9, 9.5), 7.67 (dd, 1H, H-6, *J* = 6.5, 8.0), 7.52 (dd, 1H, H-5, *J* = 8.5), 7.44 (dd, 1H, H-3, *J* = 6.2, 8.5), 7.36 (dd, 1H, H-6', *J* = 9.0), 7.28 (s, 1H, H-2'), 6.94 (d, 1H, H-5', *J* = 9.5), 3.82 (s, 2H, H-8); ¹³C NMR (125 MHz, DMSO-*d*₆) δ 206.2 (C=O), 142.6 (vinylic), 138.6 (C2), 126.5 (C3), 130.4 (C4), 132.2 (C5), 124.2 (C6), 145.6 (C7), 37.2 (C8), 36.8 (C9), 130.6 (C1'), 114.4 (C2'), 145.3 (C3'), 152.2 (C4'), 107.2 (C5'), 128.6 (C6'); IR (KBr) ν (cm⁻¹); 3600, 3330, 2657, 2824, 2764, 1655, 1596, 1505, 1248, 780, 631; HRMS *m/z*: 253.0865 ([*M* + *H*])⁺; Calcd: 253.0859.

43b. (2*Z*)-2-(3,5-dihydroxybenzylidene)-2, 3-dihydro-1*H*-inden-1-one. Yield: 50%; M.p: 158–160°C). ¹H NMR (500 MHz, CDCl₃); δ 10.50 (s, OH), 9.70 (s, OH), 7.87 (d, 1H, *J* = 10.5), 7.75 (dd, 1H, H-4, *J* = 6.5, 8.5), 7.69 (dd, 1H, H-6, *J* = 7.2, 8.5), 7.57 (dd, 1H, H-5, *J* = 6.8, 9.0), 7.54 (dd, 1H, H-3, *J* = 7.5), 7.24 (dd, 2H, H-2' & H-6', *J* = 8.2, 10.0), 6.72 (d, 1H, H-4', *J* = 10.0), 3.82 (s, 2H, H-8); ¹³C NMR (125 MHz, DMSO-*d*₆) δ 202.8 (C=O), 139.9 (vinylic), 138.2 (C2), 127.5 (C3), 130.2 (C4), 132.6 (C5), 124.2 (C6), 148.6 (C7), 39.1 (C8), 38.8 (C9), 132.2 (C1'), 116.4 (C2'), 145.2 (C3'), 122.2 (C4'), 147.2 (C5'), 127.6 (C6'); IR (KBr) ν (cm⁻¹); 3585, 3259, 2650, 2875, 2735, 1685, 1550, 1275, 1252, 745, 712; HRMS *m/z*: 253.0865 ([*M* + *H*])⁺; Calcd: 253.0860.

9.3. Results and Discussion

9.3.1. Chemistry and inhibition kinetics

In terms of the structure- activity relationships, compound **42b** ((2*Z*)-2-(3, 4-dihydroxybenzylidene)-2, 3-dihydro-1*H*-inden-1-one) exhibited the most potent tyrosinase inhibitory activity with inhibition of 74.6%. This could be accounted to the presence of a 3, 4-dihydroxy group in the B-ring that showed structural resemblance with the substrate, L-DOPA.

Compound **41b** with an ortho-para dihydroxy substitution on ring B showed an inhibition of 65.2% at 50 μM. The inhibition of both compounds **41b** and **42b** was seen to be greater than the positive control kojic acid which exhibited 45.2% inhibition at 50 μM. The inhibitory activities of these newly synthesized compounds were compared to that of kojic acid as a reference standard and the results are shown in **Table 16**.

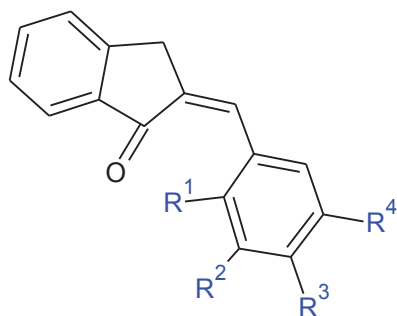


Table 16 Substitution Pattern and Inhibition Effects of 1-indanonechalcones

Compound	R ¹	R ²	R ³	R ⁴	Yield (%)	Inhibition rate (%) at 50 μ M
36a	H	NO ₂	H	H	95.5	22.6 \pm 0.44
37a	H	H	NO ₂	H	87.6	19.8 \pm 0.15
38a	OMe	H	NO ₂	H	64.2	25.4 \pm 0.55
39a	H	NO ₂	OMe	H	54.1	24.2 \pm 0.33
40a	OMe	H	OMe	H	85.4	30.6 \pm 0.47
41a	H	OMe	OMe	H	77.2	32.2 \pm 0.11
42a	H	OMe	H	OMe	70.3	38.6 \pm 0.32
41b	OH	H	OH	H	51.2	65.2 \pm 0.15
42b	H	OH	OH	H	45.2	74.6 \pm 0.14
43b	H	OH	H	OH	42.6	50.1 \pm 0.38
Kojic acid						49.2 \pm 0.22

Results indicated that both compounds **41b** and **42b** could inhibit the diphenolase activity of tyrosinase in a dose-dependent manner. With increasing concentrations of inhibitors, the remaining enzyme activity decreased exponentially. The IC₅₀ for compounds **41b** and **42b** was estimated to be 12.3 μ M and 8.2 μ M, respectively (**Figure 48**).

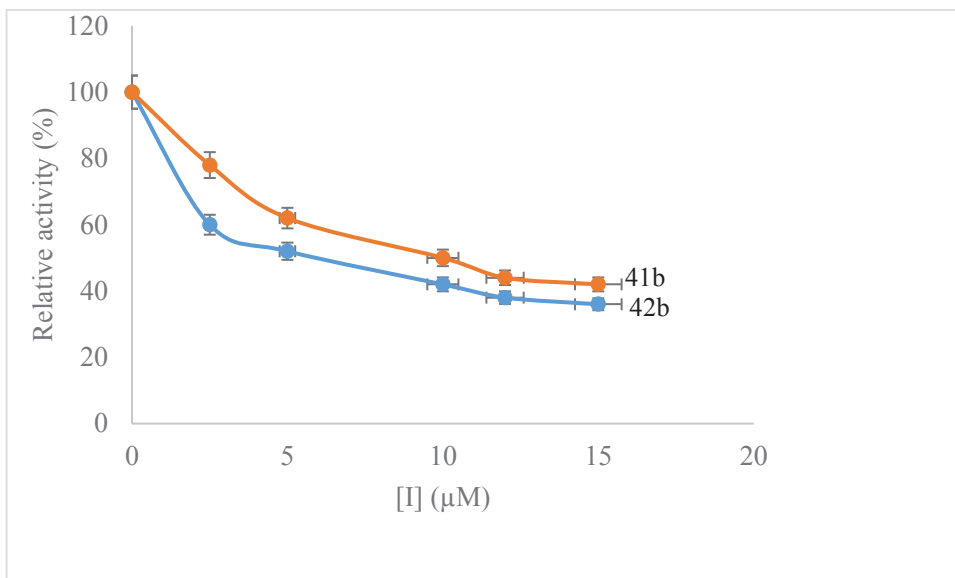


Figure 48 Inhibition effects of compounds **41b** and **42b**

Data were presented as means (n = 3).

The plots of the remaining enzyme activity versus the concentration of enzyme at different inhibitor concentrations gave a family of straight lines, which all passed through the origin. The presence of inhibitor did not reduce the amount of enzyme, but just resulted in the inhibition of enzyme activity. The results showed that both the compounds **41b** and **42b** were reversible inhibitors of mushroom tyrosinase for oxidation of L-DOPA (**Figure 49**).

Previous studies have recognized potent inhibitory effect of chalcones with hydroxyl groups on tyrosinase (Yan *et al* 2009; Yamazaki *et al* 2009; Kanade *et al* 2007; Kim *et al* 2006; Shiino, Watanabe & Umezawa 2001; Shiino, Watanabe & Umezawa 2003; Yokota *et al* 1998). The hydroxyl groups in compounds carried out the nucleophilic attack on the coppers of tyrosinase active site and were directly involved in transferring protons during catalysis, which resulted in inactivation of tyrosinase (Muñoz-Muñoz *et al* 2008; Espin *et al* 2000). Furthermore, results indicated that electron-donating groups contributed more to the inhibitory activity of the compounds on mushroom tyrosinase than the electron-withdrawing groups. Electron donating groups (*e.g.* -OMe, -OH) on the atoms adjacent to the π system activated the aromatic ring by increasing the electron density on the ring through a resonance donating effect.

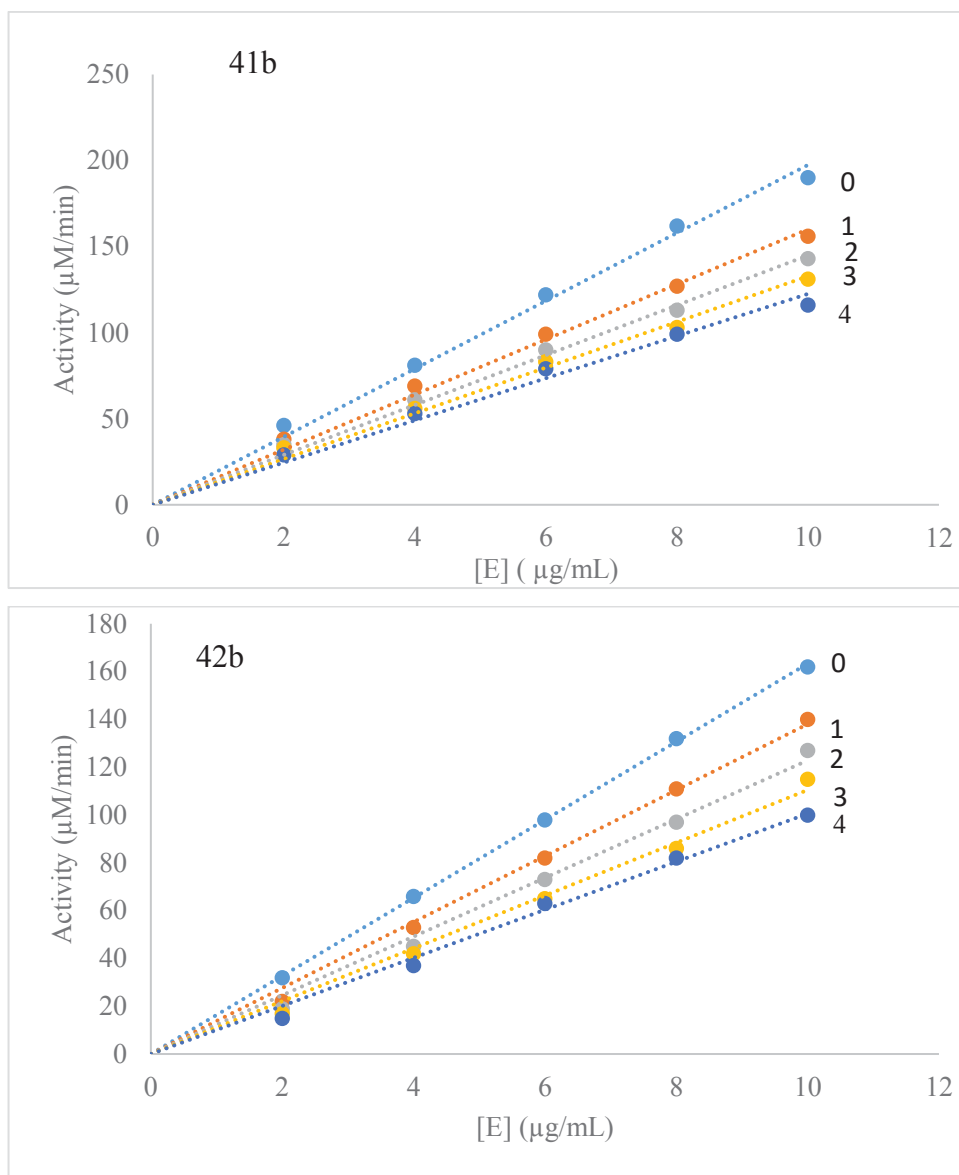


Figure 49 Inhibitory mechanism of compounds **41b** and **42b**

The concentration of inhibitor used for curves 0-4 are 0, 0.25, 0.5, 1.0 and 2.0 μM , respectively.

In this study, the tyrosinase inhibitory activities of compounds **41b** and **42b** were investigated in detail. The reaction rates were measured in the presence of active inhibitors with various concentrations of L-DOPA as a substrate. As the concentrations of active inhibitors **41b** and **42b** increased, K_m values gradually increased, but V_{\max} values did not change, thereby indicating the inhibitors to act as competitive inhibitors of mushroom tyrosinase (**Figure 50**).

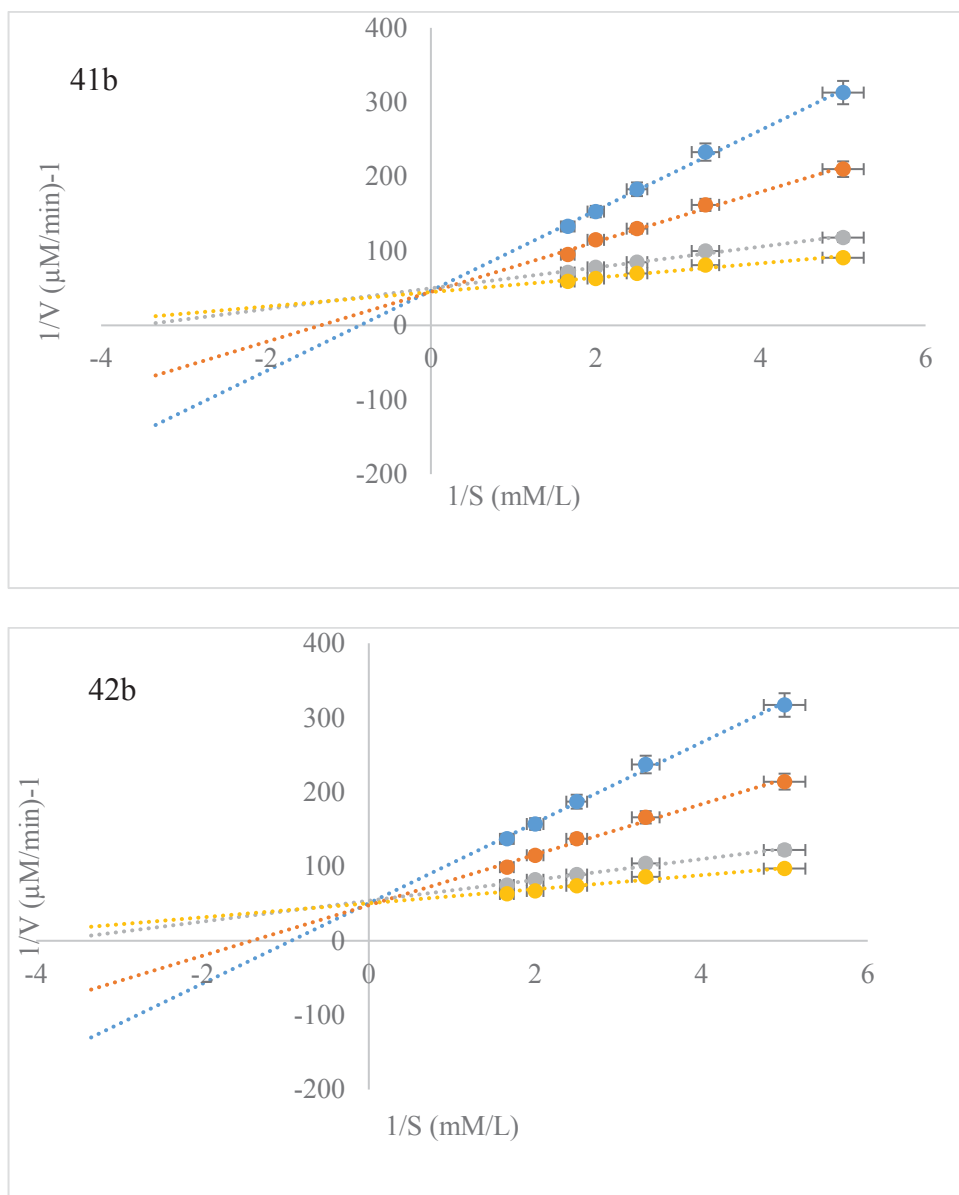


Figure 50 Lineweaver Burk plot for inhibition of compounds **41b** and **42b**

Data were obtained as mean values of $1/V$, the inverse of the absorbance increase at a wavelength of 492nm per min of three independent tests with different concentrations of L-DOPA as a substrate. The concentration of compounds **41b** and **42b** from top to bottom is 20 μM , 5 μM , 1.25 μM and 0 μM , respectively.

The inhibition kinetics were illustrated by Dixon plots, which were obtained by plotting $1/V$ versus $[I]$ with varying concentrations of substrate. Dixon plots gave a family of straight lines passing through the same point at the second quadrant, giving the inhibition constant (K_i) (**Figure 51**).

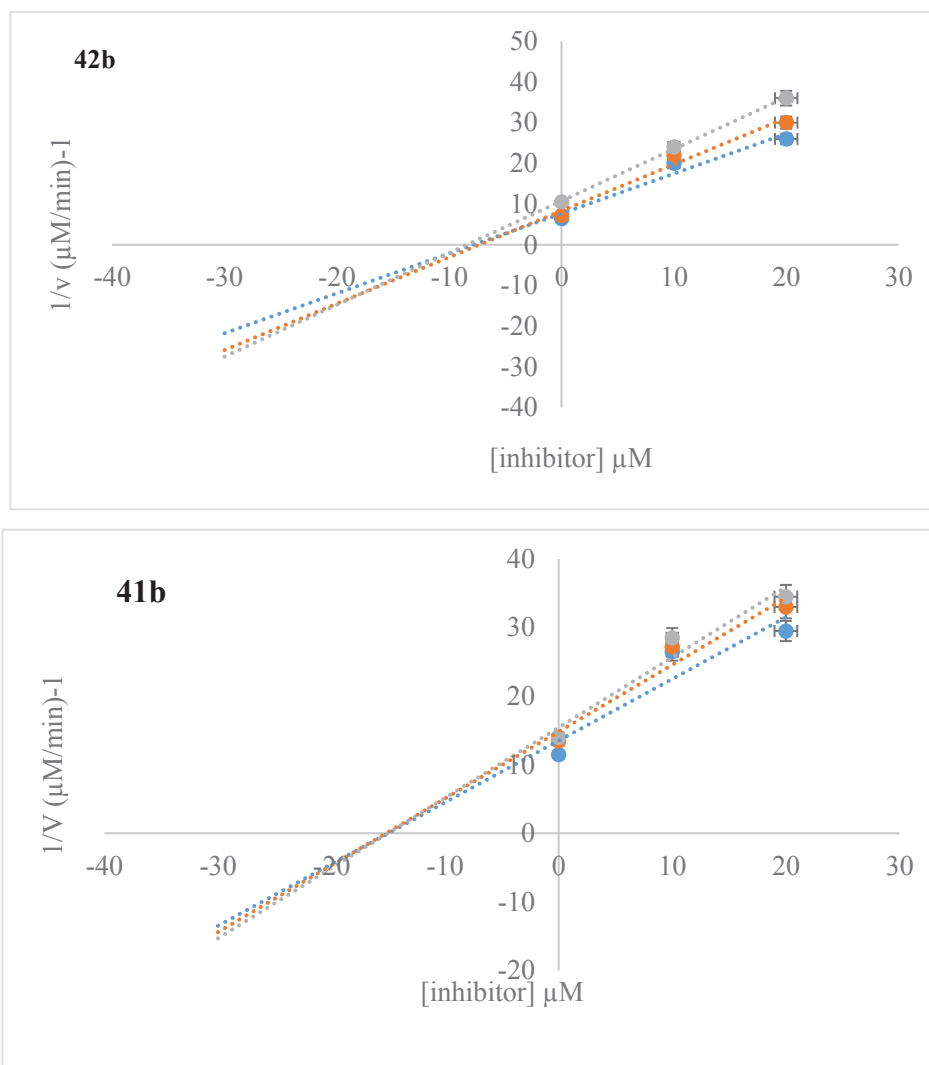


Figure 51 Dixon plot for the inhibitory effect of compounds 41b and 42b

The inhibitor concentrations were 0, 10 μM and 20 μM , respectively. The L-DOPA concentrations were 200, 400 and 600 μM .

The K_i value for the compounds **41b** and **42b** estimated from this Dixon plot was 10.3 μM and 8.7 μM , respectively. A comparison of the K_i values of the compounds with that of kojic acid revealed that they possess much higher affinity to tyrosinase than kojic acid (**Table 17**).

Table 17 Effect on tyrosinase activity and kinetic analysis of compounds

Compound	Type of inhibition	IC_{50} (μM)	RA*	K_i (μM) [#]
41b	Competitive	12.3 ± 0.22	2.23F	10.3
42b	Competitive	8.2 ± 0.44	3.35F	8.7
Kojic acid	Competitive	27.5 ± 0.56		12.2

[#]: Values were measured at 5 μM of active compounds and K_i is the (inhibitor constant). *: RA is the relative inhibitory activity compared to the standard kojic acid where 1.0F means one-time activity of kojic acid.

9.3.2. *In silico* docking studies

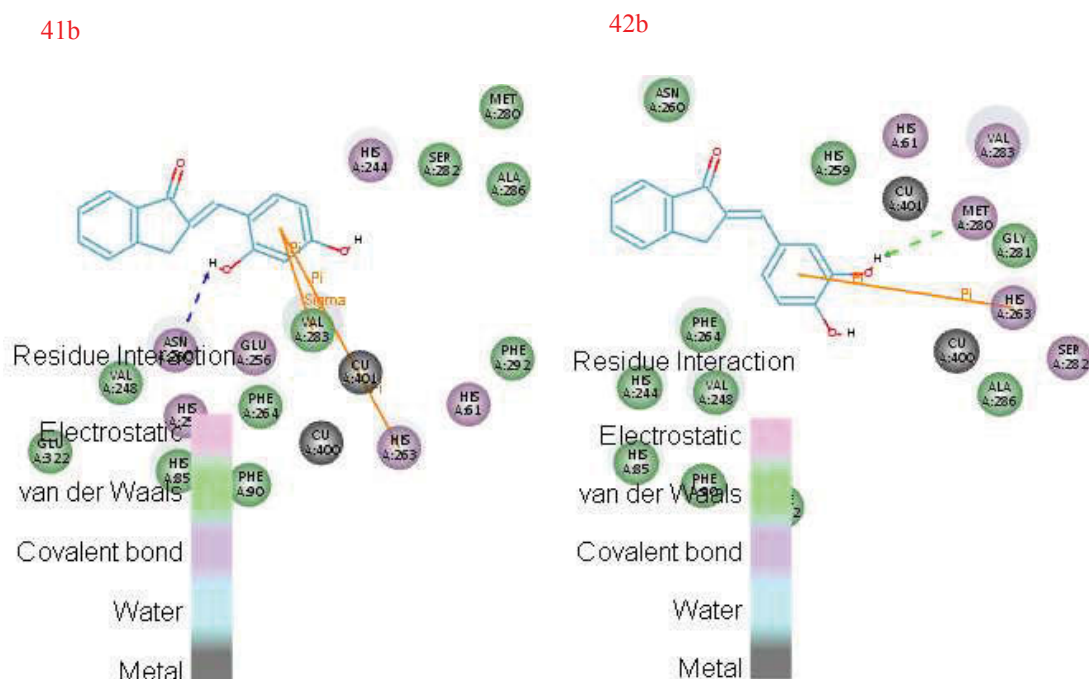
Further, the experimental results obtained were integrated with computational simulation methods to obtain a relative insight into the molecular mechanisms governing the mode of inhibition. Accelrys Discovery Studio 4.5 suite was utilized to simulate binding between the active site of mushroom tyrosinase and substituted 2, 3-dihydro-1*H*-inden-1-one chalcone-like compounds. **Figure 52** shows selected docked conformations of compounds **41b** & **42b** in the tyrosinase binding site. The docking simulation results supported the hypothesis that the binding affinities of both these compounds were higher than kojic acid, which was used as a control compound. The docking score for ligand-to-receptor binding included terms for electrostatic, van der Waals, and solvation energies. Additionally, hydrogen bonding interactions were monitored between mushroom tyrosinase and the inhibitor compounds (**Table 18**).

Table 18 Docking results of active indanone chalcone-like compounds

Compound	CDOCKER			
	energy (kcal/mol)	Type of interactions	Donor-acceptor	Distance (Å)
41b	-22.35	H-bonding	OH...O (Asn280)	1.96
		H-bonding	(His85) Hδ ₂ ... OH	2.93
		hydrophobic π-σ	ring B...Val283	2.72
		hydrophobic π-π stacking	ring B...His263	4.09
42b	-19.25	H-bonding	OH...O (Met280)	2.48
		hydrophobic π-π stacking	ring B...His263	4.07
		hydrophobic π-σ	ring B...Val283	2.75

Compounds **41b** & **42b** formed hydrogen bonds with amino-acid residues in the tyrosinase catalytic pocket. The 2-OH group in compound **41b** was actively involved in hydrogen bonding with the carboxylate oxygen of Asn280 and with the hydrogen atom of His85 at distances of 1.96 Å and 2.93 Å, respectively. Compound **42b** had a catechol moiety and hence had at least 1-OH group with low dissociation energy which could easily donate a hydrogen atom. The 3-OH group of compound **42b** formed a relatively weak hydrogen bond (2.48 Å) with the carboxylate oxygen of Met280. The residues had a key function and effect on binding affinity. It was noteworthy that replacement of 2'-

OH phenyl group in ring A with a 1'-indanone ring brought about a significant decline in tyrosinase inhibitory activity. Adding the ligand led to π - π interactions with the enzyme thereby enhancing drug permeability. Hydrophobic π - π stacking interactions were seen with His263 and ring B of the chalcone whereas the N-H proton in Ser282 and in Val283 pointing directly at a phenyl ring in a hydrogen bond led to amide- π interactions. According to the docking program, the binding residues interacting with kojic acid were Met280, Val283, Asn260 and Gly281 of tyrosinase.



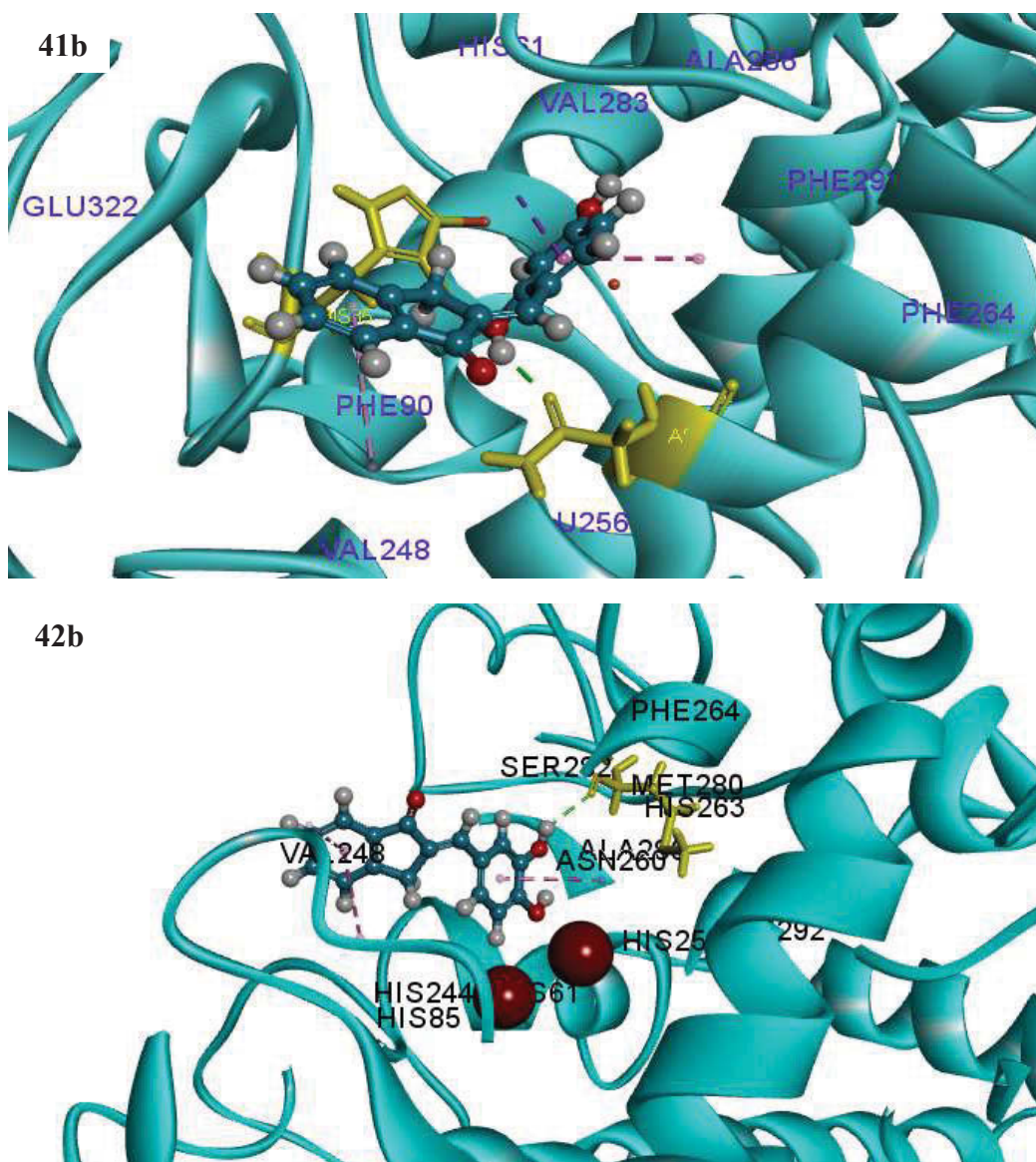


Figure 52 Docking and 2D results of compounds **41b** and **42b** in the tyrosinase pocket

Ligands **41b** and **42b** were displayed as ball and stick while the core amino acid residues were displayed as stick.

This indicated that the dealkylated derivatives of 2,3-dihydro-1*H*-inden-1-one chalcone-like compounds inhibited tyrosinase activity by binding at the active site of mushroom tyrosinase.

9.4. Conclusion

To summarize, novel 2,3-dihydro-1H-inden-1-one (1-indanone) chalcone-like compounds and their hydroxy derivatives were synthesized, and their inhibition on the diphenolase activity of mushroom tyrosinase was studied. Hydroxy substituted 1-indanone chalcone-like compounds **41b** and **42b** were found to be significantly more potent than kojic acid with their IC₅₀ values of 12.3 μ M and 8.2 μ M, respectively. Both the compounds exhibited reversible competitive inhibition. Compound **41b** with a 3,4-dihydroxy group in the B-ring had structural resemblance to the substrate L-DOPA. This led to the competitive displacement of L-DOPA from the active site of the enzyme tyrosinase in a lock-and key model. In addition, the presence of the hydroxy group at the 4- position (ring B) was indispensable for significant tyrosinase inhibition in this class of compounds. These preliminary findings justified pursuing further work on hydroxy substituted 1-indanone chalcone-like compounds to serve as a potential scaffold for the future development of active tyrosinase inhibitors.

9.5. References

Asawanonda, P, Klahan, SO 2010, 'Tetrahydrocurcuminoid cream plus targeted narrowband UVB phototherapy for vitiligo: a preliminary randomized controlled study', *Photomedicine and Laser Surgery*, Vol 28, pp. 679–684.

Espin, JC, Varon, R, Fenoll, LG, Gilabert, MA, Garcia-Ruiz, PA, Tudela, J, Garcia-Canovas, F 2000, 'Kinetic characterization of the substrate specificity and mechanism of mushroom tyrosinase', *European Journal of Biochemistry*, Vol 267, pp. 1270–1279.

Kanade, SR, Suhas, VL, Chandra, N, Gowda, LR 2007, 'Functional interaction of diphenols with polyphenol oxidase. Molecular determinants of substrate/inhibitor specificity', *FEBS Journal*, Vol 274, pp. 4177–4187.

Kim, D, Park, J, Kim, J, Han, C, Yoon, J, Kim, N, Seo, J, Lee, C 2006, 'Flavonoids as mushroom tyrosinase inhibitors: a fluorescence quenching study', *Journal of Agricultural and Food Chemistry*, Vol 54, pp. 935–941.

Lee, KH, Hall, IH, Mar, EC, Starnes, CO, Elgebaly, SA, Waddell, TG, Hadgraft, RI, Ruffner, CG, Weidner, I 1977, 'Antitumor agents. 20. Sesquiterpene antitumor agents-inhibitors of cellular metabolism', *Science*, Vol 196, pp. 533–536.

Muñoz-Muñoz, JL, Garcia-Molina, F, Garcia-Ruíz, PA, Molina-Alarcon, M, Tudela, J, Garcia-Canovas, F, Rodriguez-Lopez, JN 2008, 'Phenolic substrates and suicide inactivation of tyrosinase: kinetics and mechanism', *Biochemistry Journal*, Vol 416, pp. 431–440.

Radhakrishnan, SK, Shimmon, R, Conn, C, Baker, AT 2015, 'Azachalcones: A new class of potent polyphenol oxidase inhibitors', *Bioorganic and Medicinal Chemistry Letters*, Vol 25, pp. 1753–1756.

Shiino, M, Watanabe, Y, Umezawa, K 2001, 'Synthesis of N-substituted N-nitrosohydroxylamines as inhibitors of mushroom tyrosinase', *Bioorganic and Medicinal Chemistry*, Vol 9, pp. 1233–1240.

Shiino, M, Watanabe, Y, Umezawa, K 2003, 'Synthesis and tyrosinase inhibitory activity of novel N-hydroxybenzyl-N-nitrosohydroxylamines', *Bioorganic Chemistry*, Vol 31, pp.129–135.

Sugimoto, H 1999, 'Structure-activity relationships of acetylcholinesterase inhibitors: Donepezil hydrochloride for the treatment of Alzheimer's disease', *Pure and Applied Chemistry*, Vol 71, pp. 2031–2037.

Yamazaki, Y, Kawano, Y, Yamanaka, A, Maruyama, S 2009, 'N-[(Dihydroxyphenyl)acyl] serotoninins as potent inhibitors of tyrosinase from mouse and human melanoma cells', *Bioorganic and Medicinal Chemistry Letters*, Vol 19, pp. 4178–4182.

Yan, Q, Cao, R, Yi, W, Yu, L, Chen, Z, Ma, L, Song, H 2009, 'Synthesis and evaluation of 5-benzylidene(thio)barbiturate-beta-D-glycosides as mushroom tyrosinase inhibitors', *Bioorganic and Medicinal Chemistry Letters*, Vol 19, pp. 4055–4058.

Yokota, T, Nishio, H, Kubota, Y, Mizoguchi, M 1998, 'The inhibitory effect of glabridin from licorice extracts on melanogenesis and inflammation', *Pigment Cell Research*, Vol 11, pp. 355–361.

CHAPTER 10

CHALCONE OXIMES

(2'-acetylpyridinyl derivatives)

10.1. Introduction

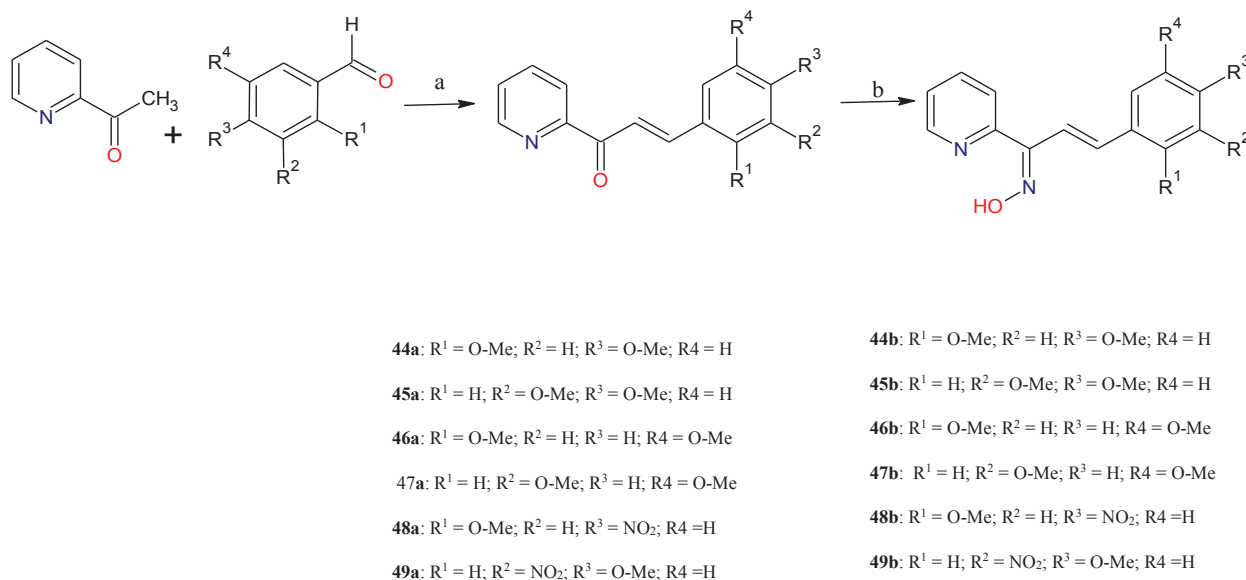
Many compounds with oxime groups displayed potent biological activities and low toxicities (Adamkova *et al* 2001). The novel chalcone oximes of phenyl and naphthyl chalcone derivatives synthesized and discussed in **Chapter 6** were found to have good tyrosinase inhibition and the results were published (Radhakrishnan (a) *et al* 2015; Radhakrishnan (b) *et al* 2015). Tyrosinase inhibitors like tropolone and kojic acid have been found to be competitive inhibitors by chelating the copper in the active site of the enzyme (Kahn & Andrawis 1985; Chang 2009). Besides, research has given rise to phenyl and naphthyl chalcones substituted with electron donating methoxy groups on ring B with significant inhibitory activities (Bandgar *et al* 2010; Ethiraj, Aranjani & Khan 2013; Shenvi *et al* 2013). Results from **Chapter 6** have shown that the placement of strongly electron-withdrawing groups such as NO₂ in ring B have culminated with enhanced tyrosinase inhibition. However, a pyridinyl nitrogen atom on ring B that formed a strong intramolecular hydrogen bond formed between the pyridinyl nitrogen and the oxygen atom of oxime group brought about a substantial decline in tyrosinase inhibitory potential.

Preliminary docking calculations prompted to synthesize a whole new template of chalconeoximes by incorporating a heterocyclic nitrogen atom into ring A of the chalcone framework. The nitrogen atom of substituted pyridinyl chalcone derivatives can possibly get protonated at physiological pH and might act as a positive center capable of interacting with anionic or partially anionic groups of amino acid residues existing in the tyrosinase active site. It was likely for the nitrogen atom in pyridine skeleton to coordinate with the copper atoms present in the tyrosinase active site. In a continuous effort to search for potential novel tyrosinase inhibitors and to develop a new template, efforts were extended towards the synthesis of oximes of 2'-acetylpyridinyl chalconeoxime compounds that had similar features to those of hydroxamic acids and hydroxamates which were good chelating agents. The chelation involved the oxygen belonging to the =N-OH group (Lindner & Goettlicher 1969).

10.2. Experimental

A series of 2'-acetylpyridinylchalcone compounds were synthesized by base catalyzed Claisen-Schmidt condensation of an aldehyde and an appropriate ketone in a polar

solvent like methanol. These compounds were then subsequently converted to their oxime derivatives by reaction with hydroxylamine hydrochloride (**Scheme 10**). Assays were performed with L-DOPA as the substrate, using kojic acid, a well-known effective tyrosinase inhibitor as the positive control.



Scheme 10. General method for synthesis of 2'-acetylpyridinylchalconeoximes.
Reagents and conditions: (a) MeOH, NaOH, 0^o C, 24hrs; (b) NH₂ OH. HCl

10.2.1. Method for synthesis of compound **46b**

To a stirred solution of 2'-acetylpyridine (1mM, 1.21mL) and 2, 5-dimethoxybenzaldehyde (1mM, 166mg) in 25 mL methanol, was added pulverized NaOH (2mM) and the mixture was stirred at room temperature for 24–36 h. The reaction was monitored by TLC using *n*-hexane: ethyl acetate (7:3) as mobile phase. The reaction mixture was cooled to 0^oC (ice-water bath) and acidified with HCl (10 % v/v aqueous solution) to afford total precipitation of the compound. A yellowish orange precipitate was formed, which was filtered and washed with 10 % aqueous HCl solution. The product obtained was recrystallized with ethylacetate to give the pure chalcone product **46a**.

A mixture of chalcone **46a** (1 mmol, 269mg), hydroxylamine hydrochloride (1.5 mmol, 104mg), and anhydrous sodium sulfate (1 mmol, 140mg) was refluxed in ethanol (5 mL) under stirring for the period (the reaction was followed by TLC). After completion of the reaction, the mixture was filtered, and the solvent was evaporated under reduced pressure. Then distilled water (10 mL) was added, and ethyl acetate (10 mL×3) was

added to extract organic compounds. The combined organic layers were dried over anhydrous sodium sulfate and filtered. Evaporation of the solvent in reduced pressure gave the crude product, which was purified by column chromatography on silica (200-300 mesh), eluted with petroleum ether (60-90 °C) or a mixture of petroleum ether and ethyl acetate (v/v = 1:4) to yield the pure oxime product **46b**.

10.2.2. Spectral data

44a. (2*E*)-3-(2,4-dimethoxyphenyl)-1-(pyridin-2-yl)prop-2-en-1-one. Yield: 80%; M.p: 110–112°C); ¹H NMR (500 MHz, CDCl₃): δ 8.56 (dd, 1H, *J* = 8.2, 9.5, H-3), 8.03 (dd, 1H, H-6, *J* = 7.4, 9.4), 7.97 (d, 1H, H_α, *J* = 11.0), 7.84 (t, 1H, H-5, *J* = 9.0), 7.70 (d, 1H, H-5', *J* = 10.5), 7.47 (dd, 1H, H-4, *J* = 7.8, 10.0), 6.97 (d, 1H, H_β, *J* = 11.5), 6.47 (d, 1H, H-6', *J* = 8.5), 6.40 (s, H-3', 1H), 3.89 (s, 3H, Me), 3.82 (s, 3H, Me); ¹³C NMR (125MHz, DMSO-d₆) δ 200.2 (C=O), 152.2 (C1), 147.5 (C3), 136.4 (C4), 136.7 (C5), 121.9 (C6), 109.2 (C5'), 124.9 (vinylic), 142.5 (vinylic), 165.8 (C4'), 160.1 (C6'), 109.1 (C3'), 129.1 (C2'), 120.5 (C1'), 55.1 (CH₃); IR (KBr) ν (cm⁻¹); 3375, 3055, 2924, 2865, 1871, 1695, 1659, 1568, 1465, 1255, 1186, 1020, 742; MS (ESI): 269.2([M + H])⁺.

45a. (2*E*)-3-(3,4-dimethoxyphenyl)-1-(pyridin-2-yl)prop-2-en-1-one. Yield: 75%; M.p: 132–134°C; ¹H NMR (500 MHz, CDCl₃): δ 8.32 (dd, 1H, H-3', *J* = 6.8, 9.5), 8.09 (dd, 1H, H-6', *J* = 6.9, 8.0), 7.87 (d, 1H, H_α, *J* = 11.5), 7.82 (dd, 1H, H-5', *J* = 10.5), 7.47 (dd, 1H, H-4', *J* = 9.5), 7.44 (dd, 1H, H-6, *J* = 8.5, 10.5), 7.40 (s, 1H), 6.97 (dd, 1H, H-5, *J* = 10.0), 6.94 (d, 1H, H_β, *J* = 12.0), 6.47 (dd, 1H, H-3, *J* = 8.5), 3.89 (s, 3H, Me), 3.80 (s, 3H, Me); ¹³C NMR (125MHz, DMSO-d₆) δ 199.4 (C=O), 152.2 (C1'), 144.2 (C3'), 139.2 (C4'), 132.4 (C5'), 122.2 (C6'), 130.4 (C1), 110.6 (C2), 151.2 (C3), 150.6 (C4), 110.6 (C5), 109.5 (C6), 127.7 (vinylic), 144.6 (vinylic), 57.1 (CH₃); IR (KBr) ν (cm⁻¹); 3450, 3035, 2935, 2840, 1852, 1699, 1552, 1446, 1027, 732; MS (ESI): 270.1([M + H])⁺.

46a. (2*E*)-3-(2,5-dimethoxyphenyl)-1-(pyridin-2-yl)prop-2-en-1-one. Yield: 87%; M.p: 110–112°C). ¹H NMR (CDCl₃ δ 8.36 (1H, dd, *J* = 9.0 Hz, H-3), 8.02 (1H, dd, *J* = 7.2, 9.0, Hz, H-6), 7.89 (1H, d, *J* = 12.0 Hz, H_α), 7.82 (1H, dd, *J* = 6.5, 9.5 Hz, H-5) 7.65 (1H, dd, *J* = 8.5, 10.5 Hz, H-4'), 7.49 (1H, dd, *J* = 7.5, 10.0 Hz, H-4), 6.95 (1H, d, *J* = 12.5 Hz, H_β), 6.42 (s, 1H, H-6'), 6.47 (1H, dd, *J* = 8.5 Hz, H-3'), 3.87 (s, 3H, Me), 3.80 (s, 3H, Me); ¹³C NMR (125MHz, DMSO-d₆) δ 205.1 (C=O), 150.8 (C1), 145.9 (C3),

137.2 (C4), 135.2 (C5), 120.9 (C6), 109.2 (C5'), 125.4 (vinylic), 140.6 (vinylic), 165.8 (C4'), 160.1 (C6'), 109.1 (C3'), 129.1 (C2'), 120.5 (C1'), 59.1 (CH₃), 55.5 (CH₃); IR (KBr) ν (cm⁻¹): 3389, 3045, 2942, 2855, 1865, 1694, 1642, 1550, 1450, 1224, 1024, 722; MS (ESI): 269.2([M + H])⁺.

47a. (2*E*)-3-(3,5-dimethoxyphenyl)-1-(pyridin-2-yl)prop-2-en-1-one. Yield: 84%; M.p: 128–130°C). ¹H NMR (CDCl₃ δ 8.38 (1H, dd, *J* = 10.0 Hz, H-3), 8.02 (1H, dd, *J* = 9.0 Hz, H-6), 7.89 (1H, t, *J* = 8.0 Hz, H-5), 7.97 (1H, d, *J* = 10.5 Hz, H _{α}), 7.07 (s, 2H, H-2' & H-6'), 7.47 (1H, dd, *J* = 6.7, 9.0 Hz, H-4), 6.94 (1H, d, *J* = 11.0 Hz, H _{β}), 6.47 (1H, dd, *J* = 8.5 Hz, H-3'), 3.84 (s, 6H, Me); ¹³C NMR (125MHz, DMSO-d₆) δ 199.2 (C=O), 152.3 (C1), 144.7 (C3), 139.2 (C4), 140.2 (C5), 122.8 (C6), 124.1 (vinylic), 144.5 (vinylic), 160.1 (C3' & C5'), 108.1 (C4'), 138.5 (C1'), 107.6 (C2' & C6'), 56.1(CH₃); IR (KBr) ν (cm⁻¹): 3420, 3047, 2954, 2874, 1874, 1700, 1654, 1524, 1435, 1250, 1172, 1052, 975, 722; MS (ESI); 269.2([M + H])⁺.

48a. (2*E*)-3-(2-methoxy-4-nitrophenyl)-1-(pyridin-2-yl)prop-2-en-1-one. Yield: 78%; M.p: 127–129°C). ¹H NMR (CDCl₃ δ 8.15 (s, 1H), 7.94 (1H, m, H-6', *J* = 8.5 Hz), 7.79 (1H, d, H-5', *J* = 10.5 Hz), 8.34 (1H, dd, *J* = 9.0 Hz, H-3), 8.09 (1H, dd, *J* = 8.7, 9.5 Hz, H-6), 7.87 (1H, t, *J* = 8.0 Hz, H-5), 7.99 (1H, d, *J* = 10.0 Hz, H _{α}), 7.52 (1H, dd, *J* = 9.0 Hz, H-4), 6.95 (1H, d, *J* = 10.5 Hz, H _{β}), 3.80 (s, 3H, Me); ¹³C NMR(125 MHz, DMSO-d₆) δ 199.2 (C=O), 150.6 (C1), 145.7 (C3), 140.2 (C4), 142.2 (C5), 120.8 (C6), 137.2 (C1'), 116.2 (C2'), 112.2 (C3'), 138.2 (C4'), 125.3 (C5'), 118.2 (C6'), 130.2 (vinylic), 144.5 (vinylic); IR (KBr) ν (cm⁻¹): 3375, 2965, 2928, 2860, 1700, 1565, 1352, 1250, 1209, 1124, 872, 715; HRMS *m/z*: 285.0869 ([M + H])⁺; Calcd: 285.0875.

49a. (2*E*)-3-(4-methoxy-3-nitrophenyl)-1-(pyridin-2-yl)prop-2-en-1-one. Yield: 72%; M.p: 119–121°C). ¹H NMR(CDCl₃ δ 8.18 (s, 1H), 7.89 (1H, m, H-6', *J* = 8.5 Hz), 7.80 (1H, dd, H-5', *J* = 9.5 Hz), 8.39 (1H, dd, *J* = 10.0 Hz, H-3), 8.07 (1H, dd, *J* = 7.9, 9.4 Hz, H-6), 7.85 (1H, t, *J* = 8.0 Hz, H-5), 7.94 (1H, d, *J* = 9.5 Hz, H _{α}), 7.53 (1H, dd, *J* = 6.9, 9.0 Hz, H-4), 6.95 (1H, d, *J* = 10.0 Hz, H _{β}), 3.84 (s, 3H, Me); ¹³C NMR(125 MHz, DMSO-d₆) δ 200.2 (C=O), 151.4 (C1), 146.2 (C3), 140.7 (C4), 142.4 (C5), 122.4 (C6), 137.2 (C1'), 116.2 (C2'), 142.2 (C3'), 118.2 (C4'), 126.7 (C5'), 120.2 (C6'), 132.2 (vinylic), 145.2 (vinylic); IR (KBr) ν (cm⁻¹): 3450, 2950, 2924, 2854, 1690, 1535, 1295, 1224, 1122, 877, 722; HRMS *m/z*: 285.0871 ([M + H])⁺; Calcd: 285.0875.

44b. (1*Z*, 2*E*)-3-(2,4-dimethoxyphenyl)-*N*-hydroxy-1-(pyridin-2-yl) prop-2-en-1-imine. Yield: 67%; M.p: 160–162°C). ¹H NMR (500 MHz, CDCl₃ δ 9.47 (s, 1H, OH), 8.42

(dd, 1H, $J = 9.0$, H-3), 8.09 (dd, 1H, $J = 8.2, 8.5$, H-6), 7.96 (d, 1H, $J = 10.0$, H_a), 7.80 (t, 1H, $J = 9.5$, H-5), 7.67 (d, 1H, $J = 10.5$, H-5'), 7.49 (dd, 1H, $J = 8.5, 11.0$, H-4), 6.99 (d, 1H, $J = 10.5$, H_β), 6.49 (d, 1H, $J = 8.0$, H-6'), 6.42 (s, 1H, H-3'), 3.88 (s, 3H, Me), 3.79 (s, 3H, Me); ¹³C NMR (125MHz, DMSO-d₆) δ 159.6 (C=N), 150.4 (C1), 148.2 (C3), 137.2 (C4), 135.2 (C5), 120.4 (C6), 110.2 (C5'), 127.2 (vinylic), 140.5 (vinylic), 164.2 (C4'), 159.4 (C6'), 110.1 (C3'), 130.1 (C2'), 122.5 (C1'), 57.1 (CH₃); IR (KBr) ν (cm⁻¹); 3655, 3580, 2950, 1645, 1558, 1432, 1250, 1175, 945, 722; HRMS m/z : 285.1233 ([M + H])⁺; Calcd: 285.1239.

45b. (1Z, 2E)-3-(3,4-dimethoxyphenyl)-*N*-hydroxy-1-(pyridin-2-yl) prop-2-en-1-imine. Yield: 55%; M.p: 180–184°C). ¹H NMR (500 MHz, CDCl₃ δ 9.52 (s, 1H, OH), 8.27 (dd, 1H, $J = 10.0$, H-3), 8.12 (dd, 1H, $J = 9.0$, H-6), 7.82 (t, 1H, $J = 8.5$, H-5), 7.94 (d, 1H, $J = 13.0$, H_a), 7.46 (s, 1H, H-2'), 7.44 (dd, 1H, $J = 6.5, 8.5$, H-4), 6.87 (d, 1H, $J = 13.5$, H_β), 6.39 (d, 1H, $J = 8.0$, H-6'), 6.82 (dd, 1H, $J = 7.5$, H-5'). 3.92 (s, 3H, Me), 3.84 (s, 3H, Me); ¹³C NMR (125MHz, DMSO-d₆) δ 162.4 (C=N), 148.4 (C1), 142.5 (C3), 138.5 (C4), 140.2 (C5), 124.2 (C6), 107.4 (C5'), 124.6 (vinylic), 142.3 (vinylic), 107.2 (C5'), 127.2 (C6'), 152.2 (C3'), 152.4 (C4'), 132.2 (C1'), 112.6 (C2'), 55.7(CH₃), 56.1 (CH₃); IR (KBr) ν (cm⁻¹); 3682, 3554, 2985, 1642, 1554, 1428, 1274, 1165, 950, 835, 725; HRMS m/z : 285.1231 ([M + H])⁺; Calcd: 285.1239.

46b. (1Z, 2E)-3-(2,5-dimethoxyphenyl)-*N*-hydroxy-1-(pyridin-2-yl) prop-2-en-1-imine. Yield: 60%; M.p: 154–156°C). ¹H NMR (500 MHz, CDCl₃ δ 9.52 (s, 1H, OH), 8.29 (dd, 1H, $J = 9.0$, H-3), 8.08 (dd, 1H, $J = 9.5$, H-6), 7.91 (d, 1H, $J = 10.5$, H_a), 7.87 (dd, 1H, $J = 9.5$, H-5) 7.64 (dd, 1H, $J = 10.0$, H-4'), 7.54 (dd, 1H, $J = 8.2, 10.7$, H-4), 6.89 (d, 1H, $J = 11.0$, H_β), 6.47 (s, 1H, H-6'), 6.57 (dd, 1H, $J = 8.0$, H-3'), 3.89 (s, 3H, Me), 3.84 (s, 3H, Me); ¹³C NMR (125MHz, DMSO-d₆) δ 160.1 (C=N), 154.1 (C1), 142.8 (C3), 139.1 (C4), 137.2 (C5), 122.4 (C6), 110.4 (C5'), 122.7 (vinylic), 144.4 (vinylic), 164.2 (C4'), 158.8 (C6'), 107.8 (C3'), 130.2 (C2'), 124.5 (C1'), 57.1 (CH₃), 55.5 (CH₃); IR (KBr) ν (cm⁻¹); 3690, 3550, 2975, 1650, 1550, 1434, 1264, 1160, 974, 735; HRMS m/z : 285.1236 ([M + H])⁺; Calcd: 285.1239.

47b. (1Z, 2E)-3-(3,5-dimethoxyphenyl)-*N*-hydroxy-1-(pyridin-2-yl) prop-2-en-1-imine. Yield: 50%; M.p: 172–174°C). ¹H NMR (500 MHz, CDCl₃ δ 9.71 (s, 1H, OH), 8.27 (dd, 1H, $J = 9.0, 9.5$, H-3), 8.10 (dd, 1H, $J = 9.5, 10.5$, H-6), 7.97 (d, 1H, $J = 11.0$, H_a), 7.82 (dd, 1H, $J = 6.9, 7.5$, H-5) 7.58 (dd, 1H, $J = 10.0$, H-4'), 7.59 (dd, 1H, $J = 11.5$, H-4), 6.86 (d, 1H, $J = 11.5$, H_β), 6.49 (s, 1H, H-6'), 6.62 (dd, 1H, $J = 8.0$, H-3'), 3.90 (s,

3H, Me), 3.86 (s, 3H, Me); ^{13}C NMR (125MHz, DMSO- d_6) δ 160.7 (C=N), 155.1 (C1), 144.2 (C3), 141.1 (C4), 137.6 (C5), 122.2 (C6), 110.2 (C5'), 122.4 (vinylic), 142.4 (vinylic), 160.2 (C4'), 156.4 (C6'), 109.4 (C3'), 129.2 (C2'), 125.5 (C1'), 58.1 (CH₃), 55.4 (CH₃); IR (KBr) ν (cm^{-1}): 3675, 3552, 2968, 1648, 1545, 1429, 1254, 1134, 935, 722; HRMS m/z : 285.1235 ($[\text{M} + \text{H}]^+$); Calcd: 285.1239.

48b. 2-[(1*E*,2*E*)-*N*-hydroxy-3-(2-methoxy-4-nitrophenyl)prop-2-enimidoyl]phenol. Yield: 58%; Mp: 190–192°C; ^1H NMR (500 MHz, CDCl_3): δ 12.52 (s, 1H, OH), 9.47 (s, 1H), 8.05 (s, 1H), 7.90 (m, 1H, $J = 8.5$, H-6), 7.87 (d, 1H, $J = 12.0$, H _{α}), 7.77 (d, 1H, $J = 11.0$, H-6'), 7.72 (d, 1H, $J = 9.5$, H-5), 7.50 (dd, 1H, $J = 6.9$, 8.0, H-4'), 7.24 (dd, 1H, $J = 9.5$, H-3'), 6.94 (dd, 1H, $J = 8.7$, 10.5, H-5'), 6.89 (d, 1H, $J = 12.5$, H _{β}), 3.89 (s, 3H); ^{13}C NMR (125 MHz, DMSO- d_6) δ 160.2 (C=N), 130.44 (C6'), 120.43 (C1'), 118.3 (C5'), 139.2 (C4'), 118.4 (C3'), 164.9 (C2'), 132.2 (C1), 114.9 (C2), 112.2 (C3), 137.5 (C4), 124.7 (C5), 118.5 (C6), 129.4 (vinylic), 142.5 (vinylic); IR (KBr) ν (cm^{-1}): 3650, 3582, 2650, 1648, 1550, 1265, 949, 835, 712; HRMS m/z : 315.0976 ($[\text{M} + \text{H}]^+$); Calcd: 315.0981.

49b. (1*E*, 2*E*)-*N*-hydroxy-3-(4-methoxy-3-nitrophenyl)-1-(pyridin-2-yl)prop-2-en-1-imine. Yield: 47%; Mp: 172–174°C; ^1H NMR (500 MHz, CDCl_3): δ 9.47 (s, 1H), 8.72 (dd, 1H, $J = 9.5$, 11.5, H-3), 8.42 (dd, 1H, $J = 8.5$, H-6), 8.20 (s, 1H), 7.88 (m, 1H, $J = 8.0$, H-6'), 7.82 (t, 1H, $J = 9.5$, H-5), 7.79 (d, 1H, $J = 12.0$, H _{α}), 7.75 (d, 1H, $J = 9.5$, H-5'), 7.44 (dd, 1H, $J = 8.8$, 11.5, H-4), 6.92 (d, 1H, $J = 12.5$, H _{β}), 3.88 (s, 3H); ^{13}C NMR (125 MHz, DMSO- d_6) δ 162.5 (C=N), 153.5 (C1), 118.9 (C6), 134.4 (C5), 130.4 (C4), 150.2 (C3), 136.4 (C1'), 118.2 (C2'), 114.2 (C3'), 139.7 (C4'), 125.3 (C5'), 120.2 (C6'), 144.2 (vinylic), 133.2 (vinylic); IR (KBr) ν (cm^{-1}): 3645, 3548, 2652, 1635, 1425, 1302, 1225, 805, 672; HRMS m/z : 300.0976 ($[\text{M} + \text{H}]^+$); Calcd: 300.0984.

10.3. Results and Discussion

10.3.1. Chemistry

The inhibitory activities of the synthesized oxime compounds were compared with the reference compound kojic acid. The parent 2'-acetylpyridinyl chalcones showed poor tyrosinase inhibitory activities. However, it was interesting to note that the oxime derivatives synthesized had better tyrosinase inhibitory activities when compared with the positive control kojic acid (**Table 19**).

Table 19 Inhibition effects and docking results of acetylpyridinylchalconeoximes

Compound	Tyrosinase Inhibition at 50 μ M (%) *	CDOCKER energy (kcal/mol)	Type of interactions		Donor-acceptor	Distance (Å)
44b	52.6 \pm 0.33	-22.84	H-bonding		(His85) H δ_2 ...N (oxime)	2.87
					(Val283) H α ... N	2.95
					H... O=C (Met280)	2.89
			hydrophobic stacking	π - π	ring B...His263	3.92
45b	48.9 \pm 0.35	-16.75	H-bonding		H... O=C (Met280)	2.42
			Intramolecular bonding		(Me) H... O (Me)	2.36
			hydrophobic stacking	π - π	ring B...His263	3.64
46b	67.4 \pm 0.65	-27.89	H-bonding		(His85) H δ_2 ...N (oxime)	2.98
					(His259) H ϵ_1 ...N	2.54
					(Val283) H α ... N	2.91
					(His259) H ϵ_1 ...HO-2'	2.35
					H...O (His85)	3.09
					H...O ϵ_1 (Glu322)	2.55
					H... O=C (Met280)	2.87
					(His85) H δ_2 ...N (oxime)	2.85
47b	55.5 \pm 0.14	-24.74	H-bonding		(Val283) H α ... N	2.93
					H...O (His85)	3.04
					H...O ϵ_1 (Glu322)	2.65
					H... O=C (Met280)	2.94
			hydrophobic stacking	π - π	ring B...His263	3.96
48b	60.5 \pm 0.24	-26.40	H- bonding		(His85) H δ_2 ...N (oxime)	2.89
					(His244) H ϵ_1 ...N	2.69
					(His259) H ϵ_1 ...N	2.52
					(Val283) H α ... N	2.85
					H... O=C (Met280)	2.90
			Intramolecular bonding	H-	OH (oxime)...N	2.01
49b	49.2 \pm 0.75	-17.71	H-bonding		(His85) H δ_2 ...N (oxime)	2.78
					H... O=C (Met280)	3.00
			Metal bond	coordination	Cu401...OH (oxime)	2.33
			hydrophobic stacking	π - π	ring B...His263	2.74
Kojic acid	49.5 \pm 0.66	-11.69	H-bonding		Asn260 H α ...O	2.93
					Val283 H α ...O	2.64
					H... O=C (Met280)	2.84

* Chalcone derivatives were synthesized according to the details in Scheme 1; Values indicated means \pm SE for three determinations.

The structures of the compounds synthesized were confirmed by ^1H NMR, ^{13}C NMR, FTIR and HRMS. The most noticeable feature of the structural characterization of compounds synthesized was the assignment of the proton resonances of their α , β -unsaturated moiety, which was confirmed from the values of the vicinal coupling constants. The signals for aromatic hydrogens were between 6.5 and 8.0 ppm. The coupling constants for vinylic protons appeared between 10.0–14.0 Hz which confirms their *trans* conformations.

These compounds were found to be more potent than the positive control, kojic acid (IC_{50} ; 27.95 μM). The structures of the non-cyclic moieties of the synthesized molecules had similar features to those of hydroxamic acids and hydroxamates which were good chelating agents. In terms of the structure- activity relationships, compound **46b** ((1*Z*, 2*E*)-3-(2, 5-dimethoxyphenyl)-*N*-hydroxy-1-(pyridin-2-yl) prop-2-en-1-imine) and compound **48b** (1*Z*, 2*E*)-*N*-hydroxy-3-(2-methoxy-4-nitrophenyl)-1-(pyridin-2-yl)prop-2-en-1-imine exhibited the most potent tyrosinase inhibitory activity with inhibition of 67.4% and 60.5% respectively. This could be accounted for the presence of strongly activating methoxy substituents that increased the reactivity of aromatic ring system by resonance effects. Presence of a strong electron releasing group in the ortho position (-OMe) and an electron withdrawing group (-NO₂) in the para position in compound **46b** modulated the electronic structure of ring B significantly, that accounted to its better tyrosinase inhibitory potential. Substitution with an ortho directing methoxy group and an electron withdrawing para-nitro group on ring B gave compound **46b** with an inhibitory potential (60.5%) that was still more effective than kojic acid (48.4%) while substitution with a para directing methoxy group gave compounds **44b** and **45b** that showed a considerable decline in tyrosinase inhibition (52.6% & 48.9%, respectively).

In this view, it was reasoned that the introduction of electron withdrawing groups (-NO₂) on B ring may increase the electrophilicity of the β -carbon, thus improving the bioactivity of the resulting compounds. Compounds **49b** & **47b** showed significant tyrosinase inhibitions with tyrosinase inhibitions of 49.2% and 55.5% respectively. Further, the inhibition mechanisms of the active inhibitors **46b** and **48b** was determined.

10.3.2. Inhibition mechanism of the selected compounds on mushroom tyrosinase

To explore the mechanism of active inhibitors, a study of the kinetic behaviour of tyrosinase activity was conducted in the presence of active inhibitors **46b** and **48b**. L-DOPA was used as the substrate for the effect of inhibitor compounds on the oxidation of L-DOPA by tyrosinase (diphenolase activity). The result showed that both compounds could inhibit the diphenolase activity of tyrosinase in a dose-dependent manner. With increasing concentrations of inhibitors, the remaining enzyme activity decreased exponentially. The inhibitor concentration leading to 50% activity lost (IC_{50}) for compounds **46b** and **48b** was estimated to be 6.37 μ M and 12.22 μ M, respectively (Table 20).

Table 20 Inhibitory effects of kojic acid, 46b and 48b on mushroom tyrosinase.

Sample	Concentration (μ M)	Inhibition (%)			Average of inhibition (%)	IC_{50} (μ M) ^a	K_i (μ M) [#]
Kojic acid	1.25	3.62	3.60	3.65	3.62		
	5.00	16.45	16.52	16.42	16.46	22.83 ± 0.66	9.23
	20.00	49.07	48.05	48.25	48.45		
46b	1.25	36.45	32.60	33.55	34.20	12.22 ± 0.42	
	5.00	40.60	37.20	35.25	37.68		8.15
	20.00	64.50	63.75	60.20	62.81		
48b	1.25	44.28	40.36	37.50	40.71		
	5.00	46.25	44.58	43.95	44.92	6.37 ± 1.22	4.82
	20.00	72.42	70.25	73.65	72.10		

a: 50% inhibitory concentration (IC_{50}). #: Values were measured at 5 μ M of active compounds and K_i is the (inhibitor constant).

The plots of the remaining enzyme activity versus the concentration of enzyme at different inhibitor concentrations gave a family of straight lines, which all passed through the origin. The presence of inhibitor did not reduce the amount of enzyme, but just resulted in the inhibition of enzyme activity. The results showed that both the compounds **46b** and **48b** were reversible inhibitors of mushroom tyrosinase for oxidation of L-DOPA (Figure 53).

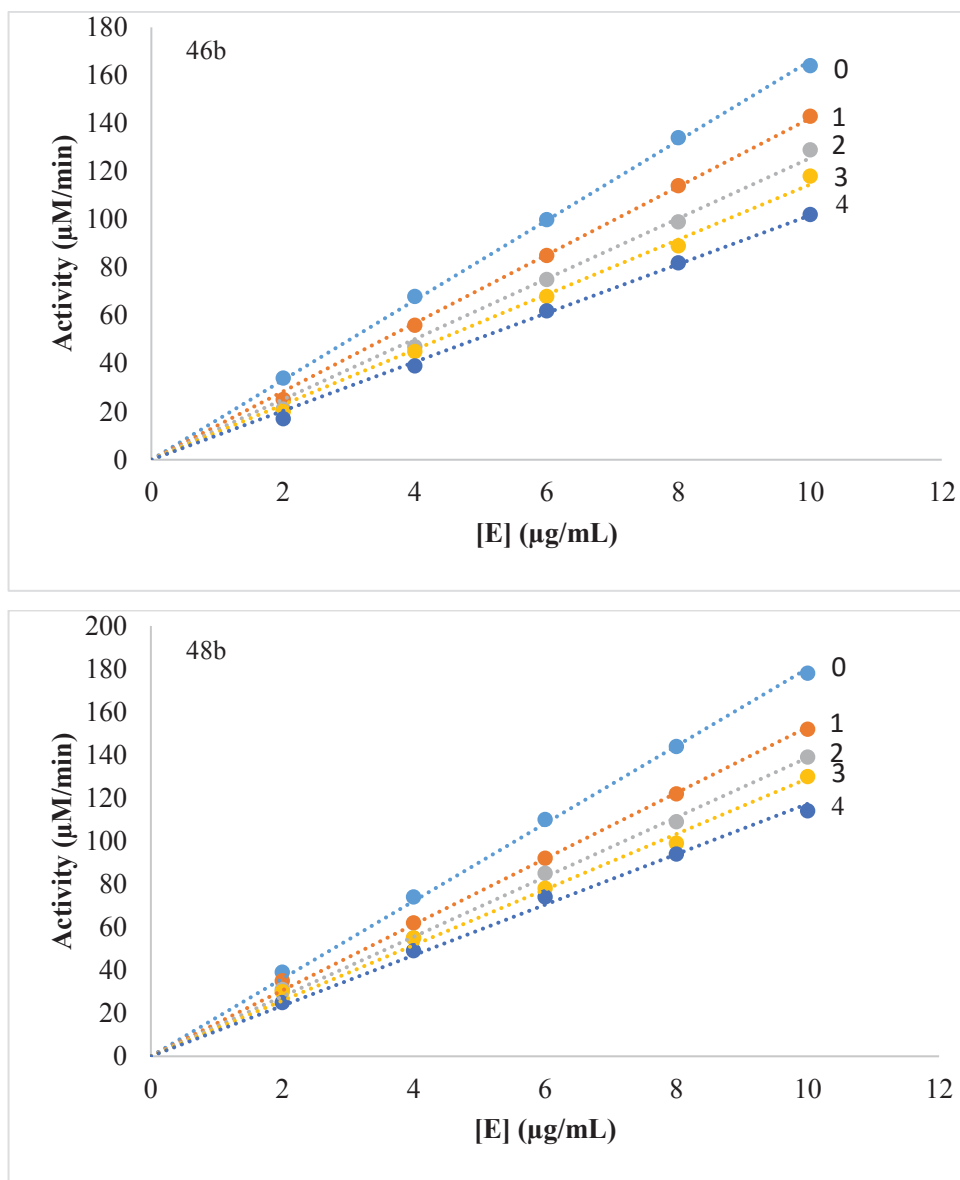


Figure 53 The inhibitory mechanism of compounds **46b** and **48b**

The concentration of inhibitor used for curves 0-4 were 0, 0.25, 0.5, 1.0 and 2.0 μM , respectively.

10.3.3. Lineweaver–Burk analysis by inhibitor compounds **46b** and **48b**.

The reaction rates were measured in the presence of active inhibitors with various concentrations of L-DOPA as a substrate. As the concentrations of active inhibitors **46b** and **48b** increased, K_m values gradually increased, but V_{\max} values did not change, thereby indicating the inhibitors act as competitive inhibitors of mushroom tyrosinase (Figure 54).

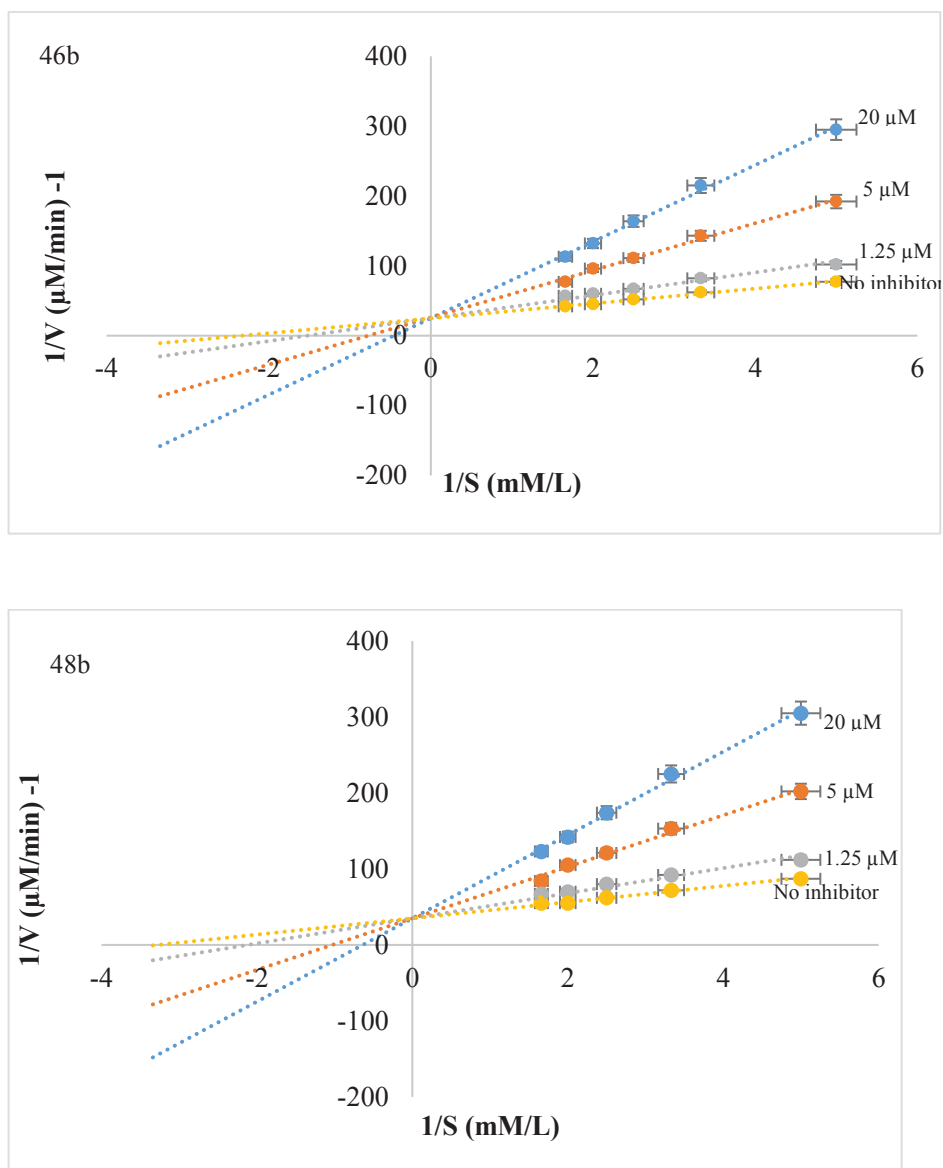


Figure 54 Lineweaver Burk plot for inhibition of compounds **46b** and **48b**

Data were obtained as mean values of $1/V$, the inverse of the absorbance increase at a wavelength of 492nm per min of three independent tests with different concentrations of L-DOPA as a substrate. The concentration of compounds **46b** and **48b** from top to bottom were 20 μM , 5 μM , 1.25 μM and 0 μM , respectively.

The inhibition kinetics was illustrated by Dixon plots, which were obtained by plotting $1/V$ versus $[I]$ with varying concentrations of substrate. Dixon plots gave a family of straight lines passing through the same point at the second quadrant, giving the inhibition constant (K_i). The K_i value estimated from this Dixon plot was 4.82 μM and 8.15 μM , respectively for the compounds **46b** and **48b** (Figure 55).

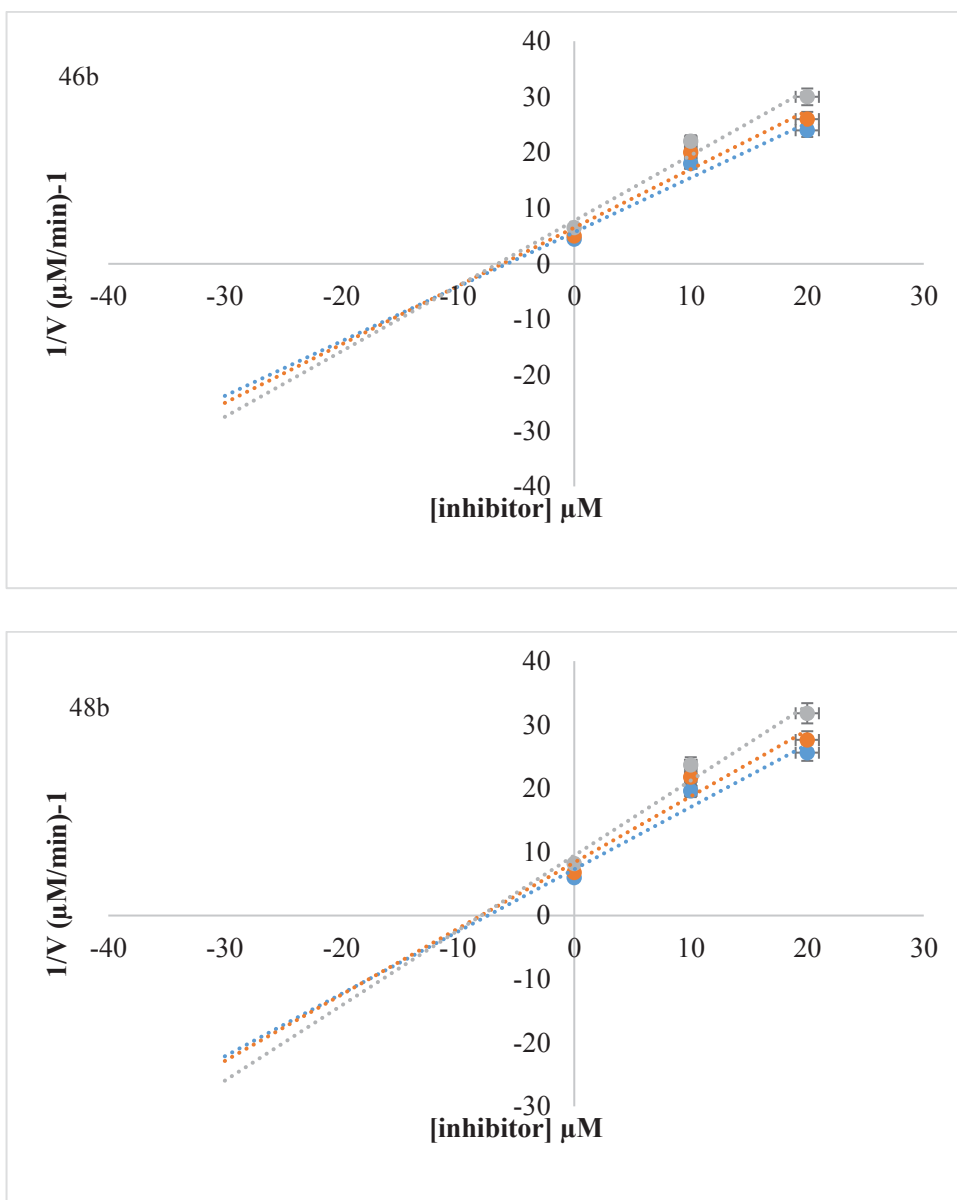


Figure 55 Dixon plot for the inhibitory effect of compounds **46b** and **48b**

The inhibitor concentrations were 0, 10 μM and 20 μM , respectively. The L-DOPA concentrations were 200 μM , 400 μM and 600 μM .

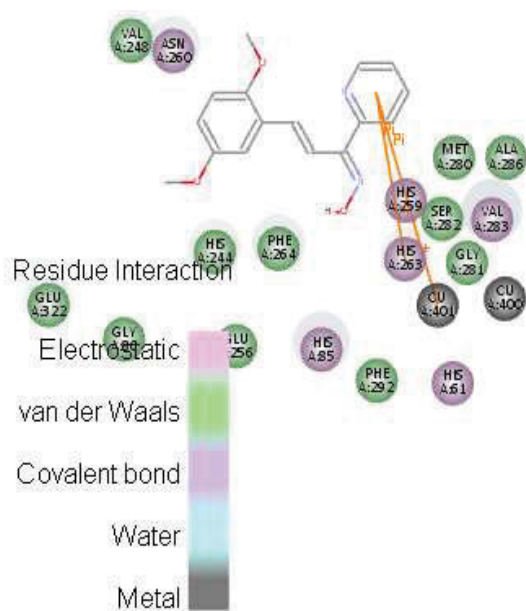
10.3.4. Docking studies

Accelrys Discovery Studio 4.5 suite was utilized to simulate binding between the active site of mushroom tyrosinase and substituted 2'-acetylpyridinyl chalcone oximes. The results of virtual screening studies indicated that the estimated CDOCKER energy of all the docked ligands ranged between -27.89 and -16.75 kcal/mol. **Figure 56** showed selected docked conformations of active inhibitors **46b** and **48b** along with the positive control, kojic acid in the tyrosinase binding site. Docking results showed that compound

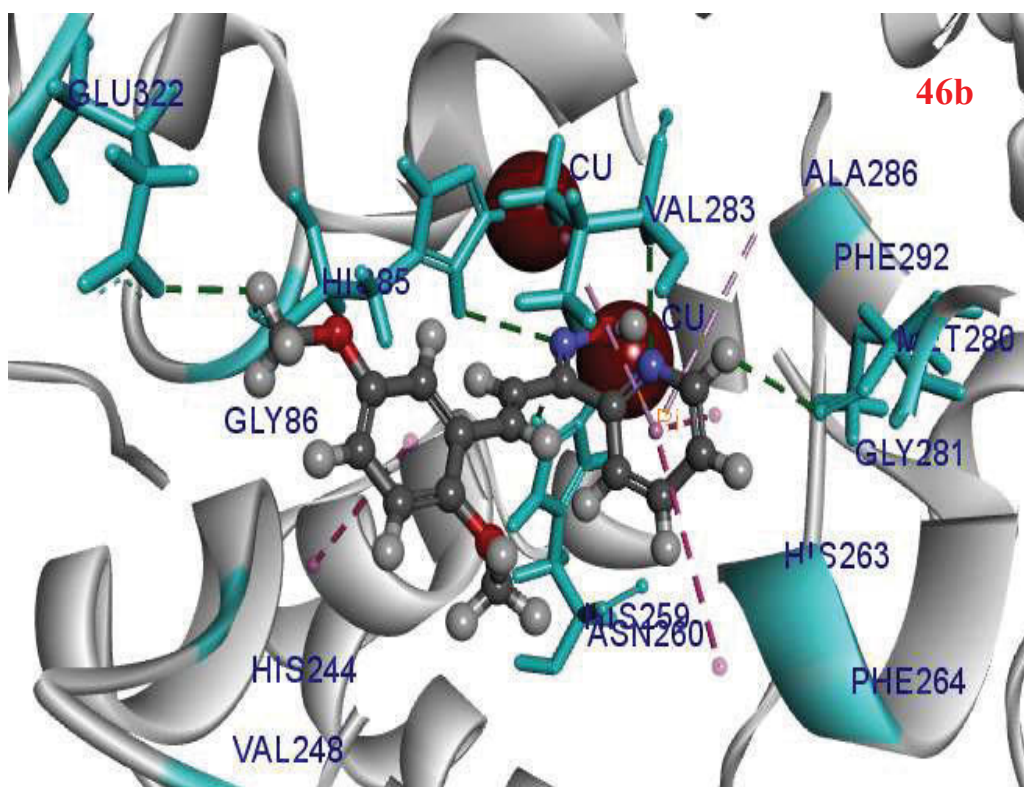
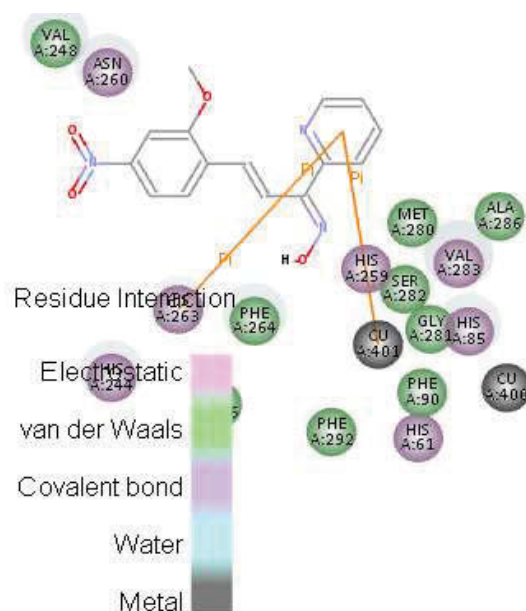
46b has the highest docking score ($-27.89 \text{ kcal mol}^{-1}$) that correlated well with the experimental results (**Table 11**). In the case of most of the oxime chalcones reported here, the oxime OH group was actively involved in hydrogen bonding interactions with amino acid residues of the tyrosinase. This could in turn, help the compounds to have a better fit to the catalytic pocket of the enzyme tyrosinase.

Compound **46b** formed 6 hydrogen bonds with amino-acid residues in the tyrosinase catalytic pocket. Hydrogen bonding with His85, His259, Val283, Met280 and Glu322 was seen for compound **46b** while compound **48b** exhibited hydrogen bonding interactions with His85, His259, Val283 and Met280. The residues had a key function and effect on binding affinity. Two weak hydrogen bonds were formed between the nitrogen atom of the oxime with the hydrogen atoms of His85 and His259 at distances of 2.98 \AA and 2.54 \AA , respectively. The heterocyclic nitrogen atom in ring A formed a weak hydrogen bond (2.91 \AA) with the hydrogen of Val283. The oxygen atoms in His85 and Glu322 each accepted a hydrogen bond from the 5-OMe hydrogens at a distance of 2.09 \AA and 2.55 \AA , respectively. Another weak hydrogen bond (2.87 \AA) was seen between the carboxylate oxygen of Met280 and the aromatic hydrogen in ring A of compound **46b**. Both the active compounds showed hydrophobic π - π stacking interactions with His263 and T-shaped edge to face aryl-aryl interactions with Phe264 and His244. According to the docking program, the binding residues interacting with kojic acid were Met280, Val283, Asn260 and Gly281 of tyrosinase. This indicated that the oxime derivatives of 2'-acetylpyridinyl chalcones inhibited tyrosinase activity by binding at the active site of mushroom tyrosinase.

46b



48b



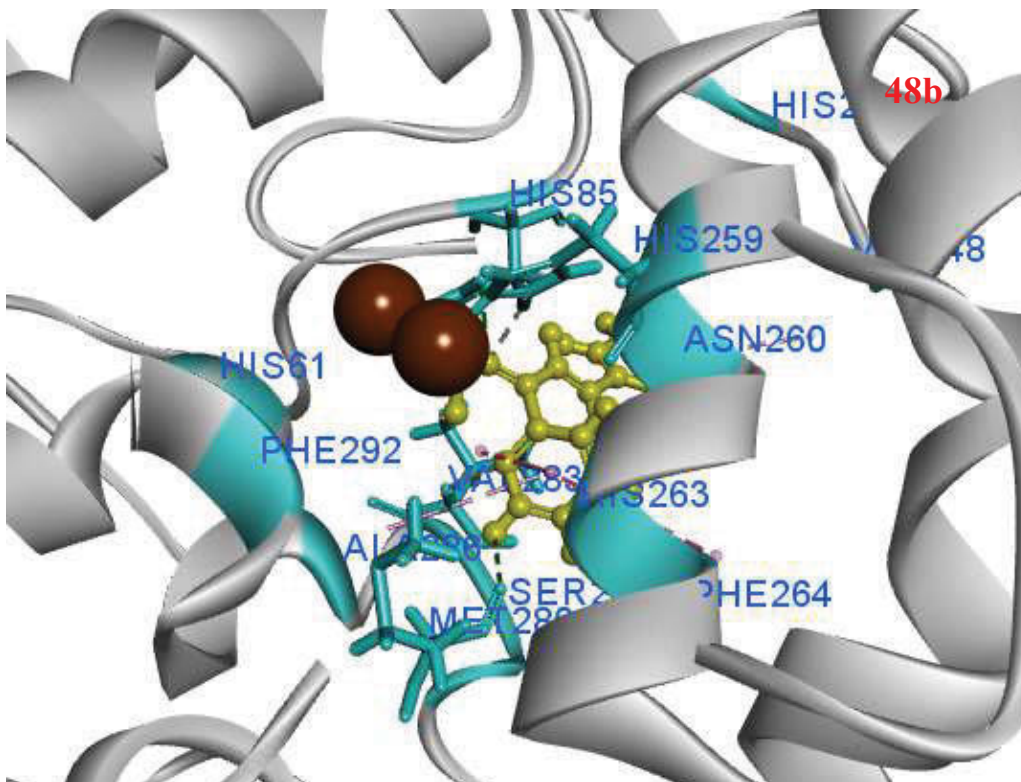


Figure 56 Docking and 2D results of compounds **46b** and **48b** in the tyrosinase catalytic pocket

Ligands **46b** and **48b** were displayed as ball and stick while the core amino acid residues were displayed as stick. The green dotted lines showed the hydrogen bond interactions and the purple lines showed the non-bonding interactions. The ochre balls represented the copper ions.

10.4. Conclusion

In summary, a series of novel 2'-acetylpyridinylchalcone oxime compounds were synthesized, and studied for their inhibition on the diphenolase activity of mushroom tyrosinase. Compounds **46b** and **48b** were found to be significantly more potent than kojic acid with their IC_{50} values of 6.37 μ M and 12.22 μ M, respectively. The oxime OH group was actively involved, both as donor (via the O-H moiety) and as hydrogen bond acceptor (via the N=C-OH moiety), in hydrogen bonding interactions. *In silico* studies revealed that the formation of a strong intramolecular hydrogen bond formed between the pyridinyl nitrogen and the oxygen atom of oxime group brought about a substantial decline in tyrosinase inhibitory potential. The soundness of the docking results and agreement with the kinetic studies suggested that 2'-acetylpyridinyl chalcone oximes

could be conveniently exploited to design inhibitors with an improved affinity for tyrosinase. Taken together, the principal results of the study suggested the following;

- a) Compounds **46b** and **48b** competitively inhibited L-DOPA oxidation of mushroom tyrosinase.
- b) Lineweaver-Burk plots showcased competitive reversible inhibition kinetics.
- c) The oxime OH group was actively involved in hydrogen bonding interactions with amino acid residues of the tyrosinase. This in turn, helped the compounds to have a better fit with the catalytic pocket of the enzyme tyrosinase.
- d) Substitution on ring B with ortho-para electron donating groups was favourable for better tyrosinase inhibition.
- e) A design principle encouraging strong coordination with the copper ions was warranted as the metal centres were a key part of the enzyme machinery.

These findings suggested 2'-acetylpyridinyl chalcone oximes to serve as a potential scaffold for the future development of active tyrosinase inhibitors. This study warranted future prospects to explore the effect of altered substituents on the pyridinyl ring and to correlate it with tyrosinase inhibition and melanin formation.

10.5. References

Adamkova, S, Frebort, I, Sebel, M, Pec, PJ 2001, 'Probing the active site of pea seedlings amine oxidase with optical antipodes of sedamine alkaloids', *Journal of enzyme inhibition*, Vol 16, pp. 367–372.

Bandgar, BP, Gawande, SS, Bodade, RG, Totre, JV, Khobragade, CN 2010, 'Synthesis and biological evaluation of simple methoxylated chalcones as anticancer, anti-inflammatory and antioxidant agents', *Bioorganic and Medicinal Chemistry*, Vol 18, pp. 1364–1370.

Chang, TS 2009, 'An updated review of tyrosinase inhibitors', *International Journal of Molecular Sciences*, Vol 10, pp. 2440–2475.

Ethiraj, KR, Aranjani, JM, Khan, FR 2013, 'Synthesis of methoxy-substituted chalcones and in vitro evaluation of their anticancer potential', *Chemical Biology and Drug Design*, Vol 82, pp. 732–742.

Kahn, V, Andrawis, A 1985, 'Inhibition of mushroom tyrosinase by tropolone', *Phytochemistry*, Vol 24, 905–908.

Lindner, HJ, Goettlicher, S 1969, 'Crystal and molecular structure of iron(III) benzhydroxamate trihydrate', *Acta Crystallographica*, Sect. B, Vol 25, pp. 832-842.

Radhakrishnan, SK, Shimmon, R, Conn, C, Baker, AT 2015 (a), 'Integrated kinetic studies and computational analysis on naphthyl chalcones as mushroom tyrosinase inhibitors', *Bioorganic and Medicinal Chemistry Letters*, Vol 25, pp. 4085–4091.

Radhakrishnan, SK, Shimmon, R, Conn, C, Baker, AT 2015 (b), 'Evaluation of novel chalcone oximes as inhibitors of tyrosinase and melanin formation in B16 cells', *Archiv der Pharmazie*, Vol 348, pp. 1–10.

Shenvi, S, Kumar, K, Hatti, KS, Rijesh, K, Diwakar, L, Reddy, GC 2013, 'Synthesis, anticancer and antioxidant activities of 2, 4, 5-trimethoxy chalcones and analogues from asaronaldehyde: structure-activity relationship', *European Journal of Medicinal Chemistry*, Vol 62, pp. 435–442.

CHAPTER 11

CONCLUSION

The primary objective of this research study was to generate a whole new class of effective tyrosinase inhibitors that could be targeted for use as potential depigmentation agents or as food additives to curb enzymatic browning. Chalcones from natural and synthetic sources have long shown to have potent tyrosinase inhibitory activities. Chemically, chalcones were the coupling products of benzaldehydes with ketones, playing their role as intermediates in the biosynthesis of flavonoids, microtubule formation and tubulin inhibition, which is vital in cellular processes like cell replication, cytoplasmic organelle movement, mitosis and for the regulation of cell shape. Dihydroxy substitutions in the aromatic ring of chalcones have shown to be vital in exerting strong tyrosinase inhibition. Also the chalcone framework resulted in a molecular skeleton that was closely similar with the enzyme substrate. The ease of synthesis and diverse biological activities made chalcone a versatile molecule to be chosen as the pharmacophore for the current research study. Thus, the aim of the present study was to investigate the structure activity relationship and contribution of different functional groups on the chalcone skeleton with the view to optimizing the design of depigmentation agents.

Chalcone skeleton was chosen as the pharmacophore of interest because of their broad spectrum of biological activities. The promising anticancer and tyrosinase inhibitory potential of chalcones served as the impetus to evaluate a series of synthetic chalcones for their inhibitory effects on the diphenolase activity of mushroom tyrosinase and on B16F10 murine melanoma cell lines.

The current study generated the synthesis and development of a series of α , β -unsaturated carbonyl based compounds as prospective tyrosinase inhibitors that could be targeted for use as depigmentation agents in the field of cosmetics or as anti-browning additives in the field of agriculture. This research has resulted in a genre of several novel chalcone derivatives. Facile Claisen-Schmidt condensation reaction was used to synthesize a whole library of novel chalcone compounds that comprised of azachalcones, naphthylchalcones, methoxychalcones, polymethoxychalcones and 1-indanone chalcone-like compounds. Assays were performed with L-DOPA as the substrate, using kojic acid, a well-known strong tyrosinase inhibitor as the positive control. The type of enzyme inhibition, the inhibition constant (K_i) for an enzyme-inhibitor complex and their mechanisms were analyzed by Lineweaver–Burk plots and Dixon plots, respectively. To confirm that the active site of tyrosinase was the likely

242

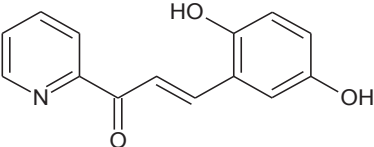
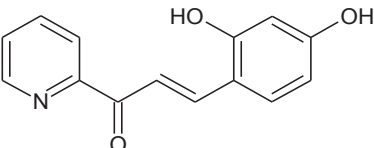
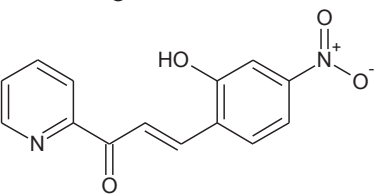
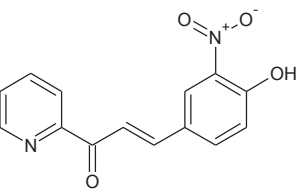
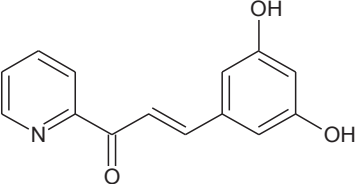
binding site of the inhibitors, modeling studies were performed using Accelrys Discovery Studio 4.5. In the present study, tyrosinase extracted from the edible mushroom *Agaricus bisporus* was used due to its easy availability and high homology with the mammalian enzyme that rendered it well suited as a model for studies on melanogenesis.

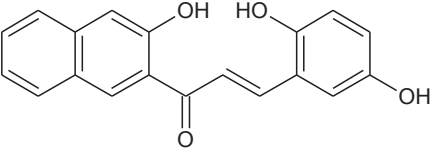
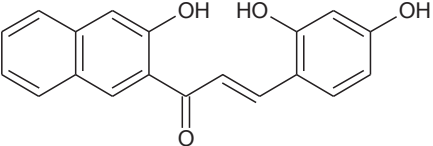
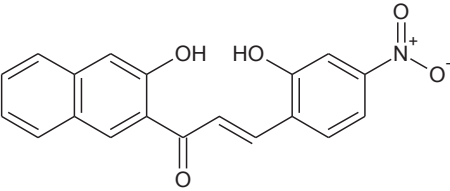
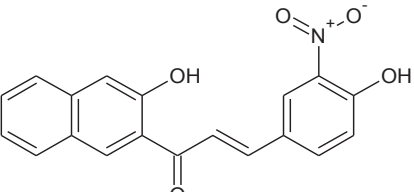
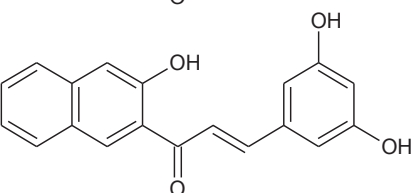
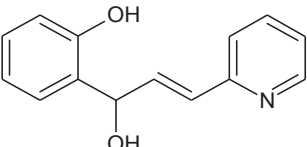
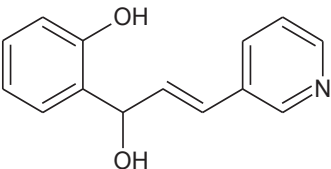
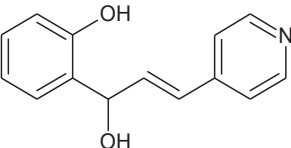
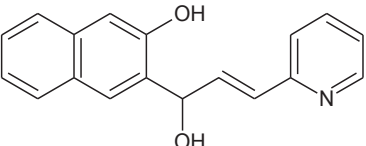
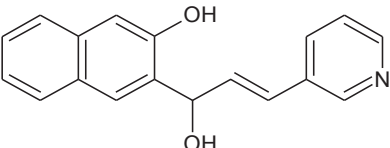
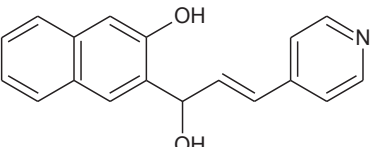
SAR studies have identified hydroxyl as the functional group indispensable for tyrosinase inhibitory activity. Replacement of 2'-hydroxy group resulted in a complete loss of tyrosinase inhibition. *In silico* docking studies showed that the hydroxyl group of the ligand could block the tyrosinase activity by binding to the copper atoms in the active site of the enzyme tyrosinase. Thus the methoxychalcones were dealkylated to their corresponding hydroxy compounds in the presence of boron tribromide. These compounds were found to be more potent than the positive control, kojic acid and the tyrosinase inhibitory activity was found to be higher when the hydroxyl group was introduced in the *p*-position with respect to the *o*-position. Also, compound (**2b**) with a 2,4-substituted resorcinol structure showed threefold better tyrosinase inhibition (K_i : 3.9 μ M) than kojic acid, probably because it had a molecular skeleton closely similar to that of the substrate L-tyrosine. Phenolic hydroxyl groups were found to coordinate with the copper atoms causing inhibition of the enzyme in competition with the catechol substrate. Additionally, the introduction of electron-withdrawing groups on ring B was found to increase the electrophilicity of the β -carbon, thus improving the bioactivity of the resulting compounds. Presence of a strong electron releasing group in the ortho position (-OH) and an electron withdrawing group (-NO₂) in the para position (**3b**) modulated the electronic structure of ring B significantly, thereby leading to its better tyrosinase inhibitory potential (50.2%). Results indicated that electron-donating groups contributed more to the inhibitory activity of the compounds on mushroom tyrosinase than the electron-withdrawing groups.

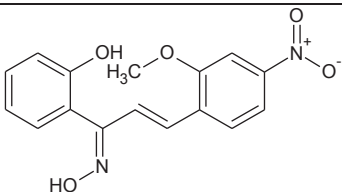
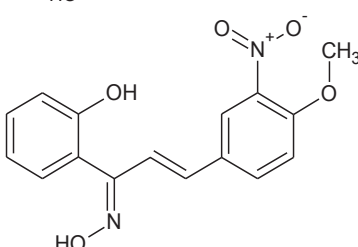
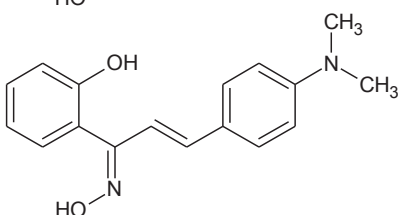
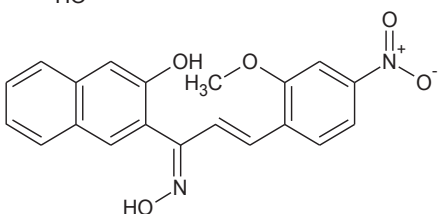
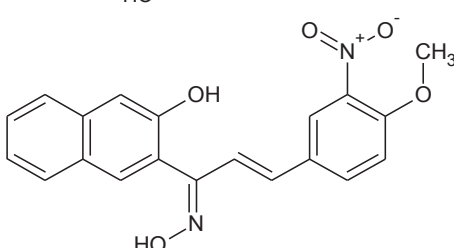
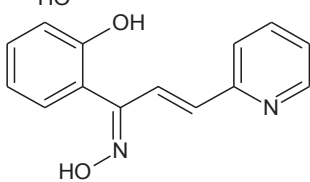
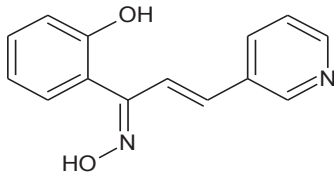
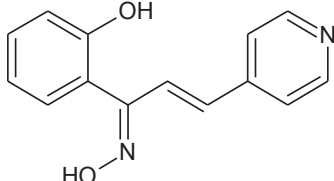
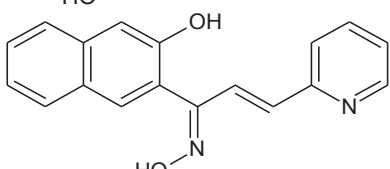
Furthermore, replacement of the phenyl group with a naphthyl group led to a significant decline in inhibitory activities indicating that the bulky naphthyl group in ring A of the chalcone compounds might cause stereo-hindrance for the inhibitors approaching the active site. However, the naphthylchalcone compounds showed better tyrosinase inhibition in comparison with the reference standard, kojic acid. A structural advantage could be attributed to the naphthyl ring that could exert a nucleophilic action on the dihydroxy phenyl ring. Also, hydroxylation at 5-position in the

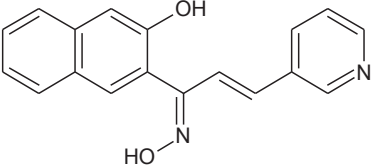
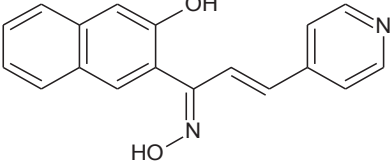
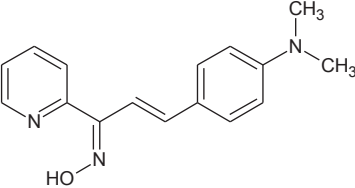
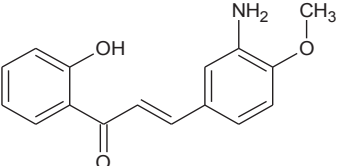
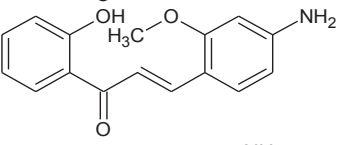
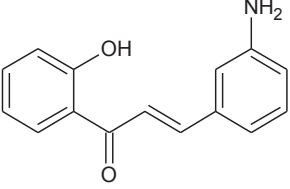
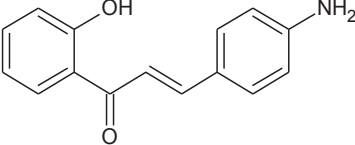
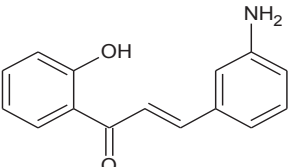
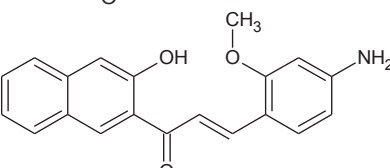
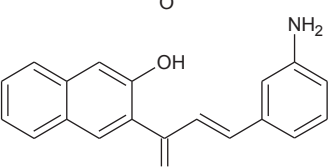
hydroxynaphthylchalcone compound (**10b**) was the molecular modification that led to a strong coordination with the copper ion in the active site of tyrosinase enzyme. The 5-OH group complexed with the binuclear copper active site of tyrosinase and interacted thereby with the hydrophobic enzyme pocket, leading to enhanced inhibitor-enzyme binding affinity and improved inhibitory effects on mushroom tyrosinase. Moreover, the binding of the inhibitor via a coordinate bond was seen to effectively block the access of the substrate to the active site of the enzyme tyrosinase. This resulted in decreasing the enzymes ability to oxidize the substrate subsequently leading to an inhibition in mushroom tyrosinase. Hence a design principle encouraging strong coordination with the copper ions was warranted as the metal centres formed a key part of the enzyme machinery.

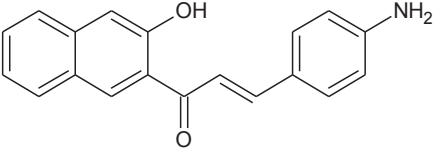
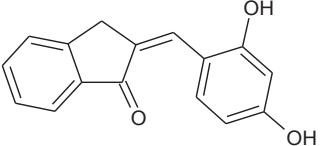
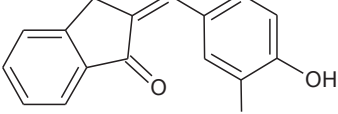
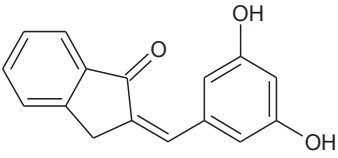
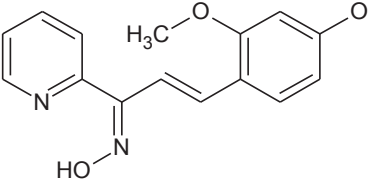
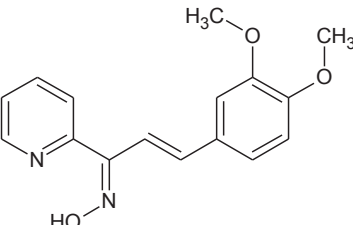
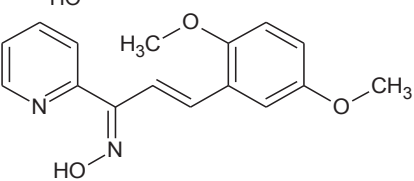
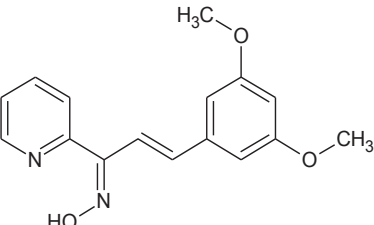
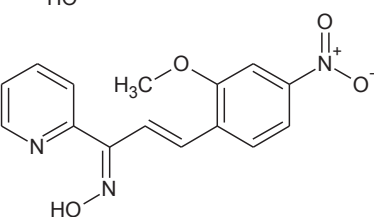
Table 21 Inhibition effects and docking results of chalcone derivatives on mushroom tyrosinase

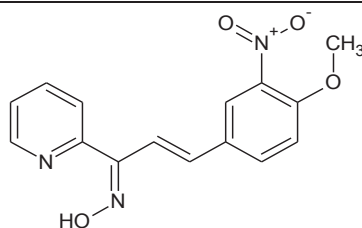
Compound	Structure	IC ₅₀ (μM)	Dock Score (kcal/mol)
1b		20.27	-21.16
2b		12.45	-25.98
3b		22.95	-20.34
4b		18.45	-23.89
5b		10.22	-27.00

6b		20.4	-22.35
7b		14.4	-19.25
8b		22.9	-16.83
9b		25.6	-16.23
10b		10.4	-22.36
11b		8.70	-24.89
12b		15.60	-20.22
13b		10.25	-21.92
14b		26.23	-10.40
15b		24.55	-12.09
16b		24.82	-12.63

17b		4.77	-28.94
18b		12.55	-18.50
19b		7.89	-25.89
20b		25.36	-14.50
21b		22.44	-16.25
22b		15.3	-27.93
23b		12.7	-27.05
24b		18.62	-24.00
25b		20.55	-13.37

26b		18.22	-18.78
27b		21.25	-13.64
28b		19.85	-14.52
29b		9.75	-25.86
30b		7.82	-26.74
31b		16.75	-23.77
32b		12.75	-24.54
33b		22.50	-13.90
34b		23.12	-11.39
35b		20.55	-12.13

36b		28.78	-7.67
41b		12.3	-22.35
42b		8.2	-19.25
43b		20.2	-12.24
44b		11.22	-22.84
45b		12.54	-16.75
46b		6.37	-27.89
47b		13.55	-24.74
48b		12.22	-26.40



14.20

-17.71

The formation of a strong intramolecular hydrogen bond (2.01 Å) between the 2'-OH and the carbonyl group was seen to hamper interactions of the ligand with the receptor. This posed an impetus to progress the research by selectively reducing the carbonyl group by Luche reduction with a Lewis acid catalyst like cerium chloride, thus leading to a new series of allyl alcohol derivatives of chalcones as tyrosinase inhibitors.

An interesting feature observed here was the facile synthesis of chalconeoximes by a solid-state solvent free method. Eliminating the carbonyl group progressively increased tyrosinase inhibitory activity. This demonstrated the negative effect of carbonyl group and identified the major role of selective carbonyl reduction that led to an enhancement in flexibility of the chalcone compound (**11b** & **13b**). The nitrogen atom in pyridine skeleton of compound **11b** was seen to coordinate with the copper atoms present in the tyrosinase active site.). There was a weak coordination between Cu401 and the hydroxy oxygen (**2'**) of the ligand **11b** at a distance of 3.21 Å. Tyrosinase substrates like L-DOPA also bind to the copper ion of tyrosinase via their OH group. Coordinate bonds thus make a major contribution to the binding of an inhibitor in the active site.

Compound **11b** formed one hydrogen bond at a distance of 2.25 Å where the hydrogen from His259 (HE₁) donated a hydrogen bond to the alcoholic oxygen on the alpha carbon atom. Additionally, the alpha-hydrogen atom formed a hydrogen bond (2.26 Å) with the carbonyl oxygen of Asn260. This helped the compound to fit into the catalytic pocket.

Literature review had shown phenyl and naphthyl chalcones substituted with electron donating methoxy groups on ring B to possess significant cytotoxic activities, when tested on cancer cell lines. This served as the impetus to extend the research findings further by exploring the effect of methoxyazachalcones and methoxynaphthylchalcones on melanin formation in murine B16F10 cells. Studies on these methoxylated chalcones suggested that the number and position of methoxy substituents on the aromatic rings appeared to be critical for cytotoxicity with position 4 being favourable, while position

3 being unfavourable for cytotoxic activity. Replacement of the phenyl ring with a naphthyl ring led to compounds with moderate cytotoxicity. The introduction of pyridinyl group in chalcone was associated with enhanced cytotoxic activity (**1c** and **3c**). Also, placement of strong electron-withdrawing groups such as NO₂ in ring B (**7c**) correlated with increase of cytotoxic activity. Docking studies revealed the extended aromatic rings or the heteroatoms to increase the binding of these compounds to appropriate receptors through a van der Waals force or hydrogen bonding.

Tyrosinase inhibitors like tropolone and kojic acid have been found to be competitive inhibitors by chelating the copper in the active site of the enzyme (Kahn & Andrawis 1985; Chang 2009). The research study was then extrapolated to synthesize a series of novel chalcone oxime compounds based on *in silico* screening studies and on the literature that has shown hydroxamate molecules, to serve as ligands for different metal ions. The chelation involves the oxygen belonging to the =N-OH group. Hydroxy substituted chalcone oxime compounds, compounds **17b** and **19b** had similar features to those of hydroxamic acids and hydroxamates which were good chelating agents. Tyrosinase inhibition of compounds **17b** and **19b** depended on the competency of the inhibitor compounds to block access by any substrate molecule in the active site of enzyme. Strong co-ordination with the copper metal, significant hydrophobic and π - π stacking interactions contributed to effective tyrosinase inhibition. Also placement of strongly electron-withdrawing groups such as NO₂ in ring B (**17b**) correlated with increase of cytotoxic activity. The presence of strongly electron-withdrawing NO₂ group provided high electrophilicity.

From all the compounds synthesized, a novel 2'-acetylpyridinylchalconeoxime compound **46b**, ((1*Z*, 2*E*)-3-(2, 5-dimethoxyphenyl)-*N*-hydroxy-1-(pyridin-2-yl)prop-2-en-1-imine), imine exhibited the most potent tyrosinase inhibitory activity with an IC₅₀ value of 6.37 μ M. Compound **46b** reversibly inhibited the diphenolase activity of mushroom tyrosinase and was found to be several times potent than the reference standard, kojic acid (IC₅₀; 27.95 μ M). The inhibition mechanism was competitive with a K_i value of 4.82 μ M. This was in complete agreement with the docking results that showed a dock score of -27.89 kcal mol⁻¹. The higher tyrosinase inhibition of compound **46b** could be accounted for the presence of strongly activating methoxy substituents that increase the reactivity of aromatic ring system by resonance effects. The oxime OH

group was actively involved, both as donor (via the O-H moiety) and as hydrogen bond acceptor (via the N=C-OH moiety), in hydrogen bonding interactions.

Several *p*-amino phenols have been reported to be useful alternatives to kojic acid as a tyrosinase inhibitor and as potent inhibitors of melanogenesis. Aminochalcones were synthesized from their respective nitrochalcone derivatives by transfer hydrogenation reaction using ammonium formate catalyzed by palladium on carbon. Amongst the series of aminochalcone compounds, compound **30b** (*(2E)*-3-(4-amino-2-methoxyphenyl)-1-(2-hydroxyphenyl)prop-2-en-1-one) exhibited the most potent tyrosinase inhibitory activity with inhibition of 75.51% and an IC₅₀ value of 7.82 μM. Copper ion (Cu400) was strongly bound by the hydroxyl group (**2'**) of compound **30b** at a distance of 1.95 Å. There was also a weak coordination between Cu401 and the hydroxy oxygen (**2'**) of the ligand **30b** at a distance of 3.15 Å. The lower tyrosinase inhibition of compound **29b** could be accounted for the formation of a strong intramolecular hydrogen bond (1.95 Å) formed between the **2'-hydroxyl** hydrogen with the carbonyl oxygen.

Kinetic studies revealed it to act as a competitive tyrosinase inhibitor with a K_i value of 1.89 μM. Presence of strong electron releasing groups in the ortho position (-OMe) and a strongly activating para amino substituent modulates the electronic structure of ring B significantly. The fact that the activity is markedly affected by altering the substituents on the aminophenyl ring, suggests that this aromatic ring makes a specific contribution to the binding via an aromatic ring orientation. Replacement of the phenyl group with a naphthyl group led to a slight decline in inhibitory activities (compounds **20b** and **21b**) indicating that the bulky naphthyl group in ring A of the aminochalcone compounds might cause stereo-hindrance for the inhibitors approaching the active site. Docking results demonstrated π-π stacking interactions between ring A of compound **30b** with the imidazole ring of His263 and T-shaped edge to face aryl-aryl interactions with Phe264 whereas amide-π interactions were observed with Ser282 and Val283. In cell based experiments, compound **30b** showed very effective inhibition of both melanin production and tyrosinase activity, suggesting amino chalcones to be a promising candidate for use as depigmentation agents in the field of cosmetics or as anti-browning food additives in the field of agriculture.

Therefore, these compounds could find applications in human medicine, particularly in dermatology and cosmetics. It was anticipated that the findings from this research study

could lead to the discovery of highly efficient pharmacological agents for the treatment of tyrosinase-related disorders.

Taken together, the principal findings of this research study included the following structural features that warranted a suitable design principle for an effective strong tyrosinase inhibitor:

- The ease of synthesis and diverse biological activities made chalcone a versatile molecule to be chosen as the pharmacophore.
- Presence of 2'-OH group in ring A was found to be indispensable for better tyrosinase inhibitory activity. The 2'-OH group formed strong coordination with Cu400 which formed a key part of the enzyme machinery. A design principle encouraging strong coordination with the copper ions was warranted, thus preventing electron transfer by the metal ion.
- The formation of a strong intramolecular hydrogen bond between the 2'-hydroxyl hydrogen with the carbonyl oxygen resulted in lowered tyrosinase inhibition. This was circumvented by selective reduction of the carbonyl moiety to its corresponding allyl alcohol derivative that had better tyrosinase inhibition.
- Heterocyclic nitrogen atom on ring A brought about a significant increase in tyrosinase inhibition as the nitrogen atom in pyridine skeleton was found to coordinate with the copper atoms present in the tyrosinase active site. However, a pyridinyl nitrogen atom on ring B that formed a strong intramolecular hydrogen bond formed between the pyridinyl nitrogen and the oxygen atom of oxime group brought about a substantial decline in tyrosinase inhibitory potential.
- The presence of strongly electron-withdrawing NO₂ group on ring B provided high electrophilicity and correlated with increase of cytotoxic activity in murine melanoma cell lines.
- Reduction of nitrochalcone compounds to their amino derivatives brought about an increase in hydrogen bonding interactions with the active site of enzyme tyrosinase, subsequently resulting in strong inhibitory potential.
- Introduction of an oxime group resulted in strong tyrosinase inhibition as the oxime OH group was actively involved, both as donor (via the O-H moiety) and as hydrogen bond acceptor (via the N=C-OH moiety), in hydrogen bonding

interactions. This in turn, helped the compounds to have a better fit to the catalytic pocket of the enzyme tyrosinase.

- It was noteworthy that replacement of 2'-OH phenyl group in ring A with a 1'-indanone ring brought about a significant decline in tyrosinase inhibitory activity.
- 1-indanone chalcone-like compounds that retained a catechol moiety showed significant tyrosinase inhibition due to a structural resemblance with the substrate L-DOPA. This led to the competitive displacement of L-DOPA from the active site of the enzyme tyrosinase in a lock-and key model.
- Extension of the aromatic ring or replacement of phenyl with a naphthyl ring brought about moderate tyrosinase inhibition, but was still greater than the reference standard.

These results presented here suggested that these molecules could serve as the interesting candidates for the treatment of tyrosinase related disorders and as the lead compounds for the development of new and potent tyrosinase inhibitors. Therefore, further studies of these compounds using human tyrosinase and a human melanoma cell line are warranted in future.

11.1. Future prospects

Malignant melanoma arises from malignant transformation of melanocytes, the pigment producing cells, which are located and evenly distributed in the basal epidermal layer of the skin. Statistics have revealed that each year in Australia, between 95-96% of skin cancers are caused by exposure to the sun. Melanin biosynthesis involves the enzyme tyrosinase that catalyzes the first two steps in the melanin-biosynthesis pathway: the hydroxylation of L-tyrosine to L-DOPA (L-3, 4-dihydroxyphenylalanine) and oxidation of L-DOPA to DOPA quinone, the primary and necessary requisite of melanogenesis is the generation of *ortho* quinones.

In cancer research, it is interesting to synthesize non-toxic prodrugs which are converted to the toxic drugs selectively at the tumor site by enzymes that are only present at the tumor. This obviates the need for administering the cytotoxic drugs themselves, which have poor selectivity for cancer cells. This necessitates the need to probe the feasibility

of involving tyrosinase in enzyme-directed selective chemotherapy strategies for melanoma. The current method involves the use of potent ortho-hydroxy substituted chalcone compounds as tyrosinase substrates to maximize the formation of reactive ortho-quinone oxidation products. If these quinones are released into the cytosol, through the defective membrane of the malignant melanocytes, they have the potential to react with vital cellular components and hence cause cell death.

This research is aimed in giving a new dimension to the treatment of malignant melanomas prevalent in Australia and world-wide through the discovery of non-toxic prodrugs. In addition, this would lead to the discovery of novel potent depigmentation agents that could be used synergistically in a formulation with sunscreens. Also, these compounds could be targeted for use as anti-browning food additives to improve the aesthetic appeal in the field of agriculture.

CHAPTER 12

GENERAL EXPERIMENTAL

12.1. Chemical reagents and instruments

Unless otherwise stated, all the materials were purchased from suppliers and were used without further purification. Tyrosinase, L-3,4-dihydroxyphenylalanine (L-DOPA), kojic acid and α -MSH (alpha- melanocyte stimulating hormone) were purchased from Sigma–Aldrich Chemical Co.

Melting points (Mp) were determined with WRS-1B melting point apparatus and the thermometer was uncorrected. NMR spectra were recorded on Agilent 500 spectrometer at 25⁰ C in CDCl₃ or DMSO-d₆. All chemical shifts (δ) are quoted in parts per million downfield from TMS and coupling constants (J) are given in Hz. Abbreviations used in the splitting pattern were as follows: *s* = singlet, *d* = doublet, *t* = triplet, *m* = multiplet. All ¹³C NMR spectra were recorded on Agilent 500 spectrometer at 25⁰ C in CDCl₃ or DMSO-d₆. HRMS spectra were recorded using the Agilent Technologies 6520 LC/MS-QTOF. All reactions were monitored by TLC (Merck Kieselgel 60 F254) and the spots were visualized under UV light. Infrared (IR) spectra were recorded on Thermo Scientific NICOLET 6700 FT-IR spectrometer in the range of 4000-600cm⁻¹. Solid samples were measured as KBr pellets.

Reactions were run in flame-dried round-bottomed flasks under an atmosphere of nitrogen or argon. All the reactions made the use of magnetic stirring bars.

12.2. General method for the synthesis of chalcone derivatives.

To a stirred solution of the appropriate ketone (1 mM) and a substituted aldehyde (1mM) in 25 ml methanol, was added pulverized NaOH (2mM) and the mixture was stirred at room temperature for 24–36 h. The reaction was monitored by TLC using *n*-hexane: ethyl acetate (7:3) as mobile phase. The reaction mixture was cooled to 0⁰C (ice-water bath) and acidified with HCl (10 % v/v aqueous solution) to afford total precipitation of the compounds. In most cases, a yellow precipitate was formed, which was filtered and washed with 10 % aqueous HCl solution. In the cases where an orange oil was formed, the mixture was extracted with CH₂Cl₂, the extracts were dried (Na₂SO₄) and the solvent was evaporated to give the respective chalcone.

12.3. Method for the synthesis of hydroxy derivatives of methoxychalcones.

A solution of BBr₃ (2.5 mL for each methoxy group) was added to a cooled solution of the corresponding methoxychalcone (1 mmol) in CH₂Cl₂ under argon. The cooling bath

was removed and the dark solution was warmed to RT and stirred for 1–5hrs. The dark solution was then poured into ice water and filtered. The aqueous layer was extracted with chloroform twice. The organic extract was washed with water followed by brine and dried over anhydrous sodium sulfate. This was then rotary evaporated to give the respective hydroxy derivative.

12.4. Method for the synthesis of allyl alcohols of chalcone compounds.

A solution of the respective azachalcone (1mmol) in methanol was treated with 2.5 equivalents of cerium(III) chloride heptahydrate at room temperature, followed by the addition of six equivalents of sodium borohydride in portions at 0° C with vigorous stirring. The reaction mixture was allowed to warm to room temperature within five hours. After monitoring the completion of the reaction with TLC, the reaction was quenched with ammonium chloride to obtain the respective compound.

12.5. General method for the synthesis of hydroxy chalcone oxime compounds

A mixture of chalcones (1 mmol), hydroxylamine hydrochloride (1.5 mmol), and anhydrous sodium sulfate (1 mmol) was refluxed in ethanol (5 mL) under stirring for the period (the reaction was followed by TLC). After completion of the reaction, the mixture was filtered, and the solvent was evaporated under reduced pressure. Then distilled water (10 mL) was added, and ethyl acetate (10 mL×3) was added to extract organic compounds. The combined organic layers were dried over anhydrous sodium sulfate and filtered. Evaporation of the solvent in reduced pressure gave the crude product, which was purified by column chromatography on silica (200-300 mesh), eluted with petroleum ether (60-90 °C) or a mixture of petroleum ether and ethyl acetate (v/v = 1:4) to yield the pure oxime products.

12.6. General method for the synthesis of amino chalcones.

To a stirred suspension of the appropriate nitro chalcones (5mmol), 0.25 g 10% palladium on charcoal in 10 cm³ dry methanol at room temperature, was added anhydrous ammonium formate (23 mmol), in a single portion under N₂. The resulting mixture was stirred at room temperature for 3 h. The catalyst was removed by filtration

through celite and washed with $2 \times 10 \text{ cm}^3$ methanol. The filtrate was evaporated under reduced pressure and the residue was taken up in CHCl_3 and washed with $3 \times 25 \text{ cm}^3$ H_2O . The organic layer was dried (Na_2SO_4) and evaporated to dryness to give the aminochalcone products.

12.7. Method for the synthesis of chalcone compounds by solid state synthesis.

A mixture of the appropriate aromatic ketone (2 mmol), aromatic aldehyde (2 mmol), and sodium hydroxide (7 mmol) was thoroughly ground with a pestle in an open mortar at room temperature for 2–3 min until the mixture turned into a melt. The initial syrupy reaction mixture solidified within 3–5 min. Grinding continued for 5–10 min more, and the reaction was monitored by TLC. The solid was washed with cold water to remove the sodium hydroxide and recrystallized from methanol to give the corresponding chalcone derivative.

12.8. Method for the synthesis of chalconeoximes by solid state synthesis.

A mixture of azachalcone (1 mmol), hydroxylamine hydrochloride (1.2 mmol) and Calcium oxide (0.6 mmol) was ground in a mortar with a pestle. On completion of the reaction as monitored by TLC, ethylacetate ($2 \times 10 \text{ mL}$) was added to the reaction mixture and filtered to separate the CaO . The filtrate was concentrated down to approximately 6 mL and then poured into crushed ice to obtain the product as a precipitate. The precipitate was filtered and dried in high vacuum to yield the pure oxime.

12.9. Tyrosinase inhibition assay

The mushroom tyrosinase inhibition activity of all tested compounds was measured using L-DOPA as substrate (Lin et al 2012). Mushroom tyrosinase, L-DOPA and tested samples were prepared by dissolving in 50 mM $\text{Na}_2\text{HPO}_4\text{--NaH}_2\text{PO}_4$ buffer (pH 6.8). Reaction mixtures containing 50 μL of $2 \text{ mmol} \cdot \text{L}^{-1}$ of L-DOPA, 50 μL of phosphate buffer and 50 μL of different concentrations (0.5 μM , 1.0 μM , 2.5 μM , 5.0 μM and 10.0 μM) of tested compounds were added in 96 well microtiter plates, followed by the addition of 50 μL of $0.2 \text{ mg} \cdot \text{mL}^{-1}$ of mushroom tyrosinase. The assay mixture was incubated at 25 $^\circ\text{C}$ for 10 min. Then the enzyme reaction was monitored by measuring the change in absorbance at 492 nm of formation of the DOPA chrome for 1 min. The

IC₅₀, that is, the concentration of compound that causes 50% inhibition for kojic acid and the active inhibitors were determined. Dose-dependent inhibition experiments were performed in triplicate to determine the IC₅₀ of test compounds. The average results from three experiments were computed.

12.10. Determination of the inhibition type of respective active compounds on mushroom tyrosinase.

Inhibitors were first dissolved in DMSO and used for the test after a 30-fold dilution. The final concentration of DMSO in the test solution was 3.33%. Mushroom tyrosinase (50 µL; 0.2 mg·mL⁻¹) was incubated with 50 µL of various concentrations of enzyme substrate ((0.2-0.6 mM) and 50 µL of phosphate buffer, and then 50 µL of different concentrations of tested samples (0, 1.25, 5.0 and 20.0 µM) were simultaneously added to the reaction mixtures. Pre-incubation and measurement time was the same as before. The measurement was performed in triplicate for each concentration and averaged before further calculation. The absorbance variations from these studies were used to generate Lineweaver–Burk plots to determine the inhibition type. The kinetic parameter (K_m) of the tyrosinase activity was calculated by linear regression from Lineweaver–Burk plots (Cho *et al* 2006). For the type of enzyme inhibition and the inhibition constant (K_i) for an enzyme-inhibitor complex, the mechanisms were analyzed by Dixon plot, which is a graphical method [plot of 1/enzyme velocity (1/V) versus inhibitor concentration (I)] with varying concentrations of the substrate.

12.11. *In silico* docking between tyrosinase and target compounds.

To further understand the binding modes of the most active compounds with mushroom tyrosinase, molecular docking studies of active chalcone compounds were performed using Discovery Studio 4.5 (Accelrys, San Diego, CA, USA). To model the tyrosinase structure, we used the crystal structure of *Agaricus bisporus* tyrosinase (PDB ID: 2Y9X), A chain. Hot spot identification revealed the natural ligand tropolone binding at the same site as that of the inhibitor compounds. Tropolone was removed and docking was done for the inhibitor compounds. From the docking results, we checked for possible hydrogen-bonding and non-bonding interactions with the amino acid residues.

12.12. *In vitro* cytotoxicity studies

12.12.1. Cell culture

B16 F10 cells (obtained from National Centre for Cell Sciences (NCCS), Pune, India) were cultured in Dulbecco's Modified Eagle's Medium (DMEM; Sigma Aldrich Co, St Louis, USA) with 10% fetal bovine serum (FBS) and penicillin/streptomycin (100 IU.50 $\mu\text{g ml}^{-1}$) in a humidified atmosphere of 5% CO_2 at 37°C. B16 cells were cultured in 24-well plates for melanin quantification and enzyme activity assays.

12.12.2. Cell viability

Cell survival was quantified by a colorimetric assay that used 3-(4, 5-dimethylthiazol-2-yl)-2, 5-diphenyltetrazolium bromide (MTT) and that measured mitochondrial activity in viable cells. This method is based on the conversion of MTT (Sigma) to MTT-formazan crystals by a mitochondrial enzyme, as previously described (Tada et al 1986). Briefly, cells seeded at a density of 3×10^4 /cell in a 48-well plate, were allowed to adhere overnight; the culture medium was then replaced with fresh serum-free DMEM. MTT was freshly prepared at 5mg/ml in phosphate-buffered saline (PBS). Aliquots of 500 μl of MTT stock solution were added to each well, and the plate was incubated at 37 °C for 4 h in a humidified 5% CO_2 incubator. After 4 h, the medium was removed. To each well, 500 μl of EtOH-DMSO (solution of a 1:1 mixture) was added to dissolve the formazan. After 10 min, the optical density of each well was measured spectrophotometric ally using a 560 nm filter.

12.12.3. Assay of murine tyrosinase activity

Tyrosinase activity was estimated by measuring the rate of L-DOPA oxidation (Kim et al 2002). Cells were plated in 24-well dishes at a density of 5×10^4 cells ml^{-1} . B16 cells were incubated in the presence or absence of 100 nM α -MSH, and then treated for 24 h with various concentrations of **2a** or **2b** (0-10 μM). Cells were washed and lysed in 100 μl of 50 mM sodium phosphate buffer (pH 6.5) containing 1% Triton X-100 (Sigma) and 0.1 mM PMSF (phenylmethylsulfonyl fluoride), and then frozen at -80 ° C for 30 min. After thawing and mixing, cellular extracts were clarified by centrifugation at 12,000 rpm for 30 min at 4 °C. An 8 μl sample of the supernatant and 20 μl of L-DOPA

(2 mg ml⁻¹) were placed in a 96-well plate, and the absorbance at 492 nm was read every 10 min for 1 h at 37 °C using an ELISA plate reader. The final activity is expressed as Δ O.D. min⁻¹ for each condition.

12.12.4. Determination of melanogenesis in B16 cells

Determination of melanin content of cells was done using a modification of the method of Bilodeau et al (Bilodeau et al 2001). In the present study, the amount of melanin was used as an index of melanogenesis. B16 F10 cells (5×10^4) were transferred to 24-well dishes and incubated in the presence or absence of 100 nM α -MSH. Cells were then incubated for 24 h with various concentrations of **2a** and **2b** (0-10 μ M). After washing twice with PBS, samples were dissolved in 100 μ l of 1N NaOH. The samples were then incubated at 60 °C for 1 h and mixed to solubilize the melanin. Absorbance at 405 nm was compared with a standard curve of synthetic melanin.

12.13. References

Bilodeau, ML, Greulich, JD, Hullinger, RL, Bertolotto, C, Ballotti, R, Andrisani, OM 2001, 'BMP-2 stimulates tyrosinase gene expression and melanogenesis in differentiated melanocytes', *Pigment Cell Research*, Vol 14, pp. 328–336.

Cho, SJ, Roh, JS, Sun, WS, Kim, SH, Park, KD 2006, 'N-Benzylbenzamides: a new class of potent tyrosinase inhibitors', *Bioorganic and Medicinal Chemistry Letters*, Vol 16, pp. 2683–2684.

Kim, DS, Kim, SY, Chung, JH, Kim, KH, Eun, HC, Park, KC 2002, 'Delayed ERK activation by ceramide reduces melanin synthesis in human melanocytes', *Cellular Signalling*, Vol 14, pp. 779–785.

Lin, YF, Hu, YH, Jia, YL, Li, ZC, Guo, YJ, Chen, QX, Lin, HT 2012, 'Inhibitory effects of naphthols on the activity of mushroom tyrosinase', *International Journal of Biological Macromolecules*, Vol 51, pp. 32–36.

Tada, H, Shiho, O, Kuroshima, K, Koyama, M, Tsukamoto, K 1986, 'An improved colorimetric assay for interleukin 2', *Journal of immunological methods*, Vol 93, pp. 157–165.

CHAPTER 13

APPENDIX

13.1. Kinetics of mushroom tyrosinase

All energetically favourable biochemical reactions (i. e., those occurring with a decrease in the free energy), need to overcome a potential energy barrier, known as the activation energy, before the reaction can take place. Enzymes act as catalysts by allowing the formation of different, more stable, transition states, and thus reduce the activation energy. In effect, the position of chemical equilibrium remains unchanged, but it is reached much faster than the corresponding unanalyzed reaction. Enzymes react with substrates to form enzyme-substrate complexes. These are quite distinct from the transition states which also occur as part of the process of enzyme catalysis. A single substrate enzyme-catalyzed reaction can therefore be described by the equation



[E], [S] and [ES] are the concentrations of the enzyme, substrate and the enzyme-substrate complex at time t, respectively. Michaelis and Menten, in 1913, hypothesized that an equilibrium was obtained and maintained between E, S and ES. Therefore, a hyperbolic relationship exists between the initial velocity, v_0 , and initial substrate concentration [S], such that at a constant total enzyme concentration, [E];

$$v_0 = (V_{\max}[S]) / [S] + K_m$$

This is referred to as the Michaelis-Menten equation. K_m is the Michaelis-Menten constant and V_{\max} is the limiting initial velocity at a particular total enzyme concentration. K_m is independent of enzyme concentration, while V_{\max} increases as the total concentration of the enzyme present increases, i.e., $V_{\max} = k_{\text{cat}} [E]$. Thus equation can be rewritten such that;

$$v_0 = (k_{\text{cat}}/K_m) [E] [S]$$

where; k_{cat} is the turnover number, and [E] is the concentration of the free enzyme. The turnover number describes the maximum number of substrate molecules which can be converted to products per molecule of enzyme per unit time. These parameters, because they are unique to the system being studied, are usually used to characterize and identify a particular enzyme. K_m values describe the affinity of the enzyme for the substrate. The term k_{cat}/K_m is known as the catalytic efficiency. A comparison of k_{cat}/K_m values for

different substrates can be used as a measure of the specificity of the enzyme. Hence, the value of the kinetic parameters V_{\max} , K_m and k_{cat} often have to be determined.

Mushroom tyrosinase is a homo tetrameric protein, with a total molecular weight of 128,000. There are four atoms of copper (Cu^+) associated with the active enzyme. Two types of substrate binding sites exist in the enzyme, one type for the phenolic substrate and one type for the dioxygen molecule. L-DOPA is a natural substrate for this mushroom tyrosinase. The mechanism of enzyme catalyzed reactions is often studied by making kinetic measurements on enzyme-substrate reaction systems. These studies include measuring rates of the enzyme-catalyzed reactions at different substrate and enzyme concentrations. The kinetics of mushroom tyrosinase is observed by monitoring the oxidation of L-DOPA and measuring the increase in absorbance at 475nm. The rate of the reaction is determined for several different concentrations of substrate (L-DOPA) and enzyme (tyrosinase) with the pH, and temperature held constant for all runs. The rate at which tyrosinase enzyme works is influenced by several factors such as substrate concentration, temperature, pH and the presence of inhibitors. The oxidation of DOPA to DOPA-quinone is the rate determining step in the reaction sequence, and subsequent reactions occur very rapidly. Thus, the rate of formation of Dopachrome is almost the same as the rate of formation of DOPA quinone. At low concentrations of the substrate L-DOPA there is a linear increase in the initial velocity (**Figure 57**).

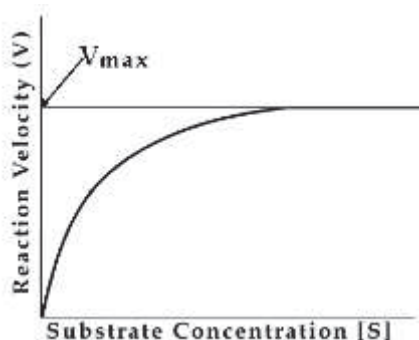


Figure 57 Tyrosinase assay

As the concentration of L-DOPA increases V assumes a rectangular hyperbola. The maximum reaction velocity is designated as V_{\max} . At V_{\max} , all enzyme molecules are complexed with substrate, and thus any additional substrate added to the reaction has no effect on the rate of reaction. The substrate concentration that

produces a velocity that is one-half of V_{\max} is designated the Michaelis-Menten constant, K_m . The lower the K_m , the greater the affinity or strength of binding between the enzyme and the substrate.

The mechanism of action of the inhibitor could be determined based on the Michaelis-Menten parameters obtained from the tyrosinase inhibition assays (Dixon & Webb 1976).

As per the Michaelis-Menten equation, the maximum conversion rate of substrate to product (V_{\max}) would be directly related to the concentration of the enzyme ($[E]$) present and the catalytic rate at which individual enzymes converted substrate molecules to product (k_{cat}). Plotting the reciprocals of the same data points yields a “double-reciprocal plot” This provides a more precise way to determine V_{\max} and K_m . A plot of $1/V$ vs. $1/[S]$ would give a straight line with a y-intercept = $-1/V_{\max}$ and a slope = K_m/V_{\max} . This plot is called a Lineweaver-Burke plot (**Figure 58**).

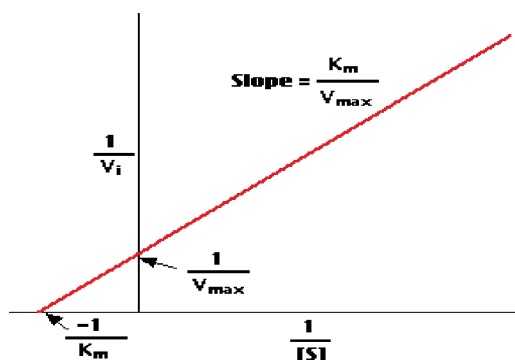


Figure 58 Lineweaver –Burk plot.

Hence, the smaller the value of K_m , the more efficient is the catalyst (Ferdinand 1976; Palmer 1991).

13.2. Enzyme inhibitors

Enzyme inhibitors are compounds which decrease the rate of an enzyme catalyzed reaction, by interacting with the enzyme, cofactor or substrate. In drug discovery, several drug analogues are chosen and/or designed to inhibit specific enzymes. However, detoxification or reduced toxic effect of many antitoxins is also accomplished mainly due to their enzyme inhibitory action. Therefore, studying the aforementioned enzyme kinetics and structure-function relationship is vital to understand the kinetics of

enzyme inhibition that in turn is fundamental to the modern design of pharmaceuticals in industries (Sami *et al* 2011).

There are two types of inhibitors reversible and irreversible. Irreversible inhibitors cannot be physically separated from the enzyme and their degree of inhibition tends to increase with time. In contrast, reversible inhibitors can be physically separated from the enzyme, e.g. by dialysis, to restore full enzymatic activity. They induce a definite degree of inhibition such that a steady-state equilibrium is usually obtained. Hence, they obey Michaelis-Menten kinetics. On the basis of the inhibition mechanism and its effects on the kinetic parameters, reversible inhibition for a single-intermediate enzymatic reaction can be described as competitive, uncompetitive, non-competitive, mixed effects or allosteric inhibition (Bitton & Dutka 1986; Michal 1978).

13.2.1. Reversible enzyme inhibition

Reversible enzyme inhibition can be competitive, uncompetitive, or linear mixed type. Some tyrosinase inhibitors are defined as competitive inhibitors, whereas others are non-competitive. For example, among the phenolic compounds, *p*-hydroxy benzoic acid is a competitive inhibitor of tyrosinase when L-DOPA is used as substrate whereas under the same experimental conditions, *o*-hydroxy benzoic acid, also called salicylic acid, is found to be a non-competitive inhibitor of tyrosinase (Kubo, Yokokawa & Kinst-Hori 1995; Kubo, Kinst-Hori & Yokokawa 1994).

13.2.2. Competitive inhibition

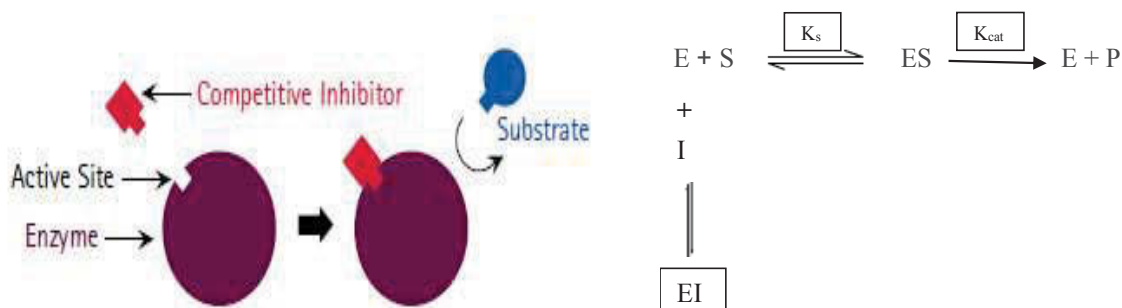


Figure 59 A simplified model of competitive inhibition

In this type of reversible inhibition (**Fig. 59**), a compound competes with an enzyme's substrate for binding to the active site (Palmer 1993; Leadlay 1978). This results in an apparent increase in the enzyme-substrate dissociation constant (K_s) (i.e., an apparent decrease in the affinity of enzyme for substrate) without affecting the enzyme's maximum velocity (V_{\max}).

The competitive inhibitor reduces the availability of free enzyme for the substrate binding. The Michaelis-Menten equation for competitive inhibitors becomes;

$$V_0 = \frac{V_{\max}[S]}{K_m + [S]}$$

For competitive inhibition, one can determine K_i , the inhibition constant, which is the dissociation constant for the enzyme-inhibitor complex. The lower the K_i value, the lower is the amount of inhibitor required to reduce the rate of reaction. The result of competitive inhibition can be presented in a Lineweaver-Burk plot (**Figure 60**). As the inhibitor concentration increases, K_m increases further and the X-intercept moves even closer to the origin. All lines go through the same Y-intercept, because a competitive inhibitor does not affect V_{\max} .

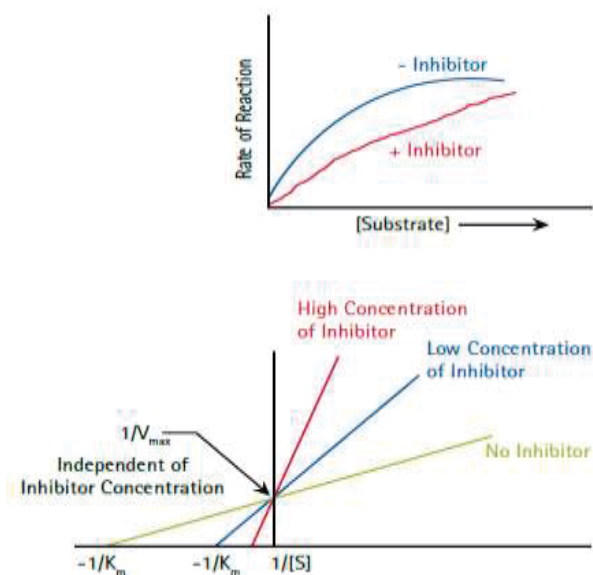


Figure 60 Kinetics of competitive inhibition

13.2.3. Non-competitive inhibition

In this type of inhibition, the inhibitor acts by binding to the active site or by inducing a conformational change which affects the active site, but either way it does not affect

substrate binding (**Fig. 61**). Therefore, for a single substrate reaction in the presence of a non-competitive inhibitor, the reaction scheme is as shown;

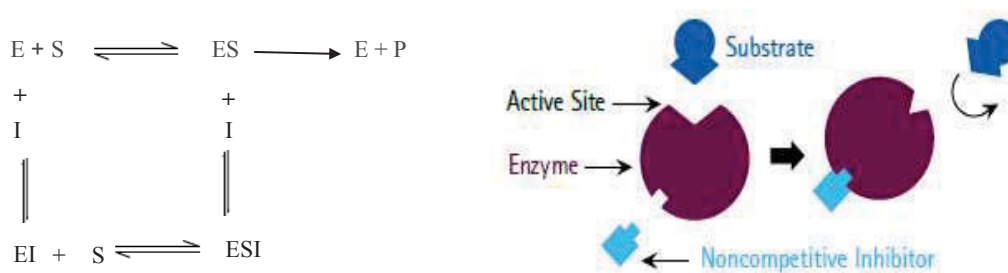


Figure 61. A simplified model of noncompetitive inhibition

Therefore, while K_m remains unchanged, V_{max} decreases in the presence of a non-competitive inhibitor. The degree of inhibition depends on the concentration of the inhibitor and its affinity for the enzyme or the enzyme-substrate complex. The effect of a noncompetitive inhibitor is graphically presented in **Fig. 62**. Since the Y intercept is $1/V_{max}$, as V_{max} decreases, $1/V_{max}$ increases. However, K_m remains the same for any concentration of the noncompetitive inhibitor. Hence, all lines go through the same X-intercept (Bennett & Frieden 1969; Holum 1968; Martinek 1969; Harrow & Mazur 1958; Pfeiffer 1954).

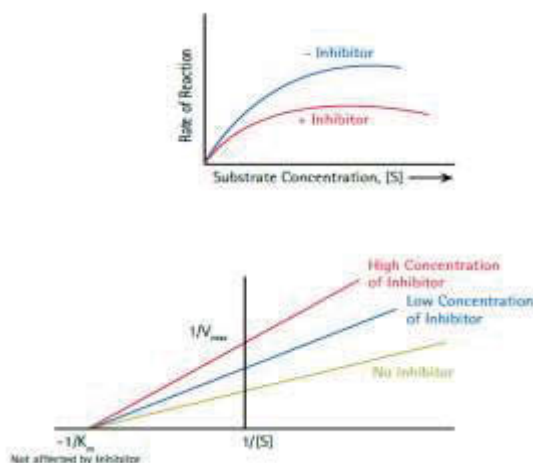


Figure 62 Kinetics of noncompetitive inhibition

13.2.4. Mixed type inhibition

In certain cases, an inhibitor can bind to both the free enzyme (with dissociation constant K_i) as well as the enzyme-substrate [ES] complex (with dissociation constant

K'_i). Here, the inhibitor binding can be reduced by adding more substrate, but inhibition cannot be totally overcome as in competitive inhibition. Mixed type inhibitors interfere with binding and reduce the effectiveness of turnover. This type of inhibition is mostly allosteric in nature, where the inhibitor binds to a site other than the active site to cause a conformational change in the enzyme structure, reducing the affinity of substrate for the active site. Hence, K_m is increased while V_{max} is reduced (**Fig. 63**). Kinetically, mixed type inhibition causes changes in the Michaelis-Menten equation so as;

$$V_0 = \frac{V_{max}[S]}{aK_m + a'[S]}$$

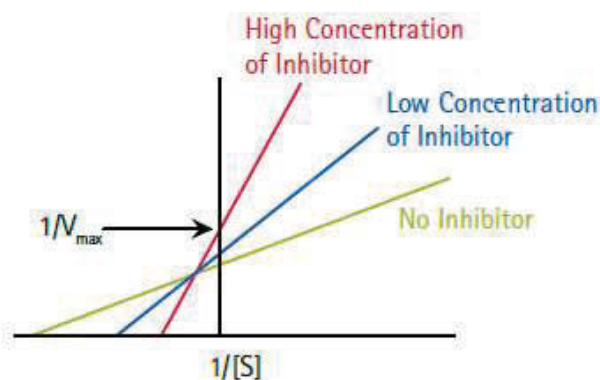


Figure 63 Kinetics of mixed inhibition

13.2.5. Uncompetitive inhibition

In this type of inhibition, the inhibitor does not affect the enzyme substrate binding. It binds to the enzyme-substrate complex but not to the free enzyme.

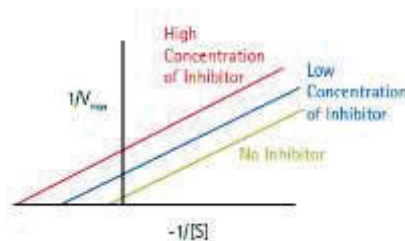
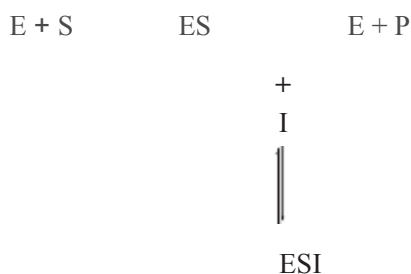


Figure 64 Kinetics of uncompetitive inhibition

Kinetically, uncompetitive inhibition modifies the Michaelis-Menten equation as;

$$V_0 = \frac{V_{\max}[S]}{aK_m + a'[S]}$$

In uncompetitive inhibition, V_{\max} is reduced because of the removal of activated enzyme-substrate complex. The amount of ESI complex depends on the concentration of the inhibitor. In uncompetitive inhibition, both K_m and V_{\max} decrease at the same time and at the same rate. In other words, V_{\max}/K_m is unaltered. **Fig. 64** shows that with uncompetitive inhibitor, $1/V_{\max}$ is increased. Hence, the Y-intercept moves up. Inhibition also increases $1/K_m$ to a degree that maintains the ratio of K_m/V_{\max} , which is the slope of the curve. For this reason, Lineweaver-Burk plots for uncompetitive inhibition are parallel, with and without inhibitor.

13.2.6. Irreversible inhibitors

Irreversible inhibitors are noncompetitive in nature. They include nonspecific protein denaturing agents, such as acids and alkalis, and specific agents, which attack a specific component of the holoenzyme system. Specific inhibitors can be grouped as: (a) coenzyme inhibitors; (b) inhibitors of specific ion cofactor; (c) prosthetic group inhibitors; (d) apoenzyme inhibitors; and (e) physiological modulators of the reaction, such as the pH and temperature that denature the enzyme catalytic site. Most irreversible inhibitors interact with functional groups on the enzyme and destroy enzyme activity. These interactions are covalent in nature. These inhibitors are highly useful in studying reaction mechanisms.

13.2.7. Suicide inhibition

A special group of irreversible inhibitors is known as suicide inhibitors. They are relatively unreactive until they bind to the active site of the enzyme. They are powerful tools in the study of kinetic and chemical mechanisms of enzymes. They often are also used as therapeutic agents in the *in vivo* modulation of the activity of target enzymes (Kitz & Wilson 1962; Ator & Ortiz De Montellano 1990; Walsh 1982; Walsh 1984). A suicide inhibitor is a relatively chemically stable molecule with latent reactivity such that when it undergoes enzyme catalysis, a highly reactive, generally electrophilic species (I^*) is produced. This species then reacts with the enzyme/coenzyme in a second step that is not part of normal catalysis, to form a covalent bond between I^* and E.

For a compound to be an ideal suicide inhibitor, it should be very specific for the target enzyme. The inhibitor should be stable under biological conditions and in the presence of various biologically active compounds and proteins. The enzyme-generated species I^* should be sufficiently reactive to be trapped by an amino acid side chain, or coenzyme, at the active site of the enzyme and not be released from the enzyme to solution. In general, addition of a suicide inhibitor to an enzyme assay will result in a time-dependent, exponential decrease to complete inactivation of the enzyme. The reactions do not always follow first-order kinetics. If $[I]$ decreases significantly throughout the progress of the assay, due either to compound instability or enzyme consumption, rates will deviate from first-order behavior and incomplete inhibition may be observed. Because they use the normal enzyme reaction mechanism to inactivate the enzyme, they are also known as mechanism-based inhibitors or transition state analogs (Silverman, 1995). Prodrugs undergo initial reactions to form an overall electrostatic and three-dimensional intermediate transition state complex form with close similarity to that of the substrate. These prodrugs serve as guidelines to further develop transition state molecules with modifications.

Tyrosinase suffers inactivation when it reacts with its *o*-diphenolic and triphenolic substrates (Escribano *et al.* 1989; Munoz-Munoz *et al.* 2010; Muñoz-Muñoz *et al.* 2008; Muñoz-Muñoz, *et al.* 2010; Chang 2007; Chang, Lin & Lin 2010; Tai, *et al.* 2009; Land, Ramsden & Riley, 2007). During the hydroxylation of monophenols to *o*-diphenols, whereby it was proposed that from the (enzyme–diphenol) complex generated, the *o*-diphenol may be oxidized to *o*-quinone, or be released to the medium as *o*-diphenol. This suicide inactivation is the result of catecholic substrates being processed by the cresolase route. As a result of this, one of the copper atoms at the active site is reduced to zero-valent copper ($Cu(0)$) which no longer binds to the enzyme and is eliminated (reductive elimination). This reductive elimination of a zero-valent copper atom rationalizes the resulting loss of 50% of the copper from the active site. The inactivation reaction is pH-sensitive and is suppressed by a competing cresolic substrate. To date, three types of mechanism have been proposed to explain the suicide inactivation of tyrosinase:

(a) an attack by the *o*-quinone product on a sensitive nucleophilic group vicinal to the active site (Ingraham, Corse & Makower, 1952)

(b) a free radical attack on the active site by the reactive oxygen species generated during the catalytic oxidation (Seiji, Sasaki & Tomita, 1978) and, more recently, (c) the processing of a catechol as though it was a monophenol (“cresolase”-type presentation). Kinetic studies in the transition phase and the steady state have shown that the o-diphenols bind to the form met-tyrosinase (E_m) more rapidly than to the form oxy-tyrosinase (E_{ox}) (Dietler & Lerch, 1982).

13.3. Docking and ligand-receptor interactions

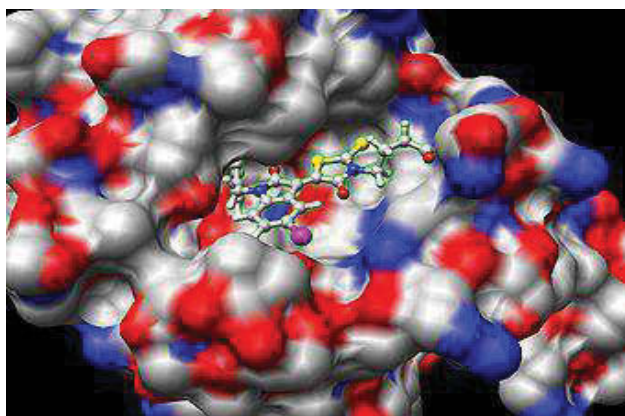


Figure 65 Molecule docked to a protein

It is important to know the 3-dimensional structure of receptor macromolecules so as to estimate the stability and stable structure of the drug-receptor complex. The conformation which a drug molecule or a natural substrate molecule adopts on its receptor is called the active conformation. The active conformation is not necessarily the most stable conformation. Knowledge of the active conformation helps evaluate structure activity relationships. Thus we can estimate stability of the ligand molecule with arbitrary conformation at arbitrary relative position, search for the mode of minimum energy binding and determine its stability. Such approaches are called docking studies (Taylor, Jewsbury & Essex, 2002). Hence docking is a computational procedure that predicts the non-covalent binding of macromolecules or of a receptor and a ligand utilizing their unbound structures obtained from molecular dynamic simulations or homology modelling. Docking studies are used to examine the mode and stability of binding of drugs to the target receptor in drug design (Wu *et al.* 2003). For this, the ligand molecule is subjected to a series of interactive three-dimensional manipulations (translation, rotation and bond rotation) inside the ligand binding site of

the protein with docking simulation studies (Lengauer & Rarey, 1996; Kitchen *et al.* 2004; Jorgensen, 1991). The protein-ligand interaction energy is a good indicator in modelling ligand molecules with strong affinity to the target protein (Wei *et al.* 2004). Empirical energy function and force field parameters are used for estimating the intermolecular and intramolecular energy stability of macromolecules. The results of docking can be used to find inhibitors for specific target proteins and thus to design new drugs. (Hartmann, Antes & Lengauer, 2009).

Aromatic interactions are intermolecular forces involving electron rich molecules.

These interactions offer great potential in drug design, structural biology, conformational analysis and asymmetric catalysis. The structure and dynamics of ligand-receptor interactions are affected by two types of non-covalent interactions: H-bonding and parallel aromatic stacking. A hydrogen bond is a weak type of force that forms a special type of dipole-dipole attraction which occurs when a hydrogen atom bonded to a strongly electronegative atom exists in the vicinity of another electronegative atom with a lone pair of electrons. These bonds are generally stronger than ordinary dipole-dipole and dispersion forces, but weaker than true covalent and ionic bonds. In a hydrogen bond, the electronegative atom not covalently attached to the hydrogen is named proton acceptor, whereas the one covalently bound to the hydrogen is named the proton donor. Hydrogen bonds can occur between molecules (*intermolecular*) or within different parts of a single *molecule* (*intramolecular*).

Depending on geometry and environment, the hydrogen bond free energy content is between 1 and 5 kcal/mole. This makes it stronger than a van der Waals interaction, but weaker than covalent or ionic bonds. H-bonding is mostly governed by electrostatics while aromatic stacking is mostly governed by London dispersion forces. It was found that parallel stacking rather than T-shaped stacking improves the hydrogen bond accepting capacity and that this effect is larger for electron donating benzene substituents. Computational studies of substituent effects on π - π interactions showed that in the parallel stacked benzene dimers, substituted benzenes with electron-withdrawing or electron-donating substituents bind stronger to benzene than unsubstituted benzene.

Cation- π interaction is a noncovalent molecular interaction between the face of an electron-rich π system and an adjacent cation. This interaction is an example of noncovalent bonding between a monopole (cation) and a quadrupole (π system). The

most studied cation- π interactions involve binding between an aromatic π system and an alkali metal or nitrogenous cation (Sinnokrot & Sherrill, 2004). The electronic properties of the substituents also influence the strength of the attraction. Electron withdrawing groups weaken the interaction, while electron donating substituents strengthen the cation- π binding (Sinnokrot & Sherrill, 2003).

Molecular docking principally includes two components:

A search algorithm called an optimization algorithm which helps to determine the best conformation of the ligand. (Friesner *et al.* 2004), (Zsoldos *et al.* 2007). In the unbound state, both the ligand and the receptor are separately solvated and do not interact. In the bound state, both partners are partially desolvated and form interactions with each other. **Monte Carlo** or Molecular Dynamics simulations are necessary to arrive at reasonably accurate values of binding free energies.

An evaluation function, sometimes called a **score** function. This is a function providing a measure of how strongly a given ligand will interact with a particular protein. Energy force fields are often used as evaluation functions (Lensink, Méndez & Wodak 2007; Halperin *et al* 2002). These force fields calculate the energy contribution from different terms such as the known electrostatic forces between the atoms in the ligand and in the protein, forces arising from deformation of the ligand, pure electron-shell repulsion between atoms and effect from the solvent in which the interaction takes place. Molecular mechanics force field **Charm M** is used for the estimation of binding affinity. The scoring function takes a pose as input and returns a number indicating the likelihood that the pose represents a favourable binding interaction. Most scoring functions were physics-based mechanics force that estimated the energy of the pose; a low (negative) energy indicated a stable system and thus a likely binding interaction

The active site of the protein can be viewed as a **lock**, and the ligand can be thought of as a **key**. Molecular docking is the process of testing whether a given key fits a particular lock. During the course of the process, the ligand and the protein adjust their conformation to achieve an overall “best- fit” and this kind of conformational adjustments resulting in the overall binding is referred to as “induced- fit” (Suresh *et al* 2008).

13.3.1. Target Characterization

The target protein (2y9x) is purified by removing the water molecules, unnecessary residues and natural ligands. The major ligands found are Holmium atom, Copper(II) ion and 2-Hydroxy cyclo hepta-2,4,6-trien-1-one.

Protein-Geometry optimization details:

1. Minimization Algorithm: Smart Minimizer
2. Minimization Energy Change :0.0
3. Dielectric Constant: 1
4. Implicit Solvent Dielectric Constant: 80
5. Nonbond List Radius: 14.0
6. Nonbond Higher Cutoff Distance :12.0
7. Nonbond Lower Cutoff Distance: 10.0
8. Electrostatics: Spherical Cutoff
9. Kappa: 0.34
10. Order: 4

13.3.2. Hot spot identification

Site Identification by Ligand Competitive Saturation (SILCS) technique is employed. The method involves simultaneously incorporating ligands representatives of all the functionalities and doing 'Molecular Dynamics simulation', It is an in silico free energy-based competition assay that generates three-dimensional probability maps of fragment binding (FragMaps) indicating favourable fragment-protein interactions. The identified hot spot is :

Active site-1

Input Site Sphere -26.5623, -11.3566, -43.1285, 12

The protein has been subjected to 'normal mode analysis' after removing the metal and ligands. Out of all modes, first ten modes obtained on the basis of stability have been picked up. These purified protein molecules are found to be relieved of much bond strain. Docking results of these protein molecules with the same ligand is supporting the above observation. Their docking scores have been improved even up to three times in same poses.

13.3.3. Current challenges or limitations facing molecular docking

- Representation of the ligand

Before docking it is necessary to provide an appropriate 2-dimensional (2D) and 3-dimensional (3D) representation of the ligand. The key issues in the 2D representation of the ligand are its charge and tautomeric state (C/T state). This problem is made even more difficult because a ligand can change its C/T state in response to the environment of the protein. In individual docking, a skilled modeler would consider all relevant states and dock each state against the protein, but in VS applications this approach is not practical. In this work a rule-based approach is used to enumerate plausible alternative states of the ligand and these states are docked individually. The best scoring state is then the one chosen for further analysis.

- Representation of the protein.

One of the key challenges facing docking today is the problem of protein flexibility, because most docking programs assume a rigid receptor. However, proteins are known to change conformation in response to ligand binding (Davis, Teague & Kleywegt 2003). Large-scale movements are particularly difficult to predict, except in situations where the key conformation states are associated with the mechanism of the protein and are known to occur in related proteins (e.g., the movement of the activation loop in kinases (Nagar *et al* 2002). Smaller movements of sidechains are easier to predict *de novo* and some docking methods attempt to do this automatically. A pragmatic solution to protein flexibility in docking applications is to dock against distinct, experimentally determined protein conformations and choose the best ligand solution obtained against this ensemble.

- Water mediation.

Water molecules often mediate favourable interactions between the protein and the ligand. In this case, for the purpose of molecular docking, the water can often be thought of as part of the protein. However, such water molecules can also be displaced by ligands and the energetics of displacement will depend, on

whether the loss of water-protein interactions is sufficiently compensated by the ligand-protein interactions plus the gain in entropy of the displaced water. The challenge for molecular docking is to determine for a particular ligand whether potential mediating waters should be included in the docking or whether they will be displaced. A pragmatic solution would be to dock against forms of the protein in which the relevant waters were (i) all omitted, (ii) some omitted, or (iii) all included in the binding site model. The simplest approach would then be to take the lowest energy ligand solution against this ensemble of protein-water states.

- Scoring

Docking functions minimize a scoring function and the ideal scoring function would have a deep, broad global minimum at, or close to the experimentally observed structure for all classes of ligands and their associated protein targets. In practical applications of virtual screening, a crude scoring function is used to score the single binding mode produced by molecular docking. Popular choices are molecular mechanics functions, empirical scoring functions and knowledge-based functions (Ajay & Murcko 1995).

A decoy analysis is advised to check whether the molecule is a ligand or decoy. Furthermore, the effect of solvation has to be studied. A detailed study on the molecular dynamics and quantum mechanics is warranted to unravel the mechanisms of enzyme inhibition.

13.4. Receptor-Ligand Interactions

Structure-based design plays an increasingly important role in this endeavor and is now an integral part of medicinal chemistry (Bohacek, McMartin & Guida, 1996; Babine & Bender, 1997). The vast majority of the currently available drugs act via non-covalent interaction with the target protein. Therefore, non-bonded interactions are of particular interest in drug design. There is a high level of steric complementarity between the protein and the ligand. This observation is also described as the lock-and-key paradigm. Lipophilic parts of the ligands are most frequently found to be in contact with lipophilic parts of the protein. Polar groups are usually paired with suitable polar protein groups to form hydrogen bonds or ionic interactions. The ligand usually binds in an energetically

favorable conformation. Generally speaking, direct interactions between the protein and the ligand are very important for binding. Therefore, in the ligand design process one has to ensure that polar functional groups, either of the protein or the ligand, will find suitable counterparts if they become buried upon ligand binding. Another situation that leads to a decreased binding affinity is imperfect steric fit, leading to holes at the lipophilic part of the protein-ligand interface.

13.5. Applications of Docking:

- A binding interaction between a ligand and an enzyme protein may result in activation or inhibition of the enzyme. If the protein is a receptor, ligand binding may result in agonism or antagonism. Hence docking plays an important role in the rational design of drugs.
- Hit identification – docking combined with a scoring function can be used to quickly screen potential drugs *in silico*.
- Lead optimization – Docking can be used to predict the binding mode or pose of a ligand to a protein which in turn could be used to design selective analogs.
- Using CHARMM based docking software (CDOCKER) of the Discovery Studio 4.1 (Accelrys Inc., San Diego, CA, USA) suite of programs, docking studies were carried out to evaluate which proteins are the most likely targets of tyrosinase inhibitors and determine the exact binding mechanism of the molecule with its target protein. CDOCKER applies grid-based molecular dynamics simulated annealing protocol by using CHARMM force field while devising the appropriate position of the ligand in the active pocket. The algorithm offers flexible ligand docking where the non-bonded interactions are softened during the docking procedure but removed during the final minimization process.

13.6. References

Ajay-Murcko, MA 1995, 'Computational methods to predict binding free energy in ligand-receptor complexes', *Journal of Medicinal Chemistry*, Vol 38, pp. 4953–4967.

Babine, RS, Bender, SL 1997, 'Molecular recognition of protein minus sign ligand complexes: Applications to Drug Design', *Chemical Reviews*, Vol 97, pp. 1359–1472.

Bennett, TP, Frieden, E 1969, 'Modern topics in biochemistry', Macmillan, London, pp. 43–45.

Bitton, G, Dutka, BJ 1986, 'Toxicity testing using microorganisms', Vol 2, CRC Press, New York, pp. 28–55.

Bohacek, RS, McMartin, C, Guida, WC 1996, 'The art and practice of structure-based drug design: A molecular modeling perspective', *Medicinal Research Reviews*, Vol 16, pp. 3–50.

Chang, TS 2007, 'Two potent suicide substrates of mushroom tyrosinase', *Journal of Agricultural and Food Chemistry*, Vol 55, pp. 2010–2015.

Chang, TS, Lin, MY, Lin, HJ 2010, 'Identifying 8-hydroxynaringenin as a suicide substrate of mushroom tyrosinase', *Journal of Cosmetic Science*, Vol 61, pp. 205–210.

Davis, AM, Teague, SJ, Kleywegt, GJ 2003, 'Application and limitations of X-ray crystallographic data in structure-based ligand and drug design', *Angewandte Chemie International Edition (English)*, Vol 42, pp. 2718–2736.

Dietler, C, Lerch 1982 'Reaction inactivation of tyrosinase. In: *Oxidases and Related Redox Systems*', edited by T. E. King, H. S. Mason & M. Morrison, Pergamon Press, NY, pp. 305–317.

Dixon, M, Webb, EC 1976, 'Enzymes' Academic Press, New York, 1979, p. 47–231, 332–468.

Escribano, J, Tudela, J, Garcia-Carmona, F 1989, 'A kinetic study of the suicide inactivation of an enzyme measured through coupling reactions', *Biochemistry Journal*, Vol 262, pp. 597–603.

- Ferdinand, W 1976, 'The Enzyme Molecule' John Wiley, New York, 1976, p. 21–37.
- Fisher, AA 1983, 'Current contact news. Hydroquinone uses and abnormal reactions', *Cutis*, Vol 31, pp. 240–244.
- Friesner, RA, Banks, JL, Murphy, RB, Halgren, TA, Klicic, JJ, Mainz, DT, Repasky, MP, Knoll, EH, Shelley, M, Perry, JK, Shaw, DE, Francis, P, Shenkin, PS 2004, 'Glide: a new approach for rapid, accurate docking and scoring 1. Method and assessment of docking accuracy', *Journal of Medicinal Chemistry*, Vol 47, pp. 1739–1749.
- Halperin, I, Ma, B, Wolfson, H, Nussinov, R 2002, 'Principles of docking: An overview of search algorithms and a guide to scoring functions', *Proteins*, Vol 47, pp. 409–443.
- Harrow, B, Mazur, A 1958 '*Textbook of Biochemistry*', Saunders, Philadelphia, pp. 109.
- Hartmann, C, Antes, I, Lengauer, T 2009, 'Docking and scoring with alternative side-chain conformations', *Proteins*, Vol 74, pp. 712–726.
- Holum, J 1969, 'Elements of General and Biological Chemistry', 2nd ed., Wiley, NY pp. 377.
- Ingraham, LL, Corse, J, Makower, B 1952, 'Enzymatic browning of fruits. III. Kinetics of the reaction inactivation of polyphenol oxidase', *The Journal of the American Chemical Society*, Vol 74, pp. 2623–2626.
- Jorgensen, WL 1991, 'Rusting of the lock and key model for protein-ligand binding', *Science*, Vol 254, pp. 954–955.
- Kitchen, DB, Decornez, H, Furr, JR, Bajorath, J 2004, 'Docking and scoring in virtual screening for drug discovery: methods and applications', *Nature reviews Drug discovery*, Vol 3, pp. 935–49.
- Kubo, I, Kinst-Hori, I, Yokokawa, Y 1994, 'Tyrosinase inhibitors from *Anacardium occidentale* fruits', *Journal of Natural Products*, Vol 57, pp. 545–551.

Kubo, I, Yokokawa, Y, Kinst-Hori, I 1995, 'Tyrosinase inhibitors from bolivian medicinal plants', *Journal of Natural Products*, Vol 58, pp. 739–743.

Land, EJ, Ramsden, CA, Riley, PA 2007, 'The mechanism of suicide-inactivation of tyrosinase: a substrate structure investigation', *The Tohoku Journal of Experimental Medicine*, Vol 212, pp. 341–348.

Lensink, MF, Méndez, R, Wodak, SJ 2007, 'Docking and scoring protein complexes: CAPRI 3rd Edition', *Proteins Structure Function and Bioinformatics*, Vol 69, pp. 704.

Lengauer, T, Rarey, M 1996, 'Computational methods for biomolecular docking', *Current Opinion in Structural Biology*, Vol 6, pp. 402–406.

Martinek, R 1969, 'Practical Clinical Enzymology', *The American Journal of. Medical. Technology*, Vol 31, pp. 162

Michal, G 1978, 'Determination of Michaelis constants and Inhibitor constants', In: *Principles of Enzymatic Analysis*, Bergmeyer H. U (E d), Wemharn VCH, New York, pp. 29–40.

Muñoz-Muñoz, JL, Garcia-Molina, F, Garcia-Ruiz, PA, Molina-Alarcon, M, Tudela, J, Garcia-Canovas, F, Rodriguez-Lopez, JN 2008, 'Phenolic substrates and suicide inactivation of tyrosinase: kinetics and mechanism', *Biochemistry Journal*, Vol 416, pp. 413–440.

Munoz-Munoz, JL, Garcia-Molina, F, Varon, R, Garcia-Ruiz, PA, Tudela, J, Garcia-Canovas, F, Rodriguez-Lopez, JN 2010, 'Suicide inactivation of the diphenolase and monophenolase activities of tyrosinase', *IUBMB Life*, Vol 62, pp. 539–547.

Muñoz-Muñoz, JL, Acosta-Motos, JR, Garcia-Molina, F, Varon, R, Garcia-Ruiz, PA, Tudela, J, Garcia-Cánovas, F, Rodríguez-López, JN 2010, 'Tyrosinase inactivation in its action on L-dopa', *Biochimica Et Biophysica Acta*, Vol 1804, pp. 1467–1475.

Nagar, B, Bornmann, WG, Pellicena, P, Schindler, T, Veach, DR, Miller, WT, Clarkson, B, Kuriyan, J 2002, 'Crystal structures of the kinase domain of c-Abl in complex with the small molecule inhibitors PD173955 and imatinib (STI-571)', *Cancer Research*, Vol 62, pp. 4236–4243.

Palmer, T 1991, 'Understanding Enzymes' Ellis Horwood series in Biochemistry and Biotechnology, Wiseman A (Ed), Ellis Horwood, England, p. 1–28.

Pfeiffer, J 1954, '*Enzymes, the Physics and Chemistry of Life*', Simon and Schuster, pp. 171–173.

Sami, AJ, Shakoor, AR 2011, 'Cellulose activity inhibition and growth retardation of associated bacterial strains of *Aulacophora foveicollis* by two glycosylated flavonoids isolated from *Mangifera indica* leaves', *Journal of Medicinal Plants Research*, Vol 5, pp. 184–190.

Seiji, M, Sasaki, M, Tomita, Y 1978 'Nature of tyrosinase inactivation in melanosomes', *Tohoku Journal of Experimental Medicine*, Vol 125, pp. 233–245.

Sinnokrot, MO and Sherrill, CD 2003, 'Unexpected substituent effects in face-to-face π -stacking interactions', *The Journal of Physical Chemistry A*, Vol 107, pp. 8377–8379.

Sinnokrot, MO and Sherrill, CD 2004, 'Substituent effects in π - π interactions sandwich and T-shaped configurations', *Journal of the American Chemical Society*, Vol 126, pp. 7690–7697

Tai, SSK, Lin, CG, Wu, MH, Chang, TS 2009, 'Evaluation of depigmenting activity by 8-hydroxydaidzein in mouse B16 melanoma cells and human volunteers', *International Journal of Molecular Science*, Vol 10, pp. 4257–4266.

Taylor, RD, Jewsbury, PJ, Essex, JW 2002, 'A review of protein-small molecule docking methods', *Journal of Computer Aided Molecular Design*, Vol 16, pp. 151–166.

Wu, G, Robertson, DH, Brooks, CL, Vieth, M 2003, 'Detailed analysis of grid-based molecular docking: A case study of CDOCKER-A CHARMM-based MD docking algorithm', *Journal of Computational Chemistry*, Vol 24, pp. 1549–1462.

Zsoldos, Z, Reid, D, Simon, A, Sadjad, SB, Johnson, AP 2007, 'eHiTS: A new fast, exhaustive flexible ligand docking system', *Journal of Molecular Graphics and Modelling*, Vol 26, pp. 198–212.